University of Sevilla
Department of Organic Chemistry

Spanish National Research Council
Institute for Chemical Research

Strategies towards Selective Functionalization of Polycationic Amphiphilic Cyclodextrins (paCDs): Engineering Novel Non-viral Gene Carriers by Tailoring Self-assembling and DNA-condensing Capabilities

Iris Pflueger

2013

University of Sevilla
Department of Organic Chemistry

Spanish National Research Council
Institute for Chemical Research

Strategies towards Selective Functionalization of Polycationic Amphiphilic Cyclodextrins (paCDs): Engineering Novel Non-viral Gene Carriers by Tailoring Self-assembling and DNA-condensing Capabilities

Memoria presentada por
Iris Pflueger, MSc.
para optar al grado de Doctor en Química

This work was performed by Iris Pflueger at the Institute for Chemical Research (IIQ, CSIC – University of Sevilla) under the supervision of Dr. Juan M. Benito Hernández, Tenured Scientist at CSIC, and under the tutorship of Dr. Carmen Ortiz Mellet, Professor of Organic Chemistry at the University of Sevilla. This work has not previously been accepted in substance for any degree and is not being concurrently submitted in candidature of any degree.

Carmen Ortiz Mellet	Juan Manuel Benito Hernández

This Thesis is dedicated to my parents
for their endless love, support
and encouragement.

Acknowledgements

Abstract

The use of pre-organized macrocyclic scaffolds to achieve a precise alignment of functional elements has proven to be extremely useful over the years in the design of artificial receptors and ligands capable of mimicking the supramolecular events occurring in living organisms. The cyclic maltooligosaccharide (cyclodextrin, CD) nucleus is considered a privileged platform for these channels, as it combines biocompatibility, availability and a tubular symmetric framework with well-differentiated faces. CD-based architectures can additionally take advantage of their distinctive inclusion capabilities.

Recently, CDs have found their way into the field of gene delivery, giving rise to a plethora of synthetic CD-containing carriers, such as CD-embedding or pendant polymers, polyrotaxanes, and CD-centered and coated dendrimers and dendripolymers.[1] Although many of these systems have proven to be efficient vectors,[2] their essentially disperse nature handicaps both investigational studies and clinical applications. The development of monodisperse CD derivatives that are capable to self-organize in the presence of nucleic acids and deliver them into cells constitutes an interesting alternative that critically depends on the availability of efficient methods to systematically manipulate the CD topology in order to attain a precise control of the presentation and orientation of functional elements and, thereby, of their supramolecular capabilities.

In this Ph.D. Thesis, a molecular-diversity-oriented approach has been exploited for the preparation of well-defined polycationic amphiphilic cyclodextrins (paCDs) as gene delivery systems. The synthetic strategy takes advantage of the differential reactivity of primary versus secondary hydroxyl groups on the CD torus to regioselectively decorate each rim with cationic and lipophilic tails, respectively. Both the charge density and the display and the nature of the hydrophobic domain can be finely tuned by using "click chemistry" methodologies, preserving the molecular homogeneity (and architectural symmetry), thereby providing an easy-to-use tool for tight control over the hydrophilic/hydrophobic balance.

The monodisperse nature of paCDs and the modularity of the synthetic scheme are particularly well suited to correlate molecular structure with self-assembling and gene

delivery capabilities in the way that structure-activity relationship (SAR) studies are carried out in typical medicinal chemistry programs. Their self-assembling capabilities in aqueous environment have been investigated and a progressive decrease of the critical aggregation concentration (CAC) with increasing amphiphilicity of the CD conjugates was observed. Acid-base titration experiments revealed that in comparison to their non-amphiphilic analogs amphiphilic CD derivatives showed improved buffering capacities in the pH range from 7 to 5. This indicates that paCD-based nanoparticles may exhibit proton sponge capabilities upon acidification, which might help to promote endosomal escape after cell internalization. Gel electrophoresis and fluorescence quenching assays evidenced that paCDs self-assemble in the presence of calf thymus DNA (ctDNA) to provide stable nanoparticles (CDplexes) that fully protect nucleic acids from the environment. As characterized by DLS measurements, paCDs formed narrow populations of compact and ordered nanoparticles with ctDNA, exhibiting small hydrodynamic diameters (60-90 nm) and positive zeta (ζ) potentials (40-50 mV). Fluorescence tracking of CDplex dissociation promoted by heparin showed that CDplex dissociation kinetics is drastically influenced by the hydrophilic/hydrophobic balance. Furthermore, the transfection efficiency of the CDplexes was investigated in vitro on COS-7 cells in serum-containing medium and was found to be intimately dependent on architectural features.

In the following chapter of this Ph.D. Thesis, the focus has been moved to the assessment of the gene delivery potential of paCDs decorated with cyclic oligoamines as alternative polar headgroups. In particular, the goal consisted on exploiting cationic preorganized scaffolds such as cyclen and cyclam, which exhibit unique DNA-binding capabilities.

With the purpose of rationalizing the role of the cationic element in gene delivery, their structure-activity relationships were investigated and compared to acyclic oligoamine-grafted paCDs. The self-assembling capabilities of cyclen/cyclam-bearing paCDs resembled those of paCDs with acyclic polycationic elements and lipophilic tails of the same length. Cyclen/cyclam-grafted paCDs exhibited improved pH buffering abilities in the range from 7 to 5. Gel electrophoresis shift assays evidenced that paCDs furnished

with cyclic polyamines self-assemble in the presence of calf thymus DNA (ctDNA) to provide stable nanoparticles (CDplexes) that fully protect ctDNA from the environment. Hydrodynamic diameter and zeta (ζ) potential measurements indicated that modifications of the molecular structure did influence neither particle size (80-100 nm) nor surface charge (40-60mV) significantly. Moreover, the transfection efficiency of the CDplexes derived from paCDs decorated with cyclic oligoamines was investigated in vitro on COS-7 and HeLa cells, both in the absence and in presence of serum and was found to be similar to that of CDplexes formulated with paCDs bearing acyclic cationic headgroups.

The above chapters demonstrate that fine-tuning of CD topology holds a great potential to manipulate supramolecular capabilities, including nucleic acid delivery. Unfortunately, the actual toolbox for selective CD modification is still limited. The final chapter of this Ph.D. Thesis has been devoted to the development of a conceptually novel approach to the selective functionalization of cyclodextrins. This novel strategy exploits a solid matrix to display the complementary reagent functionalities sufficiently far from each other to prevent a single CD species from reacting through more than one site. Using a "*catch-and-release*" process based on the Staudinger reaction, complex CD functionalization patterns could be produced in one pot and without any purification step.

Table of Contents

List of Abbreviations

A

A	Absorbance
A. U.	Arbitrary unit
AAV	Adeno-associated virus
Ac	Acetyl
AD	Adamantane
AM-PS	Aminomethylated polystyrene
AMP	Adenosine-5'-monophosphate
AMS	(Aminomethyl)polystyrene
anh.	anhydrous
aq.	aqueous
ASGPr	Asialoglycoprotein receptors
ATP	Adenosine-5'-triphosphate
av.	average

B

BCA	Bicinchoninic acid
BHK-21	Baby hamster kidney fibroblast cell line
Bn	Benzyl
BNL-CL2	A murine embryonic hepatocyte cell line
Boc	*tert*-Butoxycarbonyl
bp	Base pair
BPA	Bis(pyridyl)amine
bPEI	Branched PEI
Bu	Butyl
But	Butanoyl

C

CAC	Critical aggregation concentration
CD	Cyclodextrin

CDE	Clathrin-dependent endocytosis
CDP	Linear polymers with alternating CD and cationic segments
CDplex	paCD-DNA complex
chol	Cholesterol
CIE	Clathrin-independent endocytosis
conc.	concentrated
COS-7	A fibroblast-like cell line derived from African Green Monkey, *Cercopithecus aethiops*, kidney tissue, carrying the SV40 genetic material
COSY	Correlation spectroscopy
ctDNA	Calf thymus DNA
CuAAC	Copper-catalyzed azide-alkyne cycloaddition

D

δ	Chemical shift
DABCO	1,4-Diazabicyclo[2.2.2]octane
DBF	Dibenzofulvene
DBU	1,8-Diazobicyclo[5.4.0]undec-7-ene
DC-Chol	3b-[*N*-(*N*',*N*'-Dimethylaminoethane)-carbamoyl] cholesterol
DCM	Dichloromethane
DETA	Diethylenetriamine
DIBAL-H	Diisobutylaluminium hydride
DIC	Diisopropylcarbodiimide
dios	Diosgenin
DIPEA	Diisopropylethylamine
DLS	Dynamic light scattering
DMAP	4-(Dimethylamino)pyridine
DMEM	Dulbecco’s modified Eagle’s medium
DMF	*N*,*N*-Dimethylformamide
DMSO	Dimethyl sulfoxide
DNA	Deoxyribonucleic acid

DOGS	Dioctadecylamidoglycylspermine
DOPE	1,2-Dioleoyl-*sn*-glycero-3-phosphoethanolamine
DOSK	Dioleoyl succinyl kanamycin A
DOSP	Dioleoyl succinyl paromomycin
DOSPA	2,3-Dioleyloxy-*N*-[2-(sperminecarboxamido)ethyl]-*N*,*N*-dimethyl-1-propanaminium trifluoroacetate
DOTA	N^1,N^4,N^7,N^{10}-cyclentetraacetic acid
DOTAM	N^1,N^4,N^7,N^{10}-cyclentetraacetic acid amide
DOTAP	*N*-[1-(2,3,Dioleoyloxypropyl)]-*N*,*N*,*N*-trimethylammonium chloride
DOTMA	*N*-[1-(2,3,Dioleyloxypropyl)]-*N*,*N*,*N*-trimethylammonium chloride
DVB	Divinylbenzene

E

EDA	Ethylenediamine
EDTA	Ethylenediaminetetraacetic acid
ELS	Evaporative light scattering
EMA	European Medicines Agency
ENA	Ethylene-bridged nucleic acids
eq	Equivalent
ESI-MS	Electrospray ionization mass spectrometry
Et	Ethyl

F

FCS	Fetal calf serum
FDA	Food and Drug Administration
Fmoc	9-Fluorenylmethoxycarbonyl
FTIR	Fourier transform infrared spectroscopy

H

H9c2	Embryonic rat cardiomyoblast cell line
HA	Haemagglutinin

HeLa	Human epithelioid cervix carcinoma cell line
HEPES	2-[4-(2-Hydroxyethyl)piperazin-1-yl]ethanesulfonic acid
HepG2	Human epithelial-like liver hepatocellular carcinoma cell line
Hex	Hexanoyl
HIV	Human immunodeficiency virus
HMQC	Heteronuclear multiple quantum correlation
HPβCD	Hydroxypropyl-β-cyclodextrin
HPLC	High performance liquid chromatography

I

I	Intensity
IR	Infrared

K

K_a	Acid dissociation constant

L

LC	Liquid Chromatography
LG	Leaving group
LNA	Locked nucleic acid
LNP	Lipid nanoparticle
lPEI	Linear PEI
LPLD	Lipoprotein lipase deficiency
LS	Light scattering

M

m/z	Mass-to-charge ratio
M3-PALS	Mixed mode measurement-phase analysis light scattering
Me	Methyl
MeβCD	Methyl-β-cyclodextrin
MP	Macropinocytosis
MRI	Magnetic resonance imaging
MS	Mass spectrometry
MSNT	1-(2-Mesitylenesulfonyl)-3-nitro-1*H*-1,2,4-triazol

µw	Microwave
N	
N/P	Number of protonable amino groups (N) of the vector per phosphate (P) of DNA
NIS	*N*-Iodosuccinimide
NMR	Nuclear magnetic resonance
O	
OEI	Oligoethyleneimine
P	
paCD	Polycationic amphiphilic cyclodextrin
PAMAM	Poly(amidoamine)
PBS	Phosphate buffered saline
PDI	Polydispersity index
pDMAEMA	Poly[2-(dimethylamino)ethyl methacrylate]
pDNA	Plasmid DNA
PEG	Polyethylene glycol
PEGA	Poly[acryloyl-bis(aminopropyl)polyethylene glycol]
PEI	Polyethyleneimine
PET	Positron emission tomography
PG	Protecting group
PGAA	Polyglycoamidoamine
pGaCD	Glycosylated paCD
Ph	Phenyl
PL-AMS	Aminomethylated polystyrene commercialized by Polymer Laboratories
PLL	Poly-L-lysine
PMO	Phosphorodiamidate morpholino oligomer (Morpholinos)
PNA	Peptide nucleic acid
PP_i	Pyrophosphate
Pr	Propanoyl

	PS	Polystyrene
	PTG	
	Py	Pyridine
R		
	RAFT	Radical addition-fragmentation chain transfer
	RISC	RNA-induced silencing complex
	RNA	Ribonucleic acid
	RNAi	RNA interference
	RPC	Polycationic copper chelator
	RP-HPLC	Reversed phase HPLC
	rt	Room temperature
S		
	SAR	Structure-activity relationship
	SCID	Severe combined immunodeficiency
	SEC	Size exclusion chromatography
	shRNA	Small hairpin RNA
	siRNA	Small interfering RNA
	SPECT	Single photon emission computed tomography
T		
	$t_{½}$	Reaction half-time
	TACN	1,4,7-Triazacyclononane
	TAE	Buffer containing Tris, acetic acid and EDTA
	TBTA	Tris[(1-benzyl-1*H*-1,2,3-triazol-4-yl)methyl]amine
	TBTU	*O*-(Benzotriazol-1-yl)-*N*,*N*,*N*',*N*'-tetramethyluronium tetrafluoroborate
	TCR	T-cell receptor
	TEM	Transmission electron microscopy
	Tf	Transferrin
	TFA	Trifluoroacetic acid
	THF	Tetrahydrofuran

TLC	Thin layer chromatography
TOCSY	Total correlation spectroscopy
TPP	Triphenylphosphine
Tr	Trityl
t_r	Retention time
TREN	Tris(2-aminoethyl)amine
Tris	2-Amino-2-hydroxymethyl-propane-1,3-diol
Ts	Tosyl

U

UV	Ultraviolet

CHAPTER 1 - GENERAL INTRODUCTION

1. The Gene Therapy Paradigm

It is hardly conceivable for the pharmaceutical industry nowadays, investing a vast amount of resources on high-throughput drug discovery technologies, that the strategy to bring up new drugs could simply rely on the design based on a rational set of rules of a single candidate programmed to develop the required task. This is precisely what made nucleic acids (genes, oligonucleotides, aptamers, ribozymes, DNAzymes, or small interfering RNAs) an attractive source of therapeutic agents. The intimate structure-activity relationship and their highly specific mode of action theoretically permit, when using appropriate designs, to exploit cellular machinery in a predictable fashion to either stimulate or silence the expression of virtually any protein, with reduced potential for toxicity and fewer side effects; the Holy Grail of medicinal chemistry. These issues are the foundation of Gene Therapy's high prospects to develop an alternative therapeutic modality to traditional chemotherapy.

The potential use of genes as therapeutic agents has attracted attention as a novel approach to the treatment of severe diseases. In the case of inherited disorders, the introduction of a normal copy of the affected gene can effectively restore healthy cell functioning. For the treatment of acquired disorders, such as cancer and infectious diseases, effective potential strategies involve not only the introduction of a therapeutic gene, such as the gene for a cytokine or an antigen, but also the silencing of the expression of an abnormal gene, whose expression is enhanced in the diseased tissue or cells.

Although its underlying concepts date back to the 1960s, gene therapy is a relatively young field in modern molecular medicine. The first gene transfer clinical trial dates back from 1989, consisting on the transfer of a drug resistance gene marker to a patient's lymphocytes.[3] This and other early trials, which utilized early generation retroviral vectors, provided evidence of safe in vivo gene transfer for potential therapeutic benefit.[4] In the 2000, an experimental gene therapy treatment was put forward against combined severe immunodeficiency (SCID).[5] More recently, gene therapy has also been satisfactorily

applied to β-thalassemia, an inherited autosomal recessive blood disorder.[6] In parallel, a growing number of clinical trials have been conducted over the last 20 years or are under progress, targeting a range of maladies (Figure 1).[7] However, these trials have also highlighted the need for progress on many fronts, including deeper molecular knowledge of disease target pathologies, the development of enhanced therapeutic cargoes, further insights into gene delivery mechanisms, engineering of safer carriers, and the improvement of vector manipulation processes. Initial over-optimism had to face many disappointing roadblocks and safety concerns, including the death of a trial volunteer from carrier-associated toxicity[8] or several cases of leukemia in children receiving gene therapy treatment against SCID for replacing the interleukin-2 receptor γ chain gene.[9]

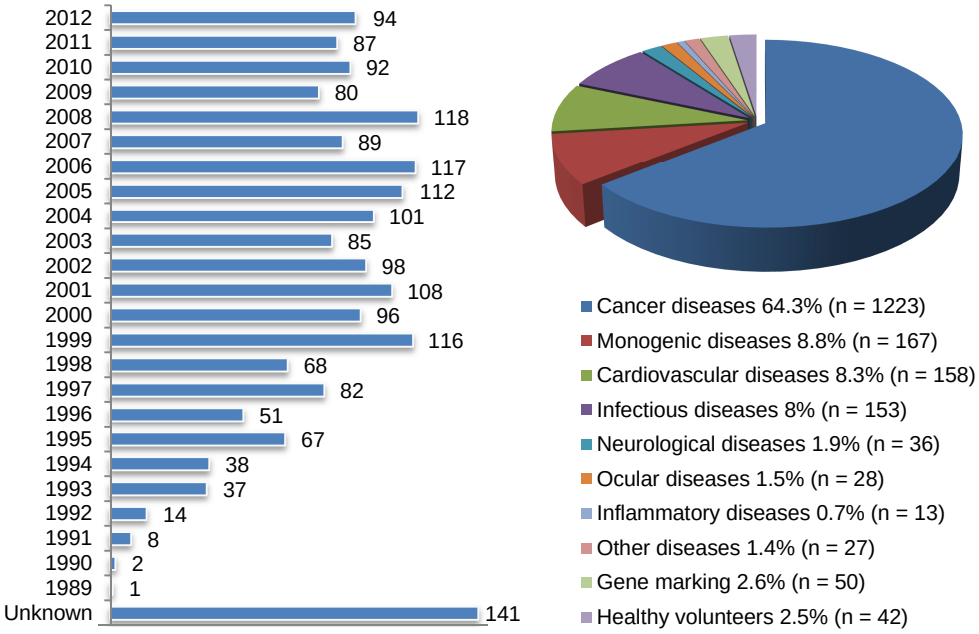

Figure 1. Gene therapy clinical trials approved worldwide 1989-2012 (left) and the indications addressed (right).[7]

The effort developed in the last decades to facilitate manipulation and engineering of oligonucleotides, together with the identification and understanding of the genetic grounds of a plethora of maladies, transformed the initial concepts into a potentially useful technology to develop novel therapeutic alternatives to known diseases. Indeed, there already exist a number of therapeutic agents based on different types of nucleic acids, which can be roughly divided into protein-coding sequences (e.g. plasmid DNA)[10] and non-coding agents (e.g. oligonucleotides,[11] ribozymes,[12,13] interfering RNAs,[14] or aptamers, Table 1).[15] Several examples of each category are undergoing clinical trials[16] for the treatment of a range of diseases, including cancer, HIV, and cardiac or neurological disorders (e.g. Parkinson and Alzheimer diseases).[17]

Table 1. Types of therapeutic nucleic acids.

Protein-coding DNA sequences	Proteins substituting missing or mutated cellular proteins Proteins modulating cellular functions Secreted growth factors and cytokines Proteins regulating cell survival and apoptosis Antigens for vaccinations Antibodies and intracellular antibodies T-cell receptor (TCR) subunits	
Non-coding nucleic acids	Oligonucleotides and modified oligonucleotides	Phosphorothioate oligonucleotides 2'-Ribose modified oligonucleotides Locked nucleic acids (LNA) and ethylene-bridged nucleic acids (ENA) Morpholinos (PMO) Peptide nucleic acids (PNA)
	Catalytic RNAs and DNAs	Ribozymes and DNAzymes
	Small regulatory RNAs	siRNAs and shRNAs, microRNAs
	Long antisense RNAs	
	Decoys	
	Aptamers	

Conventional drugs consist of a formulation of a bioactive species and a carrier, accounting the former for most of the sophistication of the design. However, in the case of biomolecular drugs such as nucleic acids, the role of the carrier becomes decisive in enabling the load to overcome the physiological barriers and reach its target in a fully functional form to carry out its designed therapeutic function. This issue was soon recognized and still remains a challenge 25 years later. Although naked oligonucleotides have been shown to transfect cells both in vitro and in vivo,[18] their transfection efficiency is generally low because of their limited bioavailability. Nucleic acids are easily degraded by nucleases in biological fluids[19] and their membrane-crossing abilities and cellular uptake are seriously limited by their inherently large size and charge (Figure 2).[20] These hurdles, evolved over millions of years, are exploited by most organisms to preserve the integrity of their genetic material from external contaminations and constitute the major impairment for the clinical success of gene therapy.

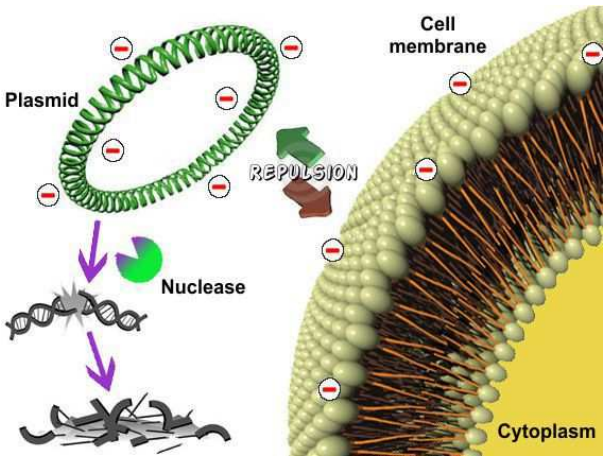

Figure 2. Schematic representation of pharmacokinetic limitations of nucleic acid-based therapeutic agents.

The myriad of technologies and strategies envisioned to improve the (therapeutic) bioavailability of nucleic acid illustrates the complications behind this challenge. Nucleic acid delivery is a multistep process and inefficiencies at any stage result in a dramatic

decrease in the pretended effects. Difficulties associated to intracellular delivery of nucleic acids are manifold, starting at cell membrane crossing, but also include distribution to the proper subcellular compartment and timely release of the cargo. In the case of DNA, an additional translocation into the nucleus is necessary, while siRNA, for instance, must be targeted to the RNA-induced silencing complex (RISC) elsewhere in the cytoplasm. Moreover, systemic delivery encounters additional hurdles, for example the unspecific interaction of nucleic acid carriers with biological milieu (e.g. blood components), uptake by the reticuloendothelial system or kidney filtration, and management of the targeting ability and the off-target toxicity.[21]

A major problem associated to extracellular gene delivery is the strong interaction of carriers with serum proteins, which leads to structural reorganization, aggregation, and/or dissociation of the carrier-nucleic acid assemblies, thereby dramatically lowering the transfection efficiency.[22] In addition, the presence of nuclease in the serum can also degrade nucleic acids if not conveniently protected by the carrier, resulting in a loss of biological activity.[23]

Cellular uptake of the carrier-nucleic acid assemblies is also major hurdle for gene therapy (Figure 3). Internalization of macromolecular entities or their aggregates does not occur passively, but exploiting cellular endocytic mechanisms.[24] The ability of the carriers to associate cell membrane and promote its uptake remarkably determines the efficacy of the transfection process. Moreover, timely escape from the internalized endosome to release the nucleic acid payload at the right intracellular spot is also crucial of the efficiency of the whole process. Unfortunately, attempting to overcome these hurdles individually is a delicate effort (often futile), since carrier manipulation usually affects several of their features simultaneously.

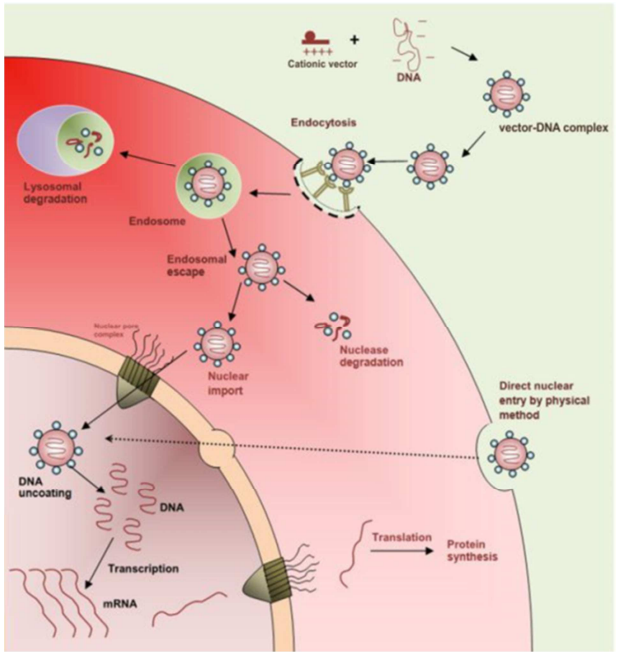

Figure 3. Schematic representation of the hurdles to gene transfer into cells.

Technological and strategic alternatives envisioned to overcome these hurdles are overwhelming. The advent of nanotechnologies and the increasing knowledge of the molecular basis of many diseases and how they are connected to gene or protein dysfunctions has attracted an unparalleled interest from the most varied fields. Unfortunately, given the cumbersome size of the challenge, as consensus solution is far from being reached. The main alternatives for nucleic acid delivery are succinctly overviewed in the following paragraphs.

2. Viral vs. Non-viral Gene Carriers

The simplest way of gene delivery consists on direct treatment of the target with naked nucleic acids, but due to their low bioavailability, a number of techniques have been developed. These can be roughly classified into two main groups: physical methods and carrier-assisted ones. The formers exploit mechanical or electric stimuli to promote uptake of the therapeutic nucleic acid into the target cell or tissue. Physical methods include *microinjection*,[25] *bio-ballistic transfection* (*gene gun*),[26] *electroporation*,[27] *ultrasounds*, or *pressure gradients*,[28] among others (Figure 4).[29] Evidently, the nature of most of these techniques makes them quite unsound for in vivo application, though they have demonstrated certain success ex vivo.[30]

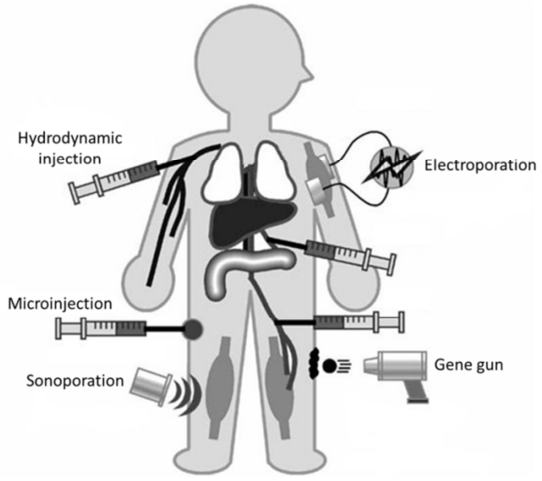

Figure 4. Physical methods used in gene therapy.

2.1. Viral-based gene carriers

Vector-assisted techniques, conversely, aim at mimicking the capabilities of natural viruses to transport nucleic acids into different targets. A successful vector should (a)

provide nucleic acid protection, (b) enable cellular uptake of its payload and delivery to its subcellular target, and (c) promote its biological action (e.g. gene transcription). Along millions of years, viruses have evolved the most fascinating mechanisms to fulfill these tasks and their capabilities were immediately recognized at the nascence of the gene therapy paradigm. Indeed, it is not surprising the recombinant viruses (devoid of replicating capabilities) were the first nucleic acid carrier candidates investigated to deliver nucleic acids at the right spot.[31,32] Unfortunately, engineering of non-replicating viruses still is nowadays an unmet challenge. Only relatively simple viruses such as retroviruses,[33] adenoviruses,[34] adeno-associated viruses (AAV),[35] the *poxvirus*,[36] the *vaccinia virus*,[37] or the *simplex herpes*[38] can be reliably modified (Figure 5).

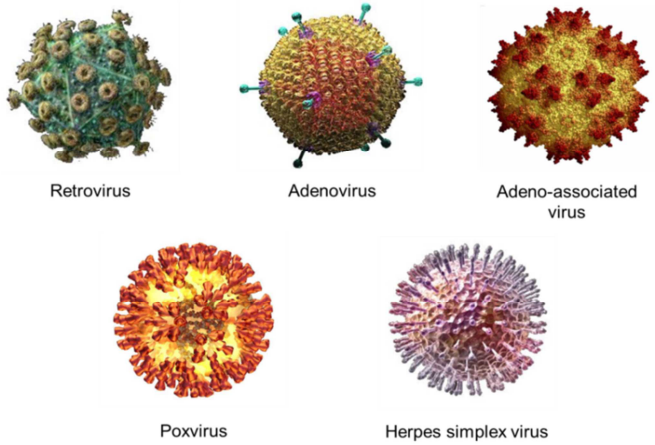

Figure 5. Some viral vectors used in gene therapy.

Despite therapeutically relevant levels of gene expression have been achieved in different organs such as kidney,[39] ovary,[40] eye,[41] and muscle tissues,[42] and over 70% of ongoing gene therapy clinical trials (approximately 1500, Figure 6) are assessing the performance of viral vectors, serious risks and limitations still exist concerning the broad applicability.[43] On one hand, viral vectors are potentially capable of recombining with replication-competent viruses. On the other, they can also induce immunogenic or inflammatory response, or eventually, undesired insertion on the host genome.[43,44]

Moreover, large scale manufacturing of even the simplest viral carriers still is far from obvious. In fact, due to these drawbacks, only one viral-vector-based gene therapy treatment has received so far the green light from the European Medicines Agency (EMA): Glybera® (UniQure), an AAV vector encoding the human lipoprotein lipase gene indicated for the treatment of lipoprotein lipase deficiency (LPLD), a very rare inherited condition that is associated with pancreatic inflammation.[45] The FDA has not approved any formulation yet. The more relaxed Chinese authorities granted Shenzhen SiBionoGenTech the use of Gendicine, a modified adenovirus vector encoding the p53 tumor suppressor gene for treating head and neck cancer in 2003.[46] Two years later, Sunway Biotech gained approval in China for H101, a recombinant oncolytic adenovirus that targets p53-deficient tumor cells.[47] Western authorities questioned both decisions due to a lack of available information on the two therapies.[48]

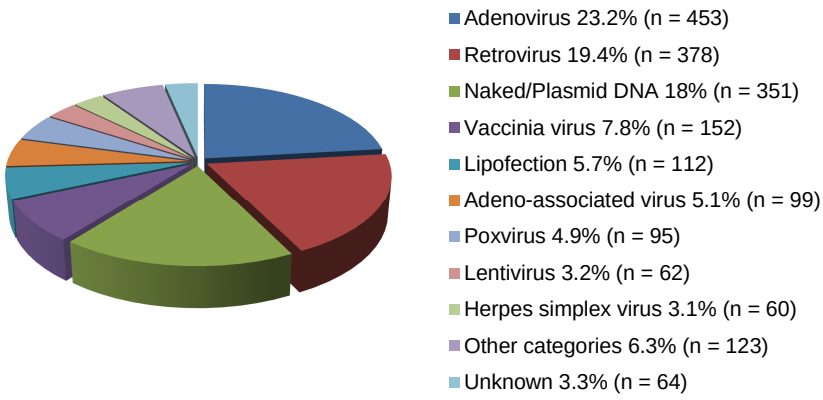

Figure 6. Vectors used in gene therapy clinical trials.[7]

Very recently, Naldini and co-workers published the results of two clinical trials using lentiviral vectors for stem cell gene therapy in patients with Wiskott-Aldrich Syndrome,[49] an inherited disease that disables the immune system, and a methachromatic leukodystrophy,[50] a metabolic disease. Three years after the start of the clinical trials, disease progression stopped in all six patients and some of them showed no symptoms for 18 to 32 month following the therapy.[51] Even after fairly long-term follow up, the

therapy appears to be safe and effective, as the risk of the corrected gene inserting itself next to the cancer-activating one could be reduced.[52]

However, despite the progress achieved in the treatment of challenging diseases such as muscular dystrophy,[42] HIV,[53] or cancer,[54] (two thirds of investigational gene therapies are focused at cancer treatment), gene therapy is immature and clinical success is still distant.

2.2. Non-viral gene carriers

Alternatively, non-viral-based vectors have gathered momentum. In the era of nanotechnologies, synthetic materials can be designed and constructed using bottom-up approaches to tailor the desired functional features in terms of bioavailability and biocompatibility, nucleic acid complexation, protecting and packing capabilities, or membrane-crossing and targeting abilities.

As the understanding of the self-assembling processes involved in aggregate formation between nucleic acids and synthetic vectors increases, the range of designed biomaterials for this purpose open wider (literally hundreds).[55,56] Most of these non-viral nucleic acid vectors fall within the category of cationic lipids[57] or polymers[58] (Figure 7 and Figure 8, respectively), featuring functional groups that electrostatically neutralize nucleic acids and cooperatively promote compaction into colloidal nanoparticles (termed *lipo*- and *polyplexes*, respectively) with increased metabolic stability and membrane permeability. Nanoparticle stability and transfection efficiency largely depend on the structural features of the cationic vector, the type of nucleic acid to be delivered and the relative formulation ratio.

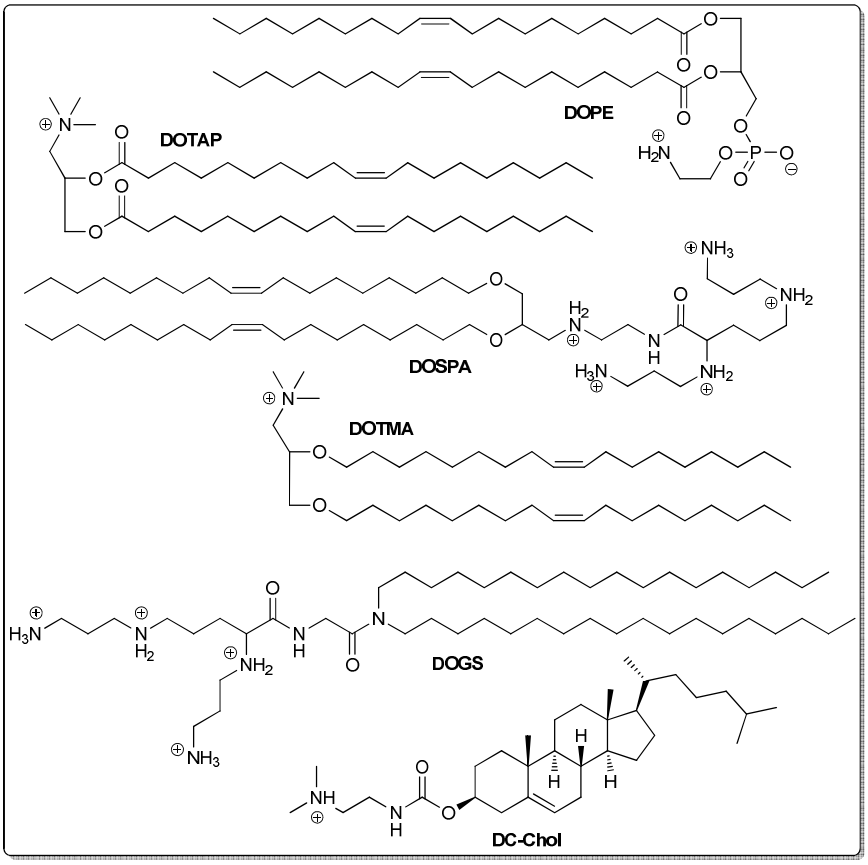

Figure 7. Illustrative examples of cationic lipids used as non-viral vectors.

Non-viral vectors are, in principle, less prone to elicit the immune system response. Moreover, they are more flexible than viral particles regarding the type and size of the payload and far easier to produce. However, they still may trigger inflammatory response and their delivery efficiency and selectivity, despite few exceptions,[2] are far from that of their viral counterparts. This is not surprising considering that most of the first generation non-viral candidates were not purposely conceived for such task, but just *off-the-shelf* materials, such as poly-L-lysine (PLL) or polyethylenenimine (PEI), for which gene delivery capabilities were incidentally discovered. Their densely charged nature does not usually furnish them with the optimal biocompatibility and cytotoxicity profiles.[59]

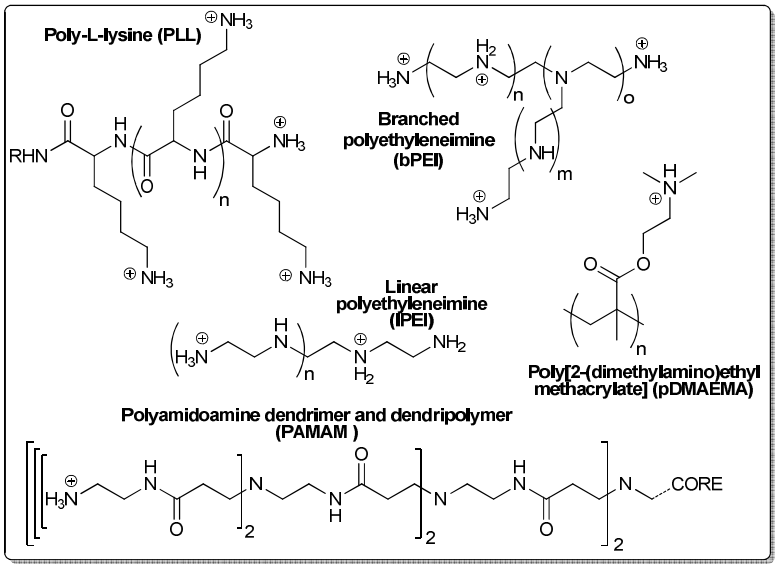

Figure 8. Illustrative examples of cationic polymers used as non-viral vectors.

In the last decade, the efforts in field have been focused on furnishing these off-the-self non-viral carriers with the functional elements that viruses exploit to overcome the physiological barriers to improve their inherently poor efficiency. That is, elaborating artificial viruses (Figure 9).[58b,60] Either covalent or supramolecular chemical manipulation of these carriers has been implemented to interfere in and improve their performance in several folds:[61]

- improving nucleic acid condensation and protection in the extracellular milieu,[62]
- enhancing cellular uptake by specific mechanisms by, for instance, grafting cell surface receptor complementary ligands,[63]
- promoting endosome release by including membrane destabilizing agents[64] or pH-sensitive architectures,[65]
- exploiting intracellular active transport machineries to selectively move through the cytoplasm,[66]
- targeting nuclear membrane pores by using nuclear localization antennae,[67]

- or improving biocompatibility and bioavailability (eventually also biodegradability) in order to prevent interferences with the immune system or undesired unspecific interactions in the biological milieu[68] by, for instance, shielding carriers with polyethylene glycol (PEG) chains.[69,70]

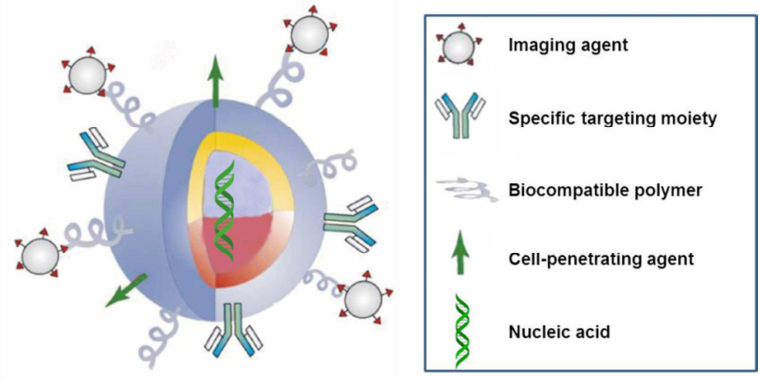

Figure 9. Schematic representation of the components of an *artificial virus* for nucleic acid delivery.

Cationic lipids are amphiphilic molecules consisting on a charged head group linked to a hydrophobic domain that self-assemble in aqueous media in the presence of nucleic acids into more or less defined liposomes. Their use in non-viral gene delivery dates back from 1987, when Felgner described an improvement of two orders of magnitude in gene expression efficiency by using DOTMA (Figure 7) as compared to other non-viral carriers.[71] This milestone inspired a number of contributions focused on assessing structure-activity relationships (SAR).[72] Nucleic acid condensation by cationic lipids is supposed to be a two-step process initiated by an initial electrostatic interaction between cationic heads and the anionic polyphosphate backbone. Then, entropy-driven desolvation by clustering of the hydrophobic domains produces aggregate compaction. It has been suggested that, once internalized into cells, cationic lipids in lipoplexes interact with anionic lipids of the endosome, causing destabilization of the endosomal membrane (Figure 10).[73]

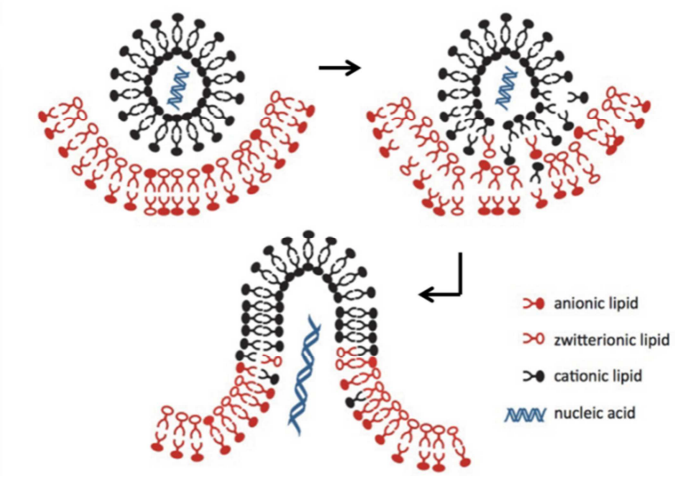

Figure 10. Illustration of the proposed mechanism for endosomal escape of cationic lipids.[74]

The length of the lipophilic tail(s), nature of the cationic head group (size and charge), the linker between both domains, or their susceptibility to changes in the biological media have been shown to exert major roles in their performance.[75] Several generations of cationic lipids have evolved improving the performance of the formers. For instance, *N*-[1-(2,3-dioleoyloxy)propyl]-*N,N,N*-trimethylammonium methyl sulfate (DOTAP, Figure 7) has been successfully applied to correct lung endothelial dysfunction via antisense oligodeoxynucleotide delivery in mice.[76] Huang have shown that the use of cholesterol-based cationic lipids feature reduced toxicity, allowing them to be the first cationic lipids entering clinical trials in humans.[77] The well-defined molecular structure of cationic lipids has allowed the rational fine-tuning of their self-assembling capabilities. As an illustrative case, Behr combined the enhanced nucleotide binding ability of polyamines within the cationic lipid framework in dioctadecylamido-glycylspermine (DOGS, Figure 7).[78] The improved gene transfer capability of DOGS was attributed to the enhanced DNA compaction and protection achieved by multipoint cationic lipid-nucleic acid interaction.[79]

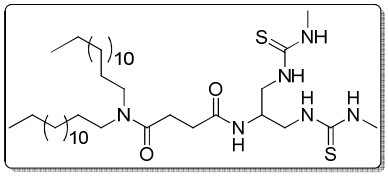

Figure 11. Example of a neutral lipopolythiourea described by Herscovici and Leblond.[80]

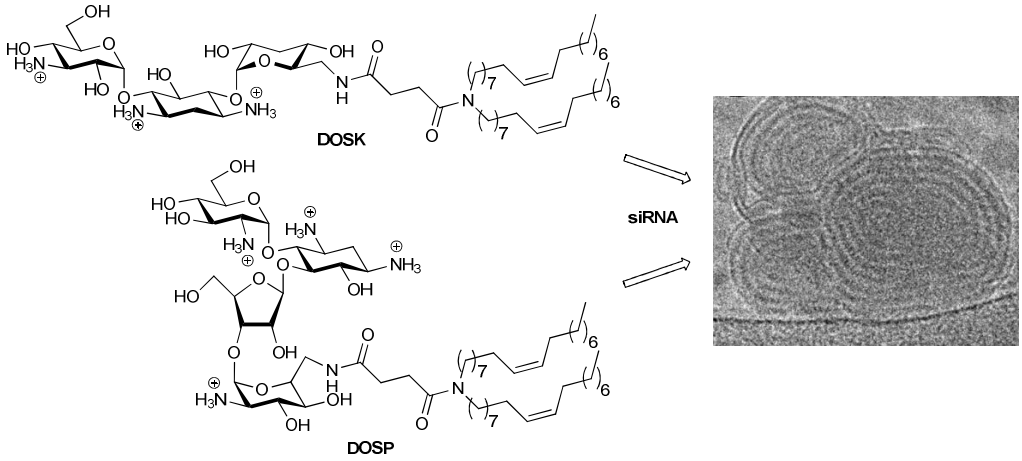

Figure 12. Structure of some lipidic aminoglycoside derivatives (dioleylsuccinyl kanamycin A, DOSK, and dioleylsuccinylparomomycin, DOSP) and a representative Cryo-TEM micrograph of their siRNA complexes (Reproduced from ref. 81b).

Other synthetic alternatives have been reported to modulate cationic lipid-nucleic acid condensation. For instance, though the vector-nucleic acid interaction in lipoplexes is essentially electrostatic, recently Herscovici and Leblond[80] have shown that neutral lipopolythioureas (Figure 11) may promote DNA condensation and compaction by cooperative phosphate-thiourea H-bonding and hydrophobic clustering. Probably due to their neutral character, these series of carriers exhibit remarkably low toxicity, though their gene transfer efficiency is comparatively lower than that reported for structurally related cationic lipids.[81] The diversity of cationic lipids architecture has been further extended exploiting nucleic acid binding epitopes such as complementary

oligonucleotides,[82] peptides[83] or carbohydrates.[81a] As illustrative example, Pitard and co-workers have designed a series of cationic lipids inspired in the structure of RNA-binding aminoglycosides (Figure 12), their lipoplexes exhibiting enhanced colloidal stability as compared with conventional cationic lipids. Remarkably, lipoplex particle features and performance could be related to lipid aminoglycoside structure and siRNA binding capabilities, finely illustrating the potential of rational design in nucleic acid delivery.[81b]

In a seminal contribution, Zuber and Behr designed a novel family of environmental sensitive non-viral vectors consisting undimerizable cationic lipids programmed to protect more efficiently the nucleic acid payload in the extracellular milieu while facilitating intracellular release (Figure 13). Once formulated with DNA, their thiolated lipids undergo air-mediated oxidation producing more stable lipoplexes. In the glutathione-rich intracellular environment, disulfide tethers are reduced, facilitating plasmid release.[84]

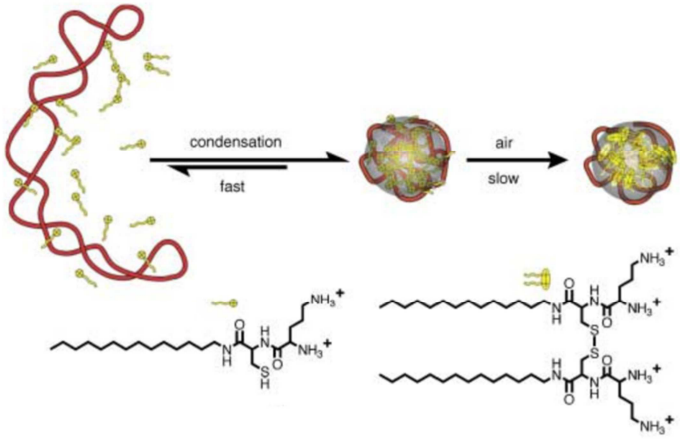

Figure 13. Dimerizable polycationic lipids reported by Zuber and co-workers.[84]

Cationic polymers, conversely, have been around much longer. Their nucleic acid binding capabilities were already noticed in the 70s',[85] but it was not until Behr reported the outstanding gene carrier features polyethyleneimine (PEI, Figure 8)[86] that their development was initiated. Upon formulation with nucleic acids, cationic polymers form positively charged complexes (*polyplexes*) by purely electrostatic interactions. Cationic

polymers are more easily manipulated as compared to cationic lipids, though their inherently polydisperse nature has consistently limited the thorough assessment of their SAR. They are generally regarded as more effective than cationic lipids, though their heavy charged structures are usually linked to higher cytotoxicity.[87]

Among a continuously growing catalog,[55] poly-L-lysine (PLL, Figure 8) was the first cationic polymer evaluated as non-viral gene carrier.[88] Despite its high DNA-binding avidity and excellent cellular uptake efficiency of the corresponding polyplexes, expression efficiency is limited due to the poor endosomal escaping capabilities.[89] Conversely, high molecular weight poly[2-(dimethylamino)ethyl methacrylate] (pDMAEMA, Figure 8) has shown excellent in vitro gene transfer capabilities,[90] probably associated to more efficient endosome escaping mechanisms, though in vivo performance resulted poor.[91]

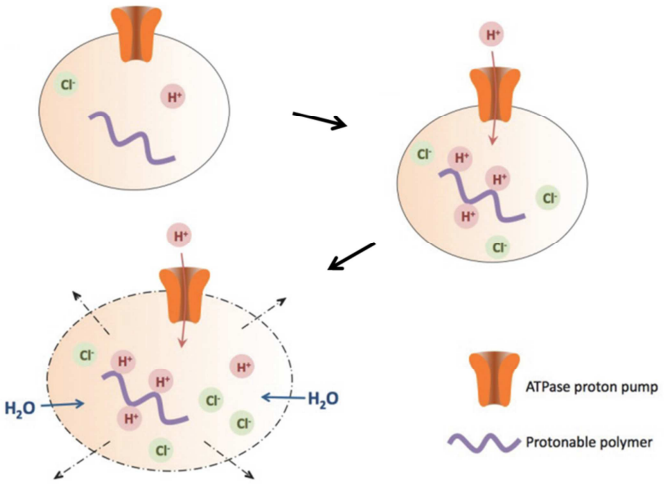

Figure 14. Illustration of the proposed mechanism for endosomal escape of cationic polymers by virtue of the proton sponge effect.[74]

Behr's PEI has considerably eclipsed the success achieved with other polymers.[86] Though the precise mechanism leading to this unparalleled efficiency still is a matter of debate, it is widely accepted that the PEI backbone should impart buffering capacity to

the polyplexes in the pH range between cytosolic (ca. 7.5) and endosomal (5.5) values. Upon endosome acidification, there is a significant increase of protonated amino groups in PEI. Such “proton sponge” effect[65] leads to endosome swelling and polyplex destabilization, thereby facilitating nucleic acid release (Figure 14). Its inherent efficacy as gene carrier, together with its architectural flexibility, allowing for a precise control of polymer size and dispersity and easiness for chemically introducing additional functionalities has pushed the commercialization of investigational vectors such as JetPEI or ExGen500.

A great deal of effort has been devoted to ameliorate its intrinsic toxicity by combining PEI and other cationic polymers with biocompatible elements (e.g. shielding from undesired interactions), while preserving its nucleic acid carrier capabilities. Evidently, the production, characterization and screening of each subtle structural modification is a limitation, but high throughput tools to speed up SAR analysis are being developed for both cationic lipids[92] and polymers.[93] Grafting polyethylene glycol chains[94] or cholesterol,[95] together with quaternarization of amino groups,[96] are among the most investigated PEI modifications.[55,94,97]

Biocompatibility and, eventually, biodegradability are precisely at the grounds of the incorporation of carbohydrates as constitutive elements in these and other type of cationic polymers, a topic that is discussed in the following section.

3. Glycotransporters in Gene Delivery

As above mentioned, most efforts in non-viral carrier development aimed at overcoming the physiological barriers to gene delivery while minimizing off-target interaction.[60b,98] Carbohydrates have proven particularly useful towards these goals. Similarly to PEG coating (pegylation),[70] glycocoating can sterically shield the positively charged surface of colloidal aggregates by improving solvation, thus preventing from non-specific interactions with intra- and extracellular components. Glycoconjugates can also be specifically recognized by cell membrane receptors and intracellular trafficking machineries, whose expression depends not only in cell type but also in cell developmental state.[99,100] Nature already offers many examples illustrating the potential of carbohydrate polymers as non-viral nucleic acid vectors, chitosan (Figure 15) being probably the most exhaustively investigated,[101] though many others have also demonstrated remarkable features themselves or after chemical manipulation.[102,103]

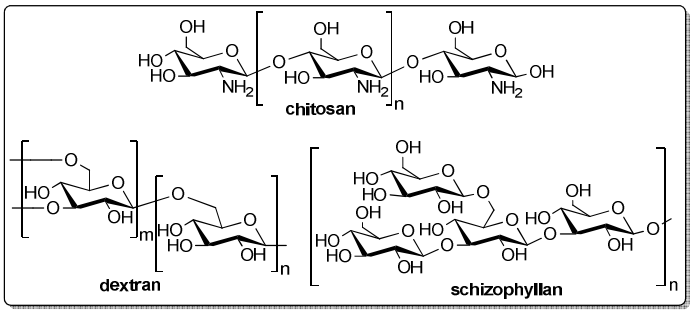

Figure 15. Naturally occurring carbohydrate polymers used as gene carriers.

Non-viral gene delivery has benefited from the large structural and functional diversity of carbohydrates, offering broad opportunities to interfere and manipulate gene transfer capabilities of first generation non-viral vectors. Moreover, the inherent flexibility of carbohydrate and glycoconjugate chemistry has enlarged the range of functional materials that can be conceived. Systematic studies on SAR of such synthetic materials

have shed light on the impact that carrier composition, hydrophobic/hydrophilic balance or charge and functional group distribution exert on nucleic acid transfer ability. This section will highlight the trending topics on the exploitation of the structural and functional features of carbohydrates in the design of non-viral gene delivery systems, focusing on two separate aspects: i) the effect of glycosylation in the performance of first generation non-viral gene vectors, and ii) the *de novo* design of carbohydrate-based cationic polymers as a tool to tailor nucleic acid shuttling capabilities. In a following section, the design of molecularly well-defined conjugates using pre-organized carbohydrate-based scaffolds (cyclodextrins, CDs) will be discussed as a mean to correlate molecular structure with gene transfer capabilities.

3.1. Carbohydrate-grafted cationic polymers and lipids

Despite their investigational utility, the functional features of most of first generation non-viral vectors resulted suboptimal. Cationic polymers, while structurally diverse (e.g. PEI, pDMAEMA, PLL, or dendrimers; see Figure 8), are usually restrained in terms of precise structural modification. The polymer molecular weight, dispersity or branching degree are known to determine their physicochemical properties and thereby, delivery efficiency or toxicity profiles.[90b,104] Improved polymerization technologies have rendered low polydisperse materials,[105] but finely tuning these parameters is very rarely sufficient to achieve clinically useful performances.[106] The situation with cationic lipids does not significantly differ. Decoration of these scaffolds with functional epitopes, such as carbohydrates, however, offers excellent opportunities to manipulate a number of features, including their nucleic acid condensation capability, biocompatibility, or extra- and intracellular trafficking of the carrier. The utility of this approach is demonstrated by the large array of glycosylated non-viral carriers reported to date and the diversity of synthetic strategies to prepare them.[107]

It has been shown that cationic polymer glycosylation may serve to modulate nucleic acid condensation and packing. For instance, Aigner and co-workers[108] have recently observed that covalent grafting of maltose onto PEI alter pDNA and siRNA condensation

thermodynamics and nanoparticle stability, consequently affecting a number of other features of the aggregates. On the other hand, Strand and co-workers have found that the kinetics of DNA complexation and release can be modulated re-engineering the glycosyl residues decorating chitosan backbone.[109] Interestingly, glycomodulation of nucleic acid-carrier interaction is not limited to cationic polymers. As above commented, Pitard and co-workers observed an enhanced colloidal stability of aminoglycoside-based cationic lipids (Figure 12) as compared with conventional ones. Remarkably, lipoplex particle features and performance could be related to lipid aminoglycoside structure and siRNA binding capabilities, finely illustrating the potential of rational design in nucleic acid delivery.[81]

Structural modification of a gene carrier does not only affect a single property, but simultaneously several features. Ascertain the precise effect of each structural change is, thus, complicated. For instance, oligomaltosylation of PEI did not only affect nucleic acid binding dynamics, but also render complexes that are largely unaffected by the presence of serum proteins, are far less toxic, and exploit different cell uptake mechanisms as compared to naked PEI.[108] A number of other polymeric scaffolds have been glycocoated in order to modulate their biocompatibility and bioavailability with gene delivery purposes. Carbon nanotubes,[110] gold nanoparticles,[111] quantum dots,[112] or (pseudo)rotaxanes[113] are some relevant examples that further provide peculiar functionalities to the gene carrier.

From the chronological point of view, carbohydrate specific recognition by biological receptors first attracted the attention. In fact, the first ever-reported evidence of specific non-viral gene delivery used a galactose-terminated PLL carrier targeted to the asialoglycoprotein receptors (ASGPr) on hepatocyte cell membrane.[114] The topic has received a sustained interest ever since. Galactose (or lactose) and mannose have been mostly exploited as glycoligands due to their hepatic and immune system cell targeting abilities, respectively. But also glucosamine, targeting vimentin,[115] and galactosamine[116] have been recently used. Glycotargeted versions of the most usual cationic polymers (including PEI,[117] PLL,[118] or PAMAM)[119] and lipids[120] have been described. The increase in gene expression when using glycoligands is associated to the improved receptor-mediated uptake of the carriers, but only to a certain extent. As above outlined, many

other features of nucleic acid-carrier interaction and nanoparticle pharmacodynamics can be altered upon glycosylation, which makes it difficult to quantify the precise role of the saccharide antennae. For instance, Behr and co-workers demonstrated that although the ASGPr is involved in the internalization of galactosylated PEI by hepatocytes, this is not sufficient to achieve specificity since other uptake mechanisms simultaneously operate (Scheme 1). Thus, relevant transfection levels were measured upon addition of ASGPr competing agents as well as in ASGPr-devoid cells.[117a] In other cases it was observed that even though the glycosylated carriers were recognized by the target receptors, endocytosis did not take place or, if it did, the resulting endosomes were unproductive.[121]

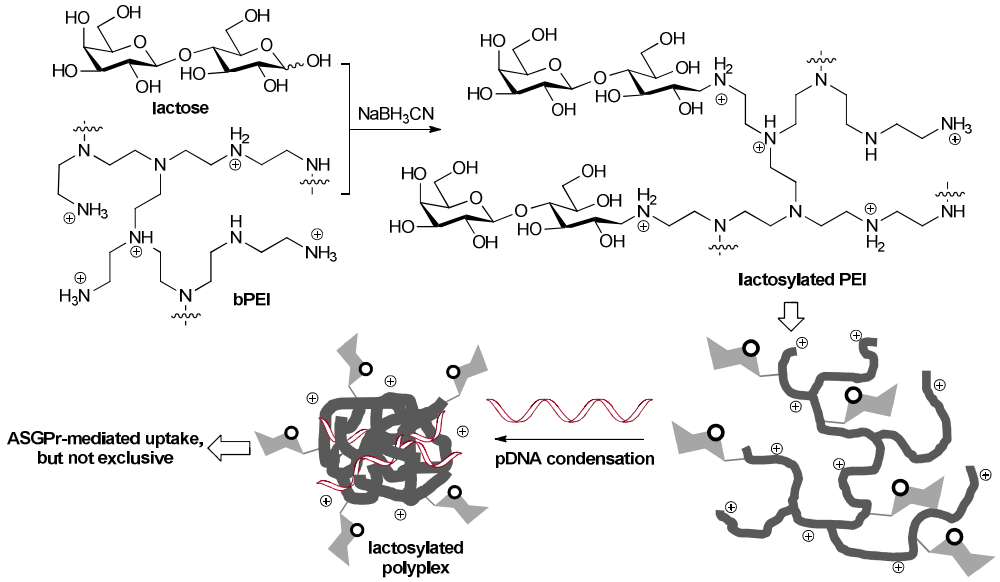

Scheme 1. Synthesis of lactosylated PEI via reductive amination and schematic representation of the condensation of lactosylated PEI with plasmid DNA into lactosylated polyplexes.

Glycoligands also exert a function in controlling the fate of the internalized nucleic acid-carrier nanocomplexes. Monsigny and co-workers showed that cytosolic and nuclear lectins might be involved in intracellular trafficking and nuclear import[122] and latter coined the term *glycofection* to refer to transfection strategies based on the glycomodulation of

intracellular barriers for gene delivery.[123] In a number of cases, lactosylated carriers appeared to induce faster escape from the late endosome/lysosome than other glycosylated counterparts and more efficiently mediated nuclear import.[124] Though these observations are still a matter of debate, recent publications by the same group[125] and others[126] highlight the potential benefits of controlling of intracellular trafficking as a prerequisite for efficient non-viral gene delivery.

3.2. *De novo* designed carbohydrate polymers

Efficiency and toxicity of polymeric vectors can be largely (and unexpectedly) affected by subtle structural changes, for example in counterion nature,[127] branching degree[128] or size,[129] which may lead even by batch-to-batch disparities. This undesired variability has been overcome to a large extent by the implementation of novel polymerization techniques, such as controlled polycondensation, radical polymerization and click chemistry reactions, which offer superior control over functional features.[130] Through the judicious choice of monomer structure and polymerization strategies a number of relevant parameters regarding gene delivery capabilities can be tailored. In this context, the *de novo* design of polymeric gene carriers from carbohydrate-derived building blocks has been very appealing, given the structural diversity and availability of simple saccharides. This section surveys a number of examples that illustrate the nucleic acid delivery capabilities of synthetic carbohydrate-based polymers.

One of the most representative examples of the potential of synthetic glycopolymers at tailoring non-viral gene vectors is the case of polyglycoamidoamines (PGAAs).[131] The first insight into the gene delivery capabilities of PGAAs were almost simultaneously reported by Reineke[132] and Guan[133] (Figure 16). In both cases the diversity, availability and biocompatibility of carbohydrates and their readily conversion to polymerizable building blocks was the main motivation. Reineke and co-workers focused on imitating the structure of linear PEI polymers by co-polymerizing their carbohydrate building blocks with a set of short oligoethyleneimine (OEI) chains. Guan's design aimed at mimicking

the structure of poly-L-lysine (PLL) by condensing carbohydrate bricks with lysine segments. Both studies revealed significantly reduced cytotoxicity of the resulting PGAAs as compared to PEI and PLL, respectively, while maintained comparable pDNA transfection efficiencies.

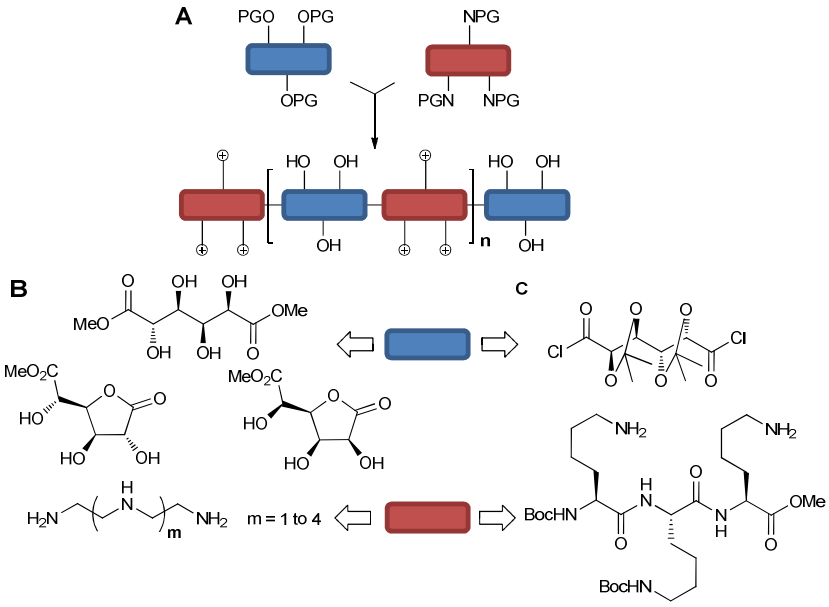

Figure 16. Schematic representation of the synthesis of polyglycoamidoamines (A) and building blocks used by Reineke's[132] (B) and Guan's[133] (C) groups.

Reineke and co-workers have thoroughly analyzed the influence of architectural issues of their PEI-inspired PGAAs on nucleic acid complexation, nanoparticle topology and stability, cell uptake, toxicity and gene expression efficiency.[134] By screening a library of cationic PGAAs, synthesized from a range of linear OEIs and esterified aldaric acid and lactone co-monomers (Figure 17), they identified vector candidates that mediated high gene expression levels in several cell lines (HeLa, H9c2(2-1), HepG2, or BHK-21). pDNA transfer efficiency peaked for the polymers containing the longer OEI chains tested.[135] Transfection efficiency compares favorably to that achieved with PEI, but with a less toxic profile. They hypothesized that the iterative interruption of OEI charge density

by carbohydrate blocks was at the origin of the reduced toxicity as compared to PEI, though their rapid hydrolysis in biological media might also account for this merit.[136]

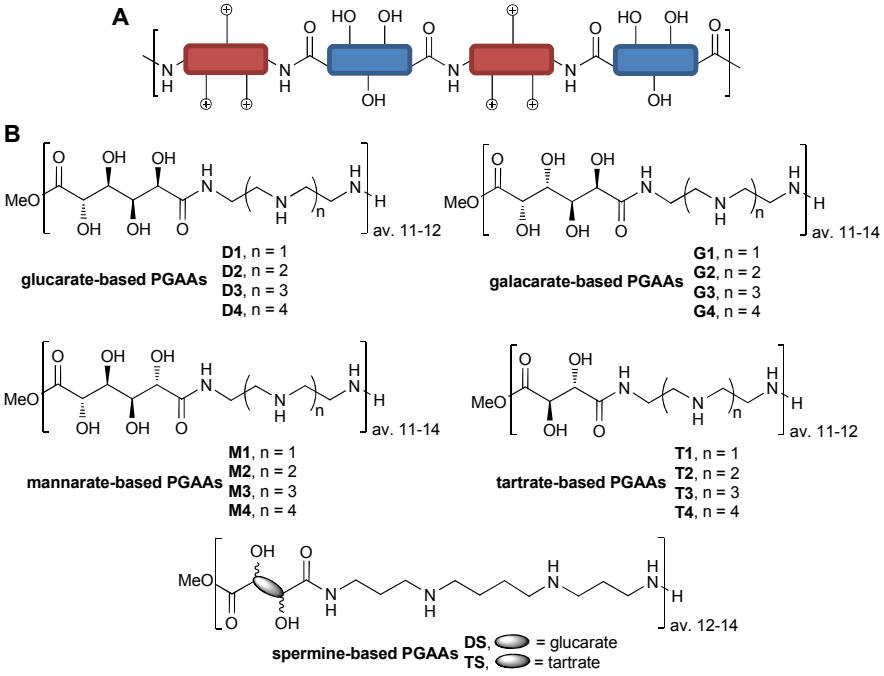

Figure 17. General structure of PGAAs studied by Reineke and co-workers (A) with indication of their structural diversity (B).

PGAAs with longer OEI segments did not significantly influenced cell uptake and overall transgene expression, but significantly improved polyplex stability in serum-containing media. Unfortunately, increased toxicity was also observed.[137] Polymers with longer inter-amine spacers (e.g. spermine) also exhibited increased toxicity, highlighting a critical relationship between charge density distribution and biocompatibility.[138] The nature of the saccharide segment, though modestly, also influenced polymer performance, apparently by altering the buffering capabilities of the system. Since the response of polyplexes at the increase of pH in the endosomes closely relates to the pDNA release dynamics, it should be expected certain folding differences upon pDNA-

PGAA complex formation. Overall, PGAA G4, combining pentaethylenehexaamine and galactarate segments (Figure 17), was identified as the best performing candidate. PGAA G4, shown to induce long lasting transgene expression (over 7 days) without appreciable cytotoxicity,[139] was recently licensed to Techulon to be commercialized as Glycofect^{TM}.[140]

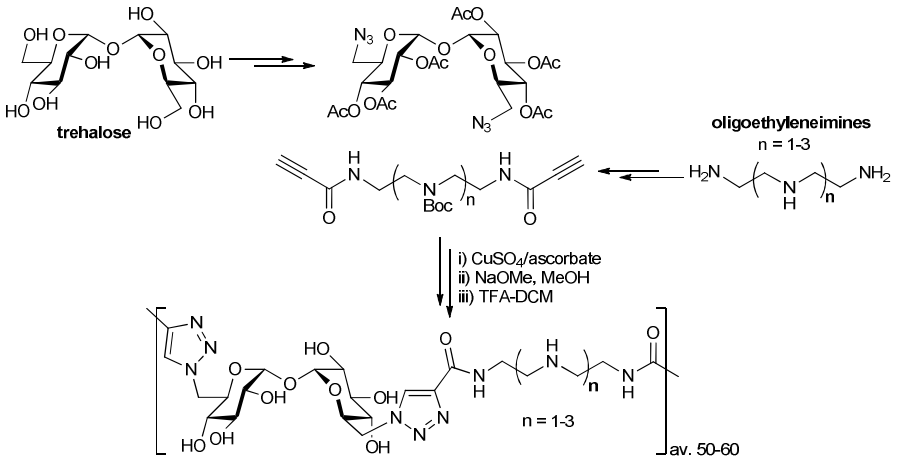

Scheme 2. Synthesis of trehalose-based cationic "click" polymers.[142]

Alternatively, carbohydrate-based cationic polymers with amidine[141] or triazole linking tethers[142] have also been explored. Though polyamidines usually exhibit severe cytotoxicity, Reineke and Davis observed that this could be overcome by intercalating saccharidic moieties (e.g. trehalose) between the cationic elements while maintaining the gene transfer capabilities.[141] The closer the amidine and the carbohydrate units are located in the polymer chain, the more efficiently the cytotoxicity is reduced. Trehalose, moreover, seems to impart additional favorable properties to polymeric gene vectors, such as shielding aggregation of the resulting polyplexes with proteins and lipids.[143] To fully benefit from this, Reineke and co-workers have devised a strategy to build a new family of cationic trehalose-embedding polymers that exploits the Cu(I)-catalyzed azide-alkyne cycloaddition (CuAAC) reaction.[144] By coupling diazido-functionalized trehalose units with a diverse set of α,ω-dipropargylated OEIs (Scheme 2), a series of polymers were obtained that allowed the systematic investigation of architectural effects (OEI size

and polymer length) on pDNA complexation, nanoparticle properties, cellular uptake and transgene expression. Transfection efficiencies that paralleled that of JetPEI-based polyplexes were achieved using trehalose “click” polymers with 3-4 ethylenediamine segments.[142a] Dynamic light scattering (DLS) revealed that polyplexes formulated with larger polymers exhibited the best tolerance to serum-containing media, but displayed higher toxicity.[142b] This unfavorable feature was alleviated by the fact that “click” polymers required far lower N/P ratios, as compared to PGAAs, to achieve similar gene expression levels.

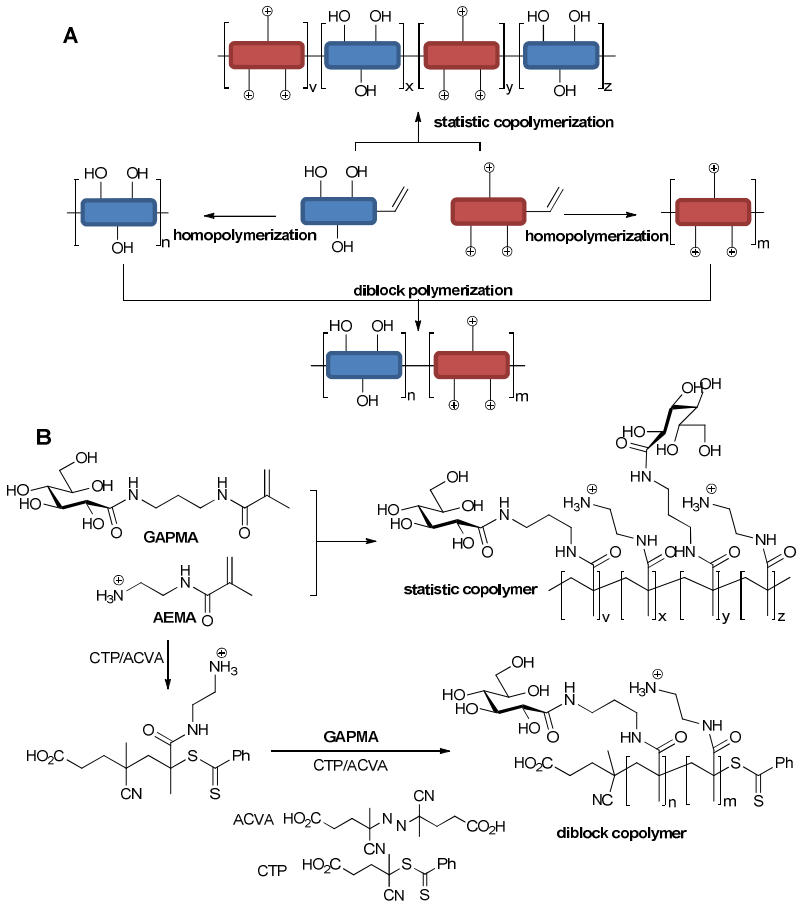

Scheme 3. Schematic synthesis of statistical vs. diblock copolymers (A) illustrated with the cationic glycopolymers synthesized by Ahmed and Narain (B).[146]

Ahmed and Narain have recently used radical addition-fragmentation chain transfer (RAFT) polymerization to synthesize a library of carbohydrate-pendant cationic polymers, where carbohydrate and cationic units can be either statistically distributed (random polymers) or segregated into separate blocks (diblock polymers, Scheme 3).[145]

Precise control on chain length, monomer ratio and polydispersity allowed the authors to rationalize the large influence that polymer architecture exerts on gene delivery capabilities. Statistical copolymers with high molecular weight produced superior gene expression with lower toxicity as compared to the corresponding diblock copolymers, both in the presence or absence of serum.[146] On the other hand, diblock copolymers resulted in nanoparticles that were shielded against non-specific interactions in a similar way of pegylated cationic polymers. However, current examples of diblock glycopolymers do not perform as other synthetic glycopolymers, the control over polymer structure open new opportunities in the field of non-viral gene delivery. Targeted delivery for instance, where non-specific interactions have to be shielded at the same time that specific uptake is promoted, might be one of those channels.

3.3. Cyclodextrins in gene delivery

The above evidences point to significant advantages of using non-viral carriers that include carbohydrates in their structure.[102] Indeed this is not just restricted to naturally occurring carbohydrate polymers or glycocoated cationic vectors. In the last decade, a growing awareness has been gathered on the remarkable features of cyclodextrins (CDs) for such purpose. First identified from bacterial digests of starch by Villiers[147] at the fall of 19th century and latter isolated by Schardinger during the first decades of the past century,[148] CDs largely remained as chemical curiosities for over half a century. By the mid-20th century, Freudenberg and co-workers unveiled their macrocyclic structure, composed of $\alpha(1\rightarrow4)$-linked glucopyranose units featuring a basket-shaped topology in which glucose hydroxyls orient to the outer space flanking the upper and lower rims, while methinic protons (H-5 and H-3) point to the inner cavity (Figure 18),[149] and reported

on their ability to form inclusion complexes with hydrophobic guests.[150] This observation represented a milestone that certainly switched the course of CD research history and steered it for the second half to the century. Indeed, the academic and (bio)technological interest for cyclodextrins has been dominated by this unique feature.[151]

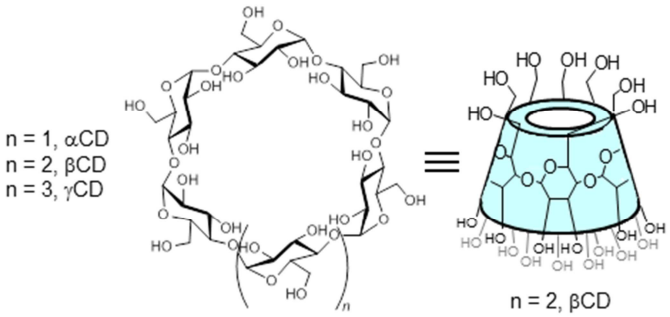

Figure 18. General structure of cyclodextrins (CDs).

CDs have long occupied a prominent position in most pharmaceutical laboratories as "off-the-shelve" tools to manipulate the pharmacokinetics and dynamics of a broad range of active principles (e.g. drugs).[152] But a body of evidence also indicates that CDs might be useful for formulation improvement on biomacromolecule delivery in general[153] and in gene therapy in particular.[1,154] In the following paragraphs, selected examples are described to illustrate the significant contribution of CDs to the field of non-viral-mediated gene therapy.

The potential of native CDs as transfection enhancers, ascribed at least in part to their ability to host cell membrane components such as cholesterol in their hydrophobic cavity, has been long known and exploited to improve the gene delivery capabilities of polycationic lipidic or polymeric non-viral vectors.[155] However, the major breakthrough in the field was reported by Davis and co-workers. They conceived a class of cationic polymers based on the controlled condensation of bifunctional CD monomers, such as bis-(C-6)-cysteaminylated βCD, and cationic co-monomers, in order to yield linear chains with alternating CD and cationic segments (CDP, A in Figure 19).[2,156] Electrostatically-

driven complexation of the resulting cationic CDPs and negatively charged pDNA (~5 kpb) rendered nanometric complexes (polyCDplexes; 100-150 nm) featuring in vitro cell transfection efficiency comparable to that obtained with PEI and Lipofectamine™, while preserving a reduced toxicity.

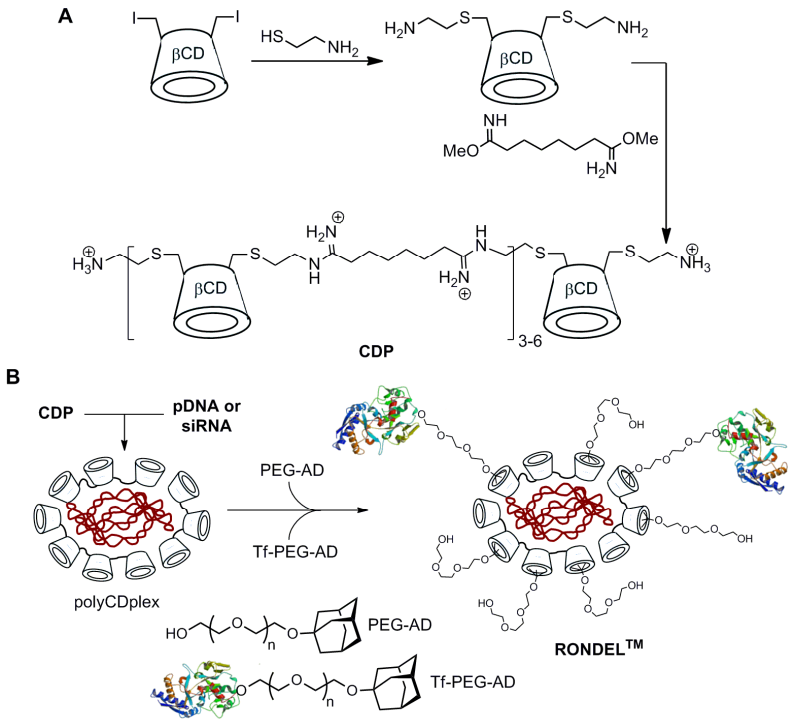

Figure 19. Schematic representation of the transferrin-targeted nucleic acid-CDP nanoparticles (RONDEL™) developed by Davis and co-workers.[2]

This milestone was followed by a series of reports in which the effect of structural modifications of CDPs on the gene delivery capabilities were investigated.[141,157] Most interestingly, supramolecular host-guest CD chemistry could be put forward to further decorate the nanoparticle surface. Thus, inclusion of the adamantane (AD) moiety of AD-PEG conjugates into CD cavities of polyCDplexes could prevent from non-specific

interactions with biological components[158] and also biorecognizable ligands could be installed at the distal end of these PEG chains to target the polyCDplexes to specific tissues (B in Figure 19).[159] Using transferrin (Tf) as the peripheral ligand, whose receptor is known to be up-regulated in malignant cells, the resulting polyCDplexes were shown to selectively target and efficiently transfect different tumor tissues in vivo in mammals (murine[160] and primates).[161] This tripartite therapeutic concept (CDP as nucleic acid complexing element/ AD-PEG as surface shielding element / AD-PEG-Tf as targeting ligand) is named RONDEL™. In June 2008, CALAA-01 (Arrowhead Research), a version of RONDEL™ loaded with a specific oligonucleotide sequence (siRNA) that inhibits tumor growth via RNA interference (RNAi), entered phase I clinical trials to determine its safety and efficacy towards solid tumors refractory to standard-of-cure therapies.[162]

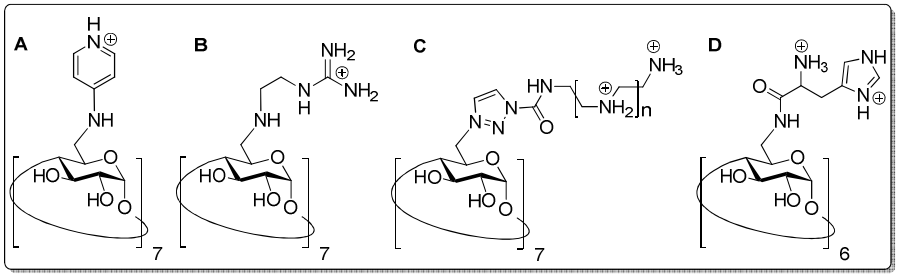

Figure 20. Examples of molecularly well-defined non-amphiphilic polycationic CDs assayed as gene vectors.

At the light of these thrilling results, research on polycationic polymeric gene vectors incorporating CDs has flourished, including linear,[163] dendritic,[119,121a,164] star-shaped,[165] or rotaxanized structures.[166] However, despite a significant success, the above systems still suffer from the inconveniences associated to polydispersity. Alternatively, attempts to overcome this limitation were made designing monodisperse polycationic clusters taking advantage of the molecular scaffolding capabilities of CDs. Using strategies for the selective chemical manipulation of CD topology, O'Driscoll and Darcy reported the first examples of monodisperse cyclodextrin-centered polycationic clusters intended for DNA complexation (A in Figure 20)[167] and demonstrated their ability to promote transfection in

vitro. Their work inspired other architectural proposals to enhance nucleic acid binding (e.g. guanidinylated,[168] oligoethyleneimine-grafted,[169] and histidine/lysine-decorated[170] CDs, B, C and D in Figure 20, respectively). The highly hydrophilic character of these materials does not help self-organization of the monomers at the surface of the oligonucleotide chain, however. Consequently, relatively large excesses are necessary to achieve full protection from the environment. Notwithstanding, some of the resulting CD-nucleic acid complexes (CDplexes) exhibited remarkable transfection capabilities.

The above examples illustrate the suitability of CDs as molecular platforms for the incorporation of cationic elements with a precise spatial orientation and the potential of the resulting monodisperse polycations as gene vectors. Most interestingly, the rim anisotropy of the basket-shaped CD structure further allows accessing compounds with segregated cationic and lipophilic domains for which, according to the "facial amphiphilicity" concept,[171] biomimetic self-assembly and gene delivery properties could be expected. Darcy and co-workers first tested this hypothesis by preparing heterogeneous βCD derivatives bearing thioalkyl chains at the primary rim and amine-terminated oligoethylene branches of variable lengths at the secondary hydroxyl positions (A in Figure 21). The resulting polycationic amphiphilic CDs (paCDs) were shown to entrap pDNA by forming CDplexes that transfected COS-7 and human hepatocellular liver carcinoma (HepG2) cells with efficiencies and toxicity profiles comparable to Lipofectamine 2000™-based lipoplexes.[172]

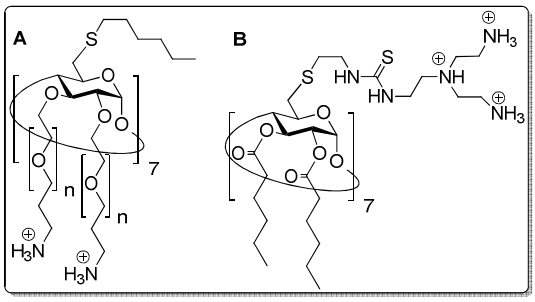

Figure 21. Examples of amphiphilic polycationic CDs assayed as gene vectors.

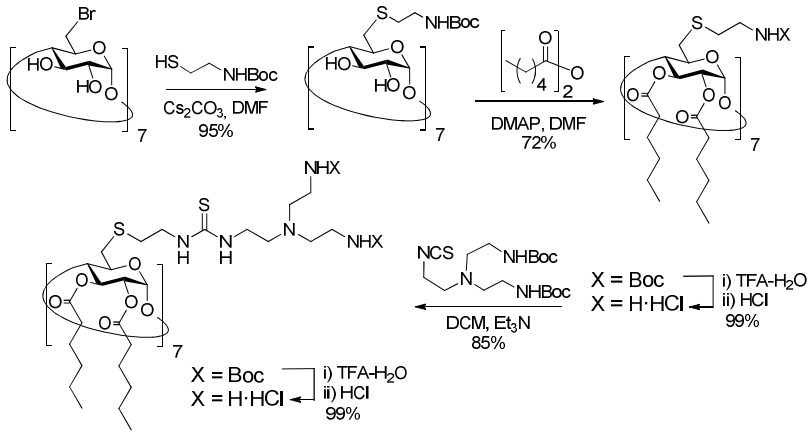

Scheme 4. Illustrative example of the synthesis of 2-aminoethylthioureido paCDs.

A dual face modification methodology has been refined in our laboratory to furnish truly monodisperse polycationic amphiphilic CDs (paCDs, B in Figure 21).[173] The synthetic strategy is based on the sequential installation of a cationic cluster on the primary rim of a CD scaffold and acylation of the secondary rim hydroxyls.[174] The sequence starts with the displacement of the halides in the heptakis(6-bromo-6-deoxy)cyclomaltoheptaose[175] by *N*-Boc protected cysteamine. Then homogeneous acylation of the secondary hydroxyls can be achieved by reaction with hexanoic anhydride in DMF using DMAP as base promoter (Scheme 4). Final acid hydrolysis of the carbamate groups afforded in excellent yield the first member of the paCD family, already featuring self-assembling capabilities in the presence of pDNA but poor gene transfer performance (e.g. 100-fold lower as compared to bPEI in BNL-CL2 cells).[174] Interestingly, the reaction of Boc-protected 2-aminoethyl isothiocyanates with this 1st generation paCD, followed by acid promoted carbamate cleavage, furnished βCD derivatives incorporating a belt of 2-aminoethylthiourea groups that behave as much more efficient phosphate anion binding epitopes.[176] The biological results indicated a significant increase in the transfection efficiency for polyaminothiourea paCD as compared with polyamine counterpart, paralleling that for polyplexes formulated with PEI at its optimal N/P 10 ratio.[174] CDplexes based on paCDs have been shown to be broad range delivery agents,

affording high transgene expression efficiencies in a most cell lines investigated and often surpassing that of PEI and Lipofectamine™. Moreover, transfection efficiency was not affected in serum-containing media, an important requisite for in vivo applications.

These facial amphiphiles efficiently condensed pDNA into stable nanocomplexes (CDplexes) of 40-50 nm diameter with very narrow polydispersity.[177] pDNA complexation is assumed to take place though a two-steps process involving, first, an electrostatic driven-interaction between the anionic polyphosphate chain and the cationic amphiphile and, then, a hydrophobic-driven compactation (Figure 22), a mechanism that is reminiscent of that operating in viral particle assembly.

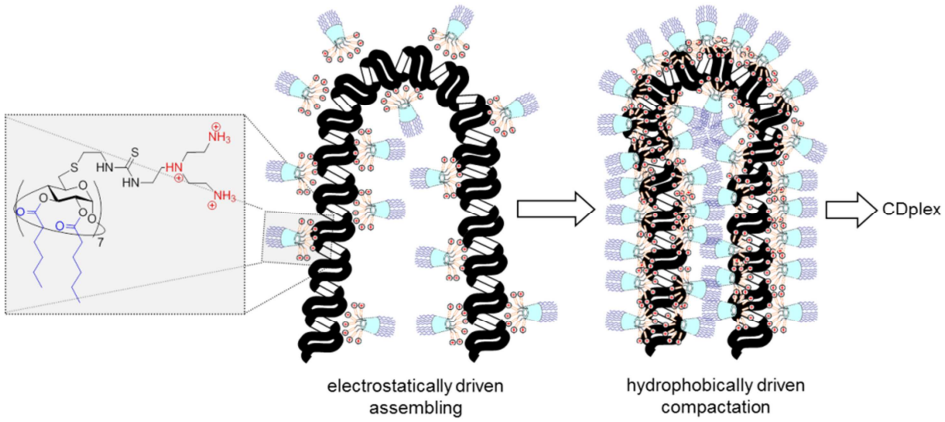

Figure 22. Schematic illustration of the proposed two-step mechanism for CDplex formation between paCDs and pDNA.

The flexibility of this synthetic methodology allowed a thorough assessment of how architectural parameters such as cationic density and display,[177,178] CD scaffold size[179] or the type of functional group tethering the cationic cluster to the CD core[180] exert on self-assembling and gene transfer capabilities both, in vitro and in vivo,[181] and the mechanisms involved in the cellular uptake of these nanoparticles (CDplexes).[182]

Most interestingly, this flexibility could be further exploited to modulate the gene transfer “promiscuity” of CDplexes. Recently, glycosylated versions of paCDs (pGaCDs) have been developed for targeting purposes.[183] The artificial glycocalyx-like surface

generated after glycoCDplex assembly can be recognized by complementary cell membrane receptors and/or intracellular trafficking machineries. As a proof of concept, an homogeneously mannosylated candidate was shown to selectively transfect MMR-positive cells (RAW264.7 macrophages) via MMR-dependent route, exhibiting very low transfection efficiency towards cell lines devoid of mannose receptors such as BNL-CL2 and COS-7 as compared to non-glycosylated CDplexes.[183a] The strategy has been also validated for the transfection of hepatocytes with galactosylated pGaCDs via specific recognition of the corresponding glyco-CDplexes by the asialoglycoprotein receptor (ASGPr).[183b]

The above ensemble of data highlights the advantages a flexible synthetic strategy leading to homogeneous gene carriers to facilitate the manipulation and optimization of their nucleic acid delivery capabilities. Most interestingly, the incorporation of additional functional elements can be undertaken at the vector or at the CDplex level, after nucleic acid complexation. Covalent as well as supramolecular ligation chemistries can be conceived in order to tailor the properties of the transfectious nanoparticles for a particular application. Unfortunately, these features are not as common it would be desired in the field of non-viral gene delivery. In most of cases, massive efforts in development of non-viral carriers yield minimal insight into the structure–function relationship of delivery agents that is relevant to adapt investigational designs to particular challenges.

Many early studies on gene delivery focused on developing tight associations of the delivery vehicle with nucleic acids such that nuclease resistance was imparted. However, such studies ignored the fact that these delivery systems needed to be capable of disassembly within the cell; an issue that still receives insufficient attention. In this Ph.D. Thesis, we would like to further exploit the competitive advantages of paCDs to gain a deeper insight into their SAR in this particular topic.

4. Objectives

Serving as a general frame, the first chapter of this Ph.D. Thesis aims to give an overview of the state of the art in non-viral gene delivery, focusing on carbohydrate-based carriers and, more particularly, on those designs based on cyclodextrins. Then, the influence of the hydrophilic/hydrophobic balance of paCDs on self-assembling, DNA-condensing and gene delivery capabilities of paCDs is investigated in the second chapter of this Ph.D. Thesis pursuing the following objectives:

- the synthesis of a series of monodisperse polycationic amphiphilic CD derivatives (paCDs) differing in their hydrophobic/hydrophilic balance,
- the investigation of their self-assembling capabilities in aqueous environment,
- the determination of pK_a values and pH buffering capabilities of CD-scaffolded polycations,
- the assessment of DNA-paCD complex (CDplex) formation and dissociation,
- and the evaluation of CDplex gene transfer capabilities towards COS-7 cells.

On the other hand, the third chapter of this Ph.D. Thesis is aimed at rationalizing the influence of the arrangement of the cationic cluster of paCDs on self-assembling and gene delivery capabilities For such purpose, in this chapter a novel series of paCDs grafted with cyclic polyamine clusters were elaborated pursuing the following goals:

- the investigation of their self-assembling capabilities in aqueous environment,
- the evaluation of their pH buffering capabilities,
- the assessment of their DNA-condensing abilities,
- and the evaluation of the gene transfer capabilities towards HeLa cells of the resulting paCD-DNA CDplexes.

Finally, despite the usefulness of CDs for engineering gene carriers, only a handful of synthetic methodologies are available for selective chemical manipulation in the CD framework. Regarding the design of CD-based gene carriers, complementing the array of regioselective functionalization strategies with methodologies facilitating installation of additional bioactive elements on the CD core would be highly desirable. Thus, in the last chapter of this Ph.D. Thesis a novel solid phase-assisted synthetic strategy towards selective functionalization of multivalent scaffolds is disclosed. Herein, implementation of the "*catch-and-release*" concept using a solid supported reagent is aimed at furnishing an array of regioselectively monofunctionalized CD derivatives in one pot.

CHAPTER 2 - INFLUENCE OF THE HYDROPHILIC/HYDROPHOBIC BALANCE ON SELF-ASSEMBLING, DNA-CONDENSING AND GENE DELIVERY CAPABILITIES OF POLYCATIONIC AMPHIPHILIC CDS (PACDS)

1. Structure-activity relationships in the rational design of novel gene carriers

A prerequisite to better understanding and consequently improving transfection efficiency of non-viral gene delivery systems is to get a deeper insight into how nucleic acid-carrier interactions and assemblies are established, the cell uptake, endosomal escaping and intracellular trafficking mechanisms involved in the process. Hence, elucidation of structure-activity relationships (SARs) is a crucial parameter for the rational design of efficient novel gene carriers.

Structure-activity correlations for DNA carrier systems are difficult to establish due to intricate cellular events involved in the multistep transfection process. Generally, there is a great difference between in vitro and in vivo experiments. Furthermore, different cell lines behave very differently when subjected to the same series of transfection experiments with a certain vector. Another difficulty is derived from the essentially polydisperse nature of many of the most prominent non-viral gene carriers, which considerably hampers inferring structure–activity links. Although there are exceptional cases, such as CD-based polymers described by Davis,2 this is a problem that breaks down many promising designs. To overcome these drawbacks, monodisperse multifunctional molecular vectors have emerged as a new generation of gene delivery systems. Chemical tailoring and systematic structural modification facilitate a deeper insight into their structure-activity relationship.

As illustrated in the preceding chapter, preorganized macrocyclic structures such as CDs could be very helpful for this task, since they can be furnished with functional elements endowing them with self-assembling capabilities in the presence of nucleic acids. In our laboratories, we have succeeded to produce a series of amphiphilic CDs to investigate the role of structural features such as architectural design (skirt[174,180b] vs. jellyfish like),[178] CD scaffold size,[179] density and display of the cationic cluster,[177] type and length of the connecting tethers (Figure 23),[180a] and the presence of selective targeting

elements[183] on their self-assembling, cellular uptake,[182] and transgene expressing capabilities have been assessed in vitro and in vivo.[181]

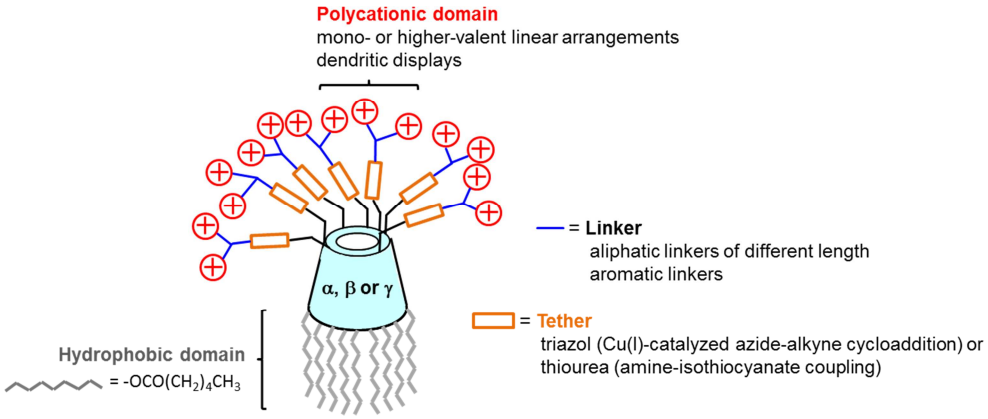

Figure 23. paCDs under investigation in SAR studies with indication of the modified structural elements.

SAR analysis on these families taught that the “skirt”-type arrangement in combination with multiple aminoethylthiourea segments presented advantages in terms of synthetic straightforwardness and architectural flexibility, and moreover, resulted in improved gene transfer efficiencies.

However, there remain a number of questions to be addressed, in special those regarding the influence of paCD structure on CDplex formation and dissociation. Towards this goal, in this Ph.D. Thesis a series of monodisperse paCDs with a precise arrangement of functional elements are prepared and used to insight on how their structural features determine their physicochemical properties and, ultimately, whether these features can be related to their DNA delivery capabilities. In particular, this chapter comprises:

- the synthesis of library of paCDs featuring subtle differences in their hydrophilic/hydrophobic balance,
- the assessment of self-assembling capabilities in aqueous environment by means of critical aggregation concentration measurements,

- the determination of pH buffering capabilities of paCD aggregates,
- the assessment of DNA-paCD complex (CDplex) formation and dissociation dynamics,
- and the determination of their pDNA delivery capabilities towards COS-7 cells.

2. Synthesis of paCDs differing in their hydrophilic/hydrophobic balance

Exploiting in-house-developed synthetic methodologies, a semi-convergent, modular strategy towards C_7-symmetric βCD derivatives differing in their hydrophobic/hydrophilic balance has been implemented for the preparation of two sub-collections of paCDs, namely (i) the linear heptacationic family and (ii) the branched 21-cationic subset, respectively, each of them containing members differing in secondary rim acyl chain lengths (Figure 24).

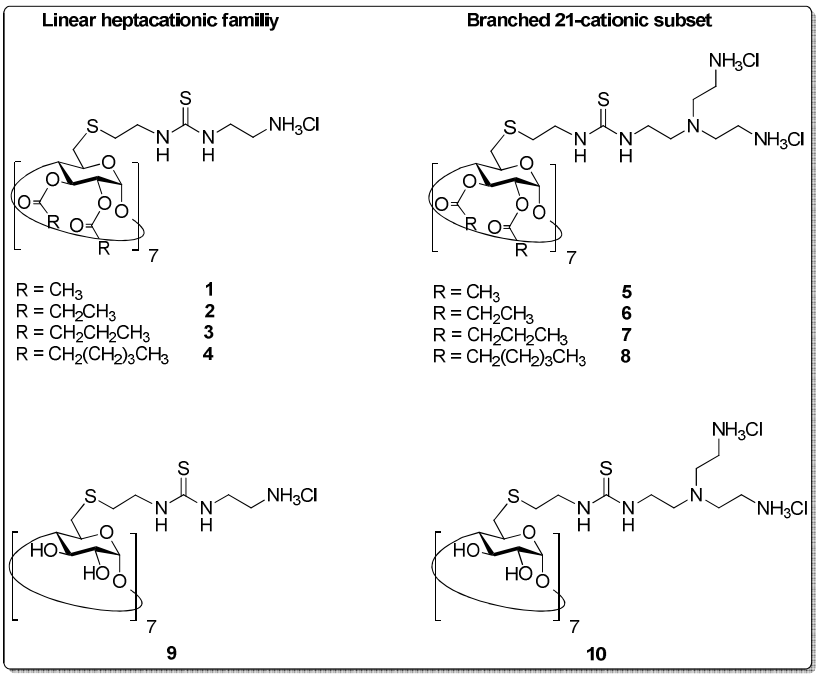

Figure 24. Structure of polycationic CD library members.

The first part of the synthetic pathway comprised the incorporation of a cysteaminyl segment into the primary βCD face and acylation of the fourteen secondary hydroxyl

groups by employing different acid anhydrides as reagents. In principle, two alternative routes can be presented, differing in the order of functionalization of the two βCD faces (Scheme 5). Although both can provide polycationic amphiphilic paCDs **18**-**21** in only four steps from commercial βCD, they differ significantly in their performance and efficiency.

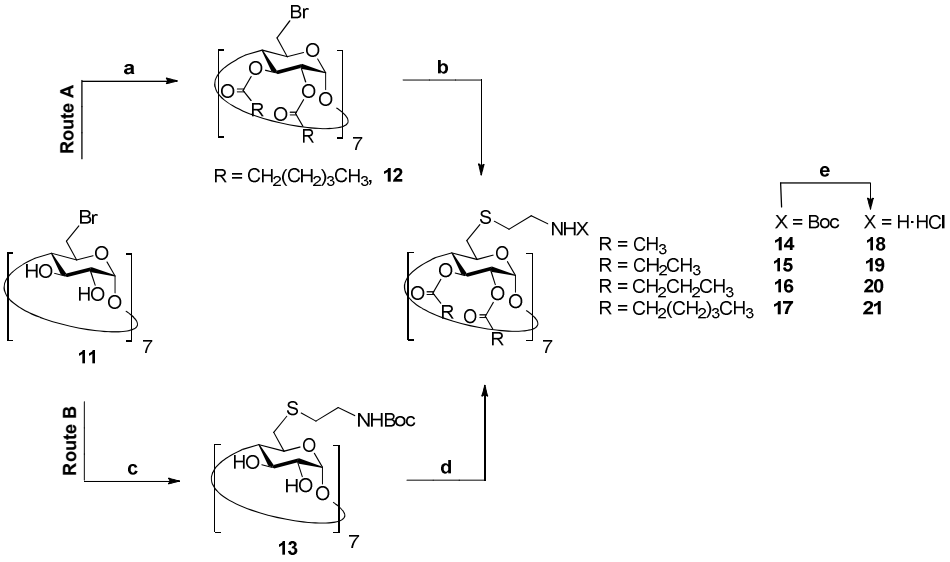

Scheme 5. Synthesis of compounds **18**-**21** (1st generation paCDs). Reagents and conditions: a) hexanoic anhydride, DMAP, Py, 16 h, 72%; b) $BocHN(CH_2)_2SH$, Cs_2CO_3, DMF, 60 ºC, 48 h, 70%; c) $BocHN(CH_2)_2SH$, Cs_2CO_3, DMF, 60 ºC, 48 h, 99%; d) 1:1 Ac_2O-Py, rt, 15 h (for R = CH_3),80%; propionic anhydride (for R = CH_2CH_3), butanoic anhydride (for R = $CH_2CH_2CH_3$), or hexanoic anhydride (for R = $(CH_2)_4CH_3$), DMAP, DMF, 70 ºC, 24 h, 73-78%; c) e) i, 1:1 TFA-DCM, 2 h; ii, HCl, 99%.

The synthesis of CD derivative **21** was explored using both synthetic pathways. Starting from heptakis(6-bromo-6-deoxy)cyclomaltoheptaose **11**, obtained from commercial βCD according to the procedure described by Defaye,[175,184] acylation of the secondary hydroxyl groups using hexanoic anhydride and DMAP was accomplished. When DMF was used as solvent for the acylation the reaction proceeded slowly. Increasing the temperature, in turn, led to concomitant nucleophilic substitution of the

halide at C-6. This drawback could be overcome by using pyridine instead, which allowed for a complete acylation of secondary hydroxyl groups without formation of side products (Scheme 5, route A). Subsequent functionalization of the primary face by nucleophilic substitution of halides with *N*-Boc-protected cysteamine in presence of cesium carbonate was achieved in good yield, although requiring purification by silica gel column chromatography.

On the other hand, compound **21** could also be obtained by reversing the order of functionalization of the two CD faces (Scheme 5, route B). Nucleophilic substitution of the halide on the primary face of **11** by *N*-Boc-protected cysteamine was carried out to yield derivative **13** in virtually quantitative yield. Subsequent acylation of the secondary hydroxyl groups in the presence of DMAP was accomplished in DMF to smoothly furnish **17** in 73% yield. This alternative synthetic route presents considerable advantages, since it reveals a more convergent character and requires only a single chromatographic purification step, i.e. after acylation of secondary hydroxyl groups. Together with its better overall performance these factors clearly privilege this synthetic pathway. Consequently, CD derivatives **18**-**20** were prepared exclusively by this route.

Under these reactions conditions using the corresponding acid anhydrides, i.e. propanoic anhydride (→**15**, 73%) or butanoic anhydride (→**16**, 78%), the formation of side products ascribed to over-acylation by the reaction of the acylating agent with carbamic nitrogen atoms was not observed in any case. Acetyls were introduced using standard conditions (1:1 mixture of Ac_2O-Py). After purification by silica gel column chromatography, homogeneity of all acylated CD derivatives was confirmed by NMR, ESI-MS and combustion analysis (see Figures S1-S4 for NMR spectra and Figures S81-S84 for MS spectra, Supporting Information). Finally, acid hydrolysis of the carbamate groups by treatment with 1:1 TFA-DCM led to paCDs **18**-**21** in quantitative yield.

The reason for choosing a 2-aminoethanothiol (cysteamine) segment to link the CD core with the cationic moieties is not trivial. Previous results of our research group have shown that the nucleophilicity of the amino group in βCD derivatives is significantly increased after insertion of the 3-atom (SCH_2CH_2) spacer in between the nitrogen atom and the CD core,[185] which in turn should facilitate interactions with phosphate anions in

the nucleic acid backbone. Moreover, distancing the amino groups from the CD core reduces steric hindrance that may limit reactivity with bulky electrophiles.

Previous insights into paCD SAR led to the identification of the 2-aminoethylthiourea segment as a privileged phosphate-binding motif.[177] This structural element has been preserved in the architectural diversification of paCDs **18**-**21**. Thus, two isothiocyanate synthons (**22**[186] and **23**,[177] Figure 25) have been coupled to each CD derivative (**18**-**21**) to furnish the linear or branched paCD subsets, respectively.

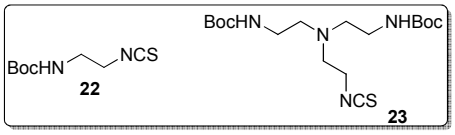

Figure 25. Isothiocyanate synthons used for the elaboration of the paCD collection.

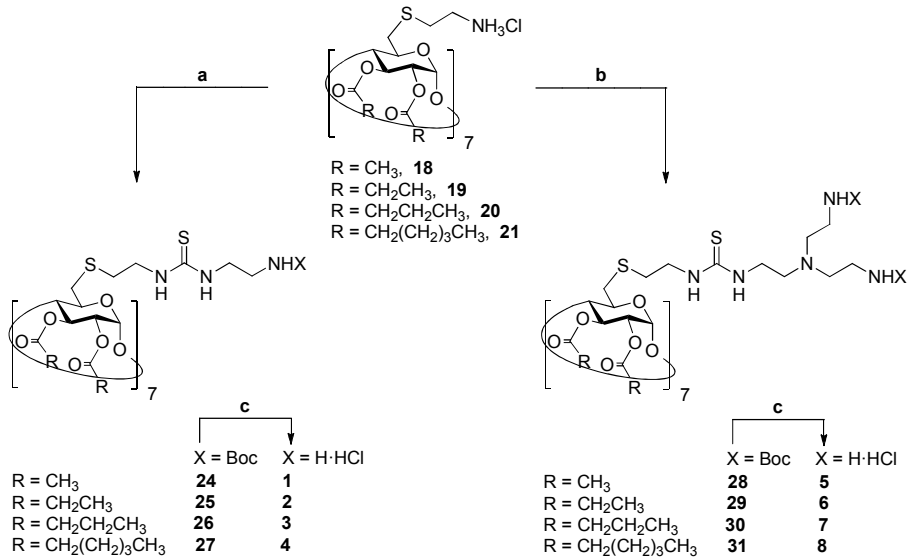

Scheme 6. Synthesis of thioureido paCDs **1**-**8**. Reagents and conditions: a) **22**, Et_3N, DCM, 15 h, 75-94%; b) **23**, Et_3N, DCM, 20 h, 62-95%; c) i, anh. TFA, 5 min; ii, HCl, 99%.

As shown in Scheme 6, Et_3N-catalyzed coupling of isothiocyanates **22** and **23** to polyamino compounds **18**-**21** in DCM led to the corresponding *N*-Boc protected linear poly(aminoethylthioureido) CD derivatives (→**24**, 94%; →**25**, 75%; →**26**, 84% and →**27**, 81%) as well as to their respective branched analogs (→**28**, 95%; →**29**, 62%; →**30**, 74% and →**31**, 71%), respectively. In all cases the thiourea formation reaction was completed in a relatively short time (2 to 3 h), as evidenced by TLC and ESI-MS (see Figures S89-S96 for MS spectra, Supporting Information) of the reaction mixture, provided pH was maintained at 8-9. The formation of products from isothiocyanate self-condensation, typically associated with long reaction times or elevated temperatures, was not observed.[187] All *N*-Boc protected products were purified by conventional silica gel column chromatography and were obtained in remarkable final yields (62-95%) keeping in mind that coupling reactions should take place at seven positions simultaneously.

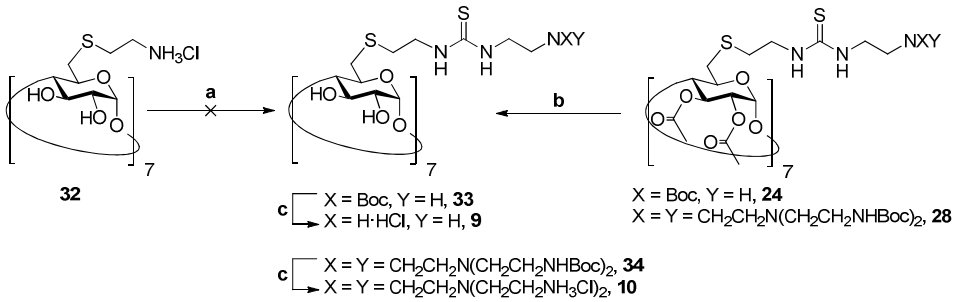

Scheme 7. Synthesis of polycationic thioureido CDs **9** and **10**. Reagents and conditions: a) **22** (→**33**), **23** (→**34**), 1:1 Py-H_2O, 24 h; b) **24** (→**33**), **28** (→**34**), NaOMe, MeOH, 14 h, 98% (→**33**), 97% (→**34**); c) i, anh. TFA, 5 min; ii, HCl, quantitative yield in both cases.

In addition to this set of compounds, the non-amphiphilic CD analogs (lacking the secondary rim acyl chains) have been synthesized. In principle, chemoselectivity of the thiourea formation reaction should allow performing the coupling without the need of protecting the secondary hydroxyls, as previously described. However, when CD derivative **32**[185a] was coupled to the isothiocyanates **22** and **23**, products resulting from partial addition precipitated from the reaction mixture, thus preventing reaction

completion. Alternatively, advantage was taken of CD derivative **24** prepared previously, which exhibits acetyl protected hydroxyl groups on the secondary face of the CD core and hence organic solvent solubility (Scheme 7). Zemplén transesterification of the acetyls gave *N*-Boc protected CD derivative **33** in excellent yield (98%). The synthesis of the corresponding branched polythioureido CD derivative **34** was performed in an analogous manner, as shown in Scheme 7.

Although all other synthetic steps to obtain the collection of linear and branched polycationic amphiphilic CDs as well as their two analogs without acyl chains on the secondary face furnished the target compounds with remarkable yields and purities, final acidic hydrolysis of the carbamate protecting groups of compounds **24**-**31**, **33** and **34** proved to be a delicate operation. In particular, two aspects have to be considered in order to prevent side reactions during acid-promoted cleavage of carbamate protecting groups. On one hand, glycosidic linkages of the βCD core are sensitive to harsh acid-promoted hydrolysis and may therefore be partially cleaved upon prolonged acidic treatment, leading to a mixture of ring opening and transglycosylation products. While CD derivatives equipped with long fatty acid ester chains seems to be unaffected, probably due to steric inaccessibility to the glycosidic bond, minimizing the reaction time is critical to obtain a homogenous products with shorter or none-acyl chains.[188] On the other hand, ester hydrolysis may take place under acidic conditions. In this regard, long fatty acid chains seem to be invulnerable, probably due to either steric crowding or the decreased rate of hydrolysis associated to longer acyl chains.[189] In any case, it was hypothesized that using anhydrous conditions in shorter reaction times should diminish the rate of hydrolysis to tolerable levels. In a first attempt, hexanoylated compounds **27** and **31** were submitted to standard Boc cleavage conditions (i.e. treatment with 1:1 DCM-TFA at rt for two hours, followed by solvent evaporation and freeze-drying from 0.1 N HCl). CDs bearing long acyl chains resisted these acid-promoted Boc cleavage conditions, as evidenced by the preserved symmetry and homogeneity of the reaction products.

However, Boc group removal in compounds furnished with shorter acyl chains revealed a completely distinct scenario. For example, a similar treatment of propanoylated CD derivative **25** furnished a heterogeneous product. As revealed by ESI-

MS, carbamate groups were completely removed, and the origin of heterogeneity was attributed to partial hydrolysis of ester chains (Figure 26). The repetitive spacing of 56 mass units between adjacent mass peaks clearly indicated the partial cleavage of propanoyl esters. However, no products derived from glycosidic bond cleavage were detected.

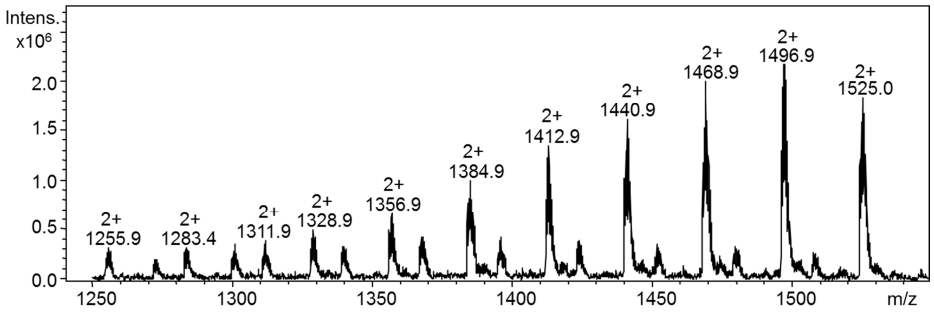

Figure 26. ESI-MS spectrum evidencing partial ester hydrolysis of compound **25** when treated with 1:1 TFA-DCM at rt for 1.5 h.

It is noteworthy that CD derivatives with butanoyl chains experienced ester hydrolysis far more slowly than their propanoyl analogs, highlighting the substantial influence of an additional carbon atom in the acyl chain.

Softening reaction conditions (i.e. lower acid proportions and shorter reaction times) did not improve the reaction outcome. Neither the use of diluted hydrochloric acid in water nor dioxane furnished homogeneous products, though results could be slightly improved.

Conversely, deprotection of amine groups under anhydrous conditions (i.e. neat anhydrous TFA at rt for 5 min, immediately followed by reaction mixture freeze-drying with a minimum amount of water) turned to be successful, as carbamate protection groups were completely removed, whereas esters (including acetyls) remained intact. Homogeneity was confirmed by ESI-MS, as depicted exemplarily for paCD **2** in Figure 27 (see Figures S97-S104 for MS spectra, Supporting Information). To facilitate handling and to provide greater stability, the crude paCD derivatives were converted into their

respective hydrochloride salts by freeze-drying them from a diluted hydrochloric acid solution.

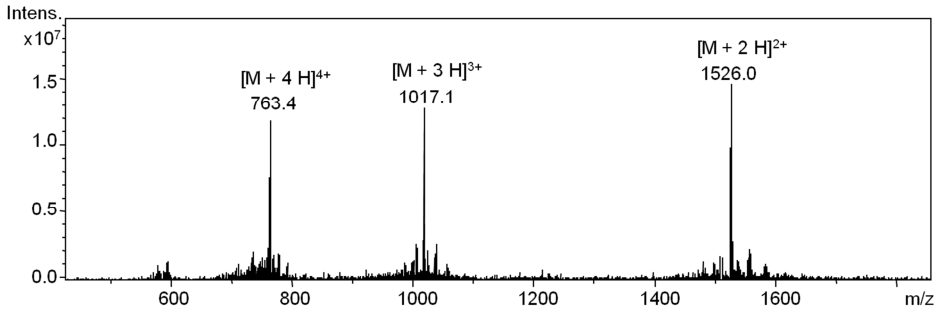

Figure 27. ESI-MS spectra of symmetric paCD **2**.

Polycationic CD derivatives with free hydroxyl groups on the secondary rim **9** and **10** could be obtained from their *N*-Boc protected precursors **33** and **34** efficiently in quantitative yields making use of the same reaction conditions as described before.

Recording NMR spectra of polycationic amphiphilic CD derivatives, some specific aspects have to be considered in order to achieve satisfactory resolution. In general, ^{1}H and ^{13}C NMR spectra of compounds furnished with thiourea moieties recorded at rt tend to show the typical line broadening associated with restricted rotation at the pseudoamide NH-C(=S) bonds.[190] This inconvenience can usually be overcome by acquiring NMR spectra at elevated temperatures (50-70 ºC), thus allowing structure confirmation. However, when ^{1}H and ^{13}C NMR spectra of compounds **1**-**10** were recorded in D_2O, MeOD or mixtures thereof at 50-60 ºC, resolution was unsatisfactory due to apparent loss of symmetry.

Two possible reasons for symmetry distortion exist, namely counter ion unbalance and self-assembly of paCDs, both solvent-dependent and probably interplaying. The self-assembling capabilities of polycationic amphiphilic compounds may lead to their aggregation not only in water but also in other solvents and their mixtures. This could be manifested in their respective NMR spectra by apparent loss of symmetry. Among the most important factors that affect self-assembling of paCDs, rank the nature of the

solvent, i.e. its polarity, sample concentration, its amphiphilicity and temperature.[191] Thus, selection of an appropriate solvent is a crucial issue.

Furthermore, we hypothesized that the counter ion species of paCDs may contribute to spectral resolution, since the presence of different kinds of counter ions, i.e. trifluoroacetate anions as well as hydrochloride anions originating from the freeze-drying process, would, depending on the solvent, result in increasingly complex NMR spectra accounting for a heterogeneous mixture of compounds.

In order to confirm this hypothesis, paCD salts were neutralized, thus getting rid of counter ions. Compound **4** was treated with a basic anion exchange resin (Dowex® Monosphere 550A hydroxide form) and, indeed, the ^{1}H NMR spectrum of the neutral amino analog featured the expected C_7 symmetry of the paCD derivative, compatible with its MS spectrum, as shown in Figure 28.

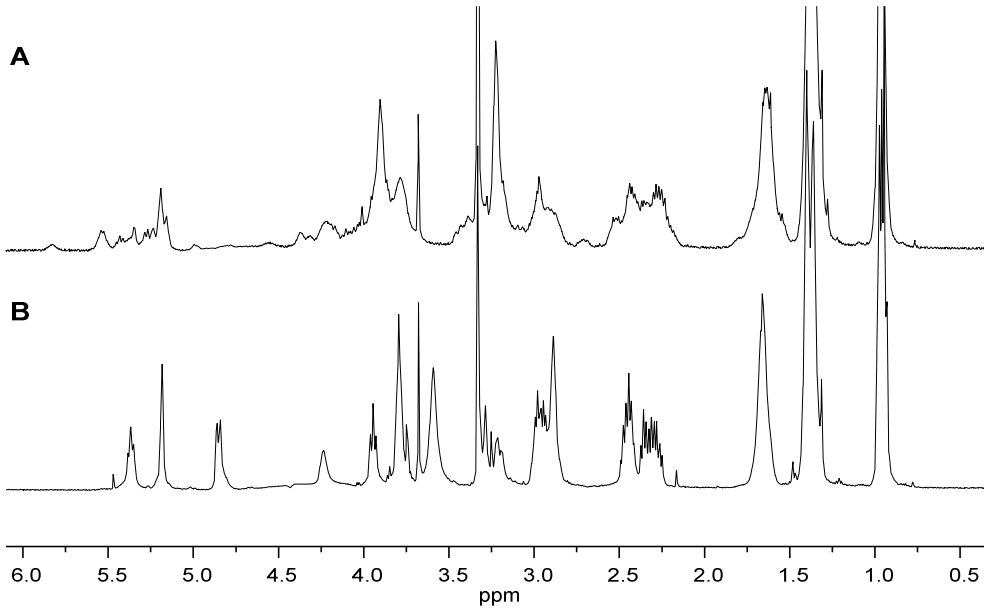

Figure 28. ^{1}H NMR spectra (500 MHz, MeOD, 323 K) of compound **4** before (A) and after (B) treatment with basic anion exchange resin. The residual HDO peak was suppressed by presaturation.

With this encouraging result in hand, the other polycationic CD compounds were subsequently treated with basic anion exchange resin. Although all amino moieties could be readily neutralized, the basic resin led to partial saponification of the more vulnerable short ester chains. In particular, hexanoyl as well as butanoyl chains of both linear and branched paCDs resisted basic treatment, whereas shorter chains, i.e. propanoyl and acetyl chains, were partially hydrolyzed, as evidenced by ESI-MS. Consequently, it has not been possible to obtain compounds **1**, **2**, **5** and **6** as their neutral amino analogs for the purpose of NMR studies.

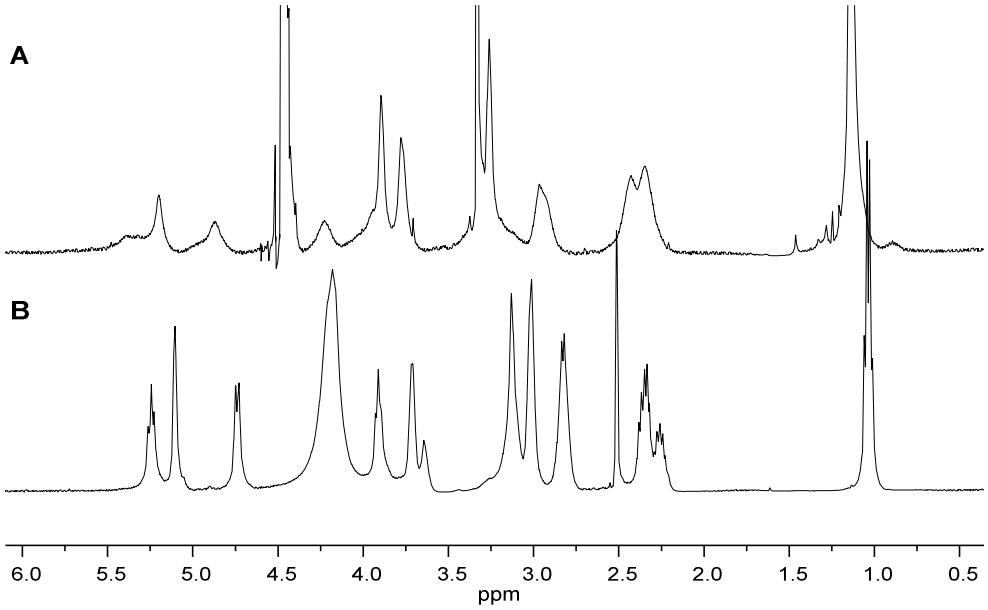

Figure 29. ^{1}H NMR spectra (500 MHz, 323 K) of compound **2** recorded in 2:1 D_2O-MeOD (A) and DMSO-d_6 (B), respectively.

As mentioned before, another reason for the apparent heterogeneity of paCDs observed in ^{1}H NMR spectra may be self-assembly. paCDs tend to self-assemble in aqueous media, while in most cases they are moderately soluble in MeOD. To strike a balance between these opposite characteristics, on first attempt NMR spectra were recorded in variable mixtures of D_2O-MeOD. However, ^{1}H NMR spectra obtained could

not prove in all cases the homogeneity of the polycationic amphiphilic compounds synthesized before. This was attributed to the fact that compounds self-assembled. When NMR spectra were recorded in DMSO-d_6, homogeneity of all paCD derivatives could be verified, indicating a weaker tendency to self-assemble in this solvent, as shown for paCD **2** in Figure 29 (see Figures S17-S24, S27 and S28 for NMR spectra, Supporting Information). Nevertheless, the self-assembling capabilities of all paCDs as well as their non-amphiphilic analogs **9** and **10** will be discussed in detail in the next section.

3. Investigation of self-assembling capabilities of paCDs in aqueous environment

For the purpose of gaining a deeper insight into their structure-activity relationship, in this Ph.D. Thesis the physicochemical properties of the synthesized paCDs were investigated. In the first place, the influence of the hydrophobic/hydrophilic balance on their self-assembling capabilities has been examined, as molecular assembly is related directly to the oligonucleotide condensing potential.

The first evidences of self-assembling in amphiphilic CDs date back from 1986,[192] when Kawabata and co-workers observed that alkanethiolated βCD derivatives obtained by nucleophilic substitution of the halides of **11**,[175,184] formed monolayers at the air-water interface with the hydroxylated face oriented towards the water (**35**-**38** in Scheme 8). However, it was not until 2000 that the self-assembling features of amphiphilic CDs were systematically analyzed.[193] Inserting oligoethyleneoxide segments in the secondary rim of the above amphiphiles (**39**-**42** in Scheme 8), Darcy and Ravoo synthesized βCD derivatives rendering different types of vesicles in aqueous environments.[194] These vesicles consisted on bilayers of CD molecules, in which the hydrophobic "tails" are directed inward and the hydrophilic "head groups" are facing water, thereby enclosing an aqueous interior (Figure 30).

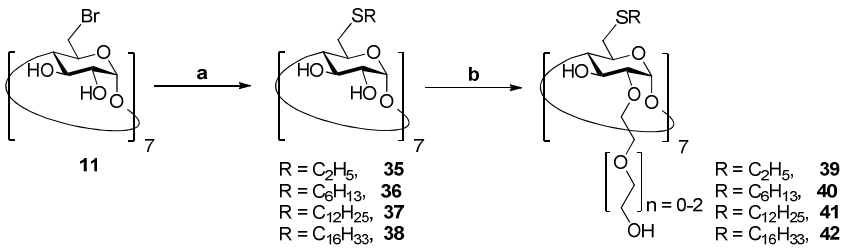

Scheme 8. Synthesis of oligo(ethylene oxide) CD amphiphiles **35**-**42**. Reagents and conditions: a) RSH, ^{t}BuOK, DMF, 80 ºC, 4 d; b) K_2CO_3, ethylene carbonate, tetramethylurea, 150 ºC, 4 h.

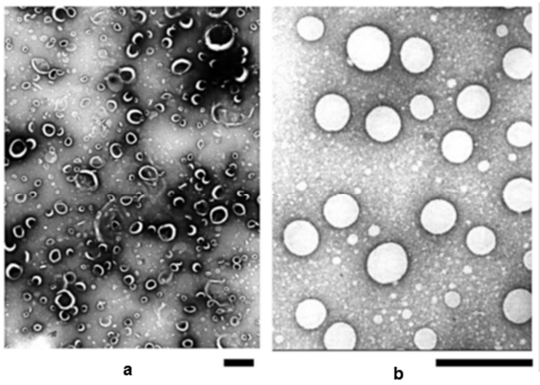

Figure 30. (a) Vesicles formed by amphiphilic CD **42** and (b) nanoparticles formed by amphiphilic glycosylated CD **45a** (scale bars = 200 nm).[195]

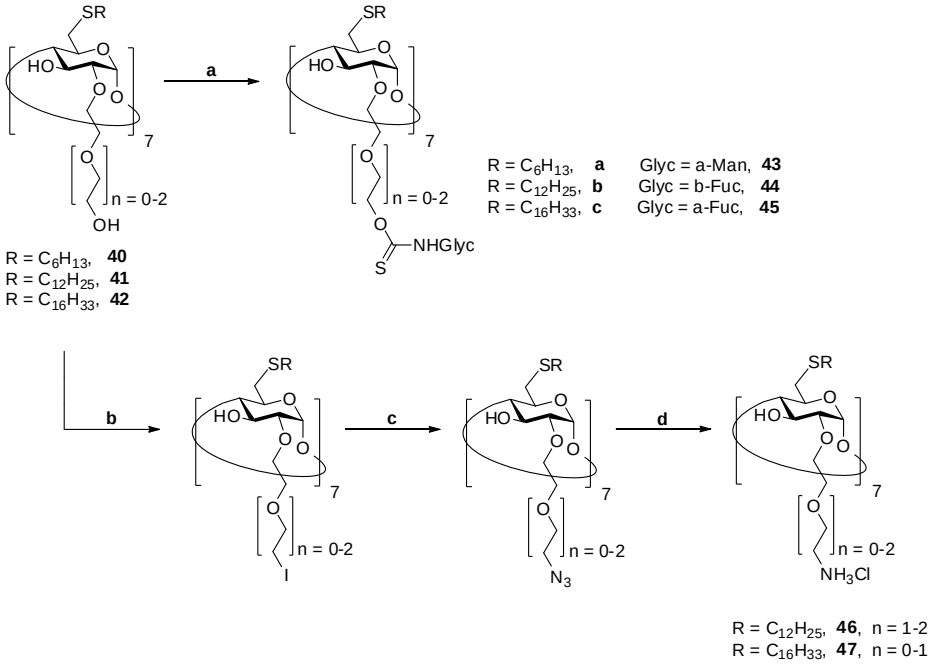

Scheme 9. Synthesis of glycosylated and cationic CD amphiphiles **43**-**47**. Reagents and conditions: a) i, acetylated Glyc-NCS, DABCO, toluene, rt; ii, NaOMe, MeOH for **43**, NaOMe, MeOH-DMF for **44** and **45**; b) NIS, TPP, DMF, 100 ºC, 4-5 h, 45-70%; c) NaN_3, DMF, 100 ºC, 4-5 d, 70%; d) i, TPP, DMF, 2 h; ii, NH_4OH, then 1 M HCl, 50-65%.

The fact that these oligo(ethylene oxide) CDs **39**-**42** exhibited significantly different self-assembling capabilities from 6-thioalkylated CDs **35**-**38** highlighted the utmost role of the hydrophilic/hydrophobic balance determining supramolecular features.[196] For instance, grafting monosaccharide moieties onto the oligo(ethylene oxide) chains of amphiphilic CD derivatives **40**-**42** directly using glycosyl isothiocyanates[197] (Scheme 9) eventually tuned amphiphilicity to render nanoparticle formation (Figure 30).[198]

In addition to non-ionic CD amphiphiles, supramolecular assemblies composed entirely of anionic[199] and cationic[200] amphiphilic CD have been described. Very recently, Darcy and co-workers[201] showed that cationic amphiphilic CDs **46** and **47**, which could be obtained from oligo(ethylene oxide) amphiphiles **41** and **42** by a iodination-azidation-reduction sequence[202] (Scheme 9), feature different self-assembling properties. While compound **47** forms bilayer vesicles in aqueous environment, **46**, equipped with shorter lipid chains tends to form micelles.

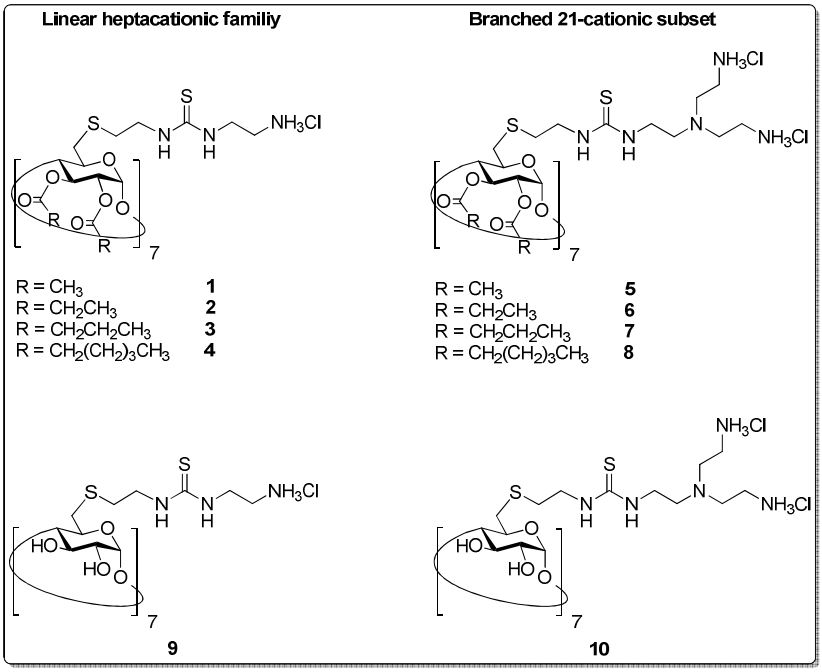

Figure 31. Library of paCDs and their respective non-amphiphilic analogs.

The intimate link between amphiphilic CD structure and self-assembling capabilities has also been demonstrated recently in our laboratory. It has been shown that subtle modifications in the nature of the functional groups installed on the primary rim of the βCD core dramatically affect the size a surface electrostatic (ζ) potential of the resulting nanoparticles.[203] In turn, these features exert an important influence of nanoparticle stability and their molecular encapsulation and release capabilities.

In a first step to correlate molecular structure of the synthesized paCDs (Figure 31) with self-assembling properties, in this section their critical aggregation concentrations (CAC) have been measured.

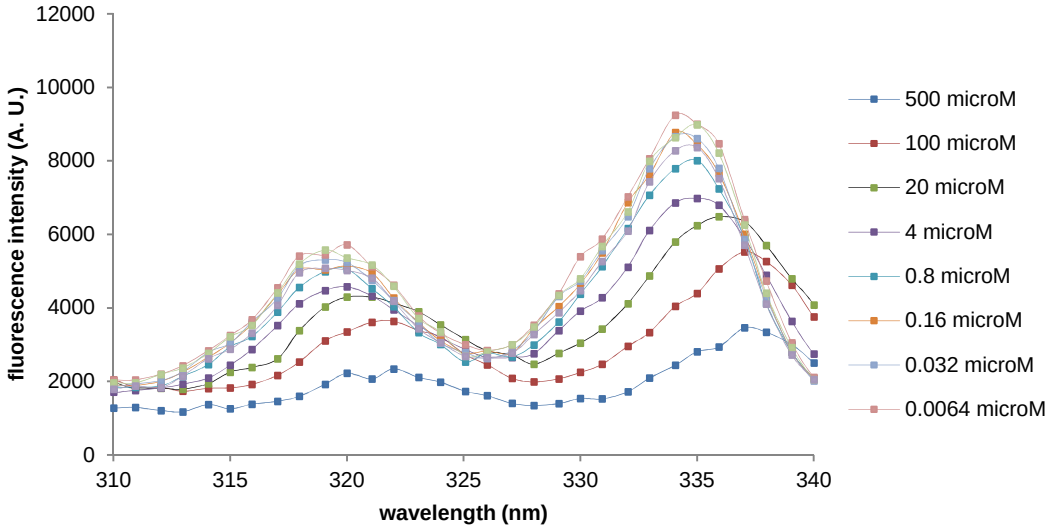

Figure 32. Fluorescence excitation spectra of pyrene (λ_{em} 375 nm) in water containing compound **4** at the indicated concentrations.

Experimentally, the critical aggregation concentration can be estimated by correlating a suitable physical property to surfactant concentration. Earlier attempts of our research group to determine the critical aggregation concentration of amphiphilic CDs by surface tension measurements based on the *Du Noüy ring method*[204] failed because measurements fell below the detection limit in the low μM range. In order to measure the

critical aggregation concentrations of the paCD collection synthesized in this Ph.D. Thesis, an established easy-to-use fluorescence technique based on the environment polarity-induced change in fluorescence spectra of pyrene[205] was applied. In aqueous environment, this extremely hydrophobic dye is preferentially incorporated in the interior of hydrophobic aggregates, leading to a significant change in its fluorescence spectrum. The onset of aggregate formation is detected by a shift of its fluorescence excitation spectra at an emission wavelength of 375 nm. A series of aqueous solutions of each paCD were prepared (0.256 nM to 500 μM), each of them containing 0.6 μM pyrene. After incubation of the samples, the fluorescence excitation spectra were registered at 375 nm (λ_{ex} 310-340 nm, Figure 32) and the fluorescence intensity at 339 nm relative to 335 nm (I_{339}/I_{335}) was plotted against Log[CD], yielding for each CD derivative a graphic as shown in Figure 33.

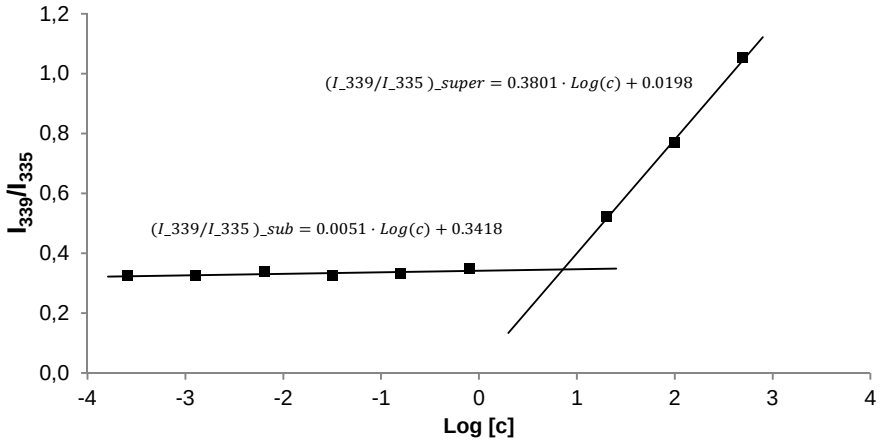

Figure 33. CAC determination for compound **4** using pyrene fluorescence excitation spectra switch at λ_{em} 375 nm.

In such representation, two linear data ranges can be distinguished: (i) a section with constant I_{339}/I_{335} ratio corresponded to CD concentrations below CAC (*sub*) and (ii) another with a linear increase in I_{339}/I_{335} ratio associated with CD concentrations above CAC (*super*). By linear fitting of both data ranges, two linear equations could be obtained:

$$\left(\frac{I_{339}}{I_{335}}\right)_{sub} = a_{sub} \cdot Log(c) + b_{sub} \quad (1)$$

$$\left(\frac{I_{339}}{I_{335}}\right)_{super} = a_{super} \cdot Log(c) + b_{super} \quad (2)$$

The critical aggregation concentrations were then determined from the intersection of both lines according to equation (3):

$$CAC = 10^{\frac{b_{super}-b_{sub}}{a_{sub}-a_{super}}} \quad (3)$$

Table 2. Critical aggregation concentrations in aqueous environment of both linear and branched paCDs and their non-amphiphilic analogs.

Acyl chain length	Linear series	CAC (μM)	Branched series	CAC (μM)
none	**9**	64.7	**10**	43.3
Ac	**1**	94.4	**5**	66.5
Pr	**2**	26.4	**6**	49.3
But	**3**	5.7	**7**	21.3
Hex	**4**	0.94	**8**	2.79

Table 2 collects the critical aggregation concentrations in aqueous environment of both linear and branched paCDs and their non-amphiphilic analogs. The expected progressive decrease of CAC with increasing acyl chain length was observed. This was in agreement with an increasing hydrophobicity of the acyl chains and thus amphiphilicity of the CD conjugates. In general, this trend could be observed in both the linear and the branched paCD series, although it was more pronounced in the linear one. CAC dispersion for the former group ranged from 1 μM (hexanoylated paCD **4**) to approximately 100 μM (acetylated paCD **1**), while CAC values of branched paCDs varied from 3 μM (hexanoyl compound **8**) to approximately 70 μM (acetylated compound **5**).

Although an increase in acyl chain length and hence in amphiphilicity of the CD conjugate resulted in a decrease of CAC, charge density also plays a major role,

evidencing that an appropriate equilibrium between acyl chain length and number of polycationic groups is decisive for the self-aggregation tendency of paCDs. The six-membered acyl chains of CD derivatives **4** and **8** seemed to be able to counterbalance arrays of both seven and fourteen cationic groups on the primary rim of the CD scaffolds, which led to low CACs in both cases. In contrast, the shorter acyl chain of the set of propanoyl compounds **2** and **6** apparently matched up better with a lower charge density. Hence, CAC of compound **2** is markedly lower than that of its branched analog **6**.

The CAC values obtained for the non-amphiphilic CD derivatives **9** and **10** are, however, unexpectedly lower than those measured for the acetylated conjugates. ^{1}H NMR registered in D_2O up to low mM concentrations gave no evidence of self-aggregation behavior for compounds **9** and **10**. Thereby, the observed effect must be the consequence of the molecular inclusion of the pyrene moiety in the CD cavity, which may also potentially lead to fluorescence spectral changes.[206] Lacking acyl chains on the secondary rim may clear the access to the cavity of compounds **9** and **10.** The experimental setup of the fluorescence technique used to determine the CACs does not allow for distinguishing whether the shift of the fluorescence excitation spectra originates from incorporation of pyrene in the interior of micelles or from the formation of inclusion complexes between CD and pyrene. As a consequence, it has not been possible to define the contribution of inclusion complex formation to the allover fluorescence shift and the actual CACs of both derivatives **9** and **10** could not be determined although they are expected to be much higher than those of their amphiphilic analogs.

In order to round investigations of self-assembling capabilities in aqueous environment out, the stability of the paCD aggregates has been studied. For such purpose, paCD **4** was chosen to be surveyed in a more detailed manner. Its pyrene-containing aqueous solutions were incubated at rt for one month and fluorescence spectra were registered at different times over that period. Measurements revealed that the CAC remained constant; hence, aggregates remained unaltered for that time.

4. Determination of pK_a values and buffering capabilities of CD-scaffolded polycations

It is generally recognized that the major obstacles to efficient gene delivery are cellular internalization and intracellular trafficking.[207,208] There have been noticed major disparities among the mechanisms used by non-viral carriers to overcome these hurdles. For instance, lipoplexes have been shown to enter the cells predominately via clathrin-dependent endocytosis (CDE).[209] PEI polyplexes, however, are internalized through several routes, being the fraction taken up via clathrin-independent (CIE) mechanisms the one that leads to gene expression.[210] Similarly to the later, in the case of CDplexes, though the largest fraction of gene complexes is taken up via CDE, the smaller fraction internalized via CIE is predominately responsible for successful transgene expression.[182]

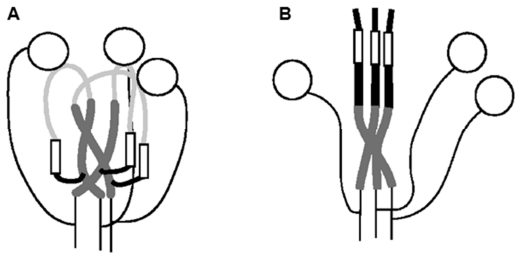

Figure 34. Schematic representation of the structure of haemagglutin (HA) at neutral pH (A) and at low pH (B).

These evidences highlight the utmost relevance of endosomal escape skills in the overall efficiency of gene carriers. Understanding of the mechanisms of viral escape from endosomes is important for improving non-viral gene delivery systems. For instance, the naturally evolved strategies by viruses are incomparably more efficient than those envisioned for non-viral vectors. Haemagglutinin (HA) protein, which is pH sensitive and membrane destabilizing, helps viral vectors to disrupt the endosome efficiently and enter the cytoplasm.[211] The escape mechanism of HA and other fusion proteins is that they shift from an ionized and hydrophilic conformation to a hydrophobic and membrane-active

conformation as the environment changes from neutral to acidic, resulting in destabilization of the endosomal membrane and its subsequent leakage (Figure 34).[212]

Though still a matter of debate, this is much alike the endosomal escape mechanism responsible for the gene transfer efficiency of lipidic vectors. The interaction of cationic lipids with anionic phospholipids, a model introduced by Xu and Szoka,[213] destabilizes endosomal membrane and facilitates its rupture (Figure 35). [214]

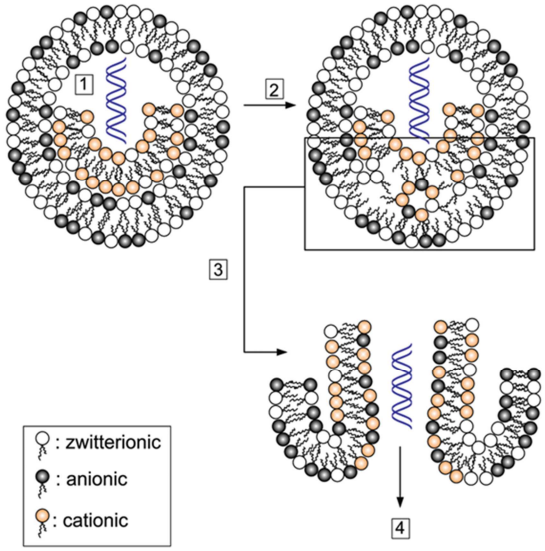

Figure 35. Proposed mechanisms of cationic lipid/nucleic acid complexes after endocytosis along the endosomal pathway: (1) cationic lipids interact with anionic lipids in endosomes by forming ion-pairs; (2) the lipid bilayer is destabilized; (3) the hexagonal phase is formed; (4) the nucleic acid is released into the cytoplasm.[215]

Conversely, the gene transfer efficiency of certain cationic polymers is associated to their pH buffering capabilities by virtue of the proton sponge effect.[65] Endosomal pH gradually drops from physiologic (ca. 7.5) to acidic (ca. 5-5.5) upon maturation, a pH range in which nearly half of high-molecular weight PEI nitrogens may protonate. This large buffering capacity may be accompanied by extensive swelling to compensate the

osmotic pressure and/or conformational changes in the DNA-carrier assembly that leads to endosome destabilization and subsequent bursting (Figure 36).[86] It is hypothesized that the proton sponge mechanism is not only valid for PEI but is more generally applicable for compounds containing amino groups with pK_a values at or below physiological pH.

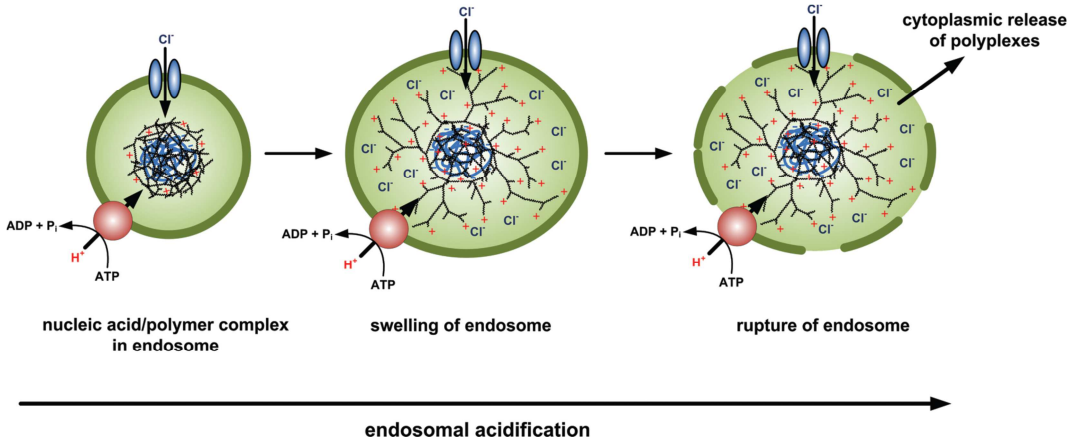

Figure 36. Endosomal rupture is mediated by polymers with a buffering capacity at the endosomal pH range that can trigger (a) the proton-sponge effect and (b) polymer swelling according to the umbrella hypothesis.[65]

Considering the similarities regarding the endocytic mechanisms between paCD CDplexes and PEI polyplexes, it was of interest to investigate the pH buffering capabilities of paCDs and their aggregates.

In general, the pK_a of each amine group in a polyamine is affected by the type of amine (primary, secondary, tertiary, or quaternary), electronic factors more than steric factors, and especially by the distance between neighboring amines.[216,217] A variety of methods for the determination of polyamine pK_a values exist. The most common is potentiometric titration, which is characterized by a high accuracy although a relatively large amount of pure compound is required.[218] Alternatively, any other property directly or indirectly affected by protonation can be used as probe for pK_a determination (UV absorption, electrophoretic mobility or LC, among others).[217] NMR-pH titration is also an

excellent technique for determining pK_a values as the protonation of a basic site leads to deshielding effects on the adjacent NMR-active nuclei, so the average chemical shifts of all the measureable NMR-active nuclei, as a function of pH, are expected to reflect the fractional protonation of each basic group of a molecule. NMR-pH titration offers the advantage of measuring pK_a in solutions that are not pure, e.g. in the presence of biological fluids or even impurities,[219] and may allow the sequence of polyamine protonation to be determined or even followed.

To determine pK_a values of a set of CD-scaffolded polycations synthesized in this Ph.D. Thesis (Figure 37), and to evaluate their buffering capacity, two different techniques were combined. ^{1}H NMR-pH titration of non-amphiphilic polycationic CDs and their respective model compounds allowed gaining a first insight into the range of their pK_a values. An advantage of this technique is that only small amounts of compounds are required, but cannot be used for self-aggregating paCDs . Alternatively, potentiometric titration was used for amphiphilic CDs instead.

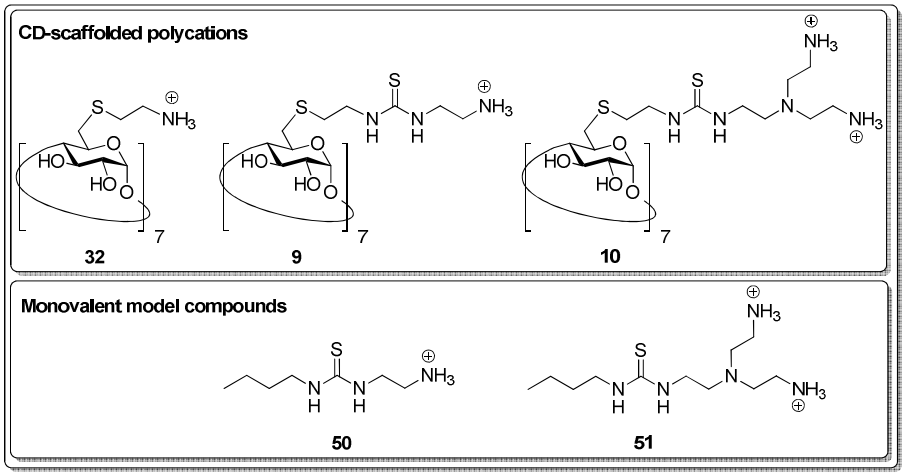

Figure 37. Compounds for ^{1}H NMR-pH titration: CD-scaffolded polycations (A) and their corresponding monovalent models (B).

Thereby, ^{1}H NMR-pH titration experiments were used to measure the pK_a values of non-amphiphilic CDs **9** and **10**, together with more simple cysteaminylated CD derivative **32**[185a] and the single branch models **50** and **51** (Figure 37). Compound **32** is the simplest one, only bearing cysteamine moieties, whereas both compound **9** and **10** additionally feature thiourea functionalities identified as the optimal tethers between the CD core and cationic cluster for gene delivery and expression. Keeping this element fixed, compound **10** has an increased density of primary amine groups in a dendritic display and is additionally furnished with a tertiary amine group. Structural modifications may have an influence on pK_a values of the primary amines corresponding to different CD derivatives. Furthermore, tertiary amines of compound **10** may have a lower pK_a than primary amines and thus enable the proton sponge effect. Model compounds **50** and **51** (Figure 37) were synthesized by reacting butylamine with isothiocyanates **22** and **23**, respectively (see Experimental Section for details) to assess the effect of the multivalent display on pK_a values.

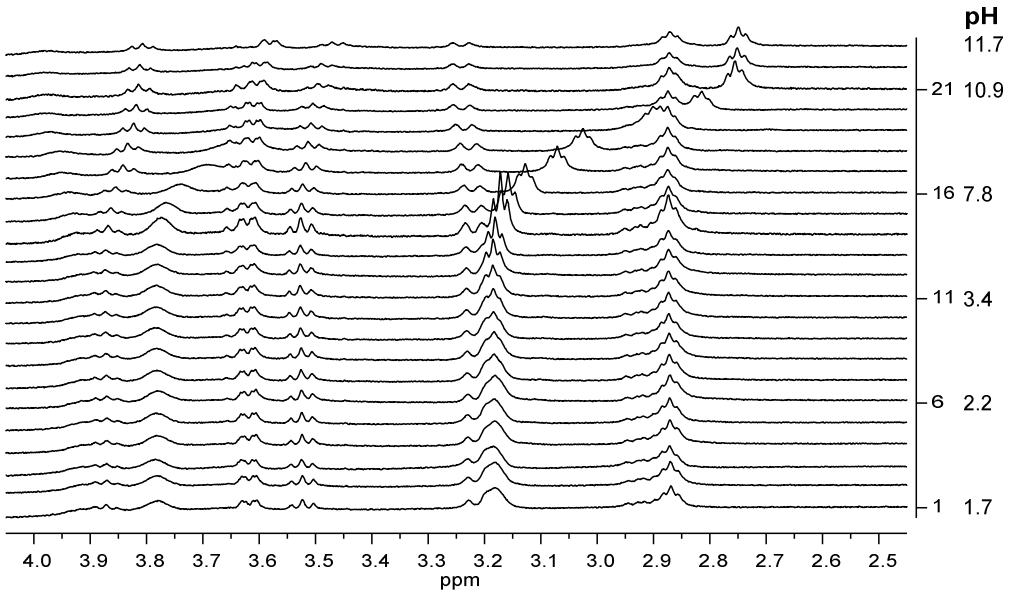

Figure 38. pH-Dependent chemical shifts of polycationic CD **9** (500 MHz, D_2O-H_2O, 298 K).

In each titration the ^{1}H NMR spectra were registered at different pH values (from 1.7 to 11.7) and the shift of each resonance was plotted vs. pH, as shown for CD derivative **9** in Figure 38 and Figure 39.

Obviously, protons adjacent to the amine groups were most influenced by the fractional deprotonation of each basic group, though this effect only took place at pH above 7.5, thus discarding the any buffering capabilities in the pH window of interest for this compound.

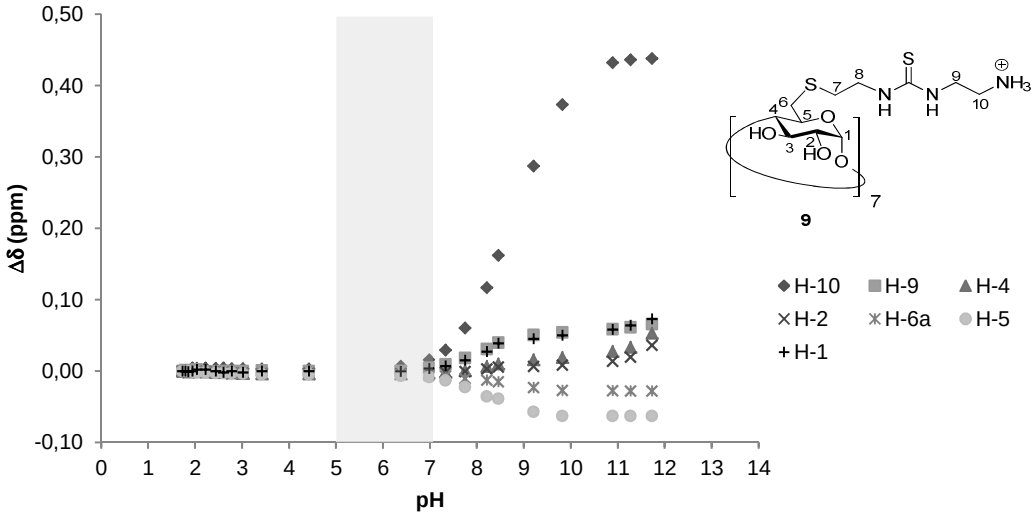

Figure 39. Sigmoidal curves representing changes in chemical shift (Δδ, ppm) of selected protons of compound **9** as a function of pH. The grey-shaded area represents the pH range where effective buffering ability may contribute to the lysis of the endosomes.

The sigmoidal curves obtained for the most representative proton resonances (those adjacent to the primary amino groups) for the rest of CDs (**10** and **32**), their corresponding models (**50** and **51**) and bPEI are collected in Figure 40. Similarly to CD **32**, **9** and **50** exhibited a single protonation equilibrium between pH 7 and 11, while for the branched derivatives **10** and **51**, and additional one was observed below pH 2, probably corresponding to the protonation of the tertiary amino group. This pK_a value is

consistent with that reported for the tertiary amine of tris(2-aminoethyl)amine (ca. 2),[220] which bears structural resemblance to compounds **10** and **51**. In any case, variations in the protonation state in the 5-to-7 pH range were unnoticed, in contrast to bPEI, exhibiting a continuous resonance shift along.

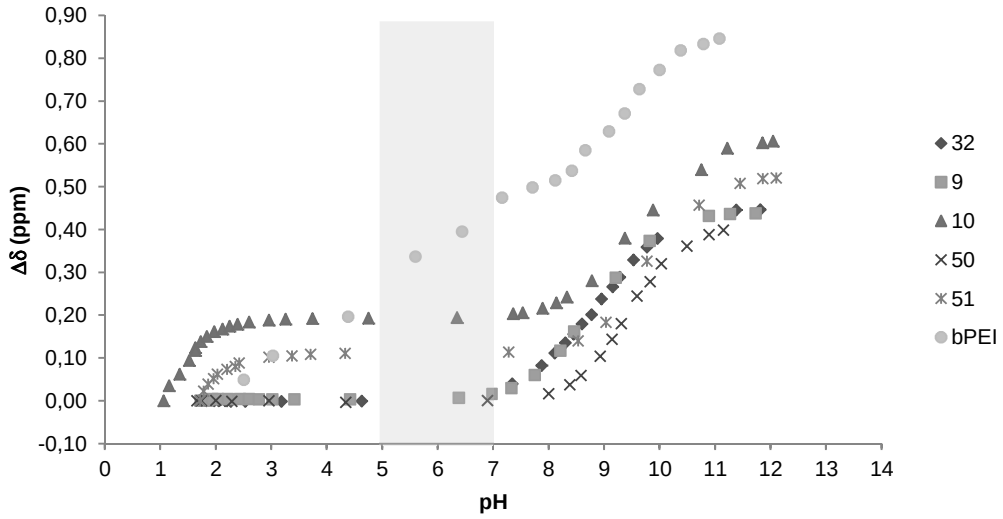

Figure 40. pH-Induced chemical shift variations (Δδ, ppm) of the resonances of protons adjacent to primary amines from non-amphiphilic polycationic CDs **32** (◆), **9** (■) and **10** (▲), their corresponding models **50** (×) and **51** (✳) and bPEI (●). The grey-shaded area represents the pH range where effective buffering ability may contribute to the lysis of the endosomes.

The pK_a values were obtained by plotting according to the Henderson-Hasselbalch equation (4),

$$pH = pK_a + log\,\frac{\delta_{acidic} - \delta_{obs}}{\delta_{obs} - \delta_{basic}} \quad (4)$$

in which δ_{acidic} and δ_{basic} are the chemical shifts of the observed signal of the fully protonated and deprotonated compound, respectively, and linear fitting, as illustrates Figure 41.

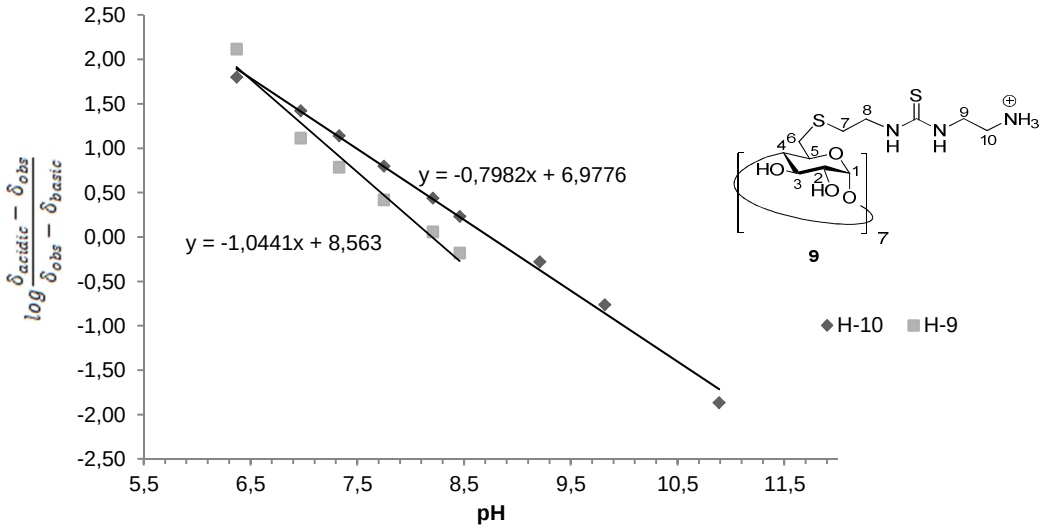

Figure 41. Logarithmic plot according to the Henderson-Hasselbalch equation and linear fitting to determine the pK_a value of CD-scaffolded polycation **9**.

Determination of pK_a values of the CD-scaffolded polycations as well as both monovalent model compounds was accomplished analogously (Table 3).

Table 3. Determination of pK_a values of CD-scaffolded polycations and their corresponding model compounds.

Polycation	pK_a	Corresponding model compound	pK_a
32	8.88	**-**	
9	8.50	**50**	9.41
10	1.88, 9.77	**51**	2.27, 8.81

No remarkable differences in the pK_a values of compounds **9** and **32**. In contrast, the pK_a value of polycation **10** is considerably higher, though still in the range for primary amines.[216,221] pK_a Values for the model compounds **50** and **51**, mimicking a “slice” of their analogous multivalent platforms **9** and **10**, deviate less than one pK_a unit. These results

led to the assumption that the multivalent character of CDs does not significantly affect the pK_a values of its amines.

In any case, as can be inferred from Figure 40, non-amphiphilic CD-scaffolded polycations apparently do not act as proton sponges upon acidification within endosomes because they lack pH-buffering capacities in the pH range from 5 to 7. This scenario, however, may change when CD-scaffolded polycations are aggregated to each other. Hydrophobic modifications of polycationic CDs might be relevant to enhance endosomal escape, because they could improve the interactions between vectors. As amphiphilic polycationic CDs self-assemble in aqueous environment, precluding ^{1}H NMR-monitored pH titration experiments, their buffering capacities were evaluated by potentiometric titration.

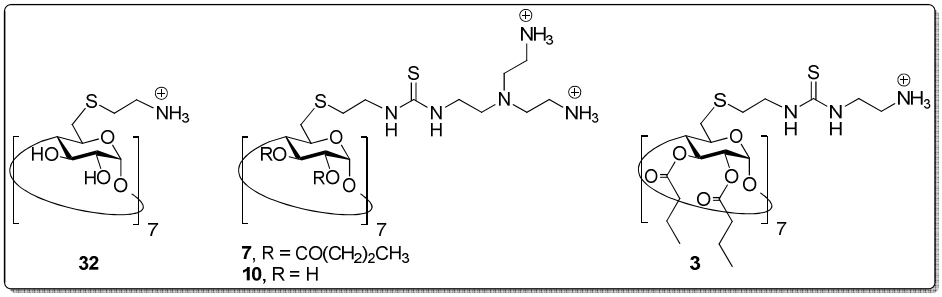

Figure 42. Amphiphilic and non-amphiphilic CD derivatives for potentiometric titration.

Representative amphiphilic and non-amphiphilic CD derivatives differing in their polycationic structure were chosen in order to assess the influence of aggregation on their buffering capacities (Figure 42). Keeping the dendritic polycationic display of compound **10** fixed, amphiphilic derivative **7** additionally bears butanoyl chains on the secondary rim. Amphiphilic compound **3** features lower charge density, while acyl chain length is similar to that of **7**. For comparative purposes, model compounds **50** and **51**, bPEI and a blank (150 mM NaCl aqueous solution) were also titrated potentiometrically in the 9-to-2 pH range.

Each compound (0.05 mmol of amino groups) was first treated with diluted NaOH to adjust pH to approximately 9, and then the pH of the solution was measured after each addition of aliquots of diluted HCl. The results are summarized in Figure 43. In agreement with ^{1}H NMR-pH titration experiments, non-amphiphilic CD-scaffolded polycations **10** and **32** do not buffer pH in the 7-to-5 range, very much alike model compounds **50** and **51**, as their acid-base titration curves drop down rapidly in this range. In contrast, amphiphilic CD derivatives **3** and **7** showed improved buffering capacities in this pH range, requiring a larger amount of HCl to drive pH to the acidic region.

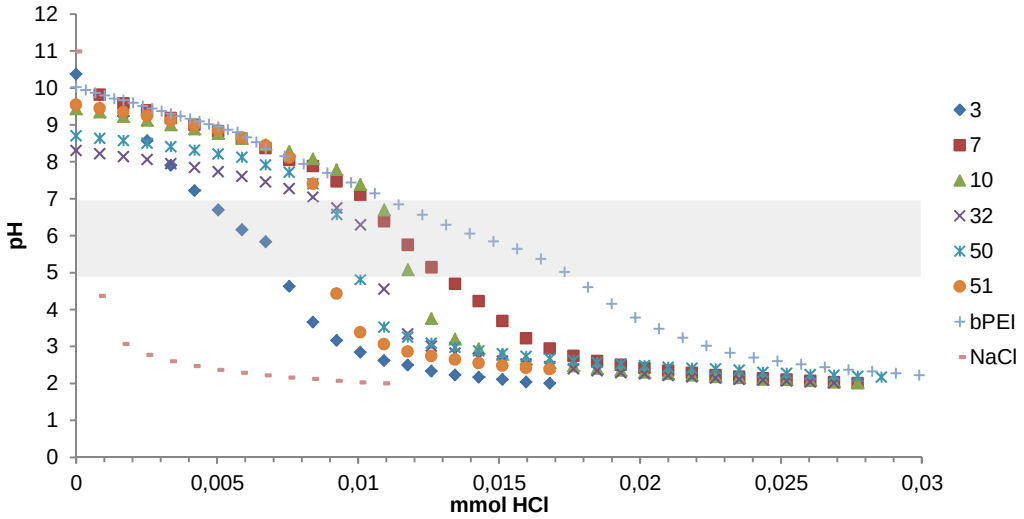

Figure 43. Potentiometric titration profiles of amphiphilic and non-amphiphilic polycationic CDs as well as their respective model compounds and bPEI. The grey-shaded area represents the pH range where effective buffering ability may contribute to the lysis of the endosomes.

As shown in Table 4, among all CD derivatives studied, branched paCD **7** exhibited the best buffering capacity, although it could not compete with the golden standard bPEI. Its linear amphiphilic analog **3** also featured good buffering ability, which clearly evidenced that amphiphilicity, and hence self-aggregation, substantially enhances the buffering capacity of CD-scaffolded polycations.

Table 4. Equivalents of HCl consumed to switch pH from 7 to 5 for amphiphilic and non-amphiphilic polycationic CDs as well as their model compounds and bPEI.

Compound	meq of HCl consumed
3	67
7	84
10	34
32	34
50	17
51	<17
bPEI	134

5. Assessment of DNA-paCD complex (CDplex) formation and dissociation

Facile cellular uptake of free DNA via plasma membrane permeation is hindered by the size and negative charge of the DNA. Although several studies have shown that naked DNA can be introduced into cells the in vivo relevance of these techniques is limited. Systemic circulation of free DNA is hindered by nuclease degradation. Thus, compaction and masking the negative charge of its polyphosphate backbone constitutes a prerequisite for effective DNA delivery. Gene-carrier complex formation is known to critically determine gene transfer efficiency. The size of the complex and stability significantly depends on the type of cationic structure used, although preparation conditions including concentration of DNA, pH, type of buffer, and N/P ratio also affect size.[55] Moreover, particle size affects the extent to which nanoparticles are taken up and are able to transfect cells, as the endocytotic machinery and cell membrane have well-defined geometries and flexibility that may restrict entry of incompatibly large or small particles.[222,223]

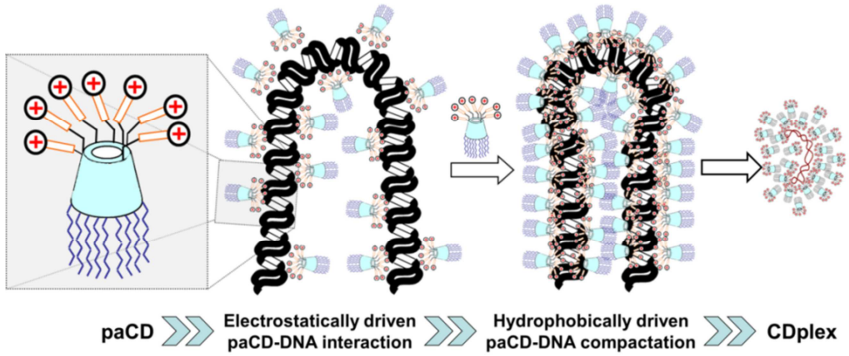

Figure 44. Two-step self-assembling mechanism of paCDs in the presence of DNA.

Along with size, surface charge (ζ potential) also critically determines particle fate and transfection efficiency. It is generally believed that positively charged nanoparticles

perform better for in vitro transfections of cells through their enhanced binding to negatively charged proteoglycans on cell surfaces,[224,225] though interaction with negatively charged serum proteins, could also be a drawback.[226] It has been shown that paCDs furnish small nanoparticles (CDplexes) with narrow polydispersity upon incubation in the presence of pDNA. These CDplexes are spherical and positively charged (av. 30 mV, Figure 45) with an average size below 100 nm. CDplex formation has been hypothesized to take place through a two-step self-assembling mechanism of paCDs in the presence of pDNA, as shown in Figure 44.[177]

The first step is a rapid and reversible electrostatically driven interaction between phosphates and the positively charged amine headgroups of paCDs, during which the paCDs act separately in an independent manner. Driven by desolvation, the second probably slower and essentially irreversible step involves the fusion and rearrangement of the paCDs, thus triggering extensive compactation by hydrophobic interactions.[227]

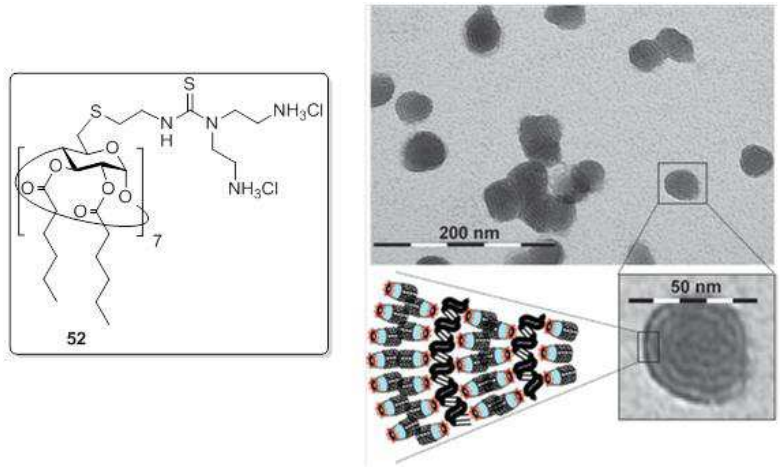

Figure 45. TEM micrograph of paCD **52**:pDNA CDplexes with amplification of the ultrafine structure of the particles and a schematic representation of the proposed arrangement of paCDs and the DNA double helix.

Transmission electron microscopy (TEM) showed the small size (40 nm) and homogeneous distribution of CDplex formulations from thioureido-cysteaminyl paCD **52**

(Figure 45).[177] At high magnification, a snail-like ultra-structure was observed, which has been attributed to the alternating lamellar arrangements of paCDs and electron-dense regions corresponding to the pDNA molecule, similarly to that reported by Pitard and co-workers (see Figure 12, Chapter 1).[81b]

The spontaneous self-assembly of CDplexes may seem very simple in its concept, yet could determine their characteristics (stability, biocompatibility, membrane-crossing ability etc.) and, thereby, their transfection potential. Control of the hydrophilic/hydrophobic balance between the CD primary and secondary faces is therefore crucial for efficient pDNA complexation and nanoparticle (CDplex) formation. Among the most important parameters that are affected by the molecular architecture of paCDs are complex size and uniformity, complex overall charge, as well as its pDNA condensation and dissociation capabilities. For a better understanding of the effects of structural variations on the molecular construct in the CDplex stability and its physicochemical properties, in this Ph.D. Thesis a deep insight on CDplex formation and dissociation capabilities of paCDs differing in their hydrophobic/hydrophilic balance was accomplished.

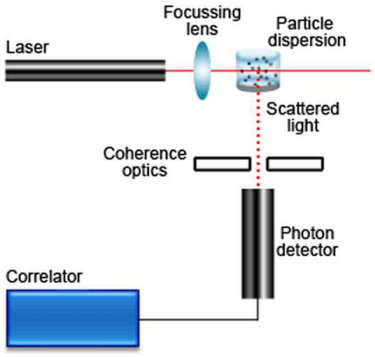

Figure 46. Schematic representation of a conventional, 90º dynamic light scattering (DLS) instrument.[228]

First, the DNA-paCD nanoparticles were characterized by dynamic light scattering (DLS) in order to determine their average hydrodynamic size and ζ potential. Briefly, the DLS technique measures the time-dependent fluctuations in the intensity of scattered

light, which occurs because the particles are undergoing random Brownian motion. Analysis of these intensity fluctuations enables the determination of the distribution of diffusion coefficients of the particles, which can be converted into a size distribution using established theories (Figure 46).

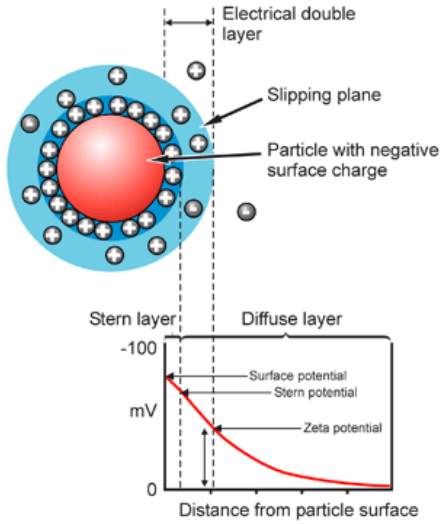

Figure 47. Schematic representation of zeta potential.[229]

In general, the surface charges of particles dispersed in an aqueous system modify the distribution of the surrounding ions, resulting in a layer around the particle that is different to the bulk solution. The ζ potential is the potential at the point in this layer where it moves past the bulk solution (slipping plane, Figure 47). ζ Potential is one of the main features that determine particle interactions, thus a high zeta potential will confer stability, i.e. the solution or dispersion will resist aggregation. ζ Potential measurement were performed by a technique called M3-PALS, which is a combination of laser Doppler velocimetry and phase analysis light scattering (PALS) to measure particle electrophoretic mobility. The mobility measured is converted to ζ potential using established theories.

The capability of the polycationic CDs differing in their hydrophobic/hydrophilic balance synthesized in this Ph.D. Thesis (Figure 48) to form stable CDplexes with DNA (calf thymus) was studied at N/P ratios 5 and 10. This ratio, which represents the ionic balance within the complexes, is referred to the number of protonable amino groups (N) in the polycationic CD per phosphate (P) of DNA. These N/P ratios were chosen since at these proportions the most efficient transfection has been achieved in earlier reports.[177,181] To avoid premature self-aggregation phenomena, the CD stock solutions were prepared in DMSO and further diluted with the DNA solution in a 20 mM 4-(2-hydroxyethyl)-1-piperazineethanesulfonic acid (HEPES) buffer at physiological pH, thereby assuring that the final DMSO content never exceeded 1% v/v.

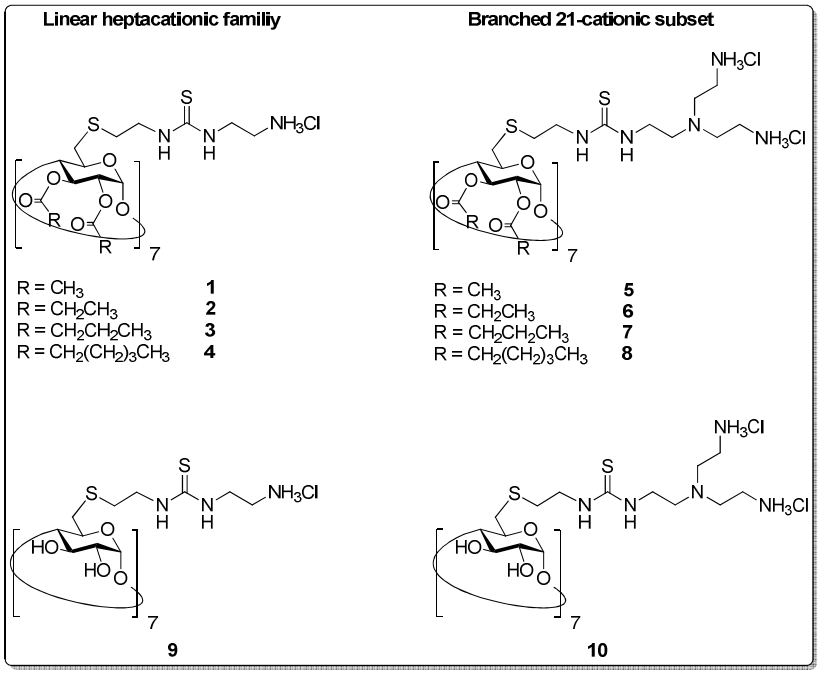

Figure 48. Library of polycationic CDs for particle size and ζ potential measurements.

The DLS results showed that all assayed polycationic amphiphilic CDs as well as their non-amphiphilic analogs formed compact, ordered and stable nanoparticles with DNA,

exhibiting rather small hydrodynamic diameters as compared with the polyplexes obtained using branched polyethyleneimine (bPEI, 25 kDa), one of the most efficient commercial gene-delivery systems (60-90 nm vs. 150 nm; Figure 49).[230,231]

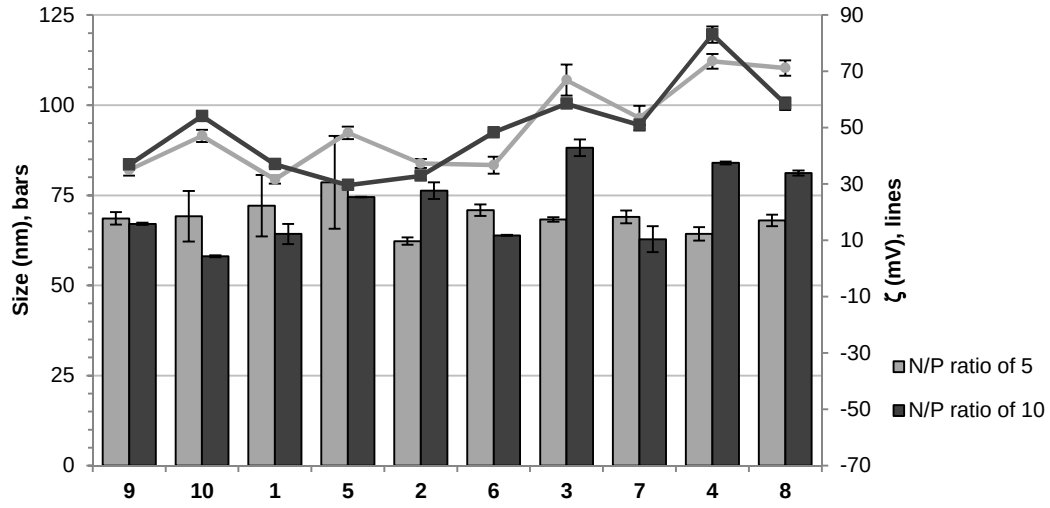

Figure 49. Size (hydrodynamic diameters, bars, nm) and ζ potential (lines, mV) of CDplexes determined by dynamic light scattering and M3-PALS analysis, respectively.

Hydrodynamic diameter measurements demonstrated that particle size scarcely depends on paCD structure. Even in the case of non-amphiphilic CDs **9** and **10**, hydrodynamic diameters could be measured in the range of 70 nm, in contrast to our previous observations,[177] but in agreement with that reported for other non-amphiphilic CD-scaffolded polycations.[169] Reineke and co-workers demonstrated that structurally-related non-amphiphilic polycationic CD condense pDNA at N/P 5 into spherical nanoparticles in the size range of 80-130 nm. These nanoparticles exhibited near neutral to positive zeta potentials (+5 < ζ < +15 mV).

In particular, non-amphiphilic CD derivatives **9** and **10** exhibited similar hydrodynamic diameters to their hexanoylated counterparts (ca. 70 nm). While this result may sound counterintuitive, their hydrodynamic diameters do not reflect how nanoparticles are

compacted and similar values could still reflect quite different behaviors for any case. The proposed two-step compaction process cannot be operating for the formation of this non-amphiphilic nanoparticles.

Additionally, narrow populations of cationic nanoparticles were observed in each individual experiment, thus indicating rather monodisperse nanoparticles (Figure 50). Such remarkable behavior (low particle size and monodispersity) has only been reported for a monomolecular condensation process that occurs upon mixing DNA with dimerizable, polycationic detergents.[84a,232,233]

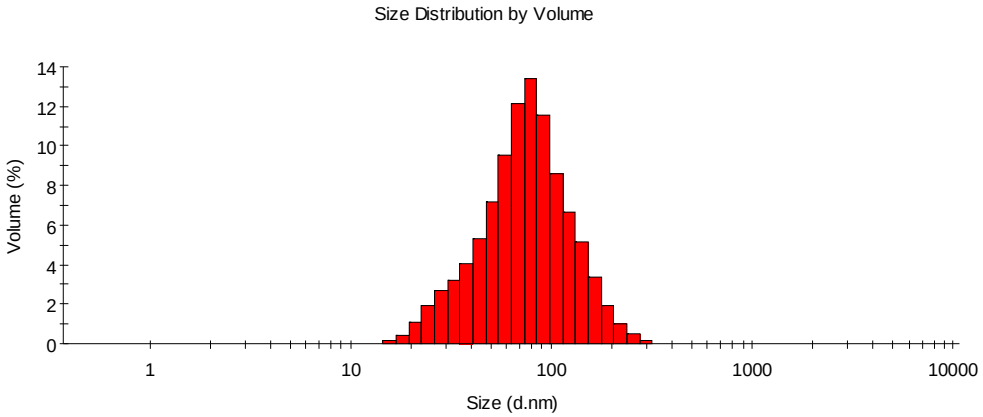

Figure 50. Particle size distribution by volume determined by DLS for paCD **8** at N/P 5 (diameter in nm).

M3-PALS measurements at both N/P ratios 5 and 10 revealed that ζ potential ranked in the range 30-70 mV, amenable values for cell-based assays. ζ potential values did not depend on the N/P ratio, which indicated that complex stoichiometry does not significantly change upon an increase of the N/P ratio. We hypothesize that excess CD does not incorporate into the CDplex nanostructure. Previous results of our research group indicated that nanoparticles of non-amphiphilic CDs exhibited zeta potential values close to neutrality even at high N/P ratio, although these CDplexes were not stable.[177] In sharp contrast, ζ potential values of CDplexes of non-amphiphilic CD derivatives **9** and **10** were

clearly in a positive range (ca. 40 and 50 mV, respectively, for both N/P ratios), thus perfectly fitting within the scope of paCDs. Results reported by Reineke and co-workers[169] support these findings, since they also demonstrated that non-amphiphilic CDs were capable of binding and compacting pDNA at N/P 5 into spherical nanoparticles with slightly positive zeta potentials.

Altogether, DLS experiments pointed out that all polycationic CD derivatives **1**-**10** were able to form nanoparticles with DNA, regardless of their hydrophilic/hydrophobic balance. All these CDplexes featured remarkably similar hydrodynamic diameters, ζ potentials and relatively narrow size distributions.

These results were contrasted using agarose gel electrophoresis shift assays. Thus, paCD:ctDNA complexes were formulated in the same manner as described before for different N/P ratios in the range of 0.5 to 20. Naked ctDNA was used for comparative purposes. A decrease of DNA migration up to complete inhibition could be observed at different N/P ratios for all tested CD derivatives. Moreover, if DNA is efficiently compacted and protected in the CDplexes, it becomes inaccessible to the GelRed™ (*Biotium*), a fluorescent intercalating agent used as staining reagent, as demonstrated by the absence of fluorescent staining in the corresponding lanes (Figure 51).

At N/P ratios higher than 1, DNA charge neutralization and migration were achieved with all assayed polycationic CDs, which was indicated by the absence of “free” mobile plasmid. However, still an intense GelRed™ stain is visible in most of the cases. At N/P ratios higher than 1, however, paCDs bearing acyl chains of different length showed essentially different behaviors, thereby evidencing the subtle differences between nanoparticles with respect to amphiphilicity. From N/P ratio 2 and up, linear amphiphilic CDs **2**, **3** and **4**, as well as branched analogs **6**, **7** and **8** were capable to efficiently compact and protect DNA in their CDplexes, which was indicated by the absence of fluorescent staining in the corresponding lanes. On the contrary, the CDplexes formulated with both acetylated (**1** and **5**) and non-amphiphilic (**9** and **10**) derivatives did not compact and protect DNA efficiently, since it remained accessible to GelRed™ in the whole range of N/P values, including even high N/P ratio 20.

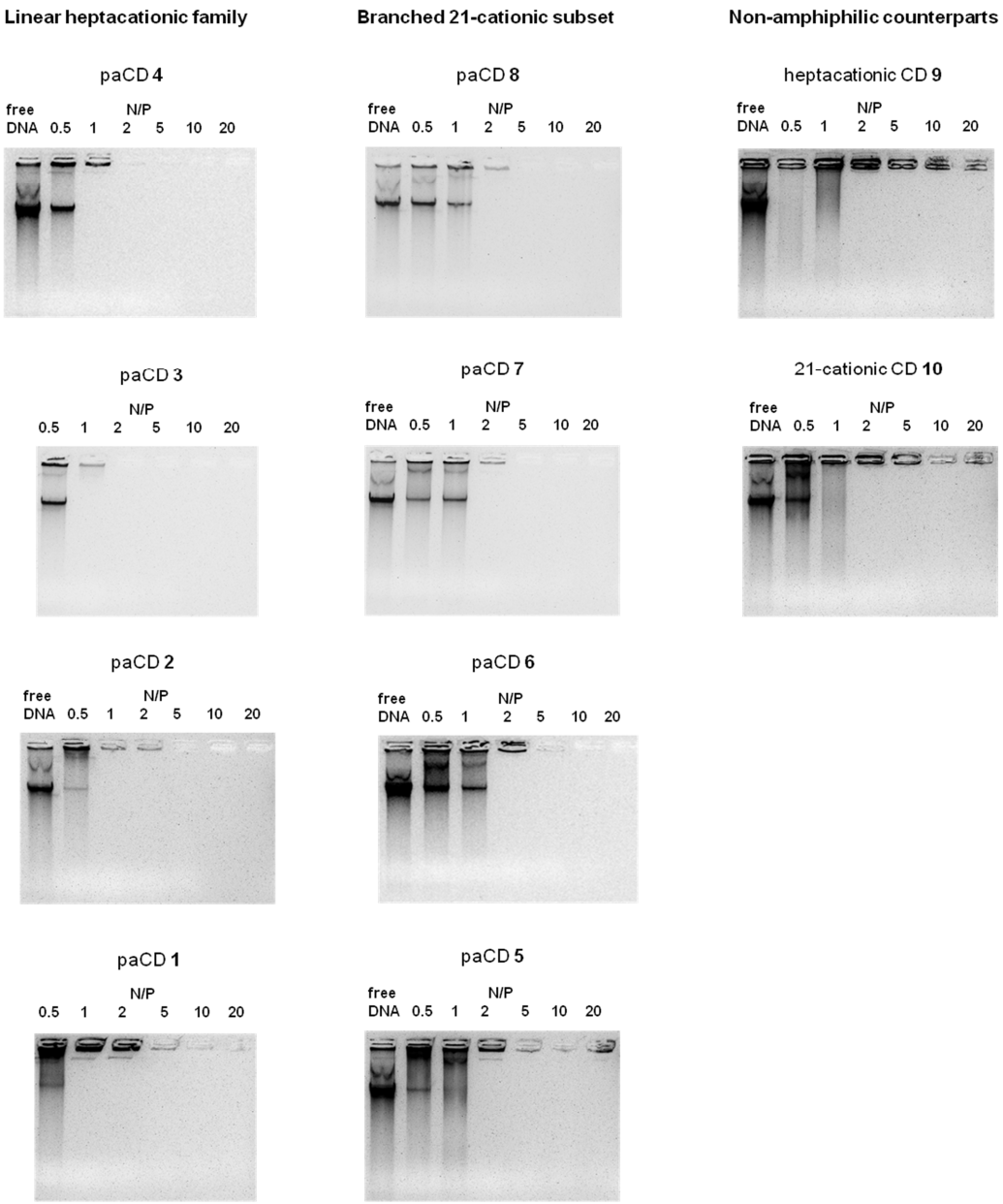

Figure 51. Protection of DNA from GelRed™ intercalation at different N/P ratios (0.5-20) by paCDs **1**-**8** and their non-amphiphilic analogs **9** and **10**.

These results clearly evidenced that CD derivatives that bear longer acyl chains cover the DNA surface more efficiently. However, no remarkable difference between paCDs featuring either four-membered or six-membered acyl chains was detected. When comparing the linear and the branched subseries among one another, it has to be kept in mind that equal N/P ratios do not correspond to equimolecular ratios. To put it differently, for the preparation of CDplexes with a given N/P ratio the number of moles of linear CD derivatives required triples that of branched CDs. This is a considerable factor because therapeutic doses of non-viral gene delivery systems are related to issues of immunogenicity and toxicity.

Additionally, for paCDs **4** and **6** gel electrophoresis shift assays were accomplished using luciferase-encoding pDNA for CDplex formation. Whereas ctDNA used so far consists of 13000-20000 base pairs (13-20 kbp), luciferase-encoding pDNA (later used for later transfection experiments) is only 5739 bp long. Hence, the question rose whether CDplexes formulated with either ctDNA or pDNA would have similar characteristics. Indeed, the results obtained for both paCDs in gel electrophoresis shift assays using luciferase-encoding pDNA were very similar to those obtained for ctDNA.

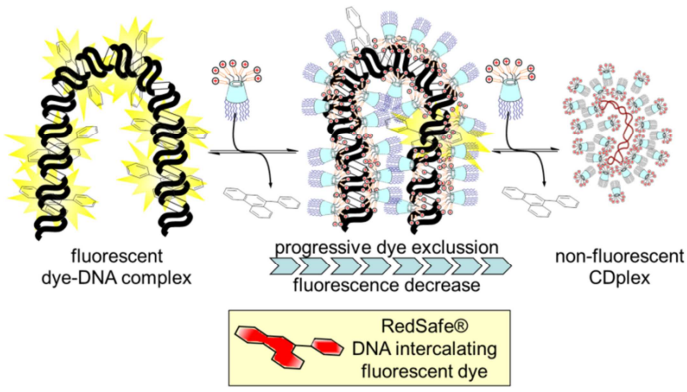

Figure 52. Schematic representation of the experiment designed for fluorescence tracking of CDplex formation and dissociation.

To get to the bottom of CDplex assembly, both paCD-DNA complex condensation and dissociation characteristics have been investigated by fluorescence spectroscopy techniques. For an insight into CDplex formation kinetics, a fluorescence quenching assay based upon exclusion of RedSafe™ (*iNtRON Biotechnology*), a DNA intercalating fluorescent dye, has been developed (Figure 52).[234] RedSafe™ forms a fluorescent complex with DNA, however, when the dye is progressively excluded due to formation of CDplexes that are capable of protecting DNA, fluorescence intensity decreases gradually. Absence of fluorescence eventually indicates complete DNA compaction.

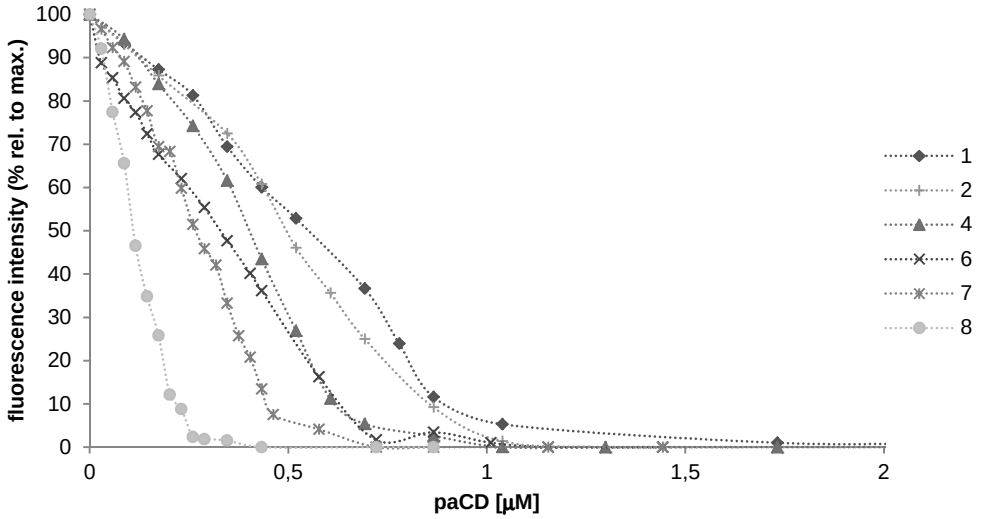

Figure 53. paCD-dependent RedSafe™ displacement assays of different paCDs.

In the title experiment, calf thymus DNA (3 µM in a base-pair basis) was incubated with different concentrations of each cationic CD in presence of the fluorescence reporter. Fluorescence intensity was monitored relative to [paCD], as depicted in Figure 53 (excitation at 295 nm and emission at 525 nm). The interactions between DNA and CD-scaffolded polycations were sufficiently strong, so that they could displace the fluorescent dye from the DNA strand, leading to a decrease in the fluorescence intensity of RedSafe™. It is worth mentioning that paCD concentration has been chosen as

independent variable of the experiment instead of N/P ratios. This facilitates comparison on a molar basis between linear and branched CD derivatives, since for the preparation of CDplexes with a given N/P ratio the number of moles of linear CD derivatives required triples that of branched CDs.

All paCDs proved to condense DNA at relatively low concentrations. However, those furnished with longer acyl chains were far more efficient to exclude the fluorescent intercalating agent, thereby reducing the fluorescence intensity. All assayed paCDs endowed with branched polycationic domains, i.e. compounds **6**, **7** and **8**, surpassed those with linear aminothioureido segments, i.e. derivatives **1**, **2** and **4**, clearly pointing out their more favorable hydrophobic/hydrophilic balance for CDplex formation. paCD **8** was the most efficient candidate at condensing DNA, followed by its analogs with shorter acyl chains. Branched paCD **6** showed comparable CDplex formation abilities to the linear derivative **4**. This undoubtedly confirms that tuning the balance of acyl chain length and charge density is crucial for efficient DNA complexation. As expected, acetylated linear paCD **1** performed worse than all other evaluated amphiphilic CDs. Fluorescent dye displacement assays of non-amphiphilic polycationic CDs **9** and **10**, however, did not match with the other results, since they seemed to displace RedSafe™ from the DNA strand at lower concentrations than their amphiphilic analogs (data not shown). As discussed before (see CAC measurements), this might be an artifact due to molecular inclusion of the fluorescent reporter into the cavity of the CD scaffold.

Despite extensive studies on the complex formation between nucleic acids and non-viral gene carriers unpacking of nucleic acids from delivery vectors is also essential to the gene delivery process. However, the dissociation mechanisms of most polycationic gene vectors are poorly known. The complexes may be dissociated in endosomes, in the cytosol or in the nucleus.[207] It has been reported that the transfection efficiency of polylysine (PLL) gene delivery systems is significantly enhanced by using low-molecular-weight PLL that can dissociate from DNA more rapidly than high-molecular-weight PLL.[235] Clearly, release of free nucleic acids from vectors is one of the most critical steps to determine the efficiency of non-viral gene delivery systems, as nucleic acids that remain bound to delivery vectors may be disabled to achieve expression. Thus, a correlation

between ease of complex dissociation and increases in transfection efficiency is quite evident.

To assess CDplex dissociation and to compare the relative stability in biological media, heparin competitive displacement assays were performed on representative paCD-DNA complexes at a complexation ratio of N/P 5. Heparin is an polyanionic polysaccharide that is present in the extracellular matrix in many tissues and are found on the cell surface.[236] Due to its anionic nature, Heparin can dissociate electrostatic complexes in a concentration dependent manner, as has been reported previously for lipoplexes,[237] polyplexes[238] and CD-based vectors.[169]

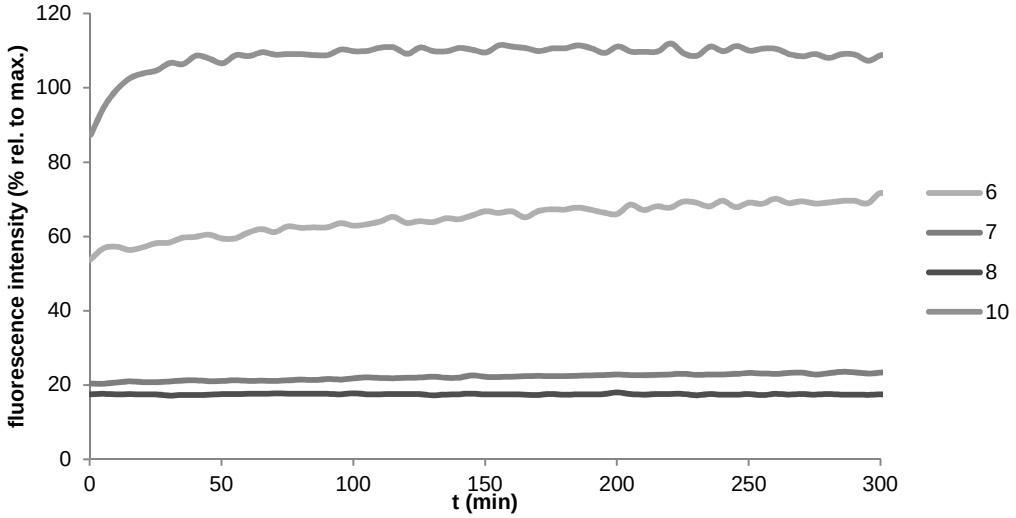

Figure 54. Time-dependent RedSafe™ displacement assays of different polycationic CDs.

To assess the stability of CDplexes towards heparin, pre-formed CDplexes were incubated with a given amount of heparin in the presence of RedSafe™ and fluorescence increase due to DNA release was monitored for several hours. Four paCDs, all belonging to the branched subseries, were assayed, i.e. compounds **6**, **7**, **8** and **10**, with the purpose of investigating the influence of acyl chain length on CDplex dissociation kinetics (Figure 54).

The results indicated that CDplex dissociation kinetics is drastically influenced by acyl chain length, thus RedSafe™ fluorescence is far faster recovered when CDs are tailored with short acyl chains or even lack them. After exposure to heparin for approximately 30 min, non-amphiphilic derivative **10** has released DNA completely, whereas its amphiphilic analogs with long acyl chains, i.e. **7** and **8**, did not show significant complex dissociation even after 5 hours. As expected, propanoylated CD **6** exhibited intermediate dissociation kinetics. In the case of CD derivative **10** the recovered fluorescence intensity surpassed the 100% mark. Since intensities were referenced to the fluorescence intensity derived from control free DNA, which is continuously being degraded, delayed DNA release may lead to relative higher fluorescence intensity. In conclusion, CDplexes composed of paCDs with longer acyl chains are more easily formed, but also very slowly dissociated. Though protection from environment is more efficient with long-acyl-chain paCDs, transfection efficiency may be hampered by slow DNA-release kinetics, thus requiring a fine balance of both features. In this sense, both the charge density and the hydrophobic/hydrophilic balance have to be finely tuned for efficient DNA complexation and subsequent release.

6. Gene transfer capabilities towards COS-7 cell lines

In collaboration with Dr. Christophe Di Giorgio (Univ. Nice-Sophia Antipolis, France) the gene transfer efficiency of CDplexes was evaluated towards COS-7 cells. For this purpose, a pDNA containing the gene encoding for luciferase (pTG11236, pCMV-SV40-luciferase-SV40pA) was used. Luciferase catalyzes the oxidation of luciferin in a light-emitting process (Scheme 10), being the amount of light produced associated to enzymatic activity and, thereby, to gene expression efficiency. In parallel, the total amount of proteins produced was also measured to estimate the metabolic activity of the transfected cells as compared to non-treated cells and the toxicity of the CDplexes.

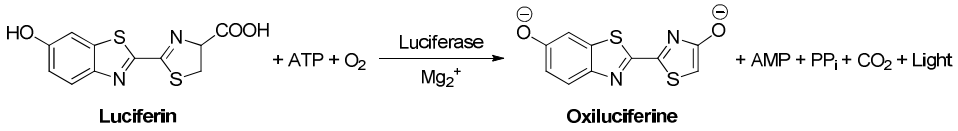

Scheme 10. Luciferase-catalyzed bioluminescent oxidation of luciferin.

The transfection conditions optimized in previous works were used.[177] CDplexes of all paCDs **1**-**8** differing in their hydrophobic/hydrophilic balance as well as their non-amphiphilic analogs CDs **9** and **10** were evaluated (Figure 55).

For comparative purposes, the naked pDNA and the commercial carrier JetPEI (22 kDa, optimal N/P ratio) were used as negative and positive controls, respectively. The assays were run with CDplexes formulated at N/P 2, 5 and 10 in serum-containing (10%) media. These N/P ratios have been previously shown to achieve the best transfection levels while preserving low to moderate toxicity profiles.[177] Conversely, despite the presence of serum proteins is known to be detrimental for gene transfer with CDplexes,[177] in order to preserve the biological relevance of the results it was decided to perform the experiments in its presence. The results, measured as the amount of expressed luciferase relative to the total proteins and expressed in a logarithmic scale, are collected in Figure 56.

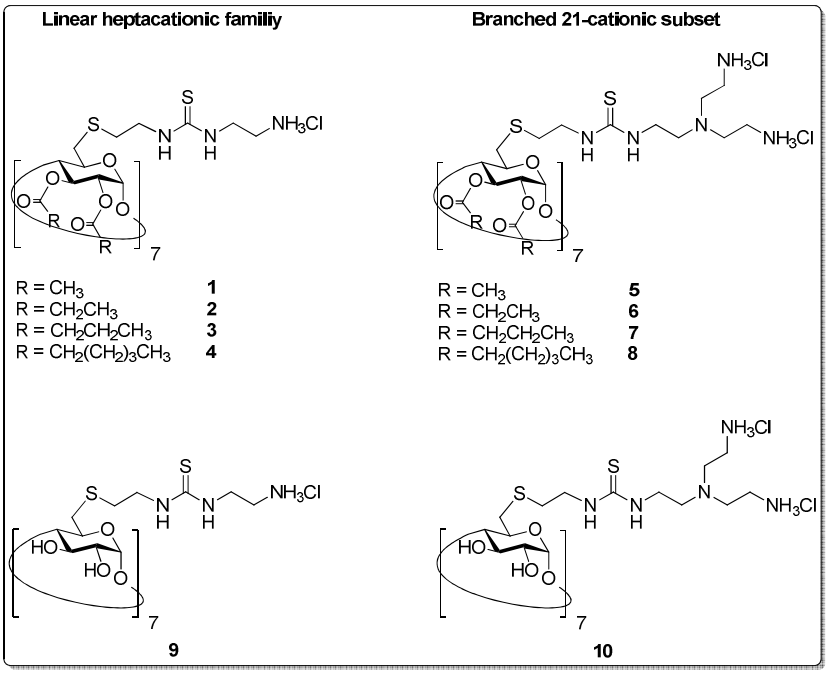

Figure 55. Library of polycationic CDs for gene transfer assays.

In agreement with previous observations in serum-devoid medium, non-amphiphilic CDs featured negligible gene transfer abilities in these experimental conditions. A barely 1-order of magnitude luciferase expression increase (as compared to naked pDNA) was achieved regardless of the number of cationic groups (7 or 21, for **9** and **10**, respectively). N/P ratio neither played a relevant role, except for the case of the CDplexes formulated with the heptacationic CD **9** at N/P 10, for with a relevant efficiency enhancement was measured but at the expense of much higher toxicity. Probably, the poor DNA-condensing abilities of these CDs are at the origin of their poor performance, although other non-amphiphilic cationic CDs have been shown to achieve remarkable efficiencies in other cell lines.[169]

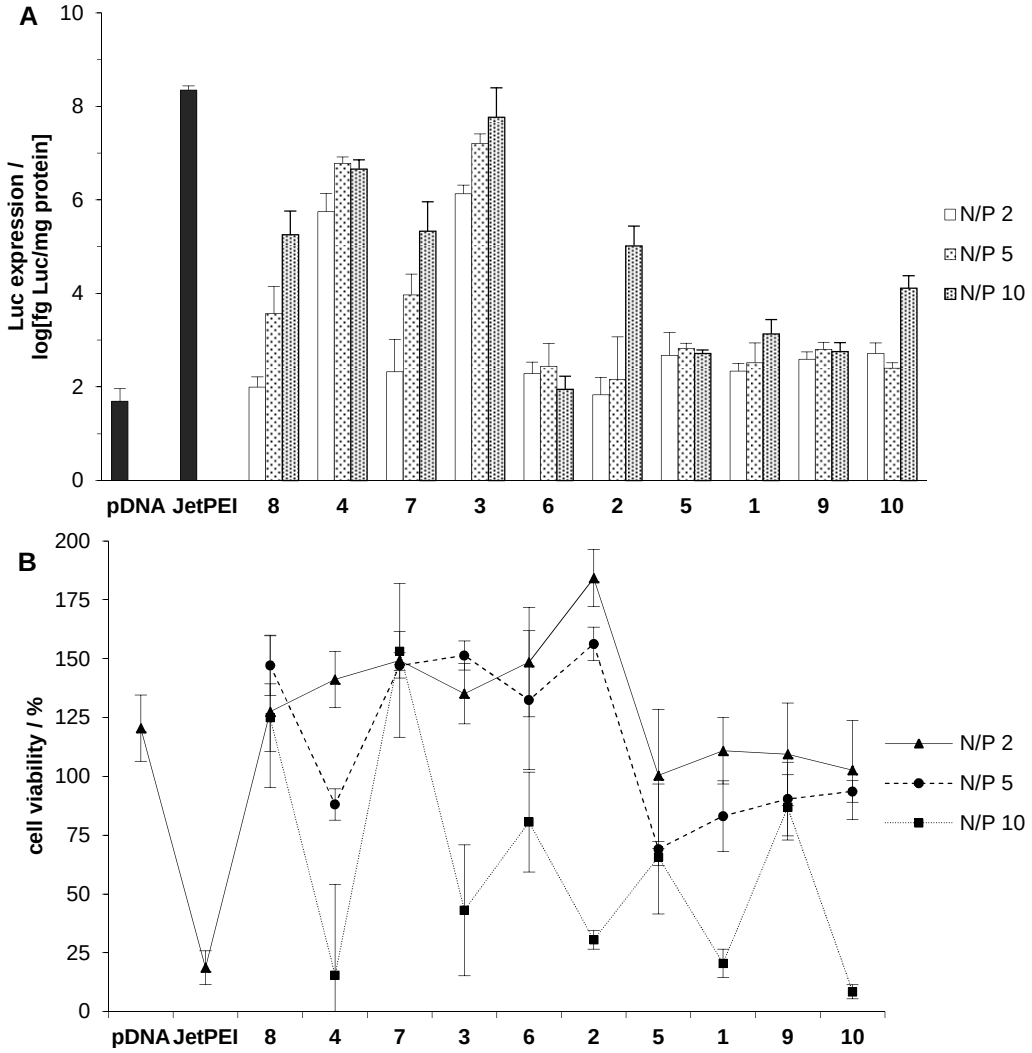

Figure 56. Luciferase-encoding gene transfer efficiency (A) and cell viability (B) in COS-7 cells treated with CDplexes formed with paCDs **1**-**8** and their non-amphiphilic counterparts **9** and **10** at N/P 2, 5 and 10. Naked pDNA and JetPEI polyplexes were used as negative and positive controls, respectively.

Despite their amphiphilic structure, the acetylated and propanoylated paCDs featured a similar behavior to the non-amphiphilic CDs. Luciferase expression increases as

compared to naked pDNA ranged between 1 to 2 orders of magnitude. Again heptacationic paCDs **1** and **2** at the highest N/P ratio (10) exhibited the largest efficiencies but also considerable toxicities. In any case, in the best performing conditions, luciferase expression resulted more than 3 orders of magnitude lower than that achieved with JetPEI. Though acetylated and propanoylated paCDs have been shown to efficiently condense and compact DNA at these N/P ratios, the stability of their CDplexes is largely compromised in competing media, as illustrated previously. We hypothesize that the reason for such poor performance may lay on the fact that serum-containing media could accelerate the dissociation of these particles, though other reasons may be considered. For instance, it has been shown that fusogenic capabilities of lipoplexes critically determine their cell membrane-binding and cell uptake abilities.[210b] These capabilities in paCDs equipped with short acyl chains are probably far from optimal.

The experiments with hexanoylated and butanoylated paCDs, however, revealed a quite distinct scenario. Both series exhibited much higher transgene expression efficiencies, which might be linked to the higher stability of their CDplexes (see preceding sections), and an N/P-dependent performance, the highest efficiencies generally achieved at N/P 10. In contrast to previously reported observations in serum-devoid media,[177] heptacationic paCDs resulted more efficient than 21-cationic ones. Even considering the paCD-pDNA mass instead of N/P ratio, heptacationic paCDs resulted more efficient than their branched counterparts. The branched paCDs **7** and **8**, regardless of the acyl chain length, featured gradual transgene expression efficiency enhancement upon N/P increase and remarkably low cytotoxicities even at N/P 10. Interestingly, the CDplexes formulated with the corresponding heptacationic conjugates **3** and **4** resulted better performing even at the lowest N/P ratio (2). In this case, efficiency increased only mildly with N/P and was handicapped due to cytotoxicity at N/P 10 (as also observed for heptacationic CDs with shorter acyl chains).

A remarkable efficiency decrease was observed for CDplexes formulated with paCD **8** in the presence of serum. paCD **8** has been previously reported to surpass JetPEI efficiency towards COS-7 cells,[177] though in 10% serum-containing media, efficiency drops by 3 orders of magnitude. It is also noticeable that the performance of its

heptacationic analog is only mildly affected by the presence of serum. And, the dramatic performance differences between butanoylated and propanoylated paCDs, which may arise from the comparatively distinct stability of their CDplexes in biological media, were even more astonishing.

Altogether, these experiments led to the identification of the butanoylated heptacationic CD **3** as the best performing candidate, exhibiting luciferase expression levels almost equaling that of JetPEI but with a slightly better cytotoxic profile (43% vs. 19% cell viability for **3** and JetPEI, respectively, at their best N/P ratio). A slightly lower but virtually non-toxic performance was achieved at N/P 5 with the same compound. These results also highlight that, despite paCD **3** is not the most efficient at DNA complexation, dynamics and kinetics of CDplex formation play a critical role in overall performance. Unfortunately, performance cannot be anticipated so far, due to the complex balance of supramolecular features that should be taken into account. But the reported results can be considered as a useful tool to experimentally tune up the carrier capabilities towards a particular target.

CHAPTER 3 - DESIGN OF CD-SCAFFOLDED CYCLIC POLYAMINE CLUSTERS: ENGINEERING OLIGONUCLEOTIDE BINDING PATTERNS IN NON-VIRAL GENE DELIVERY

1. Novel DNA binding motifs at improving the efficiency of artificial gene carriers

A large array of cationic epitopes has been explored as nucleic acid binding elements. The topic has been comprehensively reviewed very recently.[72a] Some of the most commonly used are depicted in Figure 57. Amines with different substitution and pH-dependent ionization degree are by far the most frequently used. Quaternary ammonium groups are permanently charged at any pH and consequently devoid of buffering capability.[86] Amines and ammonium groups are rarely found alone, but combined in the most bewildering way to enhance their nucleic acid binding abilities and displayed onto polymeric or lipidic platforms aimed at zipping oligonucleotides through multipoint concerted interactions.

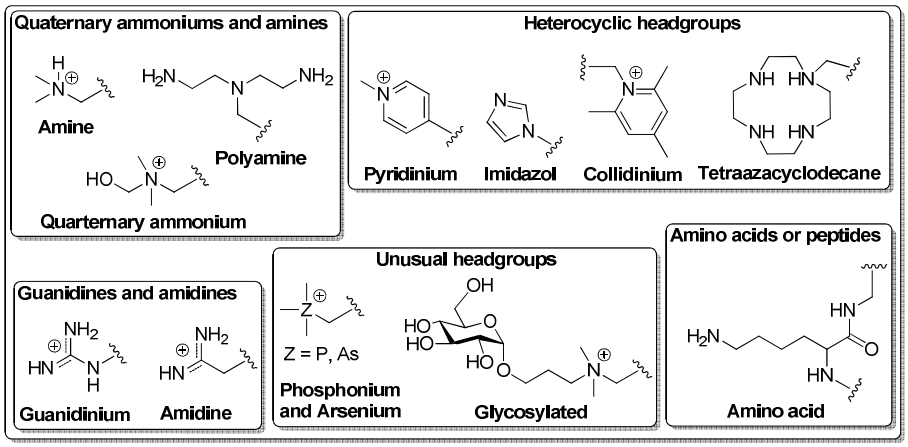

Figure 57. Illustrative examples of some commonly used of cationic headgroups for non-viral gene carrier design.

Aimed at exploring the effect of alternative cationic headgroups on paCD-based gene carriers, we have turned our attention to cyclic oligoamines, such as cyclen (1,4,7,10-tetraazacyclododecane) and cyclam (1,4,8,11-tetraazacyclotetradecane), featuring quite

unique DNA-binding.[239] Cyclen and cyclam are known to form stable complexes with transition metal ions.[240] Cyclen and its simple *N*-functionalized derivatives, such as DOTA[241] (N^1,N^4,N^7,N^{10}-cyclentetraacetic acid) and DOTAM[242] (N^1,N^4,N^7,N^{10}-cyclentetraacetamide, Figure 58) are widely used in the construction of a wide variety of functional molecules such as contrast agents for magnetic resonance imaging (MRI),[243] single photon emission computed tomography (SPECT)[244] and positron emission tomography (PET),[245] fluorescent[246] and luminescent[247] probes and metal sensors.[248] Many studies have also revealed that both cyclen[249] and its metal complexes[249b,250] may behave as artificial nucleases, featuring DNA-cleavage abilities, and protease-like catalytic activity.[251] Macrocyclic polyamines, e.g. cyclen, cyclam or bicyclam AMD3100[252] (1,1′-[1,4-phenylenebis(methylene)]bis(1,4,8,11-tetraazacyclotetradecane), Figure 58) have also exhibited antitumor and anti-HIV activity.[253]

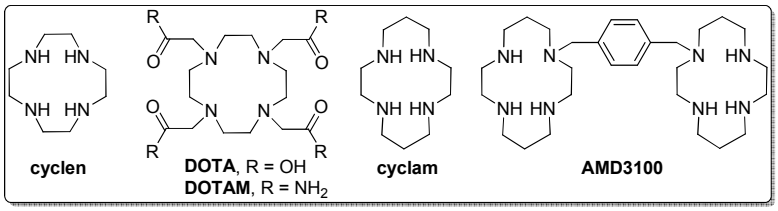

Figure 58. Structures of cyclen, its derivatives DOTA and DOTAM, cyclam and bicyclam AMD3100.

Metal complexes of cyclam such as AMD3100-^{64}Cu have been shown to be suitable PET probes for tracking cancer cells in vivo.[254] Furthermore, ADM3100-based lipidic and polycationic conjugates have been exploited as cancer cell-targeted non-viral gene vectors.[252,255]

Several factors may account for the unique oligonucleotide binding capabilities of cyclic oligoamines, such as cyclen and cyclam. The preorganization of the cyclic scaffolds may influence the phosphate binding capacity in a positive manner. The cyclen moiety is composed of repeated ethylenediamine units, comparable to those in PEI, while cyclam alternates ethylenediamine and propylenediamine segments. The cyclic arrangement of

amino groups in macrocyclic oligoamines exerts an important influence on their pK_a values (Figure 59).[256,257]

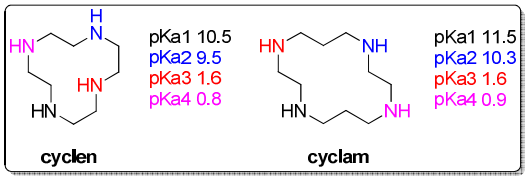

Figure 59. pK_a values of cyclic oligoamines.

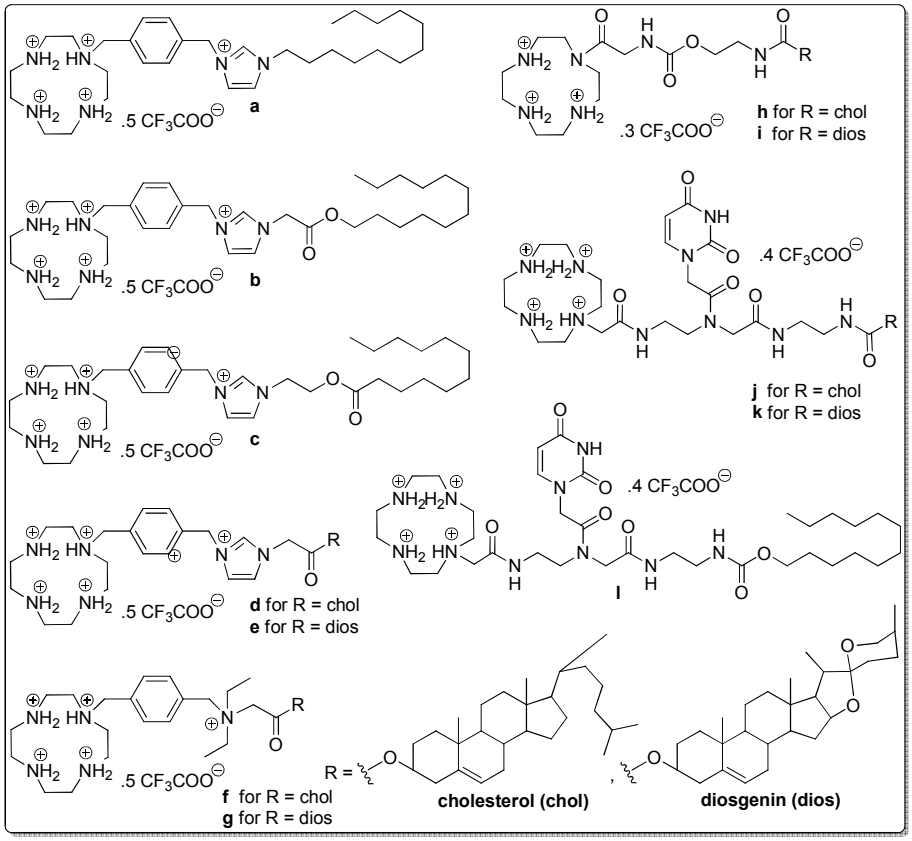

Figure 60. Molecular structures of lipids with cationic cyclen headgroups as gene vectors synthesized by Yu and co-workers.[239a,259,260]

Considering these features, it is somehow surprising that the use of cyclic oligoamines in gene delivery has being barely investigated. To the best of our knowledge, until 2008 only a single example of cyclen-based gene delivery system was reported, i.e. a dendritic polymer with a cyclen core.[258] It was only five years ago when application of cyclen as DNA binding motif in gene vectors got rolling. Yu and co-workers[239b] were the first to describe a cationic lipid with a protonated cyclen headgroup (Figure 60a), yet this imidazolium salt group-containing gene carrier showed very poor transfection efficiency. To overcome this drawback, the same research group made a considerable effort and synthesized over the years a series of lipids bearing cyclen as cationic headgroup[239a,259,260] (Figure 60b-l). By systematic modifications of both the hydrophobic tail[259] and the functional linking group[239a,260] gene delivery efficacies could be improved dramatically and transfection efficiencies of most cyclen-based cationic lipids surpassed that of Lipofectamine 2000™, thus exhibiting similar or slightly lower cytotoxicities than the lipoplexes prepared from Lipofectamine 2000™ and illustrating the potential of SAR in the improvement of transgene expression efficiency.

Arbuthnot and co-workers[261] reported a cyclen-conjugated cholersteryl derivative containing biodegradable carbamate linkers, and lipoplexes containing this lipid proved to be non-toxic DNA and siRNA delivery systems (Figure 61). Although cyclen-based lipoplexes resulted in efficient siRNA-mediated target gene silencing, almost catching up the efficiency of Lipofectamine 2000™, their efficiency was poor for DNA transfection.

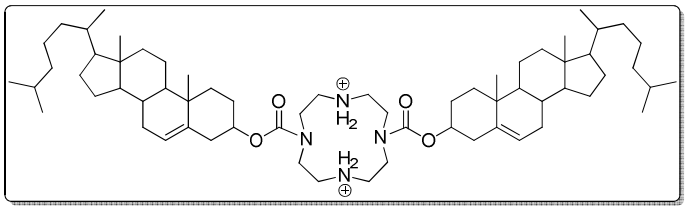

Figure 61. Molecular structure of the cyclen-conjugated cholersteryl derivative reported by Arbuthnot and co-workers.[261]

Nearly at the same time, cyclen-based polymers emerged.[262] Yu and co-workers have pioneered the field of investigating cyclen-based cationic polymers for gene delivery. Initially, a cyclen-based side-chain homopolymer capable of self-assembling in presence of pDNA has been prepared by Yu and co-workers,[262] however, its transfection efficiency has not been reported so far (Figure 62a).

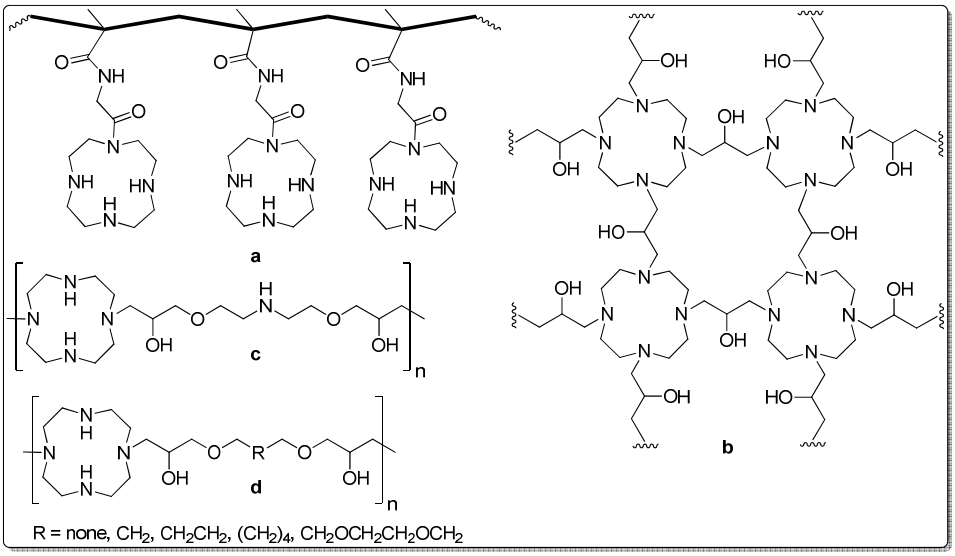

Figure 62. Molecular structures of cyclen-based cationic polymers as gene vectors synthesized by Yu and co-workers.[262,263,264,265]

Recently, the same research group has reported a variety of cyclen-based polymeric vectors, including reticular cyclen-based polymer (Figure 62b),[263] linear cyclen-based polyamine (Figure 62c),[264] as well as diolglycidyl ether-bridged cyclens (Figure 62d).[265] A biodegradable disulfide-linked version of the latter has been also reported.[266] Almost all cyclen-based cationic polymers showed transfection efficiencies close to that of PEI (20 kDa or 25 kDa) at N/P ratios in the range of 5-15 but reduced cytotoxicities.

In addition, Jiang and co-workers[267] synthesized chitosan grafted with two kinds of macrocyclic polyamines, i.e. cyclen and 1,4,7-triazacyclononane (TACN), at either C-2 or the C-6 position (Figure 63). They showed that, depending on the functionalization

position, physicochemical features could be tailored. Indeed, C-2-grafted chitosanes exhibited higher cytotoxicity and transfection efficiency than those grafted at C-6.

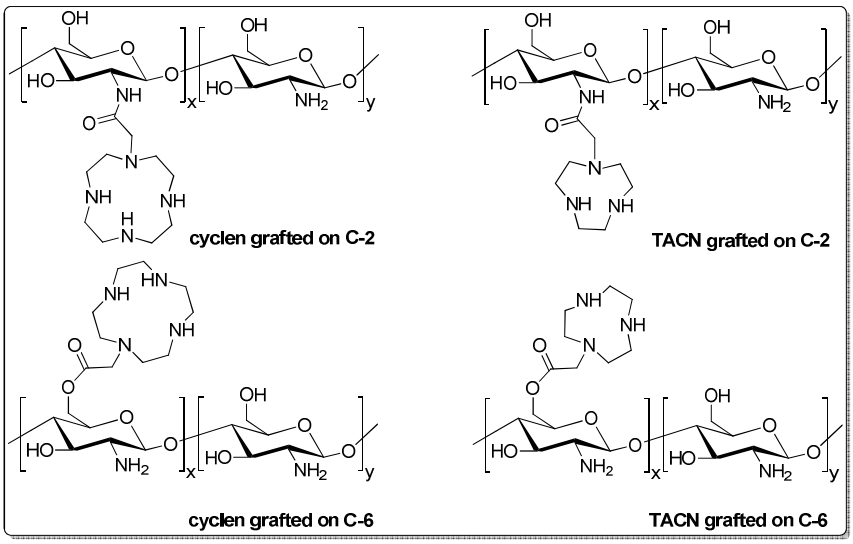

Figure 63. Structures of chitosan grafted with cyclen or TACN on different positions.

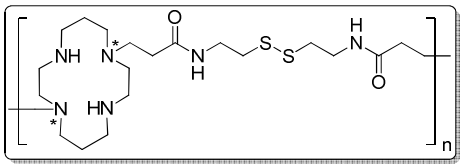

Figure 64. Structure of reducible polycationic chelators based on cyclam (The precise attachment position of the linker could not be determined. Any of the secondary amines are susceptible to modification).

Besides, Oupický and co-workers[268] described the first comprehensive report on the SAR of cyclam-based polymeric gene vectors (Figure 64). They designed a series of bio-reducible cyclam-based polycationic Cu(II) chelators (RPCs) aimed at combining gene delivery and real-time PET monitoring. The cyclam moieties in the polycations retained their ability to form complexes with Cu(II). The presence of disulfide bonds in the

polycations resulted in substantially lower cytotoxicity than 25 kDa PEI. RPCs, regardless of the presence or the absence of Cu(II) ions, exhibited high transfection activity in vivo.

With the purpose of disclosing the role of the cationic element in gene delivery, taking advantage of the modular design of paCDs, a set of monodisperse paCDs with different displays of cyclic oligoamines on the primary has been prepared using “click chemistry” methodologies and their physicochemical properties and structure-activity relationships have been explored. In particular, this chapter comprises the following aspects:

- synthesis of CD-scaffolded amphiphilic cyclic polyamine clusters,
- investigation of their self-assembling capabilities in aqueous environment,
- evaluation of their pH buffering capacities,
- assessment of their DNA-condensing abilities,
- and evaluation of their gene transfer capabilities towards COS-7 and HeLa cells.

2. Design and synthesis of amphiphilic CD-scaffolded cyclic polyamine clusters

Making use of the face-selective hydroxyl manipulation methodologies and following a similar skirt-type arrangement described before (Figure 65), lipophilic segments were introduced into the secondary rim of the CD core by esterification with long-chain acyl anhydrides in the presence of DMAP, thereby ensuring homogeneous acylation.[174] The length of the acyl chains is a critical parameter. As has been demonstrated in the preceding chapter, compounds furnished with hexanoyl functionalities proved to be the most efficient ones concerning self-assembling, DNA-condensing and gene delivery capabilities. Consequently, hexanoyl chains were used to construct the hydrophobic domain.

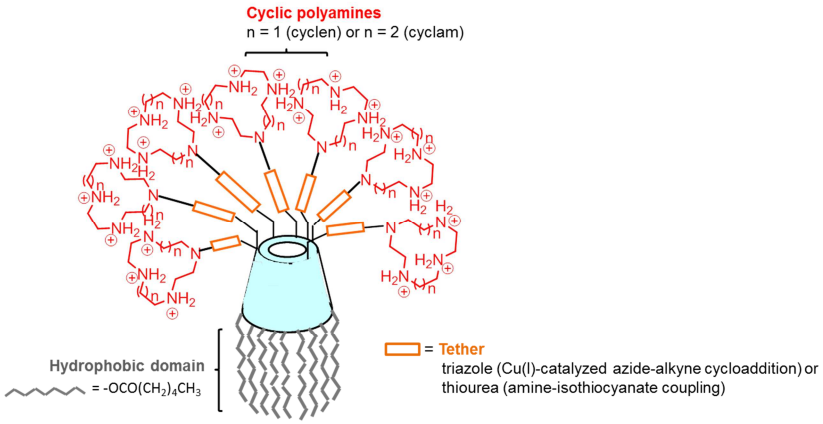

Figure 65. Schematic representation of the general structure of CD-scaffolded cyclic polyamine clusters.

The multiple coupling of the βCD core with the cationic polyamine segments is a crucial synthetic step, since very efficient reactions are required to warrant monodispersity. In addition to the thiourea-forming used in the preceding chapter, the Cu(I)-catalyzed azide-alkyne cycloaddition (CuAAC) [144,169,180] has been exploited. Both

reactions have been shown to yield homogeneous conjugates, thereby the choice would be conditioned by the nucleic acid binding capabilities of the target structure rather than the reactivity itself.

The synthetic approach comprises the preparation of secondary rim-acylated CD building blocks on the one hand, and synthesis of appropriate cyclic polyamine derivatives on the other hand. Synthesis of the CD building blocks involved installation of a suitable functional group on the primary rim of the CD core, capable of undergoing "click" coupling reactions, and subsequent esterification of the secondary rim, as shown in Scheme 11.

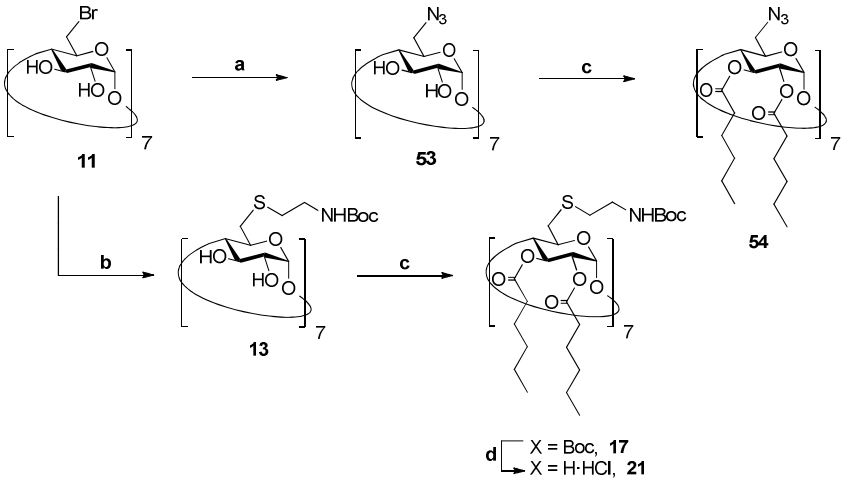

Scheme 11. Synthesis of lipophilic tail-containing CD building blocks **54**[180b] and **21**[177]. Reagents and conditions: a) NaN_3, DMF, 80 ºC, 24 h, 88%; b) $BocHN(CH_2)_2SH$, Cs_2CO_3, DMF, 60 ºC, 48 h, 70%; c) hexanoic anhydride, DMAP, DMF, 70 ºC, 16 h, 78%; d) i, 1:1 TFA-DCM, 2 h; ii, HCl, 99%.

Starting from **11**,[175] nucleophilic substitution of the bromine atoms by either azide (→ **53**)[269] or *N*-Boc-protected cysteamine (→ **13**)[185a] took place with excellent yields. Subsequent acylation of the secondary hydroxyl groups in the presence of DMAP in DMF furnished compounds **54**[180b] and **17**[177] in good yield. Finally, acidic hydrolysis of the carbamate groups of *N*-Boc protected compound **17** in quantitative yield led to the free

amine CD building block **21**.[177] Although both CD derivatives **54** and **21** could also be prepared via an alternative synthetic route, i.e. reversing the order of functionalization of the two CD faces, this alternative synthetic requires an additional chromatographic purification.

On the other hand, both cyclen and cyclam are commercial available, though due to its expensiveness of the former (226 € per g, *Aldrich*), it was synthesized following the reported methodologies.[240] Among the different strategies for the preparation of cyclen derivatives (Scheme 12)[240], the most straightforward method is the 3+1 type cyclization. This approach was used by carrying out a Richman and Atkins condensation[270] of linear 1,7-disodium salt of 1,4,7-tritosyl-1,4,7-triazaheptane **55**[271] with a biselectrophile, namely 1,3,5-tritosyl-3-azapentane **56**,[272] to obtain compound **57**[273] in good yields (Scheme 13).

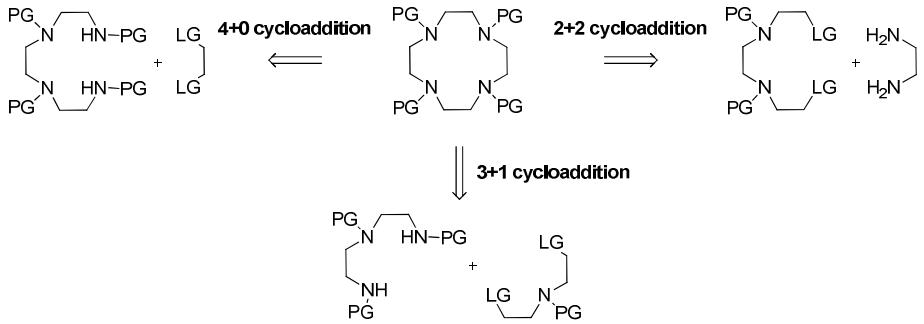

Scheme 12. Synthetic strategies for cyclen ring formation from acyclic precursors (PG protecting group, LG leaving group).

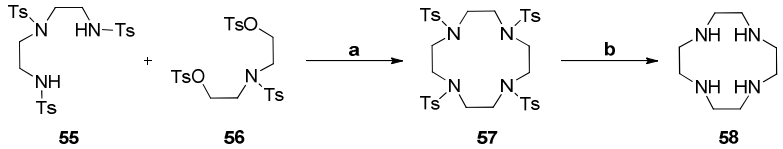

Scheme 13. Synthesis of cyclen via a 3+1 type cyclization. Reagents and conditions: a) i, treatment of 55 with EtONa in EtOH, reflux, 5 min, 100%; ii, addition of 56 in DMF, 100 ºC, 20 h, 80%; b) i, conc. H_2SO_4, 100 ºC, 72 h; ii, 50% NaOH, 77%.

The resulting tetratosylated cyclen derivative **57** underwent H_2SO_4-mediated detosylation followed by alkaline aqueous work-up, yielding cyclen **58** in 77% overall yield. It is worth mentioning that final strongly alkaline aqueous work-up is essential, since free amine groups are required to successfully perform the posterior disymmetrization of the macrocyclic tetraamine.

Tethering cyclen and cyclam to the CD scaffold requires selective functionalization with appropriate reactive groups, i.e. alkyne and isothiocyanate functionalities for click coupling to per-azido CD **54**[180b] and per-amino CD **21**,[177] respectively. The direct formation of compound **60** by obviously more straightforward *N*-monofunctionalization of cyclen **58** with propargyl bromide, however, failed to produce the target product due to cumbersome purification and poor reaction yields. Although the rather different basicity of the four amino groups present in the cyclen ring should allow in principle for selective *N*-monofunctionalizations,[274] a mixture of products was obtained and cyclen derivative **60** was isolated in a rather poor 12% yield.

Alternatively, selective protection of amines prior to *N*-monoalkylation has been considered. The disposition of amino groups on the cyclic scaffold results especially favorable for selective protection of amines as *tert*-butylcarbamates.[275] As reported in literature, reaction of cyclen with di-*tert*-butyldicarbonate gives the *N*-tri-protected product in high yield,[276] and subsequent *N*-monoalkylation proceeds smoothly. Therefore, this efficient route was employed for the synthesis of cyclic polyamine building blocks furnished with alkyne or isothiocyanate functionalities (Scheme 14).

Selective tri-*N*-Boc protection of free amine **58** was performed as described in literature[276] using DCM as solvent instead of chloroform, which proved to afford improved yield of tri-*N*-Boc-cyclen **61** to 76%. Reaction conditions were extrapolated to cyclam **59**, which could be transformed into the corresponding tri-*N*-Boc protected macrocyclic tetraamine **62** in good yield.

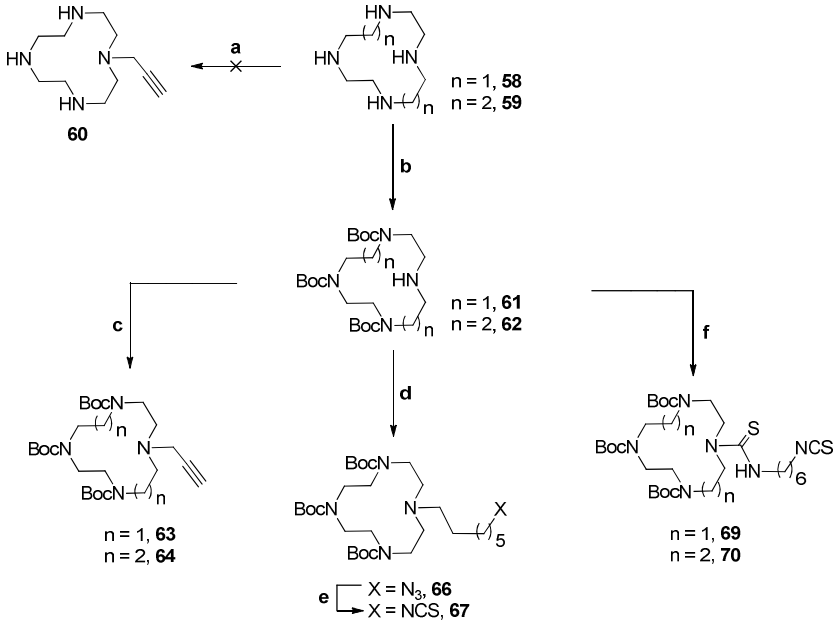

Scheme 14. Synthesis of cyclic polyamine building blocks. Reagents and conditions: a) **58**, propargyl bromide, Et_3N, $CHCl_3$, 60 ºC, 24 h, 12%; b) **58** (→**61**) or **59** (→**62**), Boc_2O, DCM, 20 h, 76% (→**61**) or 72% (→**62**); c) **61** (→**63**) or **62** (→**64**), propargyl bromide, Et_3N, CH_3CN, µw, 120 ºC, 1 h, 51% (→**63**) or 35% (→**64**); or rt, 72 h, 71% (→**63**) or 67% (→**64**); d) **61**, *n*-1-azido-7-bromoheptane **65**, Et_3N, CH_3CN, µw, 120 ºC, 1 h, 93%; e) TPP, CS_2, dioxane, 3 h, 71%; f) **61** (→**69**) or **62** (→**70**), 1,6-hexamethylenediisothiocyanate **68**, Et_3N, DCM, rt, 16 h, 85% (→**69**) or 90% (→**70**).

As both cyclen and cyclam building blocks would be linked to the CD core by either thiourea-forming reaction or by CuAAC reaction, compounds **61** and **62** have been furnished with different tethers containing the corresponding anchor groups. In order to consecutively perform CuAAC reaction with CD heptaazide **54**, compounds **61** and **62** were *N*-alkylated with propargyl bromide. In both cases, alkylation reactions proceeded slowly at room temperature, although in good yields (71% for **63** and 67% for **64**, respectively, Scheme 14). Interestingly, µw irradiation significantly shortened reaction times, but at the expense of yields.

To obtain isothiocyanate-armed cyclen and cyclam derivatives for subsequent thiourea-forming reaction with CD heptaamine **21**, initially a similar *N*-alkylation approach to that described above was used. Reaction of tri-*N*-Boc protected cyclen **61** with *n*-1-azido-7-bromoheptane **65**, prepared by statistic substitution of *n*-1,7-dibromoheptane, under μw irradiation afforded azide **66** in good yield. Aza-Wittig type reaction of azide **66** with triphenylphosphine-carbon disulfide[277] afforded the corresponding isothiocyanate **67**. Alternatively, cyclic polyamine derivatives **61** and **62** were reacted with an excess of 1,6-hexamethylenediisothiocyanate **68**[278] to afford cyclen and cyclam-derived thioureas **69** and **70**, both furnished with a terminal isothiocyanate group on the aliphatic spacer. These dissymmetrization reactions proceeded smoothly in excellent yields and formation of bis-cyclen derivatives was not observed, provided a sufficiently large excess of diisothiocyanate was used (3 eq).

In order to obtain CD-scaffolded cyclic polyamine clusters, both the CD building blocks **54** and **21** and the armed cyclen and cyclam derivatives **63**, **64**, **67**, **69** and **70** were then coupled by “click chemistry” methodologies (Scheme 15 and Scheme 16). The coupling of the CD core with the cyclic oligoamine blocks is not trivial, since coupling reactions are to take place at seven positions simultaneously, which requires very efficient procedures to warrant monodispersity.

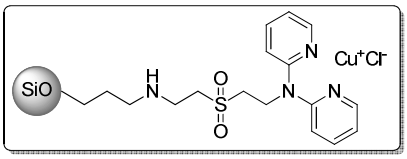

Figure 66. Structure of silica-supported heterogeneous catalyst Si-BPA·Cu^{+}.

The sevenfold Cu(I)-catalyzed azide-alkyne cycloaddition reaction between heptaazide **54** and alkynes **63** and **64** was accomplished using Si-BPA·Cu^{+} as solid-supported catalyst in refluxing 3:1 ^{t}BuOH-H_2O. Recent results had indicated the efficiency of silica-based nanoparticles incorporating bis(pyridyl)amine (BPA) Cu(I) chelating adsorbents Si-BPA·Cu^{+} to catalyze multiple CuAAC couplings[180a,279] (Figure 66).

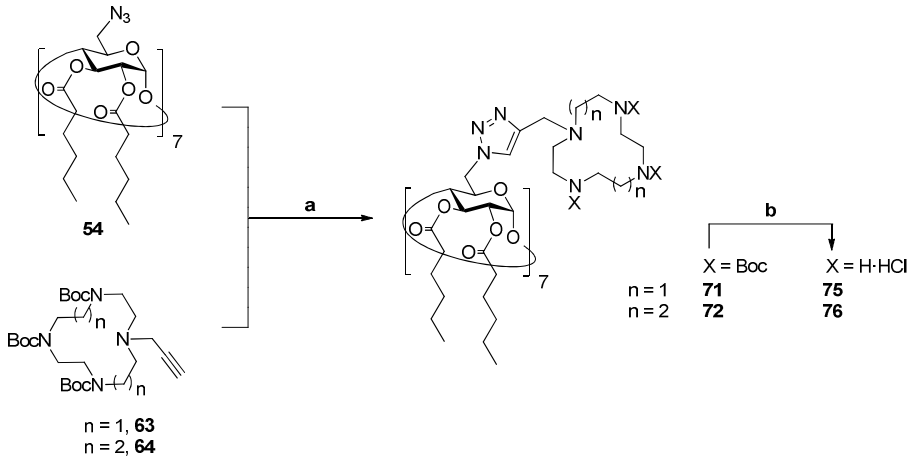

Scheme 15. Synthesis of cyclic oligoamine-grafted paCDs **75** and **76** by CuAAC reaction. Reagents and conditions: a) **63** (→**71**) or **64** (→**72**), Si-BPA·Cu^{+}, ^{t}BuOH-H_2O, reflux, 16 h, 97% (→**71**) or 84% (→**72**); b) i, 1:1 TFA-DCM, 2 h; ii, HCl, quantitative yield in both cases.

Homogeneous heptatriazoles **71** and **72** were obtained in remarkable yields (97% for **71** and 84% for **72**, respectively, Scheme 15) after purification by flash column chromatography. ESI-MS and NMR confirmed homogeneity of both compounds and neither ESI-MS nor elemental analysis detected traces of copper ions (Figure 67; see Figures S40 and S41 for NMR and Figures S119 and S120 for MS spectra, Supporting Information). Although NMR spectra of CD-scaffolded cyclic polyamine clusters **71** and **72** were recorded at elevated temperatures (60 ºC), line broadening due to restricted flexibility of Boc-protected cyclic polyamine segments was evident.

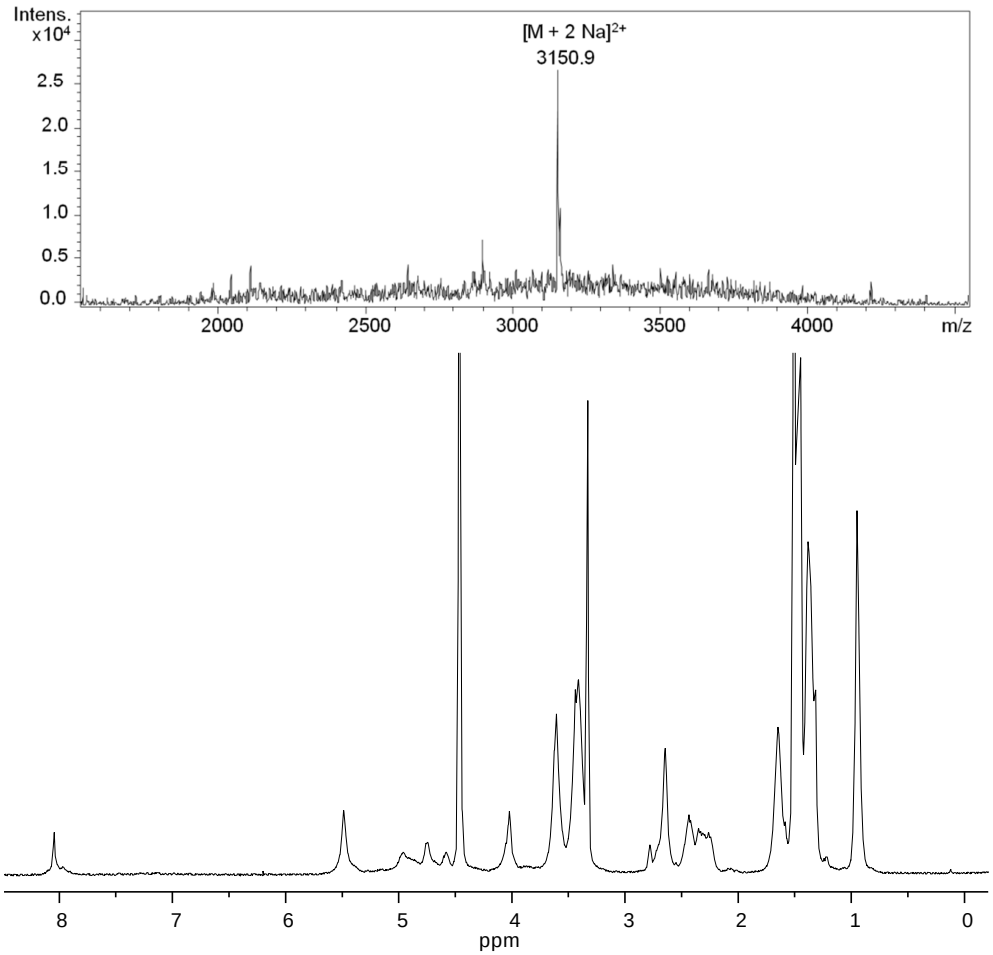

Figure 67. ESI-MS (top) and ^{1}H NMR (bottom, 500 MHz, MeOD, 333 K) spectra of compound **71**.

All attempts to couple isothiocyanate derivative **67** to heptaamine **21** in a thiourea-forming reaction failed to furnish the heptabranched product homogeneously. However, coupling of isothiocyanate derivatives **69** and **70**, respectively, and CD building block **21**, followed by purification by size exclusion chromatography, afforded monodisperse CD derivatives **73** and **74** in excellent yields, i.e. 75% for **73** and 77% for **74**, respectively (Scheme 16).

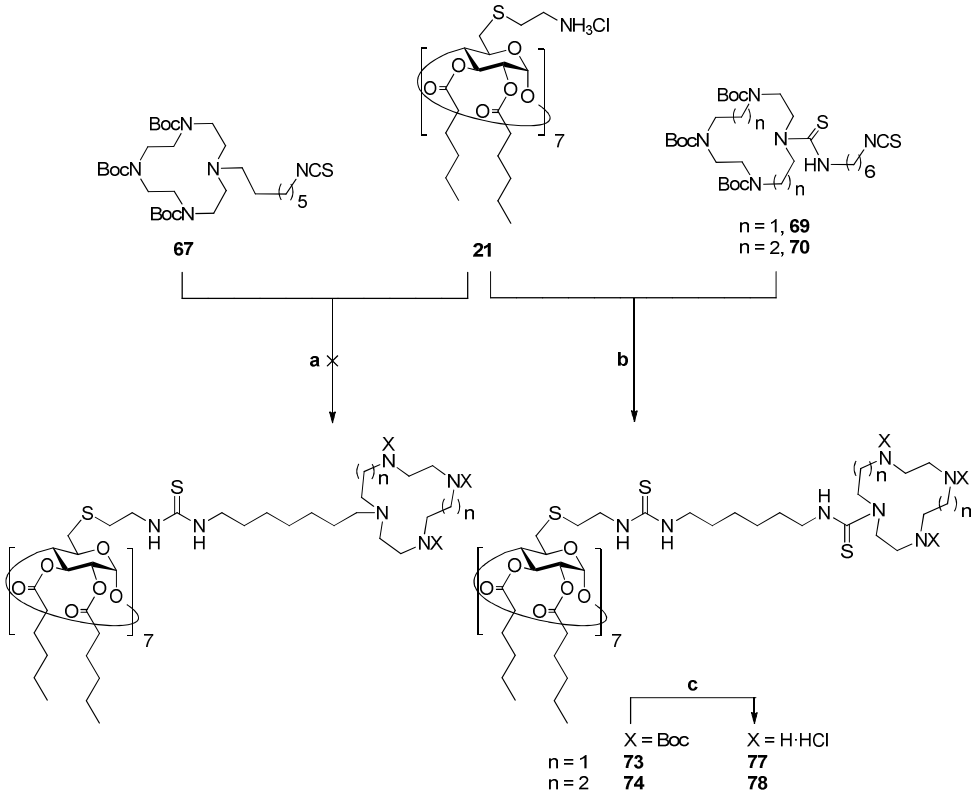

Scheme 16. Synthesis of cyclic oligoamine-grafted paCDs **77** and **78** by thiourea-forming reaction. Reagents and conditions: a) Et_3N, DCM, 40 ºC, 72 h; b) **69** (→**73**) or **70** (→**74**), Et_3N, DCM, 40 ºC, 72 h, 75% (→**73**) or 77% (→**74**); c) i, 1:1 TFA-DCM, 2 h; ii, HCl, quantitative yield in both cases.

Homogeneity of both heptathiourea derivatives was confirmed by NMR and ESI-MS, as illustrated for **74** in Figure 68 (see Figures S42 and S43 for NMR and Figures S121 and S122 for MS spectra, Supporting Information). As observed for the heptatriazole analogs, NMR spectra of compounds **73** and **74** showed broad signals even at high temperatures.

Final carbamate hydrolysis in compounds **71**-**74** using TFA-DCM afforded the target compounds **75**-**78** in virtually quantitative yields after lyophilization.

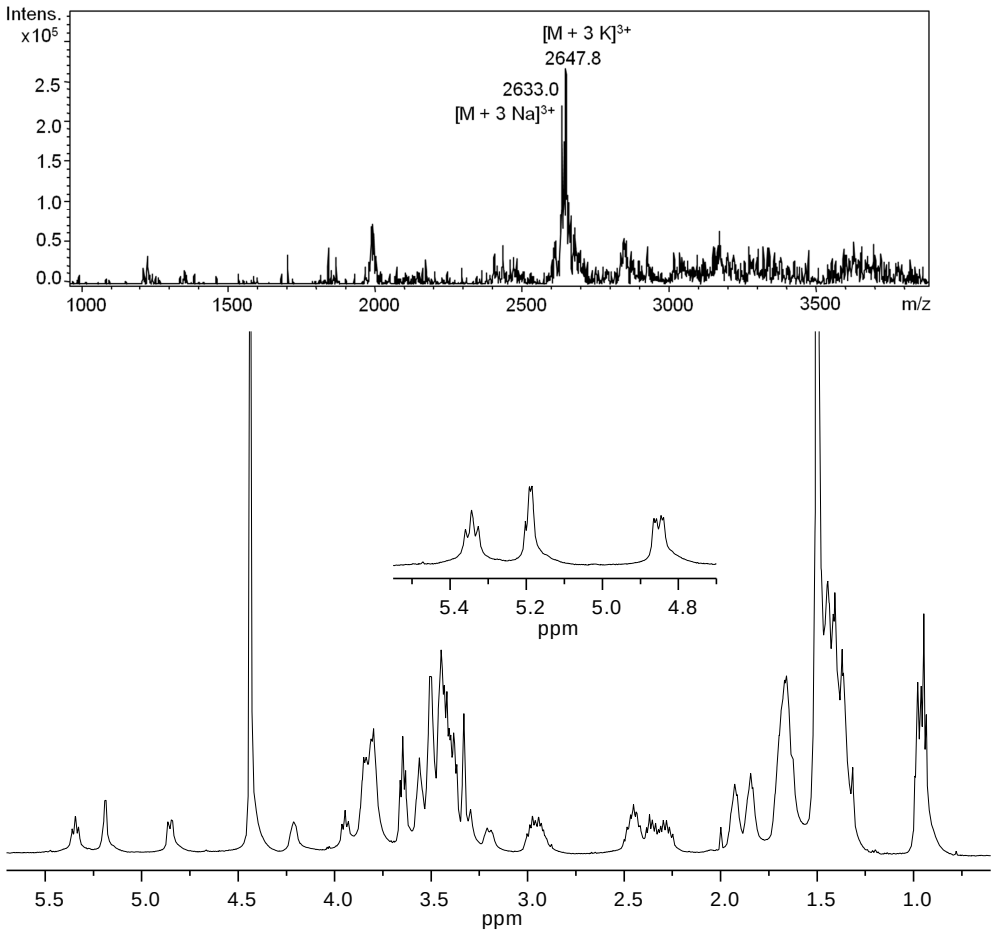

Figure 68. ESI-MS (top) and ^{1}H NMR (bottom, 500 MHz, MeOD, 333 K) spectra of compound **74**.

The set of CD-scaffolded cyclic polyamine clusters synthesized exhibits structural resemblance with the most efficient compounds studied in Chapter 2. Keeping the hydrophobic domain on the secondary rim unaltered, the polycationic head has been modified by introducing cyclic elements. The number and nature of protonable amino groups, however, differ among these compounds. Whereas branched polyamine segments contain two primary amines and one tertiary amine, cyclic polyamines possess three secondary amino groups in the case of the thiourea-tethered derivatives **77** and **78**,

and an additional tertiary amino group in the case of triazole-linked paCDs **75** and **76**. As anticipated by literature, theoretical calculations (*MarvinSketch, ChemAxon*) predict large disparities in pK_a values of each amino group, which, as later demonstrated, exert important effects on the pH buffering abilities of these compounds (Figure 69).

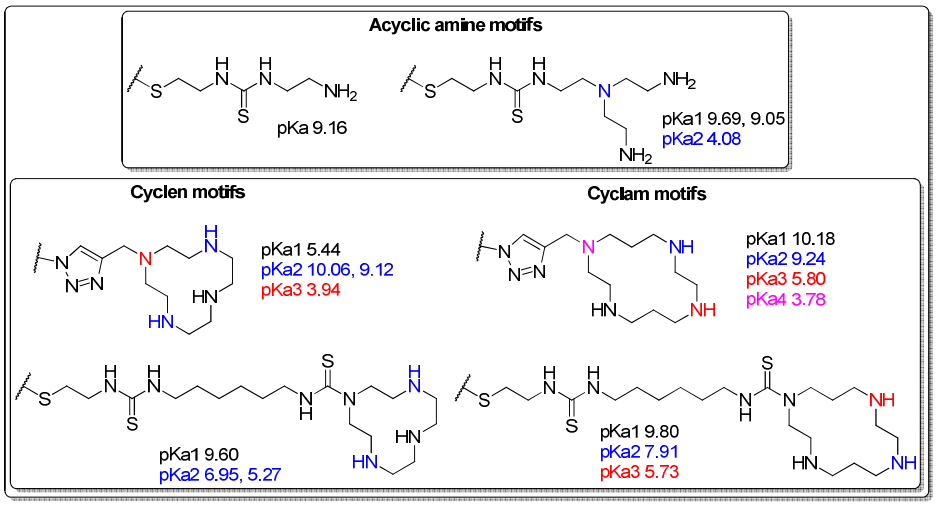

Figure 69. Calculated pK_a values for acyclic and cyclic polyamine motifs.

Cyclen derivative **60** has been also exploited as scaffold for further installing additional oligoamine branches. Thus, a series of isothiocyanate-armed Boc-protected (oligo)amines were prepared according to the sequence depicted in Scheme 17. Monotritylation of a terminal amino group and Boc-protection of the remaining amines was followed by selective trityl group cleavage. In situ treatment of the resulting monoamines with thiophosgene. furnished the target isothiocyanates derived from ethylenediamine, diethylenetriamine and spermine (**12**,[186] **85**,[177] and **86**, respectively) in good overall yields.

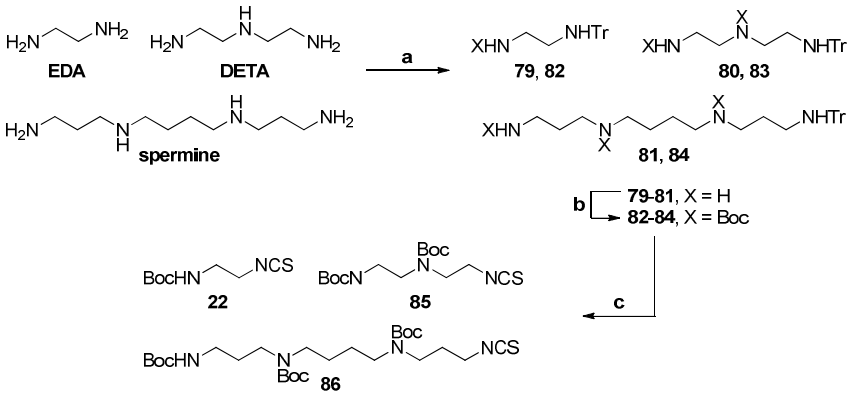

Scheme 17. Synthesis of aliphatic linear isothiocyanate compounds **22**,[186] **85**[177] and **86**. Reagents and conditions: a) EDA (→**79**), DETA (→**80**), spermine (→**81**), TrCl, DCM, 14 h, 89-95%; b) **79** (→**82**), **80** (→**83**), **81** (→**84**), Boc_2O, DCM, 15 h, 86-93%; c) **82** (→**22**), **83** (→**85**), **84** (→**86**) i, 2% TFA-DCM, 1.5 h; ii, $CSCl_2$, $CaCO_3$, 1:1 H_2O-DCM, 1 h, 73-85%.

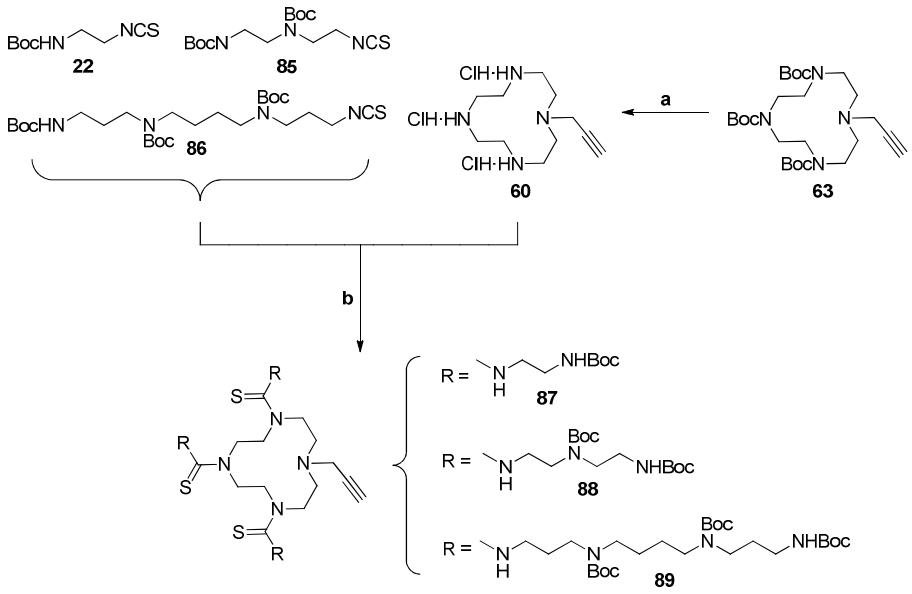

Scheme 18. Synthesis of cyclen-based multivalent polyamino displays **87**-**89**. Reagents and conditions: a) i, 1:1 TFA-DCM, 2 h; ii, HCl, 99%; b) **22** (→**87**), **85** (→**88**), **86** (→**89**), Et_3N, DCM, 15 h, 96% (→**87**), 88% (→**88**), 68% (→**89**).

Cyclen derivative **60** was obtained in almost quantitative yield from *N*-Boc protected cyclen **63** by acidic hydrolysis of carbamate groups. Coupling of the title isothiocyanates to the cyclen scaffold **60** proceeded smoothly in the presence of Et_3N and alkyne-armed compounds **87**-**89** were obtained in good yields (Scheme 18).

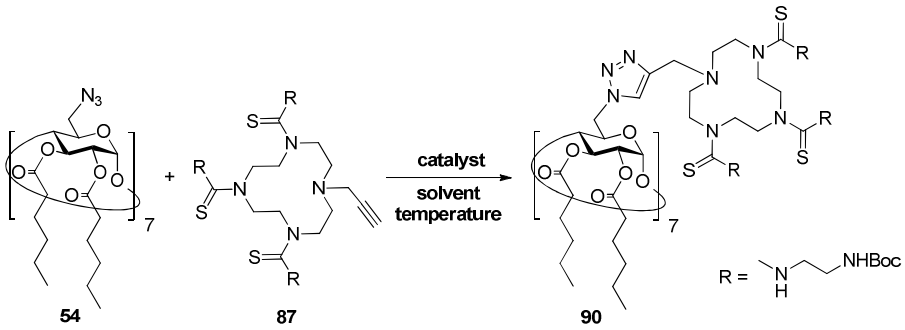

Scheme 19. CuAAC reaction of CD heptaazide **54** and cyclen-based alkyne **87**. Reaction conditions are summarized in Table 5.

To finally obtain homogeneous paCDs furnished with extended multivalent patterns of polyamino motifs, both the amphiphilic CD building block **54** and the cyclen-based multivalent polyamino displays **87**-**89** were then to be coupled by triazole-forming methodology. Unfortunately, this synthetic step turned out to be tricky. Taking advantage of the reaction conditions optimized before for the preparation of cyclen and cyclam-containing paCDs **75**-**78**, in a first attempt the reaction between CD heptaazide derivative **54** and alkyne **87** was carried out in the same conditions used to couple the Boc-protected cyclen derivative **63** (Si-BPA·Cu^+ in refluxing 3:1 ^{t}BuOH-H_2O, Scheme 19; Entry 1 in Table 5), but the reaction did not run to completion as denoted by NMR or ESI-MS. Integration of characteristic ^{1}H NMR signals of the coupling adduct indicated a conversion of ca. 12%. Similar results were obtained for the coupling of the other two isothiocyanates **88** and **89**, most probably the presence the thiourea tethers playing a role in catalyst inactivation. A variety of reaction conditions, including the use of different Cu(I) sources, solvents, reaction temperatures and times were explored, though none of them led to homogeneous conjugates. Conversion rates were estimated by integration

of characteristic ^{1}H NMR signals (Table 5) after isolation of the reaction products by size exclusion chromatography.

Table 5. Reaction conditions employed for CuAAC reaction of heptaazide **54** and cyclen-based alkyne **87** (1.1 eq relative to azide) shown in Scheme 19. The conversion rate was estimated by integration of characteristic ^{1}H NMR signals of the purified products. (For entry 5 μw irradiation was used.)

Entry	Solvent	Catalyst	T (ºC)	t (h)	Conversion
1	^{t}BuOH-H_2O 3:1	Si-BPA·Cu^+ (30 mg/mmol **87**)	85	14	12%
2	^{t}BuOH-H_2O 3:1	CuI (0.2 eq relative to **87**)	85	16	25%
3	anh. DMF	$(EtO)_3P$·CuI (0.2 eq relative to **87**)	85	16	5%
4	anh. DMF	$(EtO)_3P$·CuI (0.2 eq relative to **87**)	100	3	8%
5	^{t}BuOH-H_2O 3:1	CuI (0.2 eq relative to **87**) + TBTA (0.2 eq relative to **87**)	60	1	36%
6	^{t}BuOH-H_2O 3:1	CuI (0.2 eq relative to **87**) + DIPEA (10 eq relative to **87**)	85	15	30%

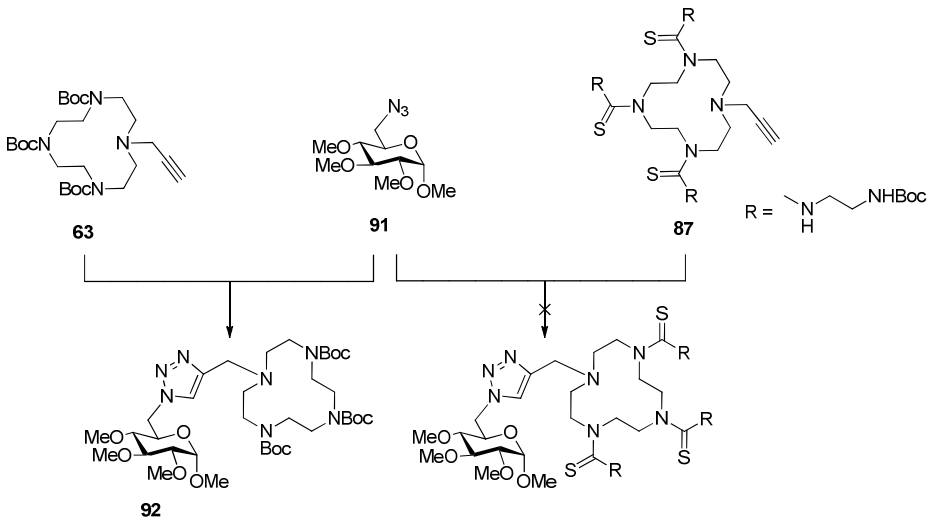

Scheme 20. CuAAC reaction of model glucopyranoside **91** with cyclen derivatives **63** and **87**. Reagents and conditions: CuI (0.2 eq relative to alkyne), 3:1 ^{t}BuOH-H_2O, rt, 1 h.

To probe the origin of such impaired reactivity a series of experiments were carried out. Firstly, 6-azido-6-deoxy-2,3,4-tri-*O*-methyl-α-D-glucopyranoside **91**[280] was used as model compound in order to study its capacity to undergo CuAAC reaction with both tri-*N*-Boc protected cyclen **63** and thiourea-functionalized analog **87** (Scheme 20).

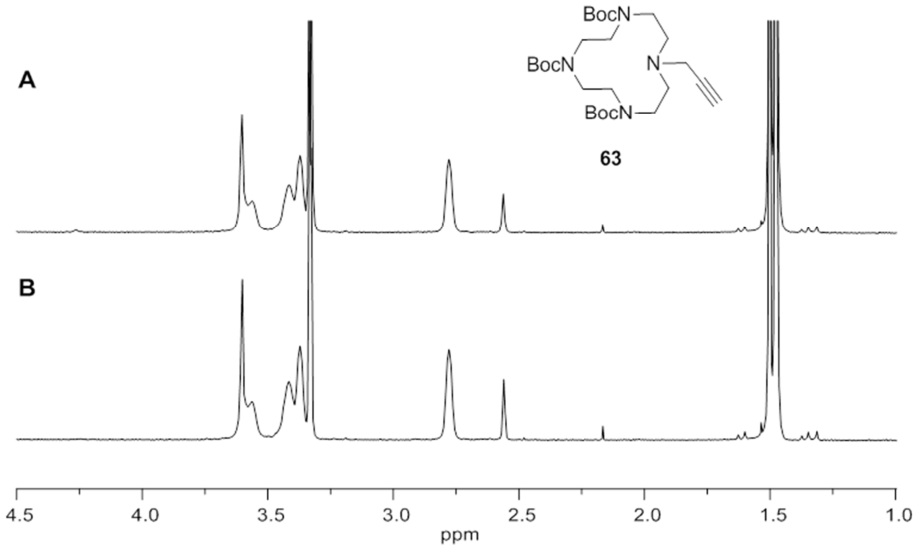

Figure 70. ^{1}H NMR spectra (500 MHz, MeOD, 323 K) of cyclen derivative **63** in absence (A) and in presence (B) of 1 eq CuI.

When CuI was used in catalytic amounts, i.e. 0.2 eq relative to alkyne, coupling of derivative **63** proceeded smoothly. In the case of cyclen derivative **87** no reaction took place under the same conditions, pointing to the Cu(I) complexing ability of the thiourea groups as the origin of catalyst inactivation. However, addition of excess CuI resulted in reaction completion at a rate similar to that observed for tri-*N*-Boc protected cyclen **63**. ^{1}H NMR spectra of both compounds **63** and **87** were recorded in absence and in presence of equimolar amounts of CuI (Figure 70 and Figure 71). Whereas the ^{1}H NMR spectrum of cyclen derivative **63** remained unaltered upon addition of CuI, in the case of thiourea-derived cyclen **87** a drastic change in its ^{1}H NMR spectrum could be observed. This alteration clearly indicated complexation of Cu(I) ions by thiourea moieties present on the

cyclen framework. Addition of a second equivalent of CuI did not further alter the ^{1}H NMR spectrum.

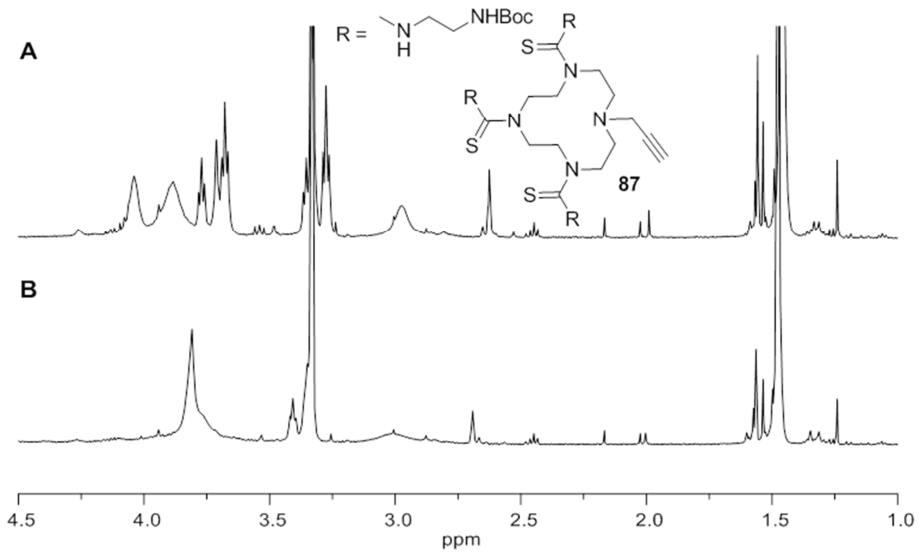

Figure 71. ^{1}H NMR spectra (500 MHz, MeOD, 323 K) of cyclen derivative **87** in absence (A) and in presence (B) of 1 eq CuI.

Interaction of thiourea moieties with metals, in particular with copper,[281] is well documented in literature,[282] nevertheless, this issue has apparently been unnoticed when performing CuAAC chemistry in the presence of thioureas before.[283] It has to be kept in mind, however, that conditions for coupling thiourea-derived cyclen **87** to an azide involve a critical complexity. The presence of three thiourea groups organized in a favorable manner on the cyclic scaffold makes compound **87** an efficient ligand for Cu(I). The complexation of Cu(I) by thiourea moieties, in turn, inactivates the metal for catalysis. Moreover, spatial proximity of the alkyne group to the three thiourea elements present on the cyclen scaffold further complicates CuAAC reaction, as Cu(I) needs to react with the alkyne to promote reaction.

In an attempt to overcome this drawback we have explored the use of Cu(I)-ligands that compete with thiourea moieties without compromising its catalytic activity. Among readily available Cu(I)-ligands TPP[284] and tris[(1-benzyl-1*H*-1,2,3-triazol-4-yl)methyl]amine (TBTA)[285] (Figure 72) were chosen, and their potential to compete with thiourea-derived cyclen for Cu(I) chelation was investigated by NMR.

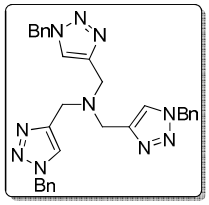

Figure 72. Structure of tris[(1-benzyl-1*H*-1,2,3-triazol-4-yl)methyl]amine (TBTA).

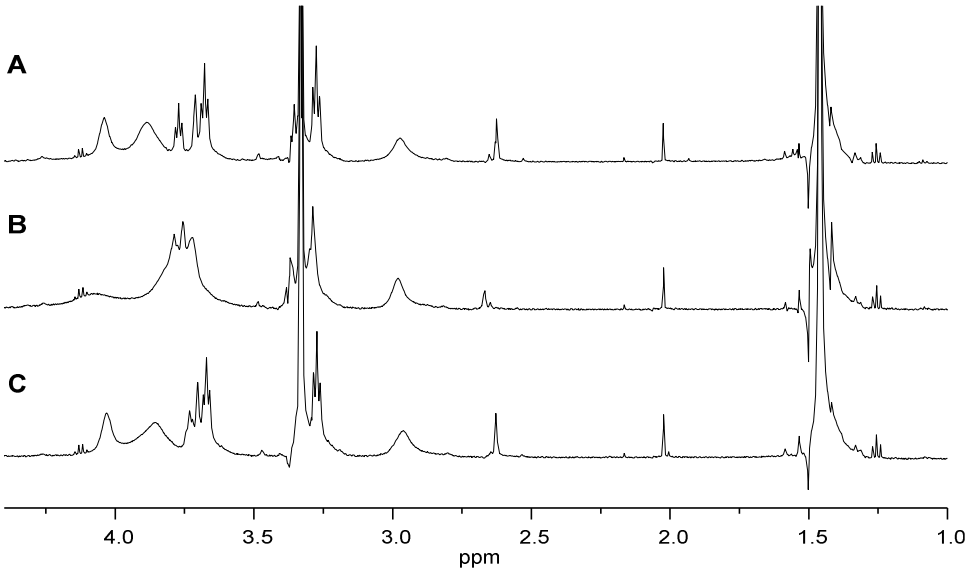

Figure 73. Selected region of the ^{1}H NMR spectra (500 MHz, MeOD, 323 K) of cyclen derivative **87** in absence (A) and in presence of 1 eq of CuI and 1 eq of TBTA (B) and 1 eq of CuI and 4 eq TPP (C).

As shown in Figure 73, TBTA and TPP exhibited rather different affinities towards Cu(I). Whereas the ^{1}H NMR spectrum of cyclen derivative **87** changed considerably when 1 eq CuI and TBTA, respectively, were added, its ^{1}H NMR spectrum remained unaltered upon addition of 1 eq CuI in the presence of 4 eq TPP. These findings indicated that **87** is a stronger chelator for Cu(I) than TBTA, but TPP can compete with it. Moreover, TPP has shown remarkable reaction rate enhancing activity of Cu(I) species in CuAAC.[284]

Table 6. Reaction conditions employed for CuAAC reaction of model glucopyranoside **91** and cyclen-based alkyne **87** (1.1 eq relative to azide) under μw irradiation at 85 ºC (results for reactions carried out at rt or under thermal heating are not shown).

Entry	Catalyst	Catalyst load (eq to alkyne)	Solvent	Rate
1	$Cu(PPh_3)_2I$ **93**	0.0	^{t}BuOH-H_2O	very slow
2			MeCN	slow
3			toluene	slow
4		0.1	^{t}BuOH-H_2O	moderate
5			MeCN	very fast
6			toluene	moderate
7		0.2	^{t}BuOH-H_2O	moderate
8			MeCN	very fast
9			toluene	fast
10	$Cu(PPh_3)_3I$ **94**	0.01	^{t}BuOH-H_2O	very slow
11			MeCN	slow
12			toluene	slow
13		0.1	^{t}BuOH-H_2O	moderate
14			MeCN	fast
15			toluene	moderate
16		0.2	^{t}BuOH-H_2O	moderate
17			MeCN	very fast
18			toluene	fast

However, care must be taken using TPP in CuAAC due to the potential competence of Staudinger reaction.[286] A variety of simple phosphine coordination complexes exist,[287,288] and they are often used in clicking reactions in organic solvents, in which cuprous salts have limited solubility. In this regard, in this Ph.D. Thesis two Cu(I)-TPP complexes,

namely $Cu(PPh_3)_2I$ (**93**)[289] and $Cu(PPh_3)_3I$ (**94**)[290] have been synthesized. To identify the optimal reaction conditions, various solvents (MeCN, toluene and 3:1 ^tBuOH-H_2O) and catalyst loads ranging from 0.01 eq to 0.2 eq (relative to alkyne), were screened for both catalysts. Furthermore, the influence of temperature and μw irradiation on the reaction rate has been examined. TLC was used to qualitatively evaluate the reaction progress (Table 6).

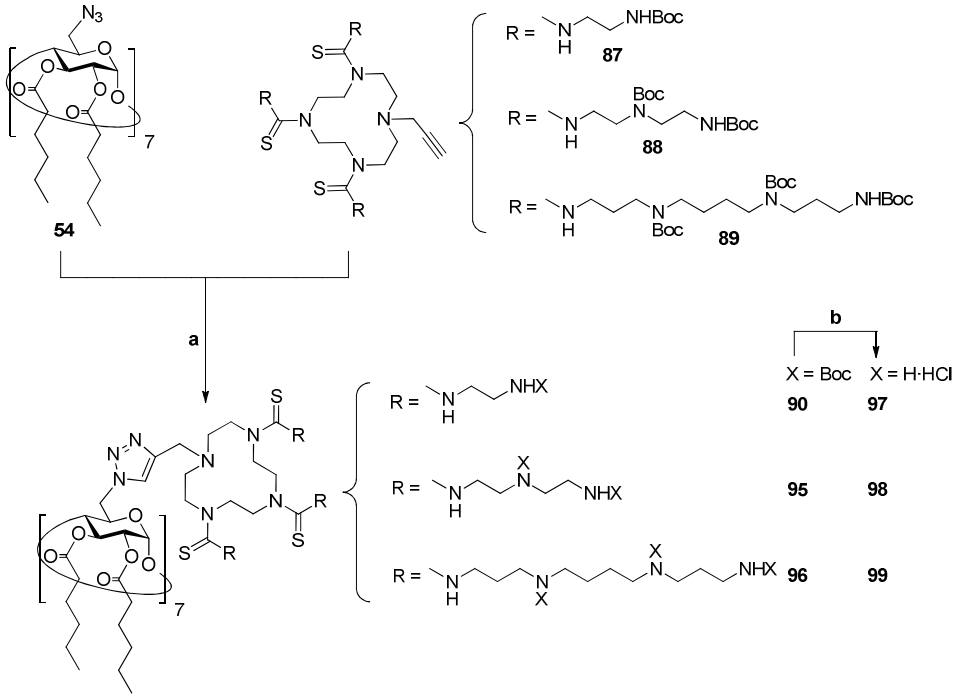

Scheme 21. Synthesis of paCDs **97**-**99** furnished with functionalized multivalent cyclen platforms. Reagents and conditions: a) **87** (→**90**), **88** (→**95**), **89** (→**96**), $Cu(PPh_3)_2I$ **93**, MeCN, μw, 85 ºC, 2.5 h, 75% (→**90**), 50% (→**95**), 31% (→**96**); b) i, 1:1 TFA-DCM, 2 h; ii, HCl, quantitative yield in all cases.

The exhaustive screening of reaction conditions revealed that the best results could be obtained when the CuAAC reaction was performed in MeCN under μw irradiation at 85 ºC and 0.1 eq of $Cu(PPh_3)_2I$ **93** was employed as catalyst. Yet, substitution of this

phosphine complex by $Cu(PPh_3)_3I$ **94** did not vary the reaction rate significantly, probably because various species coexist in the reaction mixture.

Once established these optimal reaction conditions, the triazole-forming clicking reaction of both the lipophilic tail-containing CD building block and the cyclen-based multivalent polyamino displays was tackled (Scheme 21).

Application of these conditions to the coupling of cyclen alkynes **87**-**89** to CD scaffold **54**, though TLC initially indicated acceptable reaction progress, did not yield fully homogeneous products. In the case of CD derivative **90**, conversion was estimated in approximately 85%, according to the integration of characteristic ^1H NMR signals, whereas reaction with more complex cyclen derivatives **88** and **89** resulted in slightly lower average substitution patterns (ca. 80% for **95** and 73% for **96**; see Figures S54-S56 for NMR spectra, Supporting Information). ESI-MS spectra of the crude samples are compatible with these conclusions. Nevertheless, final acidic hydrolysis of the carbamate protecting groups of heterogeneous compounds **90**, **95** and **96** took place without any difficulty.

Despite their heterogeneity, it appeared of interest to explore the self-assembling capabilities of these compounds, therefore the carbamate protecting groups were cleaved using the conventional conditions to quantitatively furnish the CD-scaffolded cyclic polyamine clusters **97**-**99**. Unfortunately, these studies could not be concluded within the frame of this Ph.D. Thesis.

3. Assessment of self-assembling and pH buffering capabilities of cyclen/cyclam-grafted paCDs in aqueous environment

Aimed at gaining insight into the relationship between structure and self-organizing capabilities of the CD-scaffolded cyclic polyamine clusters, their critical aggregation concentration and pH buffering abilities were measured accordingly to the methods reported in the preceding chapter. The study was focused on paCDs **75**-**78**, which were critically compared to hexanoylated and butanoylated paCDs described in the preceding chapter (Figure 74).

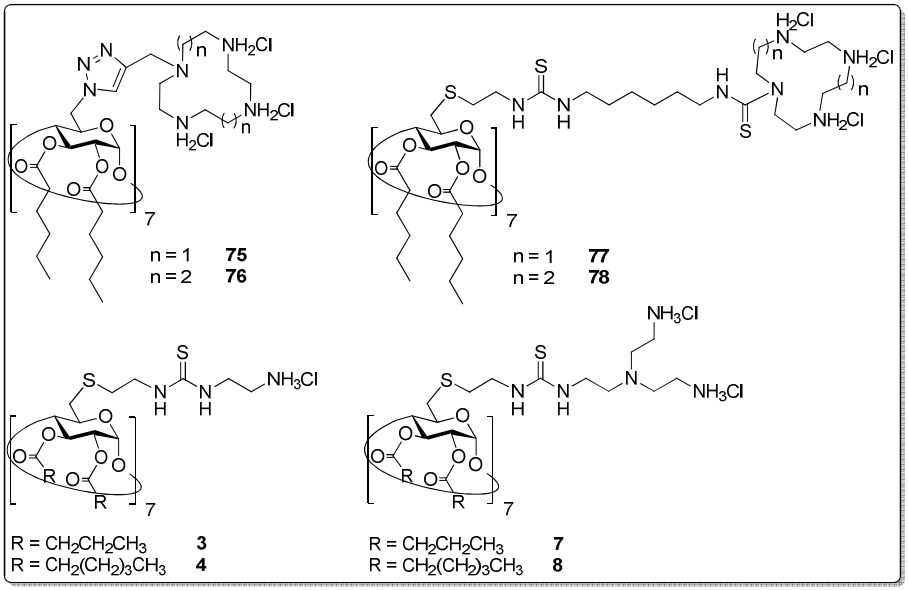

Figure 74. Series of paCDs decorated with cyclic (cyclen and cyclam) and acyclic oligoamines.

First, the influence of the hydrophobic/hydrophilic balance on the self-assembling capabilities in aqueous environment has been examined. Their critical aggregation concentrations in aqueous environment are summarized in Table 7. For comparative

purposes, CACs of hexanoylated paCDs **4** and **8** with acyclic polycationic elements have been included in this table.

Table 7. Critical aggregation concentrations in aqueous environment of cyclen/cyclam-grafted paCDs **75**-**78** and paCDs **4** and **8** with acyclic cationic elements.

paCD with cyclic amines	CAC (μM)	paCD with acyclic amines	CAC (μM)
75	2.92	**4**	0.94
76	2.85	**8**	2.79
77	0.54		
78	0.38		

All paCDs studied in this chapter are furnished with the same hexanoyl chains; therefore, possible differences in their hydrophobic/hydrophilic balance would derive exclusively from different polycationic heads. Results, however, showed that CACs of hexanoylated paCDs bearing cyclic or acyclic polycationic elements did not significantly vary, and all of them were in the range from 0.4 μM to 2.9 μM. This indicated that hexanoyl chains were able to counterbalance arrays of seven (paCD **4**), 21 (paCDs **8**, **77** and **78**) and 28 (paCDs **75** and **76**) cationic groups on the primary rim respectively, leading to low CACs in all cases. CAC values do not apparently depend on type of cyclic oligoamine (cyclen or cyclam), but on the type of tether, aggregation taking place for thiourea-linked conjugated at lower concentrations than for the corresponding triazole-tethered analogs. However, it is unclear whether this is solely due to the nature of the tether or to the number of protonable nitrogen atoms in each series.

Buffering capacities of cyclen/cyclam-grafted paCDs **75**-**78** in the pH range from 5 to 7 were evaluated by potentiometric titration, and compared to that of paCDs **3** and **7** furnished with acyclic cationic elements. The potentiometric titration studies were conducted over a pH range of 9-2. Additionally, model compounds **104**-**107**, featuring identical cationic domains as their CD-scaffolded analogs, were synthesized (Figure 75). Their protonation profiles were determined by acid-base titration and compared to **50** and **51**.

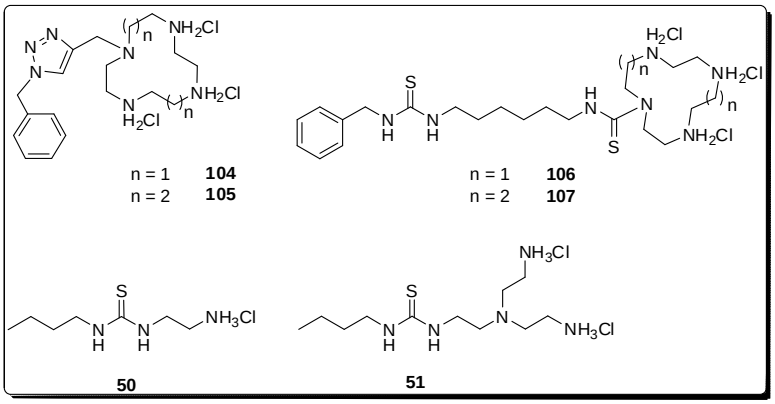

Figure 75. Monovalent model compounds used for potentiometric acid-base titrations.

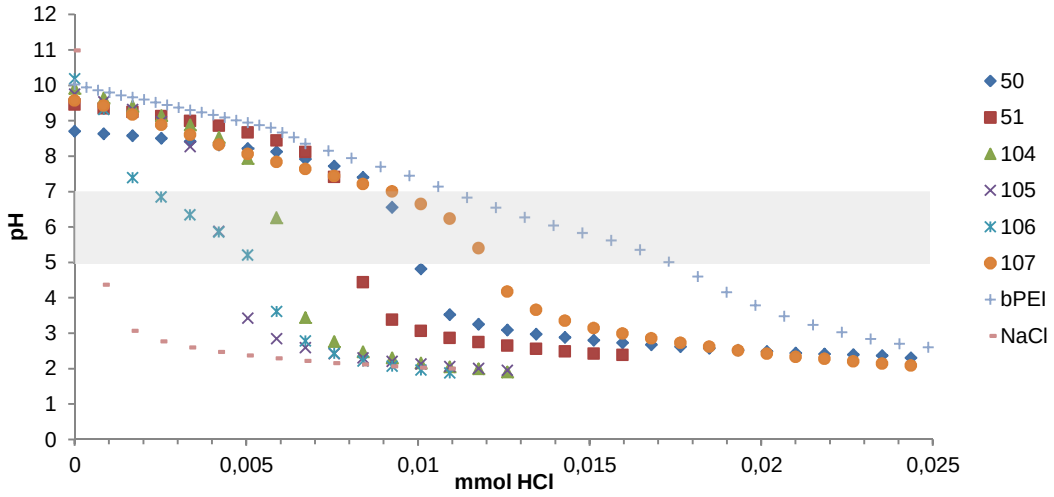

Figure 76. Potentiometric titration profiles of monovalent model compounds **50**, **51**, **104**-**107**. Titrations of NaCl and bPEI solutions are included for comparative purposes. The grey-shaded area represents the pH range where effective buffering ability may enhance lysis of the endosomes.

The results are summarized in Figure 76. Similar to model compounds **50** and **51**, whose acid-base titration curves drop down rapidly in the pH range between 7 and 5, triazole-bearing model compounds **104** and **105** apparently are devoid of buffering

capabilities in this range. In contrast, thiourea-tethered models **106** and **107** showed a certain buffering capability in this pH range.

The potentiometric titration profiles of cyclen/cyclam-grafted paCDs **75**-**78** as well as paCDs **3** and **7** furnished with acyclic cationic elements are shown in Figure 77. All paCDs exhibited buffering capacities in the pH range from 7 to 5. Whereas buffering capacities of triazole-bearing paCDs **75** and **76** resembled those of paCDs **3** and **7**, cyclen/cyclam-grafted paCDs **77** and **78** furnished with thiourea linkers presented considerably improved buffering abilities in this pH range.

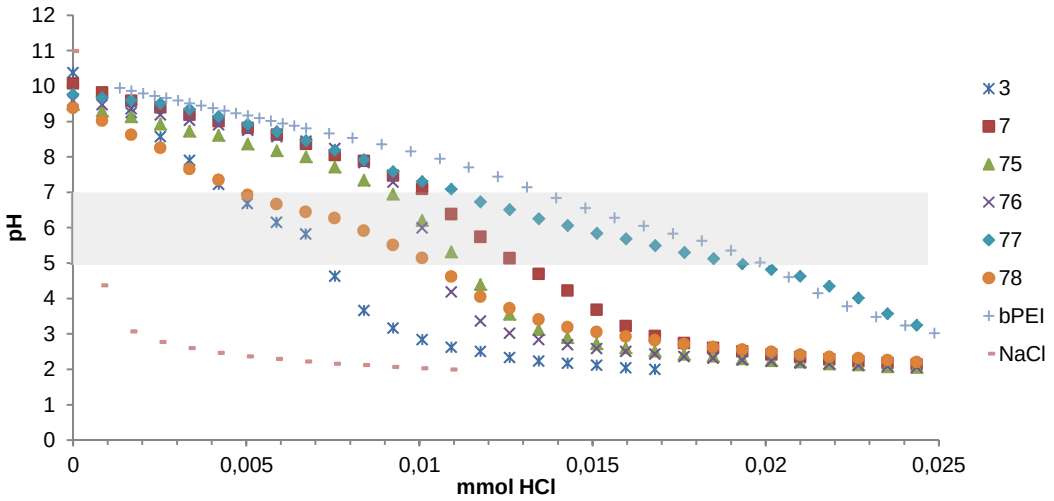

Figure 77. Potentiometric titration profiles of cyclen/cyclam-grafted paCDs **75**-**78**, and paCDs **3** and **7** with acyclic cationic elements. Titrations of NaCl and bPEI solutions are included for comparative purposes. The grey-shaded area represents the pH range where effective buffering ability may enhance lysis of the endosomes.

To study the buffering capacities of paCDs **75**-**78** and their respective model compounds **104**-**107** in a more detailed manner, for each compound the equivalents of HCl consumed to switch pH from 7 to 5 have been quantified. A comparison of the results

with those obtained for paCDs **3** and **7** and their corresponding model compounds **50** and **51** is shown in Table 8.

Table 8. Equivalents of HCl consumed to switch pH from 7 to 5 for paCDs **3**, **7** and **75**-**78**, their respective model compounds (**50**, **51**, **104**-**107**) and bPEI.

Compound	meq of HCl consumed
3	67
7	84
50	17
51	<17
75	67
76	34
77	168
78	118
104	<17
105	<17
106	50
107	50
bPEI	134

The buffering capacities of all paCDs in the pH range 7-5 were better than those of their respective monovalent model compounds, which may indicate that either the multivalency of CD platform or their aggregation abilities improve their buffering capacity. The more favorable protonation profiles of monovalent models **106** and **107**, as compared to all other model compounds, suggest that incorporation of cyclic polyamine groups into the CD scaffold via a thiourea tether adjacent to a flexible aliphatic spacer may result in improved buffering capabilities. Indeed, among all CD derivatives studied, cyclen/cyclam-grafted paCDs **77** and **78** furnished with thiourea linkers presented the best buffering capacities, catching up with the golden standard bPEI. Although slightly lower, the buffering capabilities of triazole-bearing paCDs **75** and **76** were similar to those of paCDs **3** and **7**. Regarding the type of cyclic polyamine element, i.e. cyclen vs. cyclam, the cyclen motif evidently enhances buffering capacity. For cyclic polyamines grafted to the CD scaffold via triazole or thiourea linkers, cyclen derivatives **75** and **77** showed higher buffering capacities than their cyclam-grafted analogs **76** and **78**, respectively.

4. Assessment of DNA-condensing capabilities of cyclen/cyclam-grafted paCDs

To study the influence of cyclic polyamine headgroups on DNA-condensing capabilities the CDplex formation capabilities of paCDs **75**-**78** were critically compared to paCDs grafted with acyclic oligoamines (Figure 78). First, the paCD-DNA nanoparticles were characterized by dynamic light scattering (DLS) in order to determine their average hydrodynamic size and ζ potential using ctDNA at N/P ratios 5 and 10.

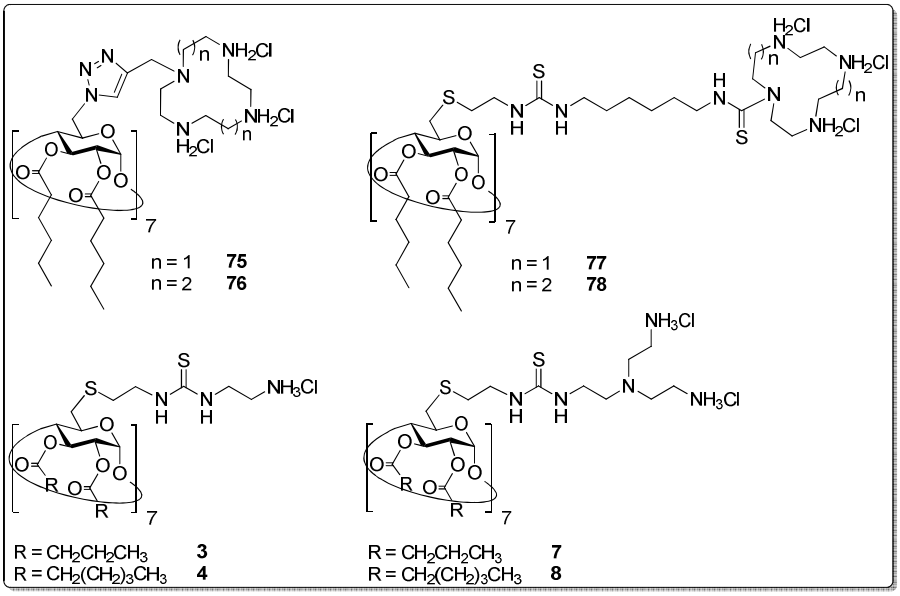

Figure 78. Library of cyclen/cyclam-grafted paCDs (**75**-**78**) and paCDs synthesized in Chapter 2 used for comparative purposes (**3**, **4**, **7** and **8**).

The DLS results showed that all assayed cyclen/cyclam-grafted paCDs formed compact and stable nanoparticles with ctDNA that, with the exception of compound **75** at N/P ratio 10, exhibited rather small hydrodynamic diameters as compared with the polyplexes obtained from 25 kDa bPEI (80-100 nm vs. 150 nm; Figure 79).

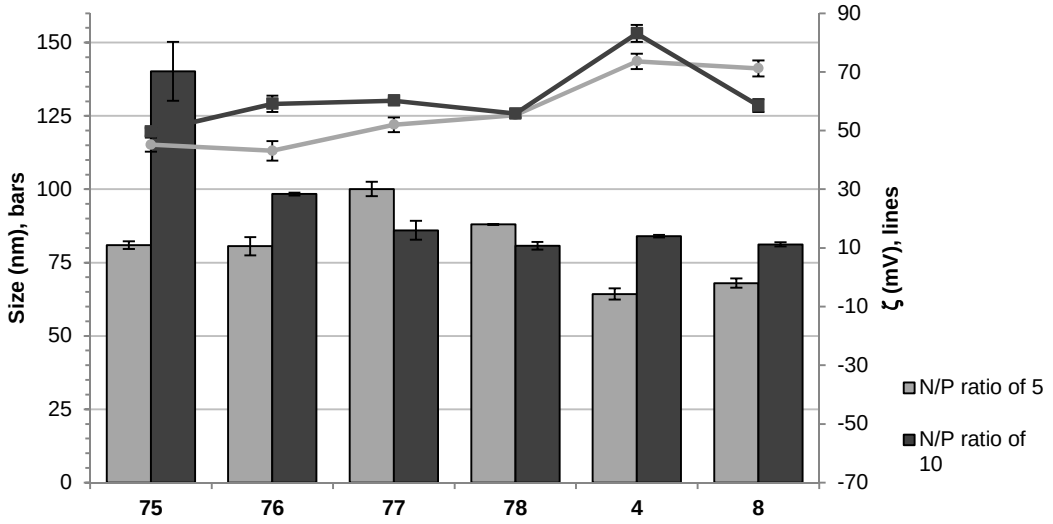

Figure 79. Size (hydrodynamic diameter, bars, nm) and ζ potential (lines, mV) of CDplexes of paCDs **75**-**78** determined by DLS and M3-PALS analysis, respectively (for comparative purposes, CDplexes of paCDs **4** and **8** are included).

Hydrodynamic diameter measurements indicated that modifications of the molecular structure of paCDs did not influence particle size significantly. Moreover, the N/P ratio did scarcely affect particle hydrodynamic diameter. Although nanoparticles of paCD derivative **75** exhibited an extraordinary large hydrodynamic diameter at N/P ratio 10, in general no substantial difference between analogous cyclen and cyclam-derived paCDs could be disclosed. Furthermore, the nature of the linking element marginally affected particle size, since paCDs **75** and **76** furnished with rigid and short methylene triazole segments and their respective analogs **77** and **78** bearing long and flexible aliphatic tethers and thiourea groups led to CDplex nanoparticles of almost the same size. These facts suggest that, despite their architectural disparity, the overall hydrophilic/hydrophobic balance is barely altered.

Similar to the results obtained for acyclic oligoamines, narrow populations of cationic nanoparticles were observed in each individual experiment, thus indicating rather monodisperse nanoparticles (Figure 80). Such remarkable behavior (relatively low

particle size and polydispersity) makes CD-scaffolded cyclic polyamine clusters suitable candidates for artificial gene carriers.

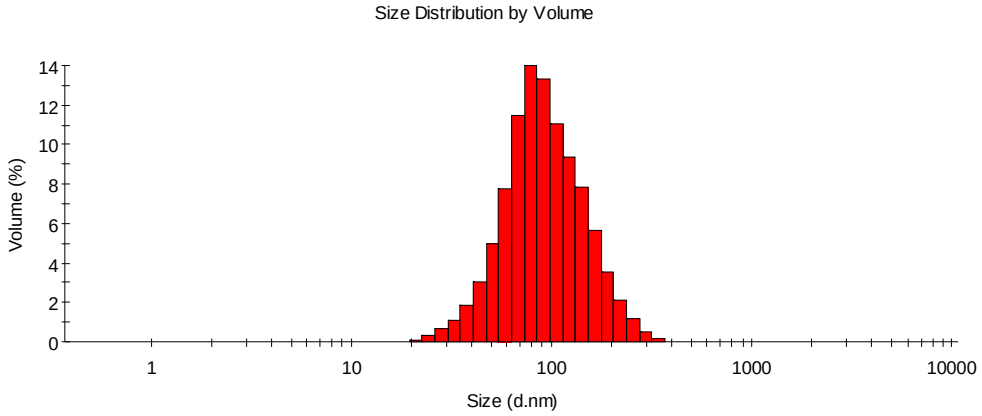

Figure 80. Particle size distribution by volume determined by DLS for ctDNA:**78** CDplexes formulated at N/P 5 (diameter in nm).

M3-PALS measurements at both N/P ratios 5 and 10 revealed that ζ potential of CDplexes formulated with cyclen/cyclam-grafted paCDs **75**-**78** ranked in the range 40-60 mV, amenable values for cell-based assays. ζ Potential values were marginally depended on the N/P ratio, thus indicating that complex stoichiometry does not change significantly upon an increase of the N/P ratio. We hypothesize that excess paCD does not incorporate into the CDplex nanostructure. ζ Potential of CDplexes formulated with paCDs **4** and **8**, however, were slightly higher than those with cyclen/cyclam-grafted paCDs (50-80 mV for paCDs **4** and **8** vs. 40-60 mV for paCDs **75**-**78**, respectively).

Altogether, DLS experiments pointed out that cyclen/cyclam-grafted paCDs **75**-**78** were able to form stable nanoparticles with DNA. These nanoparticles all featured remarkably similar hydrodynamic diameters, positive ζ potentials and relatively narrow size distributions.

Subsequently, their capabilities to compact and protect DNA were investigated by submitting the cyclen or cyclam-grafted paCDs **75**-**78** to agarose gel electrophoresis shift

assays. Therefore, paCD:ctDNA complexes were formulated in the same manner as described before for different N/P ratios in the range of 1 to 10. Naked ctDNA was used for comparative purposes. Complete inhibition of DNA migration indicated complex formation, whereas absence of fluorescent staining denoted efficient compaction and protection of DNA in the CDplexes of the corresponding lanes (Figure 81).

At N/P ratios 1 or higher, formation of the respective CDplexes was achieved for all assayed paCDs, which was indicated by the absence of “free” mobile plasmid. Starting from N/P ratio 2, both cyclen and cyclam grafted paCDs were in addition capable to efficiently compact and protect DNA in their CDplexes. Although cyclen and cyclam moieties exhibit different spatial orientation of the cationic amino groups, no appreciable difference in their DNA-condensing capabilities could be inferred and efficient covering of the DNA surface by both cyclen and cyclam grafted paCDs has been clearly evidenced.

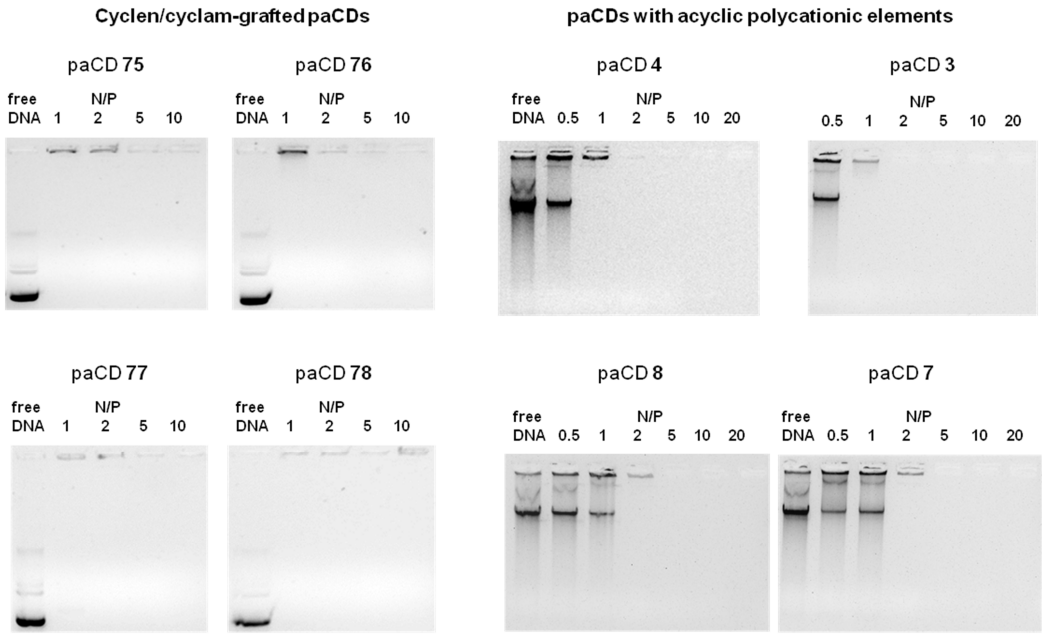

Figure 81. paCD-mediated protection of ctDNA from GelRed™ intercalation at different N/P ratios (1-10) for cyclen/cyclam-grafted paCDs **75**-**78** and paCDs with acyclic polycationic elements **3**, **4**, **7** and **8**.

However, when triazole bearing paCDs **75** and **76** were compared with their thiourea analogs **77** and **78**, respectively, a remarkable difference became apparent. Whereas triazole paCDs **75** and **76** were only capable of efficiently compacting and protecting DNA at N/P ratios 5 or higher, thiourea derivatives **77** and **78** already turned DNA inaccessible to the GelRed™ intercalating agent at N/P ratio 2. This difference might be attributed to the superior ability of thiourea segments to complement electrostatic phosphate binding via hydrogen-bonding interactions as compared to triazole tethers. Interestingly, the additional protonable nitrogen atom in the triazole-linked series, as compared to the thiourea-tethered one, does not compensate the beneficial effects added by the thiourea moieties. The presumably low pK_a value of the additional tertiary amine in the triazole-derived paCDs does not seem to favor DNA compaction and protection.[256,257]

Compared to the library of paCDs prepared in Chapter 2, which differ in the length of the lipophilic chain and are furnished with either 7 or 21 protonable amino groups, cyclen or cyclam-grafted paCDs exhibited DNA compactation and protection capabilities similar to those of linear and branched paCDs bearing butanoyl or hexanoyl chains on the secondary rim. At N/P ratio 1 cyclen and cyclam-derived paCDs showed slightly better compactation capabilities as they completely inhibited DNA migration, while linear paCDs **3** and **4** as well as branched paCDs **7** and **8**, respectively, still demonstrated partial DNA migration. Nonetheless, regarding DNA protection, the most efficient paCDs prepared in Chapter 2 performed as well as cyclen or cyclam-derived paCDs, as all of them efficiently compacted and protected DNA at N/P ratios 2 or 5 at most.

5. Gene transfer capabilities towards COS-7 and HeLa cell lines

Similarly to that reported in the preceding chapter, the gene transfer efficiency of CDplexes formed from cyclic amine-grafted paCDs was evaluated using the luciferase-encoding gene (pTG11236, pCMV-SV40-luciferase-SV40pA) as reporter towards COS-7 and HeLa cell lines.

The experiments towards COS-7 cells were developed using in-house facilities to comparatively assess the performance of triazole-tethered paCDs **75** and **76** and thiourea-tethered CDs **77** and **78** (Figure 82) in the absence of serum. JetPEI and naked pDNA were included as positive and negative controls, respectively. In addition, paCD **8**, furnished with a cluster of acyclic oligoamines,[177] was also included in the experiments as positive control (Figure 82).

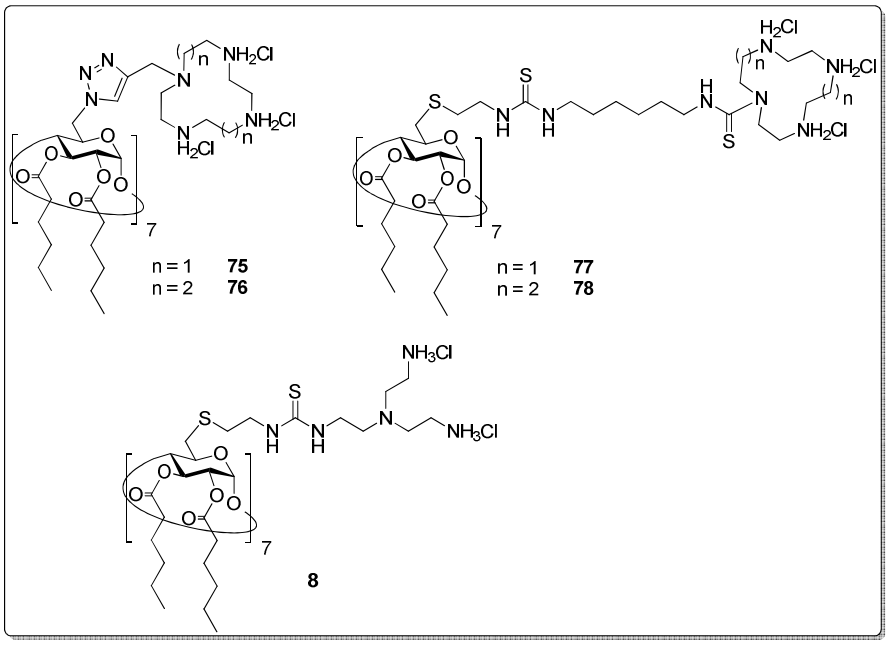

Figure 82. Library of cyclen/cyclam-grafted paCDs **75**-**78** and acyclic reference paCD **8** screened as pDNA carriers towards COS-7 and HeLa cell lines.

Previous results indicated that paCD **8** CDplexes formulated at N/P 10 mediate comparable luciferase expression levels to JetPEI in COS-7 cells, up to six orders of magnitude higher than the corresponding naked pDNA.[177] **75**- and **76**-pDNA CDplexes paralleled the efficiency of both positive controls at the same N/P (N/P 10, Figure 83), though luciferase expression levels dropped by 3 and 4 orders of magnitude at the lower N/P ratio assayed (N/P 5, data not shown). No differences due to cyclic oligoamine structure (cyclen vs. cyclam) were noticed. In stark contrast, thiourea-tethered paCDs **77** and **78** resulted far less efficient than their triazole-tethered counterparts. Though similarly performing at low N/P, they did not showed the efficiency boost at N/P 10.

The dramatic change in transgene expression efficiency due to both N/P ratio and structure highlights the relevance of architectural parameters on the formation of paCD-pDNA complexes and their stability. In all cases, the lowest N/P ratio assayed is far enough to condense pDNA into nanoparticles of similar size and ζ potential where pDNA is isolated from the media, as shown in the preceding sections. Quite remarkably, despite thiourea-tethered paCDs **77** and **78** exhibited the largest pH buffering capabilities, this feature does not seem to contribute much to their performance. Conversely, triazole-linked paCDs **75** and **76** displayed critical aggregation concentrations significantly lower than their thiourea counterparts, which may furnish their CDplexes with different capabilities to interact with their environment. Though these structural effects would require further investigation, due to time constraints, a deeper insight could not be included into this Ph.D. Thesis.

Conversely, experiments in the presence of serum-containing media (10%) masked all the above commented differences in gene transfer efficiencies (Figure 83, data for N/P 5 not shown). In this scenario, neither N/P ratio (5 or 10) nor paCD architecture significantly affected the performance of CDplexes. While in the case of thiourea-tethered paCDs similar levels of luciferase expression were measured, the triazole-tethered paCDs resulted approximately 100-fold less efficient.

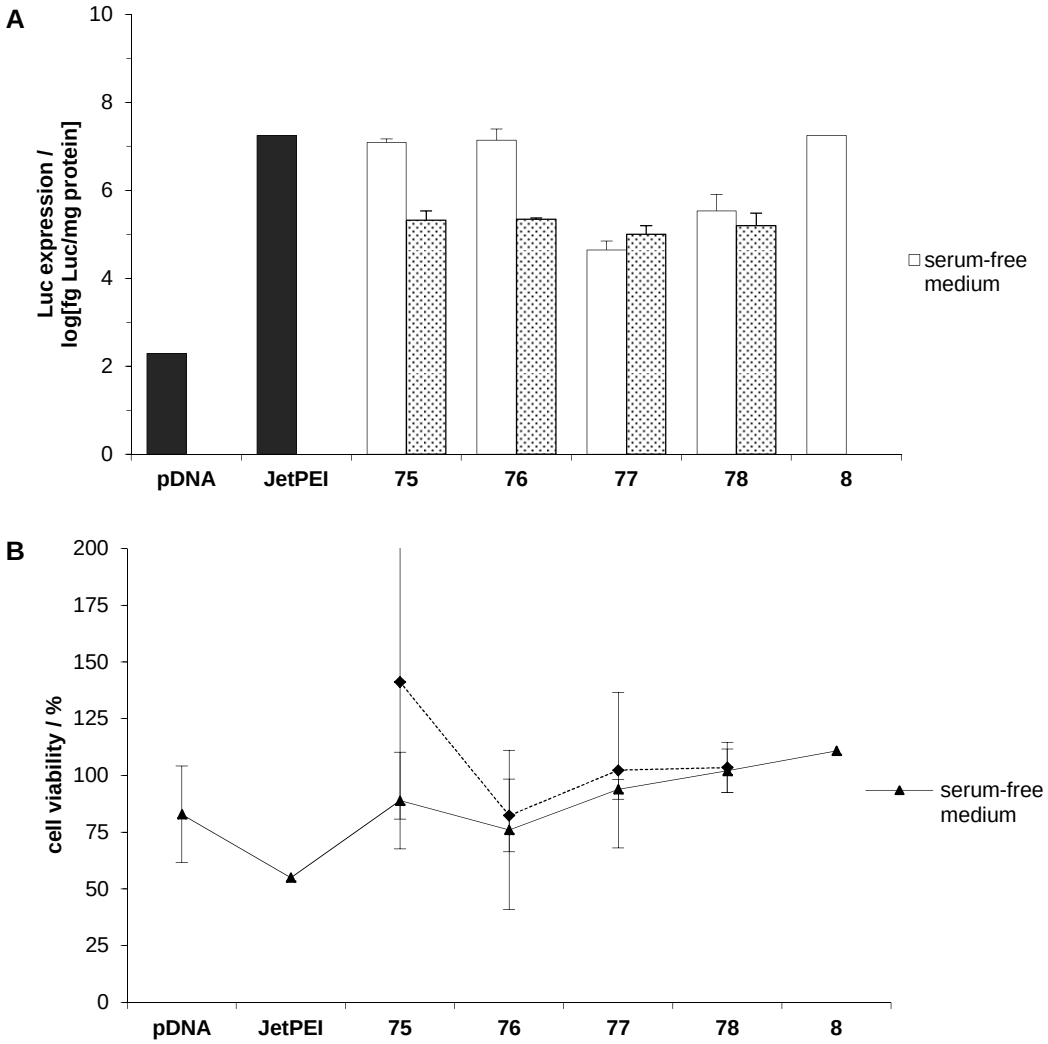

Figure 83. Luciferase-encoding gene transfer efficiency (A) and cell viability (B) in COS-7 cells treated with CDplexes formed with cyclen/cyclam-grafted paCDs **75**-**78** and the acyclic counterpart **8** at N/P 10. Naked pDNA and JetPEI polyplexes were used as negative and positive controls, respectively.

In collaboration with Prof. P. Midoux (Univ. of Orleans, France), cyclen- and cyclam-granted paCDs have been further tested in HeLa cells, and their gene carrier

performance comparatively assessed against PTG, a cationic histidine-grafted αCD derivative featuring remarkable transfection capabilities towards different cell lines.[291] Experiments were run using virtually non-toxic CDplex formulations at N/P 5 in serum-containing media (10%). The results were consistent with those observed for COS-7 cells. In these conditions, performance of cyclen- and cyclam-grafted paCDs **75**-**78** is 2 to 3 orders of magnitude lower than that measured for the acyclic oligoamine derivative **8**, which is only marginally less efficient that PTG at its optimal N/P (6) (Figure 84). As observed for COS-7 cells, there is no apparent correlation between paCD structure and gene transfer capabilities, which might indicate that the presence of serum may affect CDplex stability. As previously described, CDplexes formed from thiourea-containing paCDs may better tolerate this media,[177,180a] which could explain the better performance of the cyclam-grafted thioureido derivative **78** as compared with the rest of the cyclic oligoamine series. Nevertheless, additional experimental evidences should be gathered to fully support this hypothesis.

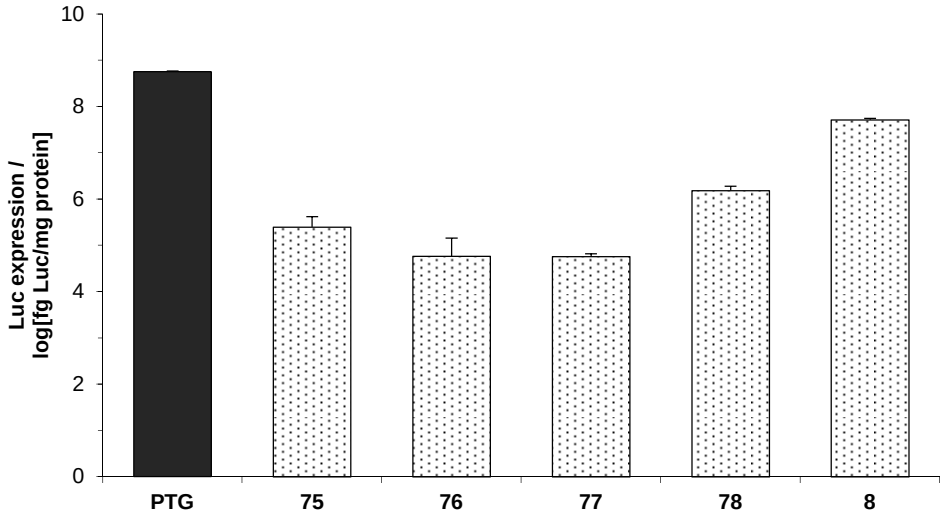

Figure 84. Luciferase-encoding gene transfer efficiency in HeLa cells treated with CDplexes formed with cyclen/cyclam-grafted paCDs **75**-**78** at N/P 5. PTG and the acyclic paCD analog **8** CDplexes at N/P 6 and 5, respectively, were used as positive controls.

CHAPTER 4 - SOLID-PHASE ASSISTED SELECTIVE FUNCTIONALIZATION OF MULTIVALENT SCAFFOLDS. APPLICATION TO SELECTIVE MONOFUNCTIONALIZATION OF CYCLODEXTRINS

1. Strategies towards selective functionalization of cyclodextrins: scope and limitations

Selective methodologies for the functionalization of cyclodextrin framework either by chemical[292] or enzymatic[293] protocols have enabled the development of a plethora of applications for CDs.[294] In addition to their utility in the design of self-assembling devices for drug and gene delivery (already covered in the previous chapters), selective functionalization strategies permitted the development of artificial enzymes,[295] sensors,[296] catalysts,[297] drugs,[298] drug carriers,[299] or molecular machines.[300] However, it is somehow curious that, despite the myriad of applications, only a handful of regioselective synthetic methodologies are available for hydroxyl differentiation in CDs. The reason for this scantiness lies in the challenge of differentiating a certain functional group among a dense display of them. Most of these selective functionalization methodologies take advantage of the CD scaffolding or molecular inclusion capabilities to force a preferential orientation between the CD and CD-modifying reagent. Despite their undeniable utility, these strategies often require a tight matching between CD and reagent pairs, thereby their CD architectural scope being very restrictive.

As illustrated in the previous chapters, the design of CD-based gene carriers has been facilitated by the use of synthetic routes that take advantage of CD facial anisotropy.1 Making use of straightforward perfunctionalization approaches, CD-based facial amphiphiles exhibiting remarkable self-assembling, DNA-condensing and gene delivery capabilities were obtained. However, installing additional functionalities onto the CD platform at selected positions requires a cumbersome synthetic effort. Despite previous reports have demonstrated the interest of grafting bioactive elements onto amphiphilic CD scaffolds (e.g. biorecognizable saccharide epitopes for targeted delivery), the methodological arsenal is still limited and synthetic schemes are cumbersome[183a,296f,299] or do not provide with homogeneous conjugates.[183b] On the other hand, installation of an additional functionality on the gene delivery vehicle, such as a PET or SPECT imaging

moiety, or a fluorescent probe for optical imaging could deliver a theranostic device, an emerging concept permitting simultaneous diagnostic and therapy.[301]

In native CDs there exist three types of hydroxyl groups attached to the C-6, C-2 and C-3 positions of the α-D-glucopyranosyl unit, respectively. Those at the C-6 position are the most basic and sterically accessible, those at the C-2 position are the most acidic, and those at the C-3 position are the least accessible.[302] These subtle reactivity differences allow for relatively straightforward chemoselective differentiation among the three types of hydroxyls,[292] but it is much more challenging to regioselectively differentiate between groups of the same type because of their identical chemical reactivity. A considerable amount of work has been invested in the search for methods to enable site selective functionalization of CDs. In general, methods for selective modification of CD can be divided into three categories:[292] (i) the "long" method, involving a series of more or less straightforward protection and deprotection steps; (ii) the "clever" method, where the supramolecular features of CD are often exploited to get the desired product by the shortest route; (iii) the "sledgehammer" method, where indiscriminate (statistical) reaction leads to complex product mixtures and then the desired product is painstakingly separated from other isomers and homologues, e.g. by chromatographic methods.

Among the "clever" methods for regioselective CD manipulation, the most successful ones are those taking advantage of a preferential approach and orientation of the CD-modifying reagent. In this way, the reaction outcome can be significantly restricted as compared to that statistically expected. An illustrative example of this kind of approach is the Cu(II)-complex directed regioselective mono-*p*-tosylation at the C-6 position of CDs.[303] Using *p*-tosyl chloride as a reagent, 6^{I}-*O*-tosylation of βCD is commonly achieved, either in pyridine[304] or with water[305] as solvent. Acyl transfer from 1-(*p*-toluenesulfonyl)imidazole in water is a valuable alternative procedure,[306] though regioselectivity is poor with these procedures. A significant improvement was described by Defaye and co-workers taking advantage of the sandwich-type chelate that βCD and Cu(II) ions form in aqueous alkaline solution (Scheme 22).[307] This complex controls the orientation of tosyl chloride upon inclusion into the βCD cavity, promoting regioselective

6^{I}-*O*-tosylation in excellent yields.[303] Mono C-6-tosylated βCD is a handy entry to selectively monofunctionalized CDs, since the tosyl group can be readily displaced by a variety of nucleophiles.

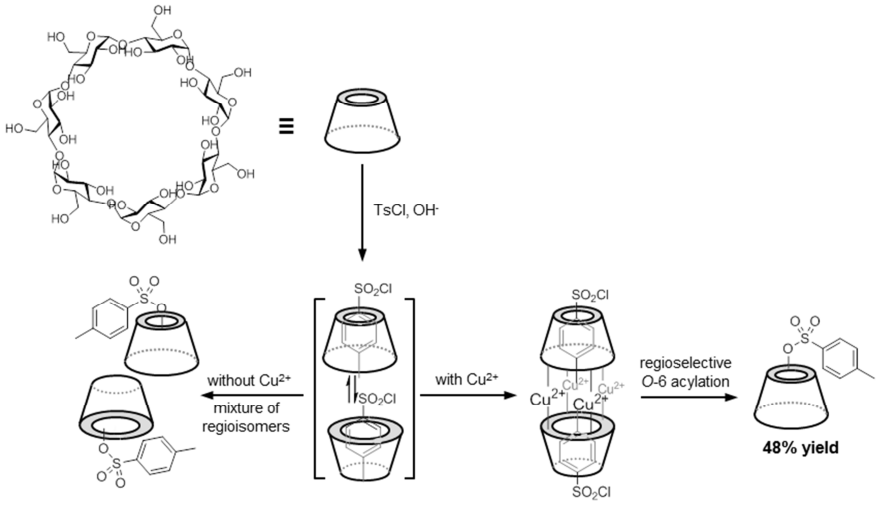

Scheme 22. Schematic representation of βCD and its inclusion complex-mediated transformation into the mono-C-6-*O*-tosyl derivative.

Taking advantage of the rigidity of the different CD scaffolds, some innovative strategies have also being devised to functionalize several selected hydroxyls at the same time.[308] For instance, using sterically hindered tritylating reagents (method A in Figure 85) Knowles and co-workers managed to selectively obtain a C-$6^{I,III,V}$-tri-tritylated αCD derivative long ago.[309]

Alternatively, bifunctional reagents have been also exploited to regioselectively produce otherwise inaccessible CD functionalization patterns (method B in Figure 85). Carefully selecting the geometry of bis-sulfonyl or bis-acyl chlorides, Tabushi and co-workers prepared the first examples of capped CDs.[310] The concept has been refined later with the use of other bis-tritylating[311] or alkylating reagents[312] which selectively react with two selected hydroxyl groups of the CD according to the length and geometry of the tether. This cap-assisted synthetic strategy[313] has mainly been developed on βCD. The

geometry of selected arene disulfonyl chlorides controls very efficiently the regiochemistry to selectively furnish AB, AC, or AD isomers (Figure 86).[314] For example, biphenyl-based capping reagents preferentially give AD isomers, benzophenone-based reagents lead to AC isomers, and 1,3-benzenedisulfonyl chlorides give AB isomers.

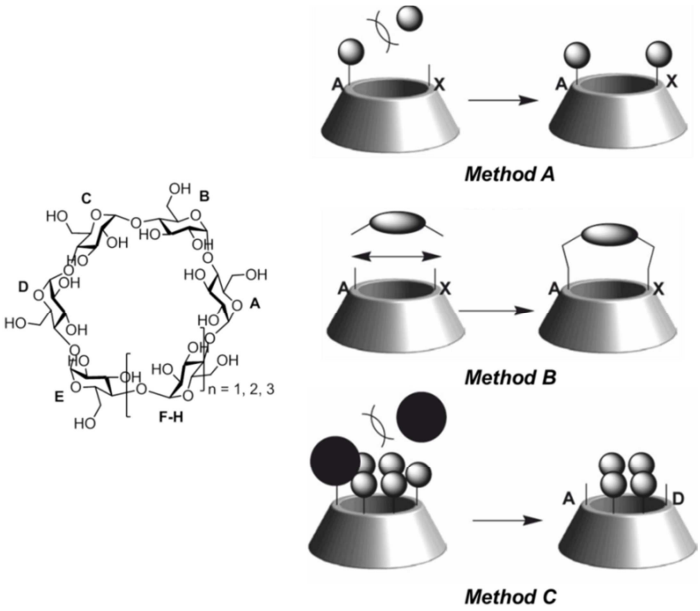

Figure 85. General methods for difunctionalization of CDs.[308]

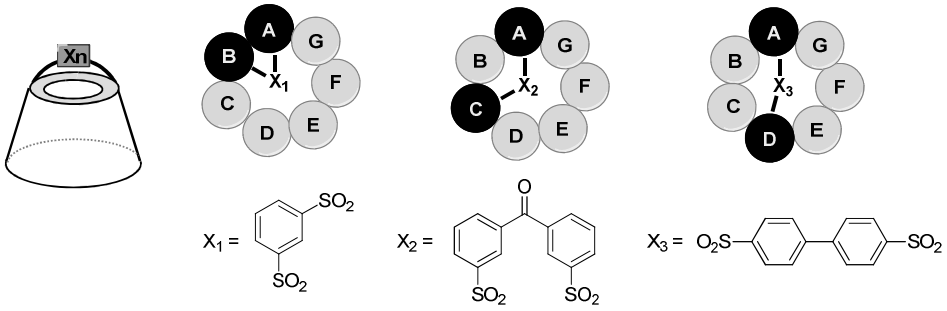

Figure 86. 6-Disulfonated βCDs: the regioselectivity depends on the choice of sulfonylating reagents.

Matt and co-workers[315] employed 1,3-bis[bis(4-*tert*-butylphenyl)chloromethyl]benzene ("bis-trityl dichloride", Figure 87) as regioselective capping reagent for the preparation of A,B-bridged α- and βCD derivatives.[311a] Taking advantage of this bulky protecting group, selectively tetrafunctionalized CD derivatives could also be accessed.[311b,316]

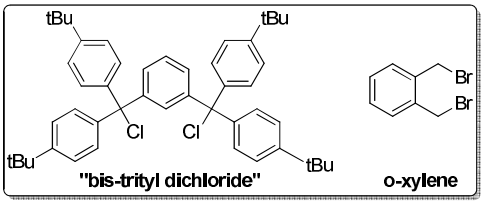

Figure 87. Capping reagents "bis-trityl dichloride" and α,α'-dibromo *o*-xylene for regioselective CD functionalization.

Small capping reagents based on phosphines, sulfides[316,317] and sulfates[318] have also been proven suitable intermediates for the preparation of tri-differentiated CD derivatives. Though most of these capping reagents were designed for primary rim hydroxyl differentiation, remarkably efficient procedures have also been envisioned for secondary hydroxyls. An in-house-developed methodology permits the straightforward preparation of 2^{I},3^{I}-*O*-capped CDs by incorporation of the *o*-xylene group (Figure 87) to the vicinal diol system presents a remarkable efficiency.[312]

But probably the strategy that has demonstrated the greatest potential for tailored manipulation of CD topology is the one based on the regioselective DIBAL-H-mediated dealkylation pioneered by Sinaÿ and Sollogoub (method C in Figure 85).[319] In a series of excellent contributions, these authors have rationalized the action of DIBAL-H over per-O-alkylated CD derivatives implementing strategies to use this reagent as a molecular scalpel to sequentially rip off selected protecting groups (mostly benzyls) with astonishing regioselectivity.[308] For example, in the cases of α- and βCDs, only benzyl group(s) attached to *O*-6 positions of the A and D units are cleaved, the selectivity probably being enhanced by the steric collapse at the primary rim due to the volume of the protecting groups and the reagent (Scheme 23). The reaction is proposed to proceed in two steps,

the first deprotection alleviating the steric crowding around the primary rim of the CD scaffold and determining the orientation of the aluminum species, thereby, and selectivity at the farthest possible site.[319b]

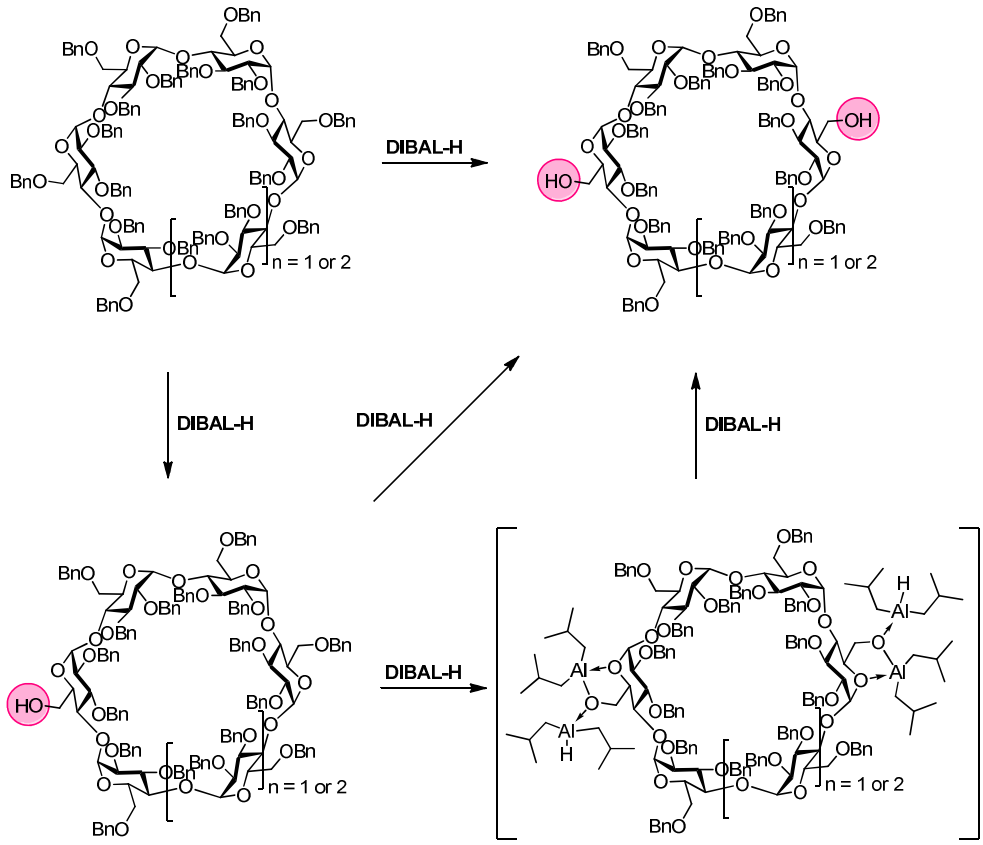

Scheme 23. Regioselective DIBAL-H promoted double debenzylation reaction pioneered by Sinaÿ and Sollogoub.

Sinaÿ and Sollogoub latter found that similar conditions can be applied to sequentially rip off methyl groups from permethylated CDs, predominately at the secondary rim.[320] Very recently, Ling and co-workers[321] showed that DIBAL-H can also be used to promote diametrically opposed di-*O*-desilylations of primary silyl ethers on CD derivatives, following a similar deprotection pattern as the related *O*-debenzylations. In further

refinement of this methodology, DIBAL-H has been used to synthesize triply and quadruply *O*-debenzylated CD derivatives in gram quantities.[322] These precisely oriented deprotections allow for the preparation of orthogonally protected, multisubstituted CDs in an efficient manner.[308,323] Besides, the DIBAL-H mediated deprotection reactions are very sensitive to concentration, and it is therefore possible to delineate reaction conditions to produce mainly monodeprotected compounds.

Such “clever” approaches have been mastered to furnish extraordinary selectivities, but their applications are often limited to tight-matching CD-reagent pairs and this fact my seriously limit their scope. Thus, development of tools to widen the accessible CD architectural scope would result in an excellent complement for these strategies.

Orienting the CD-reagent pair and preventing an additional reagent species to react the same CD molecule is crucial for the success of selective derivatization strategies. While executing this control is inherently difficult in solution, it might be easier with a reagent displayed on a solid support. In this regard, solid phase organic synthesis presents a very valuable tool. On a solid support, it is reasonably feasible to display functional or reactive elements within a predetermined distance among them by tailoring support loading and swelling. Despite this advantage, the use of solid supports for the selective functionalization of CDs has been scarcely explored. Indeed, solid-support-assisted synthesis has been already shown to successfully produce single-site functionalized 2-nm gold nanoparticles.[324] But implementation towards CD monofunctionalization has only been reported very recently by Di Fabio and co-workers.[325] They demonstrated that a solid-supported reagent can be used to graft a single label onto a series of CD scaffolds via phosphodiester linkages (Scheme 24). Only moderate yields were reported, probably due to either a suboptimal reagent display on the solid support or reaction conditions. Moreover, the precise functionalization site (primary or secondary rim) was not disclosed and final HPLC purification was required.

Aiming at refining this concept, in this Ph.D. Thesis a solid phase-assisted methodology has been developed that permits versatile and regioselective modification of CD platforms. The strategy exploits a solid matrix to display the complementary reagent

functionalities sufficiently far from each other to prevent CDs from reacting through more than one site (Scheme 25).

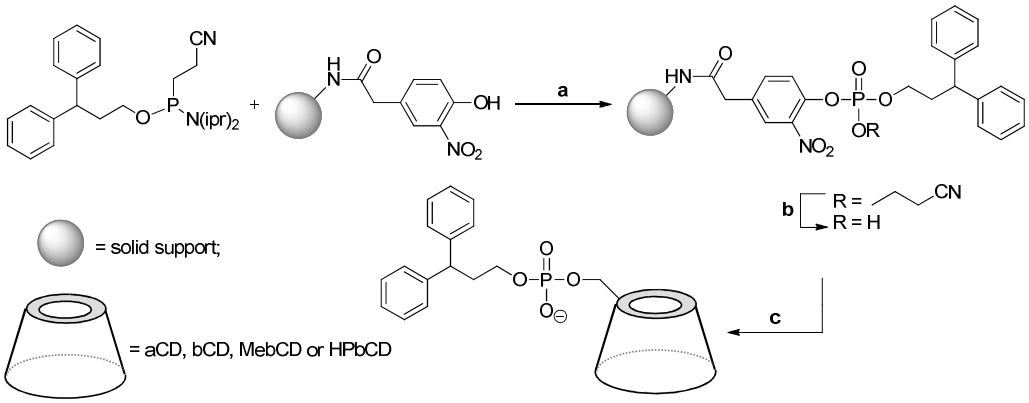

Scheme 24. Regioselective solid phase synthesis of monofunctionalized CDs using standard phosphotriester chemistry. Reagents and conditions: a) i, 1*H*-tetrazole, 30 min, rt; ii, I_2, Py, H_2O, 5 min, rt; b) 20% piperidine in DMF, 5 min, rt (3 times); c) i, αCD, βCD, MeβCD or HPβCD, MSNT, overnight, rt; ii, NH_4OH conc., 1 h, 50 ºC.

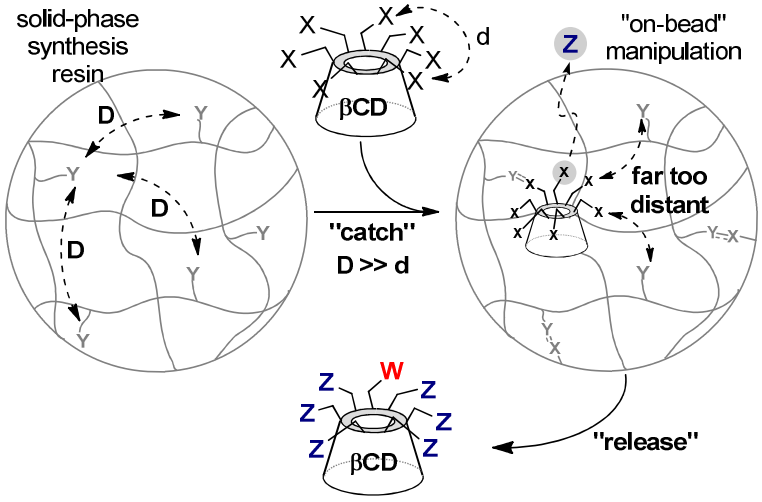

Scheme 25. Schematic representation of the solid support-assisted "*catch-and-release*" protocol for site selective CD functionalization.

For such a purpose, we have implemented an experimental setup permitting (i) the covalent capture of a fully symmetric CD derivative through a single position by a solid-supported reagent, (ii) eventual “on-bead” orthogonal elaboration of the remaining functional groups, and (iii) a final chemoselective release of the dissymmetric CD conjugate from the solid support in a sort of one-pot *“catch-and-release”* process. This strategy would allow for easily producing complex CD functionalization patterns in one pot and without any purification step.

2. Implementation of the *Catch-and-Release* concept for regioselective monofunctionalization of multivalent scaffolds

Based on the pioneering works of Merrifield[326] in 1963, the concept of solid phase synthesis revolutionized peptide and nucleotide chemistry and more than twenty years ago it set the stage for combinatorial chemistry.[327] This now widely applied technique uses a polymeric matrix or other solid material to temporarily support a substrate, which is then taken through a synthetic sequence and subsequently cleaved back into solution.

Among a wide variety of alternative methods to classic solid phase synthesis, i.e. application of solid phase reagents,[328] catalysts[329] and scavenging techniques,[328b] a hybrid methodology that combines the concept of solid phase synthesis with the idea of polymer-supported scavenging reagents has seen increased interest in polymer-assisted synthesis. Pioneered by Ley and Baxendale, this so-called "*catch-and-release*" methodology[328b,330] allows the selective trapping of specific species onto a functionalized support. After filtrating and washing to remove soluble by-products, this species may either be released in pure form from the support or subjected to further transformations by adding new reaction partners in solution. Alternatively, these reactants can simultaneously modify the substrate while cleaving it from the support.[331]

The chemical reactivity for the "*catch-and-release*" process is not a trivial choice. For this particular case, the versatility of the Staudinger reaction[332] between organic azides and phosphines has been considered (Figure 88). Staudinger reaction occurs in virtually any solvent to chemoselectively give iminophosphorane species in mild conditions and good yields. Moreover, it is relatively feasible to install such functional groups on conventional solid-phase synthesis matrixes and control the distance among them to prevent a single CD from reacting through more than a single site. For such scenario, a series of azido-functionalized compounds and phosphines were selected (Figure 89). Secondary face-per-*O*-methylated CD **110** was chosen to prevent the potential interference of secondary hydroxyls with the "*catch-and-release*" process. It is well known that methyl groups on the secondary face are stable under a wide variety of reaction

conditions, hence heptakis(6-azido-6-deoxy-2,3-di-*O*-methyl)cyclomaltoheptaose **110**[180a] represents an ideal candidate for probing the utility of the "*catch-and-release*" concept for regioselective CD modification.

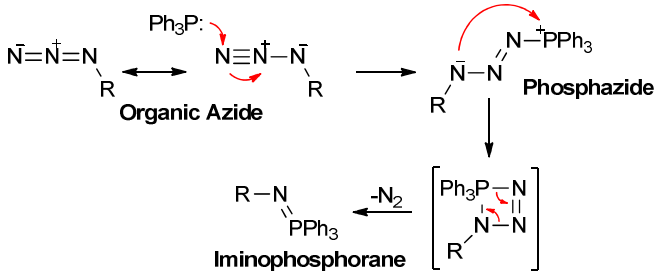

Figure 88. Formation of the corresponding iminophosphorane by Staudinger reaction between an organic azide and TPP.

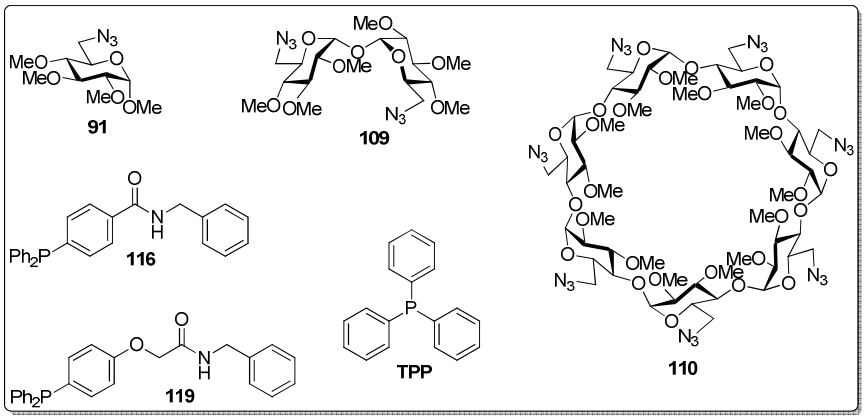

Figure 89. Structures of azides **91**, **109** and **110** and phosphines **116**, **119** and TPP investigated to optimize the Staudinger reaction.

Simpler surrogates **91** and **109** were also included as test compounds (Figure 89). Model monosaccharide methyl 6-azido-6-deoxy-2,3,4-tri-*O*-methyl-α-D-glucopyranoside **91**[280] bears only one azido group and was used incipiently to optimize solution and on-bead Staudinger reaction conditions. The distance between the two azido groups of

model disaccharide α,α'-trehalose **109** is smaller than the maximum distance between azido groups of CD **110**, which makes it a suitable model compound to study selective capture through a single position by a solid-supported reagent.

Different model phosphines have been explored for solution phase kinetics studies (Figure 89). Compounds **116** and **119** are electron-poor and electron-rich analogs of TPP that should feature reduced and enhanced reactivity, respectively, as compared to TPP. An appropriate derivative of the best-performing phosphine would be then coupled to the solid support.

Provided the reactive groups are displayed sufficiently distant on the support, the CD adduct would be reacted by a single position, being the rest too far away to further react. Once the CD derivative is covalently captured by the solid-supported reagent through a single position, the formed iminophosphorane tether might be later released from the solid matrix chemoselectively in the form of e.g. an amine, iso(thio)cyanate or (thio)urea. In addition, iminophosphorane reactivity[333] is orthogonal to other azide-involving reactions, such as the Cu(I)-catalyzed azide-alkyne cycloaddition (CuAAC) reaction,[144] which would enable further "on-bead" derivatization of the remaining functional groups.

To optimize the experimental conditions for solid phase-assisted synthesis, first the iminophosphorane formation in solution with model monosaccharide **91** and a set of aromatic phosphines has been studied. In particular, compounds **116** and **119** as well as TPP were chosen as model phosphines for solution phase kinetics studies. Their corresponding precursors **112**[334] and **118**, respectively (Scheme 26 and Scheme 27) are furnished with a carboxylic acid anchor group that later on enables coupling onto glycine-loaded aminomethylated polystyrene (AM-PS) resin by conventional peptide coupling techniques. However, as a consequence of the electron-withdrawing character of the carbonyl group directly attached to the aromatic ring, phosphine **112** should present decreased electron-donating capabilities. As this may decrease iminophosphorane formation rates, the more electron-rich phosphine **118** has alternatively been synthesized. With the purpose of gaining an insight into kinetics of solution phase iminophosphorane formation, derivatives **112** and **118** were transformed into the corresponding

benzylamides **116** and **119**, respectively, thus mimicking their ultimate form when attached to the solid support.

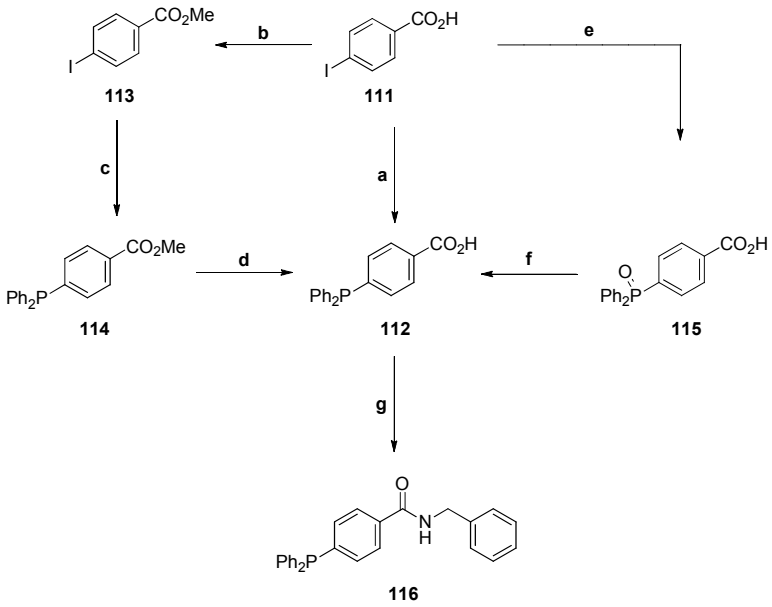

Scheme 26. Synthesis of phosphine **116**. Reagents and conditions: a) $PHPh_2$, Et_3N, $Pd(OAc)_2$, degassed MeCN, reflux, 12 h, 68%; b) K_2CO_3, MeI, 0 ºC, 1 h, 98%; c) $PHPh_2$, Cs_2CO_3, CuI, degassed toluene, reflux, 17 h, 70%; d) aq. KOH, MeOH, reflux, 12 h, 99%; e) $P(=O)HPh_2$, Et_3N, $Pd(OAc)_2$, MeCN, reflux, 12 h, 21%; f) $HSiCl_3$, dry toluene, reflux, 14 h, 97%; g) $BnNH_2$, DIPEA, TBTU, DMF, rt 20 h, 83%.

4-(Diphenylphosphino)benzoic acid **112** was obtained via different synthetic pathways, as can be seen in Scheme 26. Direct Pd(II) acetate-catalyzed cross coupling of aryl iodide **111** with diphenylphosphine proceeded only in moderate yields, yet attempts to obtain the desired compound via alternative reaction sequences did not lead to higher yields. Nevertheless, carboxylic acid derivative **112** could be converted smoothly into the corresponding benzylamide **116**. Electron-rich phosphine carboxylic acid **118** was prepared in a very similar way by direct cross coupling and was then reacted with benzylamine to give phosphine **119** in good yield (Scheme 27).

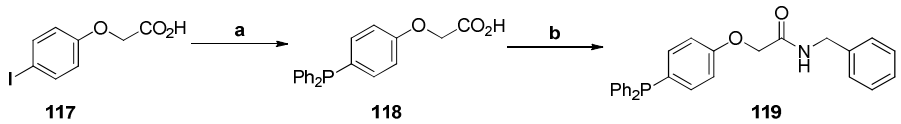

Scheme 27. Synthesis of phosphine **119**. Reagents and conditions: a) $PHPh_2$, Et_3N, $Pd(OAc)_2$, degassed MeCN, reflux, 12 h, 93%; b) $BnNH_2$, DIPEA, TBTU, DMF, rt 20 h, 59%.

To evaluate the reactivity of phosphines **116**, **119** and TPP towards model monosaccharide **91**, the Staudinger reaction was monitored by ^{31}P NMR (Scheme 28). Therefore, reactions were performed under nitrogen atmosphere in NMR tubes using anhydrous solvents to prevent hydrolysis of the formed iminophosphorane. Different solvents, such as DCM, DMF and 1,4-dioxane, were tested and reactions were carried out at either room temperature or 40 ºC. Typically 50 µmol of phosphine were mixed with 2 eq of azide **91** and ^{31}P NMR spectra of the reaction mixture were recorded every 10 min. Once the iminophosphorane had formed quantitatively, which could be observed by complete disappearance of the phosphine peak at ca. -6 ppm and the newly formed peak at ca. 9 ppm, water was added to the reaction mixture to hydrolyze the iminophosphorane, yielding the corresponding amine and phosphine oxide (peak at ca. 26 ppm, Figure 90).

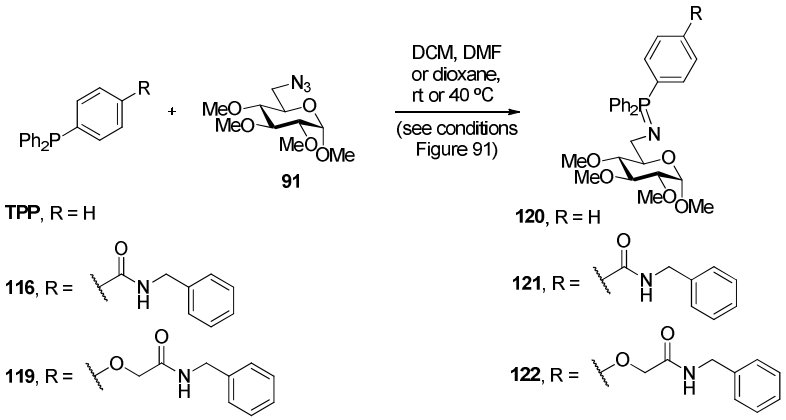

Scheme 28. Formation of the corresponding iminophosphoranes **120**-**122** by Staudinger reaction between model monosaccharide **91** and phosphines **116**, **119** and TPP, respectively.

As depicted exemplarily in Figure 90, quantitative conversion to the corresponding iminophosphorane **122** was observed within 2.5 h when 1 eq of **119** was mixed with 2 eq of azide **91** at rt in anhydrous DMF. Hydrolysis of iminophosphorane **122** took place quantitatively within 2-2.5 h when water was added to the reaction mixture.

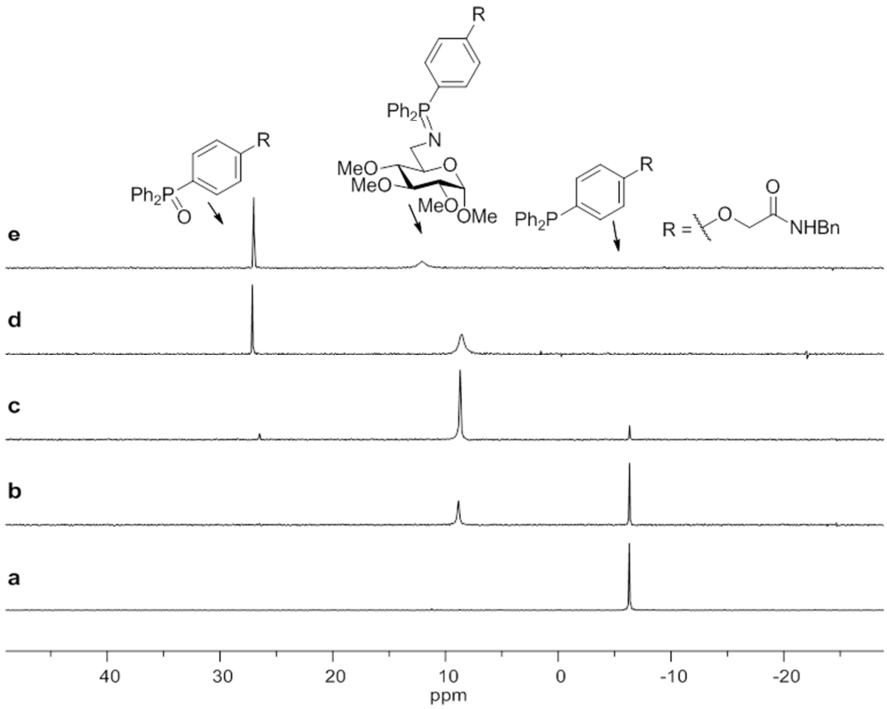

Figure 90. Monitoring of Staudinger reaction between phosphine **119** (1 eq) and azide **91** (2 eq) for 5 h at rt in anhydrous DMF by ^{31}P NMR (121 MHz, C_6D_6). The peak at ca. -6 ppm corresponds to phosphine **119**; the one at ca. 9 ppm to iminophosphorane **122**, and the one at ca. 26 ppm to phosphine oxide derived from **119**. (a) phosphine **119** alone (reference); (b) phosphine **119** + azide **91**, 30 min; (c) phosphine **119** + azide **91**, 2.5 h, (d) phosphine **119** + azide **91** + 10% H_2O, after 30 min; (e) phosphine **119** + azide **91** + 10% H_2O, after 2.5 h.

The results of the NMR-monitored kinetics studies of the formation of iminophosphoranes **120**-**122** are summarized in Figure 91. Reaction with TPP at rt indicated relatively fast kinetics with a reaction half-life of 20-30 min (○ series) in all

assayed solvents. The reaction rate of electron-lacking phosphine **116** was definitely slower ($t_{½}$ 80 min in 1,4-dioxane, △ series). Conversely, electron-rich phosphine **119** fully recovered performance of TPP, being the most appropriate choice to build on the solid-support. Moreover, the reaction rate could be significantly increased at 40 ºC ($t_{½}$ 6 min in DMF, ◆ series) with negligible iminophosphorane hydrolysis after several hours provided anhydrous conditions were preserved. The optimal performance together with good resin swelling capabilities supported the choice of DMF as solvent for the assays on the solid support.

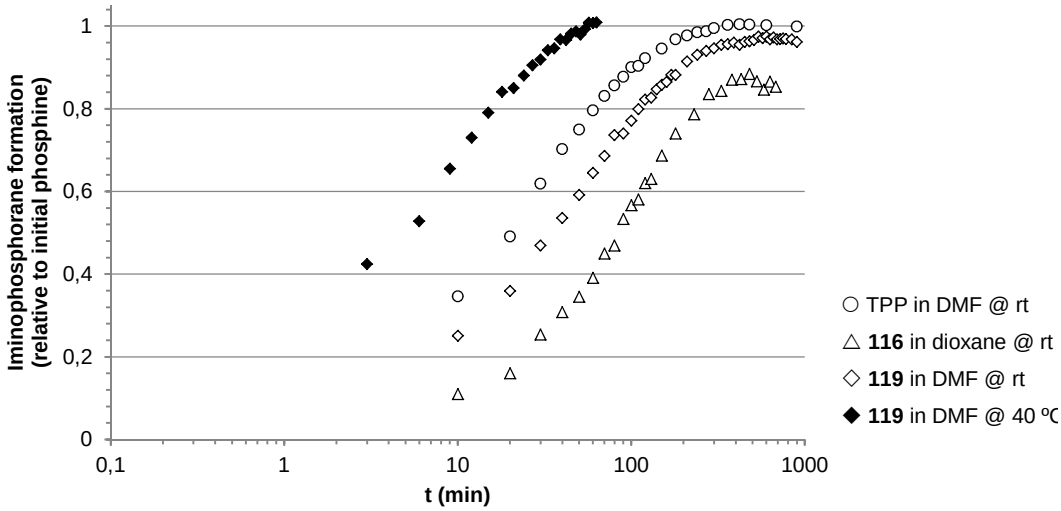

Figure 91. Iminophosphorane formation kinetics from azide **91** with phosphines **116**, **119** and TPP monitored by ^{31}P NMR.

Once the appropriate phosphine structure as well as the optimal solvent and reaction temperature have been determined, the next step comprised the synthesis of the resin-supported phosphine reagent. The choice of an appropriate solid matrix is an important issue and several aspects have to be considered. In this regard, aminomethylated polystyrene resin (AM-PS, 0.39 mmol·g^{-1}, 1% DVB) has been chosen as solid matrix. Aminomethylated polystyrene is a versatile resin that is readily modified by conventional

peptide coupling reactions. It is chemically and mechanically stable and tolerates elevated reaction temperatures without losing functional efficiency. Moreover, it presents good swelling capabilities in DMF (5-10 $mL \cdot g^{-1}$), which makes it compatible with Staudinger reaction conditions on the one hand, and on the other hand allows for controlling the distance between reactive centers.

To obtain solid-supported phosphine **123**, the resin was first loaded with *N*-Fmoc-protected glycine using conventional peptide coupling reagents TBTU and Et_3N (Scheme 29). By this means, optimal resin loading could be confirmed by spectrophotometric quantification of dibenzofulvene (DBF) released from the matrix upon treatment with either piperidine[335] or DBU (1,8-diazobicyclo[5.4.0]undec-7-ene).[336] Subsequent deprotection of the glycine amino group with 20% v/v piperidine in DMF was monitored by colorimetric off-bead assays, e.g. the Kaiser test.[337] Final coupling of carboxylic acid **118** onto glycine-loaded polystyrene by DIC-mediated activation under inert atmosphere, afforded the polymer-supported phosphine **123**.

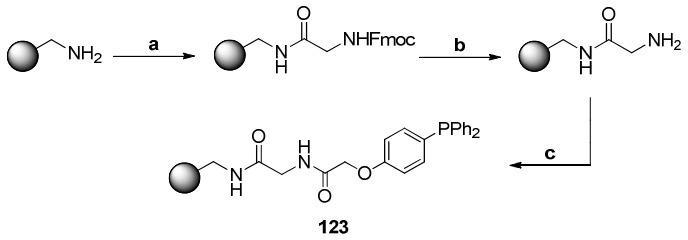

Scheme 29. Synthesis of resin-supported phosphine **123**. Reagents and conditions: a) FmocGlyOH, TBTU, Et_3N, DMF, rt, 15 h; b) 20% v/v piperidine in DMF, rt, 20 min; c) **118**, DIC, DMAP, DMF, dry DCM, rt, 15 h.

Gel-phase ^{31}P NMR was employed to confirm successful coupling of phosphine **118** to the resin. As shown in Figure 92, only a single peak showed up at ca. -8 ppm, which was in agreement with solution phase ^{31}P NMR spectra of phosphines (ca. -6 ppm). Absence of a downfield-shifted signal (ca. 26 ppm) corresponding to phosphine oxide species indicated that polymer-supported phosphine **123** is stable in the absence of moisture and oxygen.

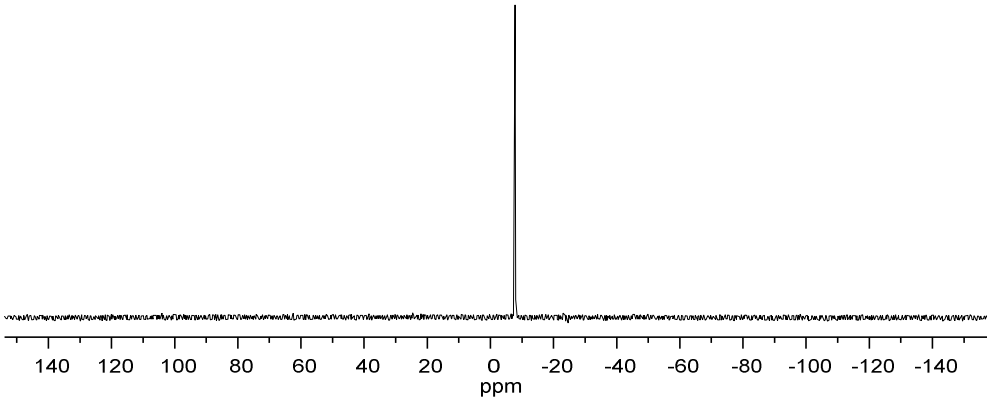

Figure 92. Gel-phase ^{31}P NMR spectrum of polymer-supported phosphine **123** (121 MHz, C_6D_6).

Gel-phase ^{31}P NMR was also used for kinetics studies of Staudinger reaction between resin-supported phosphine **123** and model monosaccharide **91**. The reaction was performed at room temperature and at 40 ºC in DMF in an analogous manner to solution phase reactions described before (Figure 93). ^{31}P NMR-monitored kinetics studies revealed a significantly slower reaction rate at room temperature ($t_{½}$ 8 h) than the corresponding reactions in solution, which can be attributed to the fact that in solid phase synthesis reaction kinetics is diffusion controlled due to restricted permeability of the reactants. The hindered diffusion of the reactants in the NMR tube due to geometrical restrictions may further decelerate the reaction rate. Moreover, nitrogen formation during the reaction creates bubbles within the resin, which also hampers diffusion. Nevertheless, by increasing reaction temperature to 40 ºC practical rates were obtained for resin-supported phosphine **123** ($t_{½}$ 50 min, series).

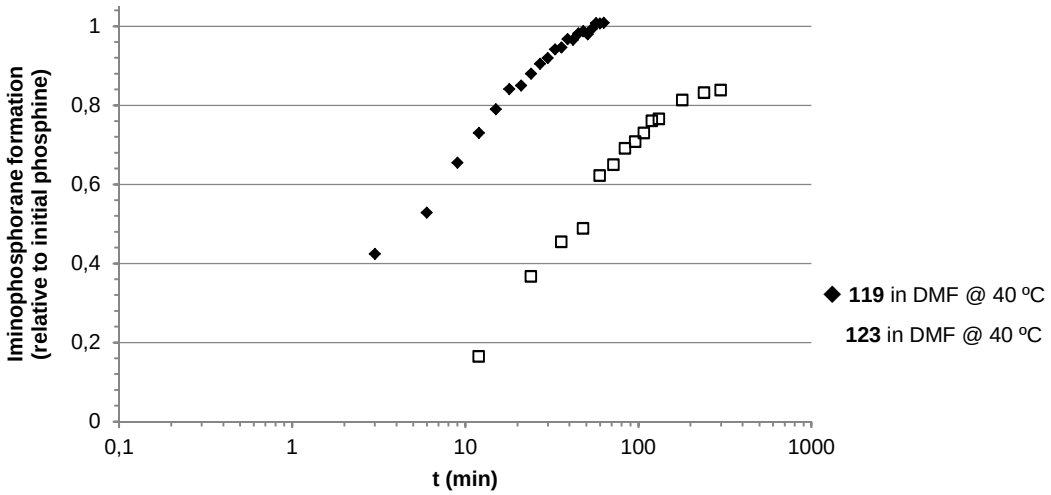

Figure 93. ^{31}P NMR-assisted comparison of iminophosphorane formation kinetics at 40 ºC from azide **91** with phosphine **119** and polymer-supported phosphine **123**, respectively.

AM-PS is not a rigid matrix, but even at the relatively high loading of 0.39 mmol·g^{-1}, and assuming a swelling in the 5-10 mL·g^{-1} range, average distance between reactive centers is estimated in ca. 4 nm. This interphosphine distance was calculated supposing an even distribution in fully swollen resins. From the total number of functional groups in a given resin volume, the volume per phosphine group and, therefore, the average distance between them was calculated. By molecular modeling using *ChemBio3D* (ChemBioOffice package, *CambridgeSoft*) maximum distances between the azido groups in α,α'-trehalose **109** and βCD **110** have been determined (Figure 94). Results showed that the maximum distance between the azido groups is 0.75 nm for α,α'-trehalose **109** and 1.3 nm for βCD **110**, respectively. The interphosphine distance in polymer **123** is three-fold larger than the maximum distance between the azido groups in βCD **110**, which points out its suitability for site-selective CD functionalization, since reagent functionalities on the solid support are situated sufficiently far from each other to prevent CDs from reacting through more than one site.

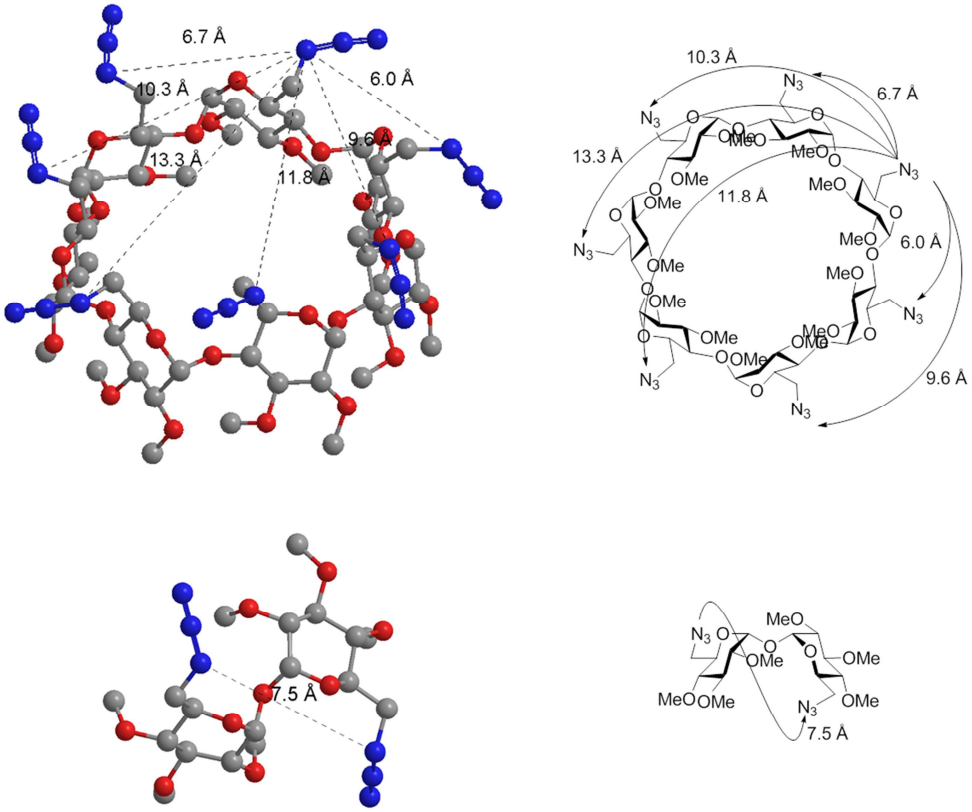

Figure 94. Molecular modeling of α,α'-trehalose **109** (bottom) and βCD **110** (top), with indication of the inter-azide distances in their more stable conformations.

The established conditions for solid-phase-assisted Staudinger reaction were first tested for model monosaccharide **91** (Scheme 30). Indeed, treating resin **123** with 2 eq of azide **91** overnight at 40 ºC in anhydrous DMF under N_2 resulted in virtually complete consumption of the supported phosphine. Premature hydrolysis of the iminophosphorane was not detected, as resin washings only contained the excess of azide. Final hydrolysis with 10% H_2O-DMF overnight at 40 ºC afforded 6-aminoglucoside **124** in 89% yield. Analytical and spectroscopic data of crude methyl 6-amino-6-deoxy-2,3,4-tri-*O*-methyl-α-D-glucopyranoside **124** matched with that of an authentic sample prepared in solution

(see experimental section, Figure S74 for NMR spectra and Figures S145 and S146 for MS spectra, Supporting Information).

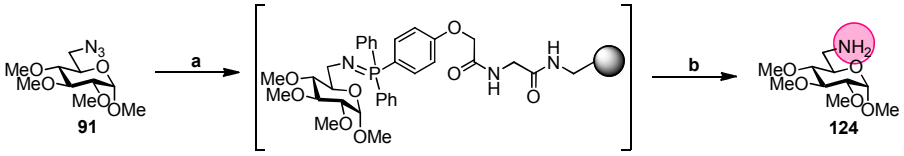

Scheme 30. Solid support-assisted synthesis of 6-aminoglucoside **124**. Reagents and conditions: a) **123** (0.5 eq), anh. DMF, 40 ºC, overnight; b) 10% H_2O-DMF, 40 ºC, overnight, 89%.

However, α,α'-trehalosediazide **109** and βCD heptaazide **110** appeared to be more demanding substrates, since only minute amounts were captured by resin **123** under the same conditions. This may be attributed to size-dependent diffusion rates, or the higher polarity of larger molecules, which hampers accessibility to non-polar PS resin. Higher "catch" temperatures increased reactivity but reduced selectivity. As evidenced by ESI-MS, even diazide **109**, featuring a maximum inter-azide distance of 0.75 nm (Figure 94), was doubly-bound by two phosphine moieties, despite the much larger average resin inter-phosphine distance. Hydrolytic release of the supported diiminophosphorane afforded α,α'-trehalosediamine **125**. An increase in temperature probably enhanced resin backbone mobility which in turn reduced the effective inter-phosphine distance. A similar effect was observed with more flexible supports (e.g. PEGA resin).[338]

To overcome this drawback, we set our sights on microwave irradiation, as we hypothesized that the larger microwave-absorption capability of DMF (as compared to non-polar PS-resin) could selectively increase reagent diffusion and reactivity inside the resin vs. resin backbone mobility. Indeed, microwave-assisted heating revealed a completely different scenario to thermal conditions. Catch efficiency increased up to 90% (estimated from the recovered azide) after irradiating resin **123** swollen in a DMF solution of either **109** or **110** at 60 ºC (2 × 10 min, 40 W) under N_2 (Scheme 31 for **109** and Scheme 32 for **110**).

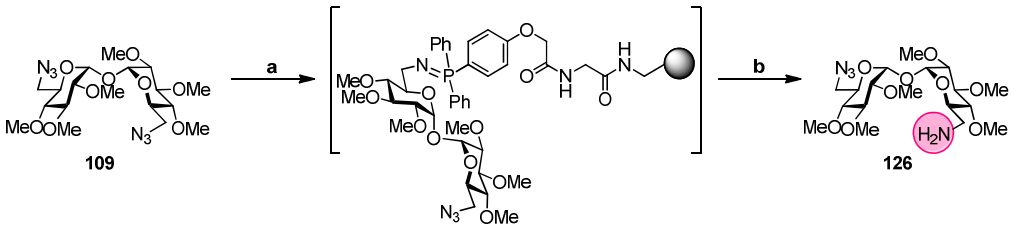

Scheme 31. Solid support-assisted synthesis of monoamine **126**. Reagents and conditions: a) **123** (0.5 eq), anh. DMF, μw, 60 ºC, 2 x 10 min; b) 10% H_2O-DMF, 40 ºC, overnight, 52%.

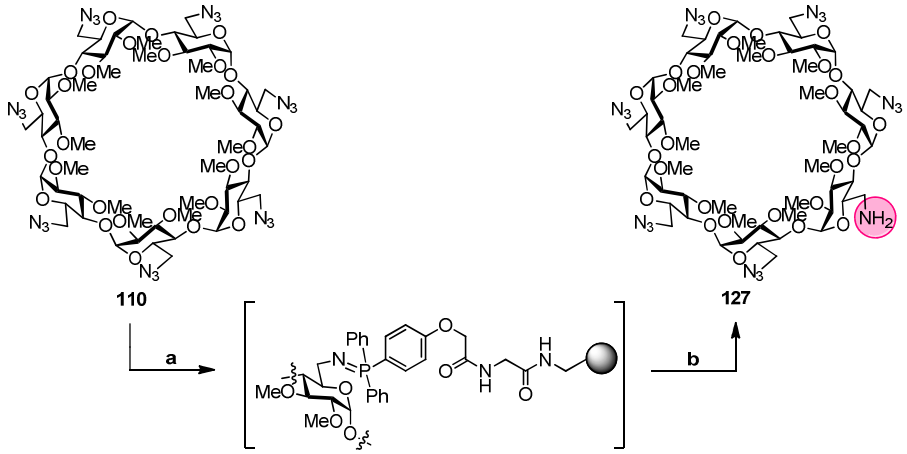

Scheme 32. Solid support-assisted synthesis of monoamine **127**. Reagents and conditions: a) **123** (0.5 eq), anh. DMF, μw, 60 ºC, 2 x 10 min; b) 10% H_2O-DMF, 40 ºC, overnight, 79%.

Hydrolytic release of the supported iminophosphoranes afforded the target mono-reduced adducts (52% and 79% yields for **126** and **127**, respectively) virtually devoid of over-reduced adducts as denoted by ESI-MS and RP-HPLC (Figure 95 and Figure 96; see Figures S76-S77 for NMR spectra and Figures S148-S151 for MS spectra, Supporting Information).

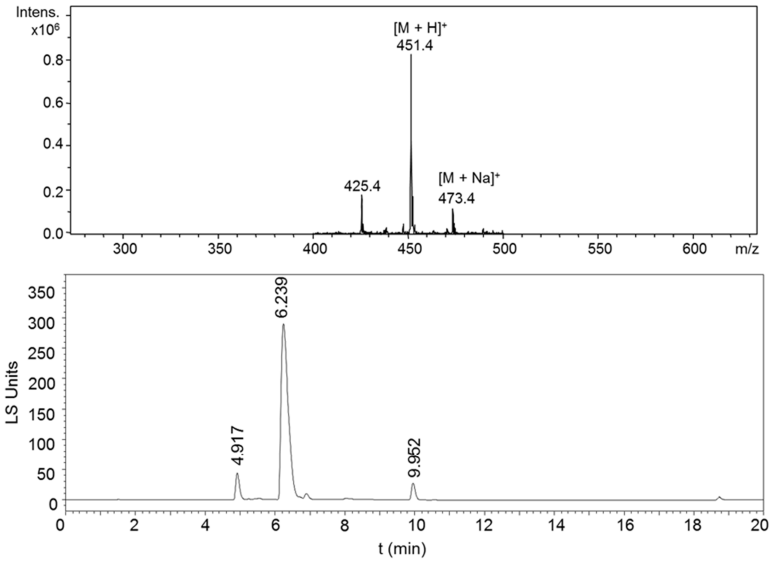

Figure 95. ESI-MS spectrum (top) and HPLC trace (bottom) of crude monoamine **126**.

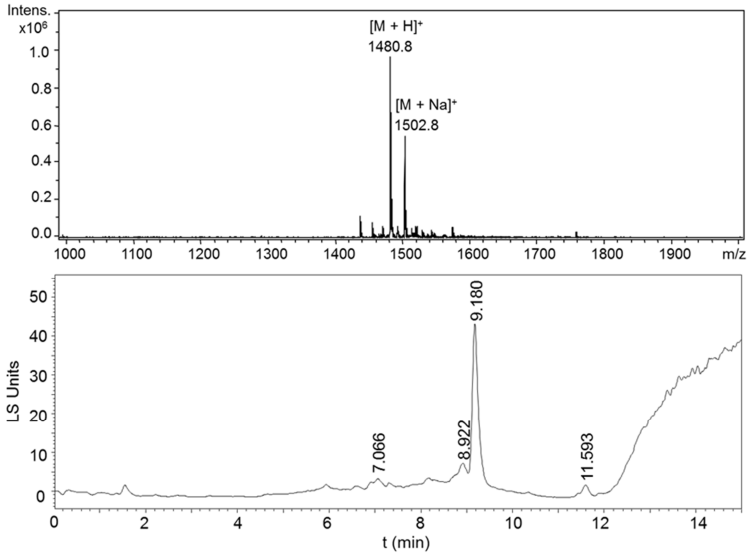

Figure 96. ESI-MS spectrum (top) and HPLC trace (bottom) of crude monoamine **127**.

To tap the full potential of the "*catch-and-release*" concept, the flexibility of iminophosphorane chemistry[333] was also exploited to produce alternative CD functionalization patterns. Aza-Wittig-type reaction of the resin-bound CD iminophosphorane with CS_2 furnished isothiocyanate **128** in 86% yield (Scheme 33).

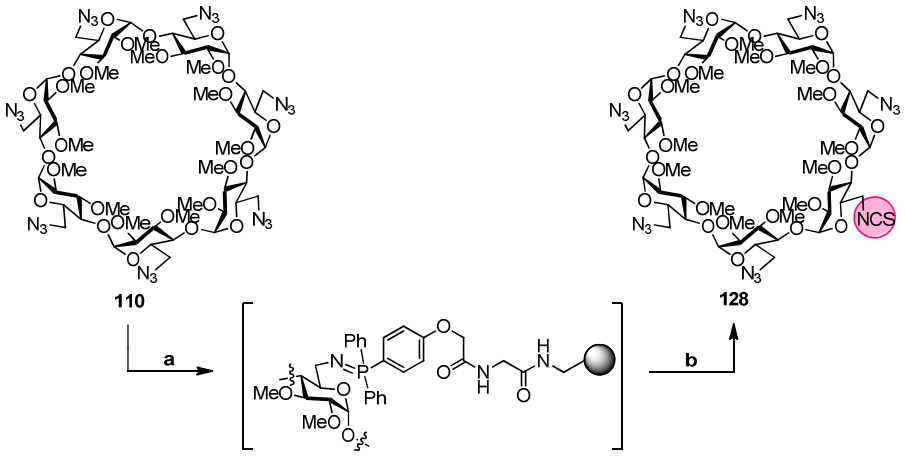

Scheme 33. Solid support-assisted synthesis of monoisothiocyanate **128**. Reagents and conditions: a) **123** (0.5 eq), anh. DMF, μw, 60 ºC, 2 x 10 min; b) CS_2, μw, 60 ºC, 2x10 min, 86%.

Although a clean HPLC trace was observed, a minor peak for diisothiocyanate conjugates was identified by ESI-MS (Figure 97). While the average inter-phosphine distance in resin **123** is estimated in ca. 4 nm (much larger than the largest between azido groups in CD **110**, see Figure 94), resin backbone mobility is a parameter that cannot be easily measured. It is feasible that such distance is not large enough to completely prevent from doubly-capturing a certain amount of CD **110**, as resin backbone mobility reduces inter-phosphine distance. Curiously, such over-reactivity was not observed in the case of amine **127**, despite the similar catch conditions. We reasoned that iminophosphorane hydrolysis may occur at a slower rate due to shrinking of the high hydrophobic PS resin in the presence of water,[339] thereby increasing the chance for doubly-linked CD units to remain bound to the matrix. This type of self-sorting mechanism that efficiently furnished monoamine **127** in excellent yields and purity, however, does not

operate in other cases. The CS_2-DMF cocktail swells the PS resin much better, facilitating the release of all bound material, including mono- and bis-iminophosphoranes.

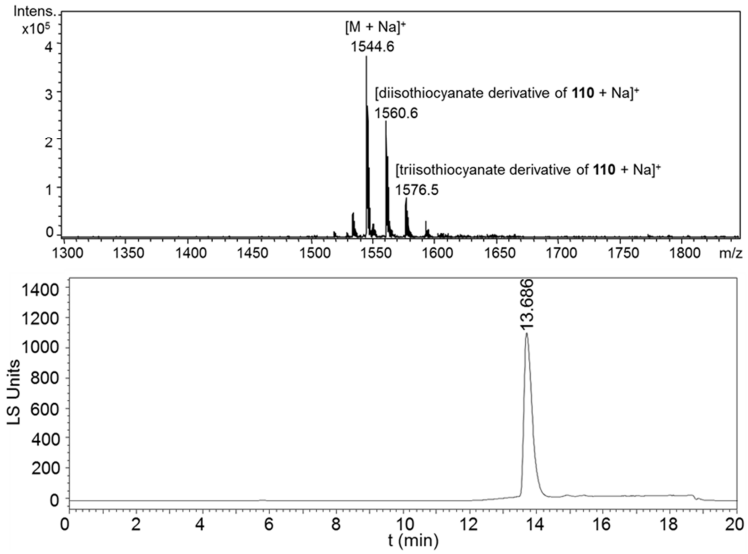

Figure 97. ESI-MS spectrum (top) and HPLC trace (bottom) of crude monoisothiocyanate **128**.

In order to minimize this drawback, a resin with larger inter-phosphine distance has been prepared. Thus, AM-PS resin was acylated with a 9:1 mixture of Boc- and Fmoc-protected glycine and the Boc groups were transformed into inert acetyl groups. Phosphine was then installed onto the remaining amino groups, resulting in a ten-fold diluted matrix, resin-supported phosphine **129**, with ca. 40 $\mu mol \cdot g^{-1}$ loading and 7-9 nm inter-phosphine average distance, calculated in an analogous manner to that described before.

To probe the performance of this support, we made use of an intermolecular aza-Wittig type reaction of immobilized iminophosphorane with a heterocumulene, i.e. isothiocyanate, to construct a carbodiimide functionality, which is a useful precursor of a variety of functional groups.[340] CD **110** was sequentially loaded on and cleaved by 3-methoxypropylisothiocyanate **130**[341] to release a carbodiimide that in situ added water to

furnish the corresponding urea **131** in 76% yield with undetectable trace of difunctionalized adducts (Scheme 34; see Figure S79 for NMR spectra and Figure S154 for MS spectrum of compound **131**, Supporting Information).

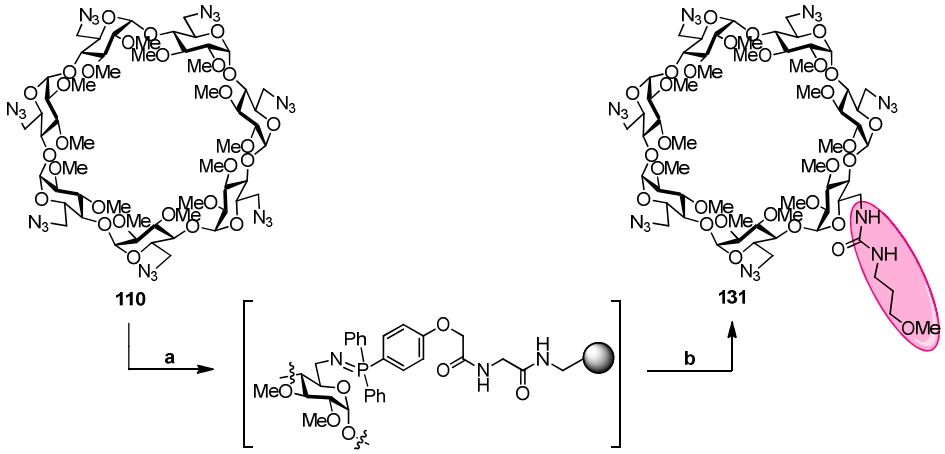

Scheme 34. Solid support-assisted synthesis of monourea **131**. Reagents and conditions: a) **129** (0.5 eq), anh. DMF, μw, 60 ºC, 2x10 min; b) i, 3-methoxypropylisothiocyanate **130**, μw, 60 ºC, 2 x 10 min; ii, AcOH-washed silica gel, MeOH, 5 min, 86%.

To push forward this strategy and taking advantage of the greater selectivity of resin **129**, on-bead manipulation of the solid-supported CD has been taken into account. The iminophosphorane tether should, in principle, remain unaffected by the conditions for CuAAC reaction. Actually, treating the supported CD iminophosphorane with an excess of a terminal alkyne, namely *N*-Boc-protected propargylamine, in the presence of catalytic CuI, followed by CS_2-mediated release, afforded the bifunctional CD derivative **132** in remarkable 59% yield without any purification step (Scheme 35).

The NMR spectrum of this conjugate is far too complex to assess purity and even identity, but RP-HPLC trace and ESI-MS spectra of the crude product doubtlessly confirmed both (Figure 98; see Figure S80 for its ^{1}H NMR spectrum, Supporting Information).

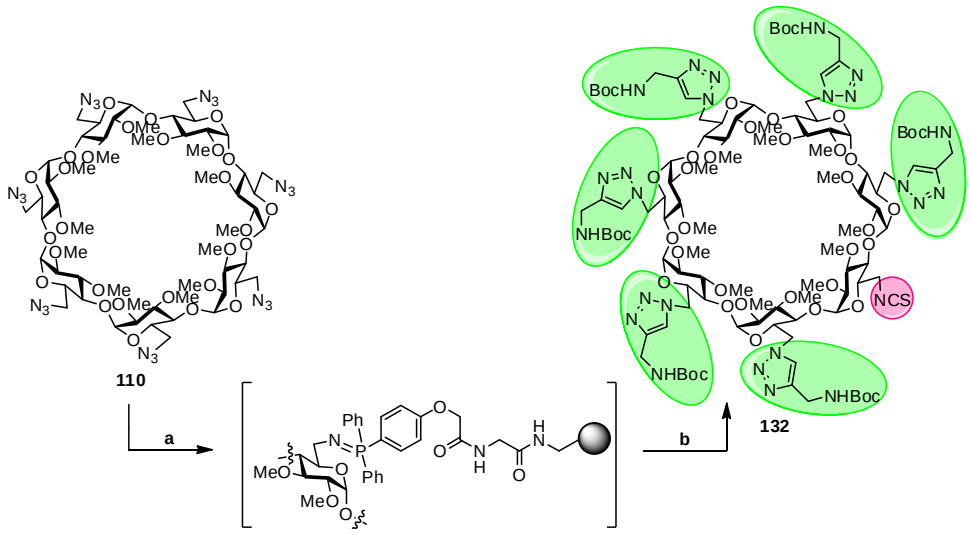

Scheme 35. Solid support-assisted synthesis of heterobifunctional CD derivative **132**. Reagents and conditions: a) **129** (0.5 eq), anh. DMF, µw, 60 ºC, 2x10 min; b) i, *N*-Boc propargylamine, CuI, DIPEA, µw, 80 ºC, 2 x 10 min; ii, CS_2, µw, 60 ºC, 2 x 10 min, 59%.

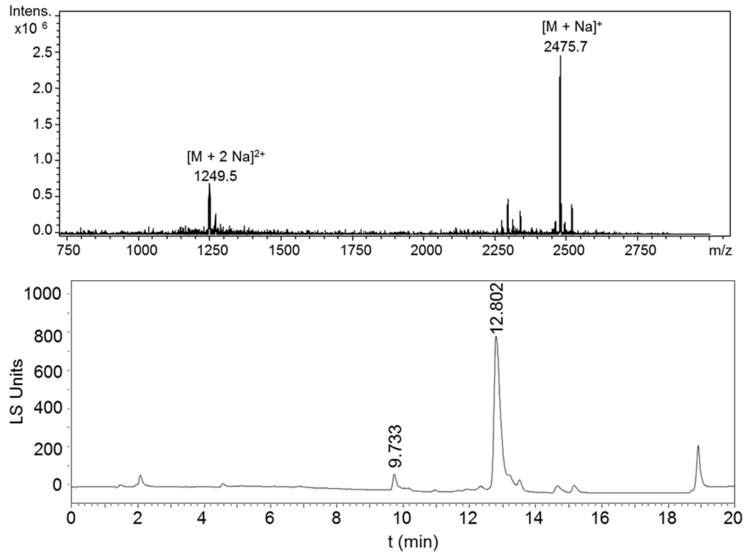

Figure 98. ESI-MS spectrum (top) and HPLC trace (bottom) of the crude heterobifunctional CD **132**.

It is worth mentioning that crude heterobifunctional CD **132** neither exhibited detectable traces of hydrolysis products, nor diisothiocyanate conjugates, but completion of the CuAAC reaction. Production of such CD functionalization patterns, despite being feasible, is far from obvious using conventional solution phase techniques. Although only βCD manipulation has been carried out, it is reasonable that this methodology would be suited for other CDs and macromolecular scaffolds.

CONCLUSIONS

The results obtained in this Ph.D. Thesis have led to the following conclusions:

1. Taking advantage of the rim anisotropy of the basket-shaped βCD structure, two libraries of monodisperse polycationic amphiphilic cyclodextrins (paCDs) with a precise and controlled arrangement of functional elements were prepared, endowing these macromolecular systems with tailored self-assembling capabilities in aqueous environment in the presence of nucleic acids. The flexible and diversity-oriented synthetic strategy was based on the sequential installation of a cationic cluster on the primary rim of the CD scaffold and acylation of the secondary hydroxyls. Systematic manipulation of the molecular structure of paCDs allowed for fine-tuning architectural parameters such as cationic density and display, the nature and flexibility of the tether or the acyl chain length, thereby maintaining C_7-symmetry of facial amphiphilic βCD derivatives. In particular, two series of paCDs were elaborated: (i) a library of paCDs furnished with acyclic cationic domains and featuring subtle disparities in their hydrophilic/hydrophobic balance, and (ii) a library of paCDs decorated with cyclic (preorganized) oligoamines as alternative cationic headgroups.

2. The correlation between amphiphilic CD structure and self-assembling capabilities in aqueous environment (in terms of the critical aggregation concentrations (CACs) of paCDs) was found to be very intimate. Self-assembling was considerably affected by the volume of the hydrophobic domain and the positive charge density, CACs progressively decreasing with increasing amphiphilicity of the CD conjugates. Conversely, the self-assembling capabilities of cyclic oligoamine-grafted paCDs resembled those of paCDs with acyclic polycationic elements and lipophilic tails of the same length.

3. ^{1}H NMR-pH titration experiments of non-amphiphilic polycationic CDs indicated that these non-aggregating polycationic CDs lack pH buffering capabilities in the pH range from 5 to 7, as pK_a values of their primary amines ranged around 9, whereas their tertiary amines exhibited very low pK_a values of ca. 2. In stark contrast, their amphiphilic analogs revealed a completely different behavior. Potentiometric titration profiles clearly

evidenced that amphiphilicity-induced self-aggregation substantially enhances the buffering capacity of CD-scaffolded polycations in the 5-to-7 pH range. Interestingly, the buffering potential is intimately dependent on the structure of the oligoamine display. Moreover, incorporation of cyclic oligoamine groups into the CD scaffold further improved paCD pH buffering capabilities in this pH range. The nature of the cyclic oligoamine motif and the type (primary, secondary, of tertiary amine) and the nature and flexibility of the tether (thiourea or triazole) considerably affects such buffering capacities.

4. DLS experiments pointed out that all polycationic CD derivatives were able to form small, positively charged nanoparticles with calf thymus DNA (ctDNA), regardless of their hydrophilic/hydrophobic balance or the nature of their polar headgroup. All these nanoparticles (CDplexes) featured remarkably similar hydrodynamic diameters, ζ potentials and relatively narrow size distributions. Gel electrophoresis and fluorescence quenching assays evidenced that the amphiphilic character and the hydrophilic/hydrophobic balance of paCDs play an important role in terms of DNA condensing and protecting capabilities. Despite their similar nanoparticle sizes and surface charges, CDplexes derived from more amphiphilic paCDs efficiently protected nucleic acids from the environment at N/P ratios at which less amphiphilic derivatives only attained DNA charge neutralization. No appreciable difference in the DNA-condensing capabilities of paCDs depending on the nature of their cationic headgroups could be inferred. Fluorescence tracking of CDplex dissociation promoted by heparin showed that CDplex dissociation kinetics is drastically influenced by the balance between the lipophilic domain and the polar headgroups. CDplexes composed of more amphiphilic paCDs are more easily formed, but also very slowly dissociated.

5. The transfection efficiency of the CDplexes towards COS-7 and HeLa cell lines was investigated in vitro both in the absence and in presence of serum, and was found to be intimately dependent on architectural features. More stable CDplexes formulated with paCDs bearing more lipophilic tails and lower charge density resulted the best performing candidates in serum-containing medium, exhibiting luciferase expression levels almost

equaling that of JetPEI but with considerably better cytotoxic profiles. Despite their enhanced pH buffering capacities, CDplexes formulated with CD-scaffolded cyclic oligoamine clusters were slightly less efficient than their acyclic counterparts, irrespective of the cyclic amine structure or the nature of the tether. These results highlighted the relevance of DNA complexation capabilities of paCDs for efficient gene delivery, but also clearly indicated that dynamics and kinetics of CDplex formation and, especially, dissociation might play a critical role in overall performance.

6. A conceptually novel approach to the selective functionalization of CDs was developed. The strategy exploited a solid matrix to display the complementary reagent functionalities sufficiently far from each other to prevent a single CD species from reacting through more than one site. Using a "*catch-and-release*" process based on the Staudinger reaction and controlling the average distance between the reactive centers displayed on the solid support, complex CD functionalization patterns could be easily produced in one pot and without any purification step.

EXPERIMENTAL PART

1. General Methods

All reagents and solvents used in this Ph.D. Thesis were purchased from commercial sources and used without further purification, unless otherwise specified.

Thin layer chromatography (TLC) was performed on aluminum sheets coated with Silica Gel 60 F_{245} (layer thickness 0.25 mm, *E. Merck*), with visualization by UV light (λ 254 nm) and by charring with 10% ethanolic H_2SO_4, 0.1% ethanolic ninhydrin, 3% ethanolic phosphomolybdic acid, or Mostain reagent (5% w/v ammonium molybdate(VI) tetrahydrate, 0.1% w/v ceric sulfate hydrate in 10% aq. H_2SO_4).

Flash column chromatography was carried out on Silica Gel 60 (*E. Merck*, 230- 400 mesh).

Size exclusion chromatography (SEC) was performed on cross-linked dextran gel *Sephadex LH-20* and *Sephadex G-25* (*GE Healthcare*) using degassed MeOH and H_2O, respectively, as eluents, with inline UV monitoring at 254 nm. A *Pharmacia Biotech Pump P-1* was used as peristaltic pump.

Microwave-assisted synthesis was carried out using a *Biotage Initiator Microwave Synthesizer* in sealed glass vials.

Optical rotation data were recorded at 20 °C in a 1 dm tube on a *Perkin-Elmer 141 MC Polarimeter*, using the D-line of a sodium lamp (λ 589 nm). Samples were dissolved in DCM or MeOH at concentrations in a range of 0.2 to 1% w/v.

IR spectra were recorded on a *Bruker* FTIR *Vector 22* spectrometer. Samples were dissolved either in MeOH or in DCM, and applied on either KBr or NaCl windows.

Electrospray ionization mass spectrometry (ESI-MS) was done on a *Bruker Esquire600* instrument. Typically, samples were dissolved at low µM concentrations in appropriate volumes of deionized MeCN, MeOH, H_2O or mixtures thereof and injected directly at a flow rate of 120 µL/h using a *Cole-Palmer* syringe pump.

Elemental analyses were performed either on a *Leco CHNS-932* instrument or on a *Leco TruSpec CHN* elemental analyzer.

^{1}H, ^{13}C and ^{31}PNMR spectra were recorded on *Bruker AVANCE 300*(300 MHz), *Bruker AVANCE DRX 400* (400 MHz) and *Bruker AVANCE DRX 500* (500 MHz) NMR

spectrometers. $CDCl_3$, MeOD, DMSO-d_6 and D_2O were used as deuterated solvents. 2D COSY (*Correlated Spectroscopy*), 1D TOCSY (*Totally Correlated Spectroscopy*) and HMQC (*Heteronuclear Multiple-Quantum Correlation*) experiments were employed to assist NMR assignments. NMR data are reported as follows: chemical shift (ppm), multiplicity (s = singlet, bs = broad singlet, d = doublet, dd = doublet of doublets, t = triplet, bt = broad triplet, q = quartet, m = multiplet), peak integration and coupling constant *J* (Hz). NMR experiments in non-deuterated solvents were performed using a sealed capillary containing an appropriate deuterated solvent to assist field lock.

Gel phase ^{31}P NMR was used to confirm successful attachment of the phosphino compounds to the resin. For this purpose, approximately 50 mg of resin were transferred under nitrogen atmosphere to a NMR tube and were then allowed to swell in dry DMF. A thin glass capillary containing a small amount of deuterated solvent (C_6D_6 or D_2O) was placed into the NMR tube in order to provide deuterium lock signal. KH_2PO_4 (1 % w/v) was added to D_2O capillaries as internal standard (6 ppm). ^{31}P NMR chemical shift of reduced phosphino compounds was about -6 ppm, whereas their oxidized analogues were shifted to lower field (approximately 27 ppm). Additionally, ^{31}P NMR was used to carry out kinetics studies concerning *Catch-and-Release* reactions (see Chapter 4), following the same procedures as described above.

Analytical **reversed-phase high performance liquid chromatography (RP-HPLC)** was performed on a *Waters® 2695 Separations Module* using an analytical *HPLC Scharlau column Kromaphase 100 C18 5 µm 150 x 3 mm* (ref. 070B53Y803) column with a flow rate of 1 mL·min^{-1}. Evaporative Light Scattering (ELS) detection (*Waters® 2420 ELS*) was used. The ELS detector was operating under the following conditions: N_2 gas pressure, 27 psi; gain, 1; nebulizer control heater level, 75%, and drift tube temperature, 60 ºC. All RP-HPLC runs were carried out at 30 ºC using buffers A (0.1 % v/v formic acid in H_2O) and B (0.1 % v/v formic acid in MeCN) filtered prior to use according to the following sequence: 1 min isocratic 0 % B, 9 min gradient to 100 % B, 6 min isocratic 100 % B, 2 min gradient to 0 % B and 2 min isocratic 0 % B (Figure 99). Samples were dissolved in acetonitrile at a concentration of 20 mg/mL and the injection volume ranged from 5 to 40 µL. The resulting chromatograms were processed using *Empower Pro Software* (2002).

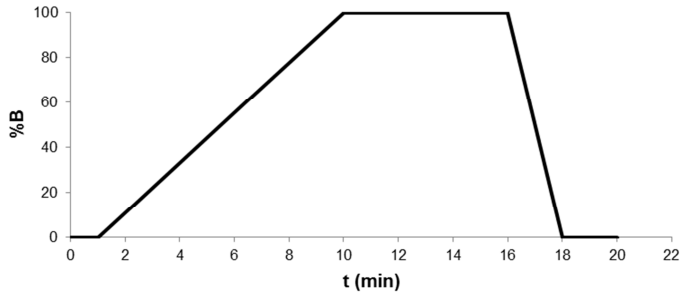

Figure 99. Gradient profile used for RP-HPLC.

1.1. General Methods for Synthesis in Solution Phase

Acetylation reactions were carried out in a mixture of Ac_2O-Py (1:1, 10 mL per gram of compound) at 0 °C, allowing the reaction mixture to warm up to rt overnight. Then, the reaction mixture was poured into H_2O/ice and extracted with DCM. The organic layer was washed successively with 2 M aq. H_2SO_4 and a saturated aqueous solution of $NaHCO_3$. Finally, the organic phase was dried over Na_2SO_4, filtered and evaporated under reduced pressure. In general, the crude product was then purified by flash column chromatography.

Deacetylation reactions were performed under Zemplén conditions.[342] Briefly, to a solution of the corresponding compound in MeOH, methanolic NaOMe (0.1 eq per mole acetate) was added and the reaction mixture was stirred at rt for approximately 5 h. After neutralization with ion exchange resin *Amberlite IR-120* (H^+), the reaction mixture was filtered and the solvent evaporated.

Hydrolysis of carbamate protecting groups was achieved by treating the compounds with a 1:1 mixture of DCM and TFA at rt for two hours. After reaction completion, the solvents were co-evaporated several times with H_2O. To obtain the compounds as their corresponding hydrochloride salts, the resulting residue was freeze-dried from 0.1 N aq. HCl.

In order to hydrolyze carbamate protecting groups belonging to amphiphilic CD derivatives which are sensitive to acidic hydrolysis, compounds were treated with anhydrous TFA at rt for 5 min and then freeze-dried immediately from 0.1 N aq. HCl, yielding the compounds as their corresponding hydrochloride salts.

1.2. General Methods for Solid-Phase Synthesis

Aminomethyl polystyrene (AM-PS) resin (PL-AMS resin, 0.39 mmol/g, 75-150 µm) was purchased from *Polymer Laboratories* (ref. 1464-3749). Solid-phase organic chemistry was performed in disposable plastic syringes fitted with sintered Teflon filters (pore size 10 µm) purchased from *Bola* (ref. N1616-20) or microwave reactor vials.

Attachment of amino acids to the amine-functionalized resin was achieved by pre-activation of the carboxylic acid functionality. Therefore, the resin was placed in the plastic syringe and allowed to swell in DMF for 20 min, which was carefully added from the top and removed from the bottom by vacuum suction. Meanwhile, 3 eq (relative to the resin nominal loading) of the *N*-protected amino acid were dissolved in a minimum amount of DMF and Et_3N (4 eq) and TBTU (2.9 eq) were sequentially added. The mixture was stirred for approximately 5 min until complete dissolution of TBTU. Then, the solution was added to the swollen resin and the mixture was incubated at rt overnight. The resin was washed with DMF (6 x 2 min) and DCM (4 x 2 min). After the final wash, the resin was dried in vacuum to a constant weight. The substitution of the resin was estimated from the weight gain of the resin. Completion of the reaction was ensured by negative Kaiser test (see below).[337]

Solid-phase reaction monitoring was accomplished by colorimetric off-bead assays. To detect primary amines, a small sample of the resin (1 - 2 mg) was removed and submitted to the Kaiser test,[337] which consists in solid-supported amino group derivatization with ninhydrin to afford the characteristic Riemann's purple complex. In a complementary manner, bromophenol blue (4,4'-(1,1-dioxido-3*H*-2,1-benzoxathiole-3,3-diyl)bis(2,6-dibromophenol)) provided a reliable test for the detection of both primary and secondary amines on the solid support. Although less sensitive than the Kaiser test, deprotonation of

the reagent by free amino groups present on the resin imparts a characteristic blue coloration.[343]

To monitor free carboxylic acid moieties on the resin the malachite green test was employed.[344] Therefore, a few beads of the resin were sampled and washed several times with DMF and MeOH. The beads were transferred to a test tube, and 1 mL of a 0.025 % w/w solution of malachite green oxalate in ethanol was added, followed by 1 drop of Et_3N. The mixture was allowed to stand at rt for 2 min and then the solution was decanted and the beads were washed several times with MeOH or EtOH until washes were colorless. A dark green coloration of the beads indicated that free acid moieties were present.

Loading measurements to determine the resin substitution grade usually involve treatment of a known quantity of Fmoc-loaded resin with piperidine in DMF and measuring spectrophotometrically the amount of the dibenzofulvene (DBF)-piperidine adduct released.[335] However, the accuracy of this approach is moderate, as the values obtained do not always correspond with the nominal values. This discrepancy may be a consequence of the equilibrium between piperidine and DBF (Scheme 36).

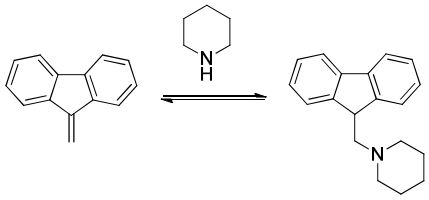

Scheme 36. Equilibrium of DBF and piperidine.

Therefore, piperidine was substituted by a base which cannot undergo Michael addition to DBF.[336] The base of choice was 1,8-diazobicyclo[5.4.0]undec-7-ene (DBU). Approximately 5 mg of resin were weighed into a vial and 2 mL of DMF were added. The suspension was allowed to stand at rt for 30 min and then 40 µL of DBU were added, affording a solution of 2 % v/v DBU in DMF. This mixture was incubated at rt for another 30 min and diluted with MeCN to 10 mL. 200 µL of this solution were then transferred to

another vial and diluted with MeCN to 2.5 mL. A reference solution was prepared in the same manner but without addition of the resin. To quantify Fmoc loading, 1 mL of the reference solution was transferred to one of a matched pair of 1 cm quartz glass cuvettes. The second cuvette was filled with 1 mL of the sample solution. A UV spectrometer was set to zero at 294 nm on the reference solution, and the absorbance of the sample solution was measured. The loading was calculated using equation (5). Alternatively, the quantitation could be performed at 304 nm and calculated using equation (6).

$$loading\ (\frac{mmol\ NH_2}{g\ resin})_{294\ nm} = \frac{A \times 142.14}{mg\ resin} \quad (5)$$

$$loading\ (\frac{mmol\ NH_2}{g\ resin})_{304\ nm} = \frac{A \times 163.96}{mg\ resin} \quad (6)$$

Removal of Fmoc protecting groups was performed with 20% v/v piperidine in DMF (approximately 10 mL/g resin). The mixture was allowed to incubate at rt for 20 min before rinsing the resin with DMF (6 x 2 min) and DCM (4 x 2 min).

Removal of Boc protecting groups was accomplished by suspending the resin in 50% v/v TFA in DCM, using 1 mL of TFA-DCM per gram of resin. The mixture was allowed to incubate at rt for 1 h, followed by rinsing the resin with DCM (4 x 2 min) and 5% v/v Et_3N in DCM (1 mL/g resin) to remove TFA.

Acetylation of solid-supported amino groups was achieved by pre-swelling the resin in DMF and subsequent adding acetic anhydride (10 eq relative to the resin amine loading) and pyridine (10 eq relative to the resin amine loading). The mixture was incubated at rt for 1 h, followed by rinsing the resin with DMF (6 x 2 min) and DCM (4 x 2 min).

Attachment of phosphinocarboxylic acids to the amine-functionalized resin was accomplished under nitrogen atmosphere in order to prevent phosphine oxidation. The resin was placed in a plastic syringe and washed several times with dry DMF (6 x 2 min) and dry DCM (4 x 2 min), which were carefully added through a septum fixed on the top of the syringe and removed from the bottom by purging with nitrogen gas through the

septum. Phosphino carboxylic acids were pre-activated. Therefore, 2.1 eq (relative to the resin amine loading) of the phosphine carboxylic acid were dissolved under nitrogen atmosphere in a minimum amount of dry DCM, and DMAP (2.1 eq) and DIC (2.1 eq) were added. The mixture was stirred for approximately 5 min. Subsequently, the solution was added to the resin and the mixture was allowed to incubate at rt overnight. Then, the resin was washed under nitrogen atmosphere with dry DCM (6 x 2 min). After the final wash, the resin was dried in vacuum to a constant weight. The resin was stored under an inert nitrogen atmosphere to avoid phosphine oxidation.

Formation of resin-supported iminophosphoranes (*Catch*) was accomplished under N_2 atmosphere in order to prevent hydrolysis of the iminophosphorane compounds. A portion of the phosphine-functionalized resin was placed in a plastic syringe and dry and degassed DMF (ca.8 mL per g resin) was added through a septum fixed on the top of the syringe. The resin was allowed to swell in DMF for 30 min at rt. Meanwhile, 1.2 eq or 2 eq respectively (relative to the resin phosphine loading) of the corresponding azide were dissolved in the minimum amount of dry DMF under N_2. Subsequently, the solution was added to the resin and the mixture was incubated at 40 ºC overnight. Evolution of N_2 during the reaction indicated the progression of the reaction. The resin was then washed with dry DMF (5 x 2 min) under N_2 to remove unreacted starting material and eventual byproducts. The combined filtrates were concentrated and freeze-dried in order to determine catch efficiency.

Alternatively, formation of resin-supported iminophosphoranes was also accomplished under microwave irradiation. In this case, the reaction mixture was heated in a sealed glass vial under microwave irradiation at 60 ºC for two cycles of 10 min (ca. 40 W) with intermediate shaking to ensure complete homogenization. The resin was then washed with dry DMF (5 x 2 min) under N_2 to remove unreacted starting material or undesired byproducts. The combined filtrates were concentrated and freeze-dried in order to determine catch efficiency.

Cleavage of resin-supported iminophosphoranes by hydrolysis to yield an amine (*Release, procedure A*) was accomplished immediately after completion of the *Catch* reaction step. The iminophosphorane-loaded resin was swollen in 10% H_2O in DMF

(approximately 8 mL per g resin) and heated either thermally to 40 ºC overnight or under microwave irradiation to 60 ºC (2 x 10 min, ca. 40 W). Then, the resin was filtered and washed with DMF (6 x 2 min) to extract the released amine. The combined filtrates were concentrated and freeze-dried in order to determine reaction yield and product purity.

Cleavage of resin-supported iminophosphoranes by reaction with CS_2 to yield an isothiocyanate (*Release, procedure B*) was accomplished immediately after completion of the *Catch* reaction step. The iminophosphorane-loaded resin was swollen in 10% CS_2 in dry DMF (approximately 8 mL per g resin) under N_2 and heated under microwave irradiation to 60 ºC (2 x 10 min, ca. 40 W). Then, the resin was filtered and washed with DMF (6 x 2 min) to obtain the released isothiocyanate. The combined filtrates were concentrated and freeze-dried in order to determine reaction yield and product purity.

Cleavage of resin-supported iminophosphoranes by reaction with an isothiocyanate to yield a urea (*Release, procedure C*) was done immediately after completion of the *Catch* reaction step. The iminophosphorane-loaded resin was swollen in a solution of 3-methoxypropylisothiocyanate **130**[341] (5 eq) in dry DMF (approximately 8 mL per g resin) under N_2 and heated under microwave irradiation to 60 ºC (2 x 10 min, 40 W). Then, the resin was filtered and washed with DMF (6 x 2 min) to obtain the released carbodiimide. To transform the carbodiimide into a urea derivative, the combined filtrates were concentrated, the residue was dissolved in MeOH and a catalytic amount of AcOH-washed silica gel was added. Then, the reaction mixture was stirred at rt for 5 min and the solvents were then co-evaporated twice with water and the resulting urea was freeze-dried in order to determine reaction yield and product purity.

CuAAC "click" reaction in solid phase prior to cleavage of resin-supported iminophosphoranes was done on the remaining free azido groups of polyazide compounds after formation of the resin-supported iminophosphorane. The iminophosphorane-loaded resin was swollen in a solution of *N*-Boc-propargylamine (2 eq per remaining solid-supported azido group), DIPEA (2.5 eq), and CuI (0.1 eq) in dry DMF (approximately 8 mL per g resin) under N_2 and heated under microwave irradiation to 80 ºC (2 x 10 min, 70 W). The resin was carefully washed as in the catch phase to remove the remaining excess of reagents in solution. The resin was then swollen in 10% CS_2 in DMF and the product was released as described in *Procedure B*. The combined filtrates

were concentrated and freeze-dried in order to determine reaction yield and product purity.

1.3. General Methods for Characterization of paCDs

The **critical aggregation concentration (CAC)** was determined using an established technique based on the dependence of the fluorescence spectrum of pyrene on the microenvironment.[205] This extremely hydrophobic probe is preferentially incorporated in the inferior of supramolecular aggregates. The onset of supramolecular aggregate formation can be observed in a shift of its fluorescence excitation spectrum at an emission wavelength of 375 nm. In the concentration range of aqueous solutions, a shift of the excitation band in the 335 nm region toward higher wavelengths confirms the incorporation of pyrene in the hydrophobic interior of aggregates.

CAC measurements were performed on a *Varian Cary Eclipse Fluorescence Spectrophotometer*. Fluorescence measurements were carried out at an emission wavelength of 375 nm (emission and excitation slits fixed at 5 nm). The ratio of the fluorescence intensities at excitation wavelengths of 339 (I_{339}) and 335 (I_{335}) nm was used to quantify the shift of the broad excitation band.

A pyrene stock solution (1 mM in THF) was diluted with Milli-Q water to give a final concentration of 0.6 µM. This pyrene solution was subsequently used to prepare stock solutions of amphiphilic CDs (500 µM). These CD stock solutions were diluted with 0.6 µM pyrene solution in order to yield solutions varying in CD concentration from 500 to $2.56 \cdot 10^{-4}$ µM. The samples were allowed to equilibrate for 1 h at 37 °C prior to fluorescence measurement. To determine aggregate stability, selected samples were incubated at rt for 5 days and one month, respectively, prior to fluorescence measurement. Finally, the critical aggregation concentrations were determined from the crossover point when representing Log[CD] vs. I_{339}/I_{335} ratio.

pK_a and pH-buffering capability determination was done by ^{1}H NMR-pH titration and by potentiometric titration. For the ^{1}H NMR-pH titration an acidic solution **A** containing 60 µL compound stock solution (10-70 mM in H_2O), 60 µL D_2O, 600 µL stock solution NaCl (0.2 M, in H_2O-D_2O 9:1, 1% MeCN), 120 µL stock solution HCl (100 mM in H_2O) and 360

µL H_2O, as well as a basic solution **B**, consisting of 125 µL compound stock solution, 125 µL D_2O, 1.25 mL stock solution NaCl, 250 µL stock solution NaOH and 750 µL H_2O, were prepared. Determination of the pK_a values of the compounds was performed by titrating the acidic solution **A** (500 µL, compound concentration 0.5 mM in 9:1 H_2O-D_2O) with the basic solution **B** and monitoring the induced chemical shifts of certain proton nuclei adjacent to pH-active groups ($\Delta\delta_{obs}$) by ^1H NMR spectroscopy at 25 ºC. The MeCN in solution **A** was used as internal reference. The dissociation constants of PEI were also determined as indicated for paCDs, starting from a 200 mM stock solution. The pH value of the solution was measured after every addition of solution **B** and just before the spectrum acquisition. To record the spectra, the water peak was suppressed using a phase-shift presaturation technique. The ionization equilibrium of a protonated amine is given by equation (7),

$$AH^+ \rightleftharpoons A + H^+ \tag{7}$$

whose equilibrium constant K_a is expressed as

$$K_a = \frac{[H^+][A]}{[AH^+]} \tag{8}$$

or

$$pK_a = pH + log\frac{[AH^+]}{[A]} \tag{9}$$

Plotting δ_{obs} as a function of pH yielded sigmoidal curves for each compound. The pK_a values were obtained by plotting according to the Henderson-Hasselbalch equation (10),

$$pH = pK_a + log\frac{\delta_{acidic} - \delta_{obs}}{\delta_{obs} - \delta_{basic}} \tag{10}$$

in which δ_{acidic} and δ_{basic} are the chemical shifts of the observed signal of the fully protonated and deprotonated compound, respectively, and linear fitting.

To determine the buffering capacity of cationic compounds, acid-base titration studies were conducted over a pH range of 2-10. Each compound (0.05 mmol of amino groups) was dissolved in 1 mL of 150 mM NaCl aqueous solution, and 0.088 N aq. NaOH (standardized using 2% w/v aq. potassium hydrogen phthalate) was added to adjust pH to 10. Aliquots (10 µL for each) of 0.084 N aq. HCl (titrated with 0.088 N aq. NaOH) were added, and the solution pH was measured with a *Basic 20 pH-meter* (*Crison*) after each addition. A blank (150 mM aq. NaCl) was used under the same experimental conditions. By plotting µL of 0.084 N aq. HCl added vs. pH, the acid-base titration profile of each compound was represented.

1.4. General Methods for Characterization of CDplexes

For the **preparation of complexes formulated from CD derivatives and DNA** two different plasmids were used; DNA sodium salt from calf thymus (ctDNA, *Sigma-Aldrich*, ref. D3664*)*, a highly polymerized DNA (10-15 million Da) which contains both double stranded and single stranded forms, being double stranded DNA the predominant form, and the luciferase-encoding plasmid pTG11236 (pCMVSV40-luciferase-SV40pA),[345] which is a plasmid of 5739 bp (base pairs). The latter was utilized for transfection assays whereas studies of physicochemical properties were carried out using commercially available DNA.

The quantities of compound used were calculated according to the desired DNA concentration, the N/P ratio, the molecular weight and the number of protonable nitrogen atoms in the corresponding cationic CD or cationic polymeric or CD reference (JetPEI (22kDa), bPEI or PTG). In particular, DNA concentrations applied were 0.06 $mg \cdot mL^{-1}$ (i.e. 180 µM phosphate) for gel electrophoresis, 0.58 $mg \cdot mL^{-1}$ (i.e. 1.75 µM phosphate) for critical aggregation concentration determination, 0.02 $mg \cdot mL^{-1}$ (i.e. 60 µM phosphate) for

nanoparticle size, polydispersity index (PDI) and ζ potential measurements, 0.002 $mg \cdot mL^{-1}$ (i.e. 6 µM phosphate) for fluorimetric pDNA-paCD-binding studies, 0.004 $mg \cdot mL^{-1}$ (i.e. 12 µM phosphate) for heparin competitive displacement assays and 5 $\mu g \cdot mL^{-1}$ (i.e. 15 µM phosphate) for in vitro transfection experiments.

For the preparation of CDplexes, typically pDNA was diluted in HEPES (20 mM, pH 7.4) to the desired final concentration as specified above, and then the desired amount of CD derivative was added from a stock solution in DMSO (typically 10 mM). The resulting mixture was vortexed thoroughly and the complexes were incubated for one hour prior to subjecting them to characterization or transfection experiments.

Nanoparticle size, polydispersity index (PDI) and ζ potential were determined by Dynamic Light Scattering (DLS).[228] The average diameter that is measured in DLS is a value that refers to how a particle diffuses within a fluid so it is referred to as a hydrodynamic diameter. The diameter that is obtained by this technique is the diameter of a hypothetical rigid sphere that has the same translational diffusion coefficient as the particle. Thus, the average particle size calculated in this manner corresponds to the apparent size of solvated particles. It is important to note that this mean size is an intensity mean. It is not a mass or number mean because it is calculated from the signal intensity. Furthermore, a dispersion width parameter is given, known as the polydispersity index (PDI).

CDplexes were prepared as previously described according to the desired pDNA concentration (60 µM phosphate) at N/P ratios 5 and 10.CDplex average sizes were measured using a *Zetasizer Nano* (*Malvern Instruments*) with the following settings: sampling time, automatic; number of measurements, 3 per sample; medium viscosity, 1.054 cP; refractive index, 1.33; scattering angle, 173°; λ 633 nm; temperature, 25 °C. Data were analyzed making use of the multimodal number distribution software included in the instrument. Results are presented as volume distribution of the major population by the mean diameter and its standard deviation.

ζ-Potential is a parameter that can be related to the surface electric charge of nanoparticles.[229] The net charge at the particle surface affects the distribution of ions in the surrounding interfacial region, resulting in an increased concentration of counter ions

close to the surface. Thus, an electrical double layer exists around each particle. ζ Potential is the potential difference between the diffuse region and the stationary layer of fluid attached to the dispersed particle. To determine ζ potential, two techniques are combined: Electrophoresis and Laser Doppler Velocimetry, being electrophoretic mobility the measured parameter (Laser Doppler Electrophoresis).

ζ Potential measurements on CDplexes were accomplished on the same *Zetasizer Nano* instrument applying "mixed-mode measurement" phase analysis light scattering (M3-PALS). M3-PALS consists of both slow field reversal and fast field reversal measurements, hence the name "mixed-mode measurement"; it improves accuracy and resolution. The following settings were applied: sampling time, automatic; number of measurements, 3 per sample; medium viscosity, 1.054 cP; medium dielectric constant, 80; temperature, 25 °C.

Before each series of experiments, performance of the instrument was calibrated with either 90 nm monodisperse latex beads (*Coulter*) for DLS or with DTS 50 standard solution (*Malvern*) for ζ potentials.

Agarose gel electrophoresis was run in 0.8% (w/w) agarose gel in TAE buffer (1:1:1 Tris/acetate/EDTA) and stained with GelRed™ (*Biotium*, 7.5 µL 10000x in 160 mL TAE). CDplexes were prepared as previously described according to the desired ctDNA concentration (180 µM phosphate) at N/P ratios ranging from 0.5 to 20. The samples were prepared by mixing 18 µL of each CDplex formulation and 2 µL of loading buffer (6x; 5 mL glycerol, 250 µL TAE 40x, 1 mL bromophenol blue and 2.75 mL H_2O). Bromophenol blue is a negatively charged dye and thus moves in the same direction as DNA during electrophoresis. This color marker is used to monitor the process on the gel, although DNA may move more rapidly than bromophenol blue. The samples were submitted to electrophoresis for approximately 20 min under 150 V. Finally, DNA was visualized after photographing (λ 302 nm) using an *Alphaimager Mini* UV transilluminator (*Cell Biosciences*).

CDplex formation and dissociation was monitored by fluorescence quenching of an intercalating agent. Experiments were performed on a *Varian Cary Eclipse Fluorescence Spectrophotometer* using ctDNA (5 µg, [bp] = 3.0 µM). For CDplex formation studies a

solution of intercalating agent RedSafe™ (*iNtRON Biotechnology*, 2.5 µL 20 000x in 50 mL HEPES 20 mM, pH 7.4) was prepared. Fluorescence emission was measured in a range from 450 to 570 nm, exhibiting RedSafe™ an emission maximum at 525 nm (λ_{ex} 295 nm, emission and excitation slits 5 nm). Fluorescence emission of the buffer solution was taken as reference. When ctDNA was added to the RedSafe™ buffer solution (final concentration 3 µM bp), the fluorescence reading of the RedSafe™-DNA solution increased drastically. Subsequently, from CD derivative stock solutions in DMSO (50-1000 µM) µL portions were added to the RedSafe™-DNA solution in order to obtain ascending N/P ratios from0.1 to 10 approximately. These N/P ratios correspond to CD concentrations ranging from ca. 0.03 to 8.6 µM. Fluorescence emission was recorded after each addition and equilibration (5 min) and as N/P ratio increases fluorescence intensity decreases, indicating the DNA condensation and subsequent dye exclusion by CDplex formation. Portions of the CD stock solution were added until no further decrease in fluorescence intensity could be observed.

To assess CDplex dissociation and to compare the relative stability, competitive displacement assays were performed on CDplexes at an N/P ratio of 5 using heparin. The effect of heparin on the stability of CDplexes was evaluated by means of the change in relative fluorescence intensity obtained with the fluorescence probe RedSafe™ (*iNtRON Biotechnology*, 20000x). Starting from a CDplex solution in HEPES (20 mM, pH 7.4, RedSafe™ 1x) containing a DNA concentration of 3.0 µM (base pairs) and the corresponding volume of a CD stock solution in DMSO (50-1000 µM), a volume of 150 µL of this solution was added to the wells of a 96-well plate. Then, different volumes of heparin stock solutions (100-10000 µg/mL in HEPES 20 mM, pH 7.4) were added to each well and after taking to a final volume of 250 µL, final heparin concentrations in the range of 5-2000 µg/mL were obtained. The samples were incubated for 10 min at rt prior to fluorescence measurement. Finally, time-dependent fluorescence intensity was measured with a *Varian Cary Eclipse Fluorescence Spectrophotometer* equipped with a microplate reader as indicated above. Naked DNA and bPEI as references were processed in a similar manner as indicated for the CDplexes.

1.5. Evaluation of the Gene Transfer Capabilities of CDplexes

In vitro transfection experiments were performed in COS-7 and HeLa cells. Twenty-four hours before transfection, cells were grown at a density of $2 \cdot 10^4$ cells per well in 96-well plates in Dulbelcco's modified Eagle's culture medium (DMEM; Gibco-BRL) containing 10% fetal calf serum (FCS; Sigma), 10 $mg \cdot mL^{-1}$ gentamycin for HeLa cells, or 100 units per mg penicillin and 100 $mg \cdot mL^{-1}$ streptomycin for COS-7 cells, in a wet (37 ºC) and 5 % CO_2 containing air atmosphere. The above-described CD:pDNA (pTG11236) complexes, JetPEI:pDNA polyplexes and PTG:pDNA complexes were diluted to 100 µL in DMEM or in DMEM supplemented with 10% FCS so as to have 0.5 µg of pDNA in the well (15 µM phosphate). The culture medium was removed and replaced by these 100 µL of the complexes. After 4 and 24 h, DMEM (50 and 100 µL) supplemented with 30% and 10% FCS, respectively, were added. After 48 h, the transfection was stopped, the culture medium was discarded, and the cells were washed twice with PBS (100 µL) and lysed with lysis buffer (50 µL; Promega, Charbonnires, France). The lysates were frozen at -32 ºC before the analysis of luciferase activity. This measurement was performed using a luminometer (*GENios PRO*, Tecan France S.A.) in dynamic mode, for 10 s on the lysis mixture (20 µL) and using the "luciferase" determination system (Promega) in 96-well plates. The total protein concentration per well was determined by the BCA test (Pierce, Montluçon, France). Luciferase activity was calculated as fg of luciferase per mg of protein. The percentage of cell viability was calculated as the ratio of the total protein amount per well of the transfected cells relative to that measured for untreated cells. The data were calculated from three or four repetitions in two fully independent experiments (formulation and transfection).

2. Starting Materials

The following starting materials were prepared as described previously in literature:

- Heptakis(6-bromo-6-deoxy)cyclomaltoheptaose **11**[175]
- Heptakis(6-bromo-6-deoxy-2,3-di-*O*-hexanoyl)cyclomaltoheptaose **12**[174]
- Heptakis[6-(2-*tert*-butoxycarbonylaminoethylthio)-6-deoxy]cyclomaltoheptaose **13**[177]
- 2-(*tert*-Butoxycarbonylamino)ethylisothiocyanate **22**[186]
- 2-[Bis(2-(*tert*-butoxycarbonylamino)ethyl)amino]ethylisothiocyanate **23**[177]
- Heptakis(6-aminoethylthio)cyclomaltoheptaose **32**[185a]
- Heptakis(6-azido-6-deoxy)cyclomaltoheptaose **53**[269]
- Heptakis(6-azido-6-deoxy-2,3-di-*O*-hexanoyl)cyclomaltoheptaose **54**[180b]
- 1,4,7-Tritosyl-1,4,7-triazaheptane **55**[271]
- 1,3,5-Tritosyl-3-azapentane **56**[272]
- 1,4,7,10-Tetratosyl-1,4,7,10-tetraazacyclododecane **57**[273]
- 1-(Prop-2-ynyl)-1,4,7,10-tetraazacyclododecane trihydrochloride **60**[274]
- 1,4,7-Tris(*tert*-butoxycarbonyl)-1,4,7,10-tetraazacyclododecane **61**[276b]
- 1,4,8-Tris(*tert*-butoxycarbonyl)-1,4,8,11-tetraazacyclotetradecane **62**[346]
- 1,6-Hexamethylenediisothiocyanate **68**[278]
- 2-[*N*-(*tert*-Butoxycarbonyl)-*N*-[2-(*tert*-butoxycarbonylamino)ethyl]amino]ethyl isothiocyanate **85**[177]
- Methyl 6-azido-6-deoxy-2,3,4-tri-*O*-methyl-α-D-glucopyranoside **91**[280]
- Bis(triphenylphosphine)copper(I)iodide **93**[289]
- Tris(triphenylphosphine)copper(I)iodide **94**[290]
- 6,6'-Diazido-6,6'-dideoxy-α,α'-trehalose **108**[269]
- Heptakis(6-azido-6-deoxy-2,3-di-*O*-methyl)cyclomaltoheptaose **110**[180a]
- 4-(Diphenylphosphino)benzoic acid **112**[334]
- Methyl 4-iodobenzoate **113**[347]
- Methyl 4-(diphenylphosphino)benzoate **114**[348]
- 4-(Diphenylphosphoryl)benzoic acid **115**[349]
- 3-Methoxypropylisothiocyanate **130**[341]

3. New Compounds

3.1. New Compounds synthesized in Chapter 2

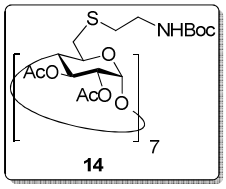

14

Heptakis[2,3-di-*O*-acetyl-6-(2-*tert*-butoxycarbonylaminoethylthio)-6-deoxy]cyclomaltoheptaose (14). Compound **13**[177] (1.03 g, 0.46 mmol) was acetylated using acetic anhydride as acetylating agent according to a standard procedure described before. The crude product was purified by flash column chromatography (40:1 → 20:1 DCM-MeOH) to yield compound **14** as a white powder (1.04 g, 80%).

R_f = 0.80 (20:1 DCM-MeOH). $[\alpha]_D$ = +18.9 (*c* = 1.0 in DCM).

^{1}H NMR (500 MHz, $CDCl_3$, 313 K, Figure S1): δ = 5.39 (bs, 7H, N*H*Boc), 5.28 (t, 7H, $J_{2,3}$ = $J_{3,4}$ = 9.4 Hz, H-3), 5.15 (d, 7H, $J_{1,2}$ = 3.9 Hz, H-1), 4.84 (dd, 7H, H-2), 4.20 (m, 7H, H-5), 3.82 (t, 7H, $J_{4,5}$ = 9.4 Hz, H-4), 3.63 (bq, 14H, $^3J_{H,H}$ = 6.5 Hz, CH_2NHBoc), 3.16 (dd, 7H, $J_{5,6a}$ = 2.1 Hz, $J_{6a,6b}$ = 11.6 Hz, H-6a), 3.06 (dd, 7H, $J_{5,6b}$ = 6.0 Hz, H-6b), 2.82 (m, 14H, CH_2S_{cyst}), 2.06, 2.02 (2 s, 21H each, $COCH_3$), 1.42 (s, 63H, $(C(CH_3)_3)$).

^{13}C NMR (75.5 MHz, $CDCl_3$, 313 K, Figure S1): δ = 171.1, 169.8 (2 CO ester), 156.4 (CO carbamate), 97.1 (C-1), 79.7 (C-4), 79.4 (CCH_3), 71.7 (C-3), 71.3 (C-2), 70.9 (C-5), 40.6 (CH_2NHBoc), 34.1 (CH_2S_{cyst}, C-6), 28.9 ($C(CH_3)_3$), 21.2 ($COCH_3$).

ESI-MS (Figure S81): *m/z* 1442.0 $[M + 2 Na]^{2+}$, 2861.7 $[M + Na]^+$.

Elemental analysis calculated (%) for $C_{119}H_{189}N_7O_{56}S_7$: C 50.36, H 6.71, N 3.45; found: C 50.21, H 6.46, N 3.35.

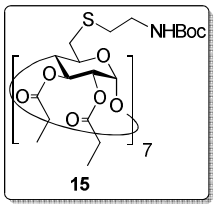

15

Heptakis[6-(2-*tert*-butoxycarbonylaminoethylthio)-6-deoxy-2,3-di-*O*-propanoyl]-cyclomaltoheptaose (15). To a solution of **13**[177] (1.0 g, 0.44 mmol) in dry DMF (30 mL) under nitrogen atmosphere, DMAP (2.28 g, 18.7 mmol, 3 eq) and propanoic anhydride (3.2 mL, 24.9 mmol, 4 eq) were added at 0 ºC. The reaction mixture was allowed to warm to rt and stirred overnight. Then, MeOH (130 mL) was added and the reaction mixture was further stirred for 1 h. The solvents were removed under reduced pressure, and subsequently H_2O (60 mL) was added to the reaction mixture which was then extracted with DCM (4 x 60 mL). The organic layer was successively washed with 1 N aq. HCl (2 x 50 mL) and a saturated aqueous solution of $NaHCO_3$ (50 mL), dried over Na_2SO_4, filtered and reduced in vacuum. The crude product was purified by flash column chromatography (1:2 → 1:1 EtOAc-petroleum ether) to yield **15** (0.98 g, 73%).

R_f = 0.29 (20:1 DCM-MeOH). $[\alpha]_D$ = +85.7 (*c* = 1.0 in DCM).

^{1}H NMR (500 MHz, $CDCl_3$, Figure S2): δ = 5.45 (bs, 7 H, N*H*Boc), 5.28 (t, 7H, $J_{2,3} = J_{3,4}$ = 8.9 Hz, H-3), 5.12 (d, 7H, $J_{1,2}$ = 3.9 Hz, H-1), 4.84 (dd, 7H, H-2), 4.20 (m, 7H, H-5), 3.80 (t, 7H, $J_{4,5}$ = 8.6 Hz, H-4), 3.35 (bq, 14H, $^3J_{H,H}$ = 6.5 Hz, CH_2NHBoc), 3.17 (dd, 7H, $J_{5,6a}$ = 2.1 Hz, $J_{6a,6b}$ = 11.7 Hz, H-6a), 3.07 (dd, 7H, $J_{5,6b}$ = 5.9 Hz, H-6b), 2.79, 2.77 (2 dt, 14H, $^2J_{H,H}$ = 13.4 Hz, $^3J_{H,H}$ = 6.7 Hz, CH_2S$_{cyst}$), 2.47-2.20 (m, 28H, CH_2CO), 1.47 (s, 63H, C$(CH_3)_3$), 1.12 (2 t, 42H, $^3J_{H,H}$ = 7.5 Hz, CH_3).

^{13}C NMR (125.7 MHz, $CDCl_3$, Figure S2): δ = 174.1, 172.6 (2 CO ester), 156.0 (CO carbamate), 96.8 (C-1), 79.4 (*C*$(CH_3)_3$), 79.0 (C-4), 71.3 (C-5), 70.7 (C-3), 70.2 (C-2), 40.4 (*C*H_2NHBoc), 33.8 (CH_2S_{cyst}, C-6), 28.5 (C(*C*$H_3)_3$), 27.3, 27.2 (*C*H_2CO), 8.9 (CH_3).

ESI-MS (Figure S82): *m/z* 1540.3 $[M + 2\ Na]^{2+}$, 3057.0 $[M + Na]^+$.

Elemental analysis calculated (%) for $C_{133}H_{217}N_7O_{56}S_7$: C 52.64, H 7.21, N 3.23, S 7.40; found: C 52.64, H 7.27, N 3.20, S 7.69.

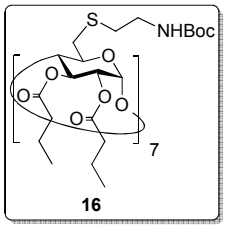

16

Heptakis[2,3-di-*O*-butanoyl-6-(2-*tert*-butoxycarbonylaminoethylthio)-6-deoxy]cyclomaltoheptaose (16). To a solution of **13**[177] (1.21 g, 0.54 mmol) in dry DMF (40 mL) under nitrogen atmosphere, DMAP (2.77 g, 22.7 mmol, 3 eq) and butanoic anhydride (4.9 mL, 30.2 mmol, 4 eq) were added at 0 ºC. The reaction mixture was allowed to warm to rt and stirred overnight. Then, MeOH (150 mL) was added and the reaction mixture was further stirred for 1 h. The solvents were removed under reduced pressure, and subsequently H_2O (70 mL) was added to the reaction mixture which was then extracted with DCM (4 x 70 mL).The organic layer was successively washed with 1 N aq. HCl (2 x 60 mL) and a saturated aqueous solution of $NaHCO_3$ (60 mL), dried over Na_2SO_4, filtered and reduced in vacuum. The crude product was purified by flash column chromatography (1:3 → 1:1 EtOAc-petroleum ether) to yield **16** as a white powder (1.36 g, 78%).

R_f = 0.31 (20:1 DCM-MeOH). $[\alpha]_D$ = +101.6 (*c* = 1.0 in DCM).

^{1}H NMR (500 MHz, $CDCl_3$, Figure S3): δ = 5.47 (bs, 7 H, N*H*Boc),5.29 (t, 7H, $J_{2,3} = J_{3,4}$ = 8.8 Hz, H-3), 5.14 (d, 7H, $J_{1,2}$ = 3.9 Hz, H-1), 4.82 (dd, 7H, H-2), 4.19 (m, 7H, H-5), 3.81 (t, 7H, $J_{4,5}$ = 8.6 Hz, H-4), 3.34 (bq, 14H, $^3J_{H,H}$ = 6.5 Hz, CH_2NHBoc), 3.16 (dd, 7H, $J_{5,6a}$ = 2.1 Hz, $J_{6a,6b}$ = 11.8 Hz, H-6a), 3.07 (dd, 7H, $J_{5,6b}$ = 5.8 Hz, H-6b), 2.79, 2.77 (2 dt, 14H, $^2J_{H,H}$ = 13.1 Hz, $^3J_{H,H}$ = 6.6 Hz, CH_2S$_{cyst}$), 2.42-2.14 (m, 28H, CH_2CO), 1.63 (m, 28H, CH_2CH$_3$), 1.47 (s, 63H, C(CH$_3$)$_3$), 0.98, 0.94 (2 t, 42H, $^3J_{H,H}$ = 7.5 Hz, CH$_3$).

^{13}C NMR (125.7 MHz, $CDCl_3$, Figure S3): δ =173.2, 171.6 (2 CO ester), 156.0 (CO carbamate), 96.5 (C-1), 79.3 (*C*(CH$_3$)$_3$), 78.8 (C-4), 71.3 (C-5), 70.4 (C-3), 70.1 (C-2), 40.4 (*C*H$_2$NHBoc), 35.9, 35.7 (*C*H$_2$CO), 33.8 (CH$_2$S$_{cyst}$, C-6), 28.5 (C(*C*H$_3$)$_3$), 18.1 (*C*H$_2$CH$_3$), 13.6, 13.5 (CH$_3$).

ESI-MS (Figure S83): *m/z* 1638.4 [M + 2 Na]$^{2+}$, 3253.4 [M + Na]$^+$.

Elemental analysis calculated (%) for $C_{147}H_{245}N_7O_{56}S_7$: C 54.65, H 7.64, N 3.03, S 6.95; found: C 54.81, H 7.34, N 2.87, S 6.97.

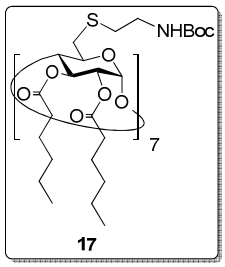

17

Heptakis[6-(2-*tert*-butoxycarbonylaminoethylthio)-6-deoxy-2,3-di-*O*-hexanoyl]cyclomaltoheptaose (17).[177] To a solution of **13**[177] (1.27 g, 0.57 mmol) in dry DMF (30 mL) under nitrogen atmosphere, DMAP (2.91 g, 23.8 mmol, 3 eq) and hexanoic anhydride (7.3 mL, 31.7 mmol, 4 eq) were added at 0 ºC. The reaction mixture was allowed to warm to rt and stirred overnight. Then, MeOH (80 mL) was added and the reaction mixture was further stirred for 2 h. The solvents were removed under reduced pressure, and subsequently H_2O (70 mL) was added to the reaction mixture which was then extracted with DCM (2 x 70 mL).The organic layer was successively washed with H_2O (2 x 50 mL), 2 N aq. H_2SO_4 (3 x 50 mL) and a saturated aqueous solution of $NaHCO_3$ (3 x 50 mL), dried over Na_2SO_4, filtered and reduced in vacuum. The crude product was purified by flash column chromatography (1:3 → 1:2EtOAc-petroleum ether) to yield **17** as a white powder (1.49 g, 73%).

R_f = 0.45 (1:2 EtOAc-petroleum ether). $[\alpha]_D$ =+84.1 (*c* = 0.9 in $CHCl_3$).

^{1}H NMR (500 MHz, $CDCl_3$, 323 K, Figure S4): δ = 5.45 (m, 7 H, N*H*Boc), 5.25 (t, 7 H, $J_{2,3}$ = $J_{3,4}$ = 9.5 Hz, H-3), 5.08 (d, 7 H, $J_{1,2}$ = 3.5 Hz, H-1), 4.76 (dd, 7 H, H-2), 4.12 (ddd, 7 H, $J_{4,5}$ = 9.5 Hz, $J_{5,6b}$ = 5.5 Hz, $J_{5,6a}$ = 2.5 Hz, H-5), 3.77 (t, 7 H, H-4), 3.30, 3.29 (2 t, 14 H, $^3J_{H,H}$ = 6.5 Hz, C*H*$_2$NHBoc), 3.10 (dd, 7 H, $J_{6a,6b}$ = 14.0 Hz, H-6a), 3.02 (dd, 7 H, H-6b), 2.74, 2.72 (2 dt, 14 H, $^2J_{H,H}$ = 13.5 Hz, $^3J_{H,H}$ = 7.0 Hz, CH_2S_{cyst}), 2.38-2.11 (m, 28 H, CH_2CO), 1.57 (m, 28 H, C*H*$_2$$CH_2CO$), 1.42 (bs, 63 H, $C(CH_3)_3$), 1.30 (m, 56 H, CH_3CH_2, $CH_3CH_2CH_2$), 0.89, 0.87 (2 t, 42 H, $^3J_{H,H}$ = 7.0 Hz, CH_3).

^{13}C NMR (125.7 MHz, $CDCl_3$, 323 K, Figure S4): δ = 173.2, 171.6 (CO ester), 155.9 (CO carbamate), 96.7 (C-1), 79.2 ($C(CH_3)_3$), 78.8 (C-4), 71.4 (C-5), 70.6 (C-3), 70.3 (C-2), 40.5 (CH_2NHBoc), 34.0 (C-6, CH_2CO), 33.9 (CH_2S_{cyst}), 33.8 (CH_2CO), 31.5, 31.3 ($CH_3CH_2CH_2$), 28.5 ($C(CH_3)_3$), 24.4, 24.3 (CH_2CH_2CO), 22.3, 22.2 (CH_3CH_2), 13.8 (CH_3).
ESI-MS (Figure S84): *m/z* 1835.6 $[M + 2 Na]^{2+}$.
Elemental analysis calculated (%) for$C_{175}H_{301}N_7O_{56}S_7$: C 58.00, H 8.37, N 2.71; found: C 57.79, H 8.19, N 2.50.

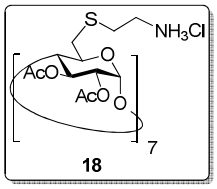

18

Heptakis[2,3-di-*O*-acetyl-6-(2-aminoethylthio)-6-deoxy]cyclomaltoheptaose hepta-hydrochloride (18). Treatment of compound **14** (304 mg, 0.11 mmol) with TFA following the procedure described in the general methods gave pure compound **18** in virtually quantitative yield (326 mg).
$[\alpha]_D$ = +51.7 (*c* = 1.0 in H_2O).
^{1}H NMR (500 MHz, MeOD, 313 K, Figure S5): δ = 5.41 (t, 7 H, $J_{2,3} = J_{3,4}$ = 9.5 Hz, H-3), 5.25 (d, 7 H, $J_{1,2}$ = 3.3 Hz, H-1), 4.84 (dd, 7 H, H-2), 4.11 (m, 7 H, H-5), 3.96 (t, 7 H, $J_{4,5}$ = 9.5 Hz, H-4), 3.26 (m, 21 H, CH_2NH_2, H-6a), 3.10-2.98 (m, 21H, H-6b, CH_2S_{cyst}), 2.13, 2.10 (2 s, 21 H each, $COCH_3$).
^{13}C NMR (125.7 MHz, MeOD, 313 K, Figure S5): δ = 172.1, 172.0 (2 CO ester), 98.1 (C-1), 80.0 (C-4), 73.9 (C-3), 72.3 (C-2), 72.0 (C-5), 40.7 (CH_2NH_2), 34.9 (C-6), 31.9 (CH_2S_{cyst}), 21.3, 21.1 ($COCH_3$).
ESI-MS (Figure S85): *m/z* 713.2 $[M + H]^{3+}$, 1069.1 $[M + 2 H]^{2+}$, 2138.1 $[M + H]^+$.
Elemental analysis calculated (%) for $C_{84}H_{140}Cl_7N_7O_{42}S_7.H_2O$: C 41.85, H 5.94, N 4.07, S 9.31; found: C 41.70, H 5.49, N 3.81, S 8.92.

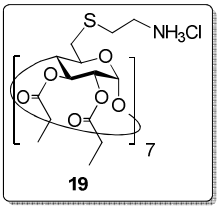

19

Heptakis[6-(2-aminoethylthio)-6-deoxy-2,3-di-*O*-propanoyl]cyclomaltoheptaose heptahydrochloride (19). Treatment of heptacarbamate **15** (307 mg, 0.10 mmol) with TFA following the standard procedure described in the general methods, followed by freeze-drying from a 0.1 N aq. HCl solution, gave pure compound **19** in quantitative yield (262 mg).

$[\alpha]_D$ = +59.2 (*c* = 1.0 in MeOH).

^{1}H NMR (500 MHz, MeOD, Figure S6): δ = 5.42 (t, 7H, $J_{2,3} = J_{3,4}$ = 9.5 Hz, H-3), 5.26 (d, 7H, $J_{1,2}$ = 3.6 Hz, H-1), 4.85 (dd, 7H, H-2), 4.15 (m, 7H, H-5), 3.99 (t, 7H, $J_{4,5}$ = 9.0 Hz, H-4), 3.30 (t, 14H, $^3J_{H,H}$ = 7.0 Hz, CH_2NH$_2$), 3.19-3.12 (m, 21H, H-6a, CH_2S$_{cyst}$), 3.07 (m, 7H, H-6b), 2.51-2.30 (m, 28H, CH_2CO), 1.15 (2 t, 42H, $^3J_{H,H}$ = 7.5 Hz, CH$_3$).

^{13}C NMR (125.7 MHz, MeOD, Figure S6): δ = 173.9, (2 CO ester), 96.4 (C-1), 78.2 (C-4), 72.4 (C-5), 70.5 (C-3), 70.4 (C-2), 38.9 (*C*H$_2$NH$_2$), 33.2 (C-6), 30.3 (CH$_2$S$_{cyst}$), 27.1, 26.9 (*C*H$_2$CO), 7.9 (CH$_3$).

ESI-MS (Figure S86): *m/z* 1167.4 $[M + 2 H]^{2+}$, 2333.9 $[M + H]^+$.

Elemental analysis calculated (%) for $C_{98}H_{168}Cl_7N_7O_{42}S_7.7H_2O$: C 43.35, H 6.76, N 3.61, S 8.27; found: C 43.42, H 6.53, N 3.72, S 7.90.

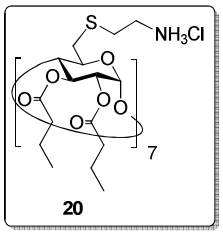

20

Heptakis[6-(2-aminoethylthio)-2,3-di-*O*-butanoyl-6-deoxy]cyclomaltoheptaose heptahydrochloride (20). Treatment of heptacarbamate **16** (300 mg, 93 µmol) with TFA following the standard procedure described in the general methods, followed by freeze-drying from a 0.1 N aq. HCl solution, gave pure compound **20** in quantitative yield (258 mg).

$[\alpha]_D$ = +65.0 (*c* = 1.0 in MeOH).

^{1}H NMR (500 MHz, MeOD, 313 K, Figure S7): δ = 5.40 (t, 7H, $J_{2,3} = J_{3,4}$ = 9.3 Hz, H-3), 5.22 (d, 7H, $J_{1,2}$ = 3.5 Hz, H-1), 4.83 (dd, 7H, H-2), 4.14 (m, 7H, H-5), 3.94 (t, 7H, $J_{4,5}$ = 8.7 Hz, H-4), 3.32-3.26 (m, 21H, CH_2NH$_2$, H-6a), 3.13-2.98 (m, 21H, H6-b, CH_2S$_{cyst}$), 2.49-2.25 (m, 28H, CH_2CO), 1.67 (m, 28H, CH_2CH$_3$), 0.98, 0.99 (2 t, 42H, $^3J_{H,H}$ = 7.4 Hz, CH$_3$).

^{13}C NMR (125.7 MHz, MeOD, 313 K, Figure S7): δ = 173.0, 172.8 (2 CO ester), 96.5 (C-1), 78.4 (C-4), 72.5 (C-5), 70.4 (C-3), 70.1 (C-2), 39.0 (*C*H$_2$NH$_2$), 35.7, 35.5 (*C*H$_2$CO), 33.3 (C-6), 30.4 (CH$_2$S$_{cyst}$), 17.8 (*C*H$_2$CH$_3$), 12.6 (CH$_3$).

ESI-MS (Figure S87): *m/z* 1265.6 $[M + 2 H]^{2+}$, 2530.1 $[M + H]^+$.

Elemental analysis calculated (%) for $C_{112}H_{196}Cl_7N_7O_{42}S_7 \cdot 7H_2O$: C 46.20, H 7.27, N 3.37, S 7.71; found: C 45.89, H 6.91, N 3.19, S 7.63.

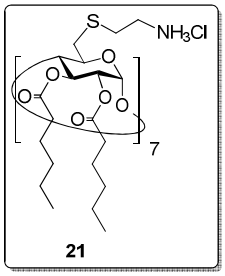

21

Heptakis[6-(2-aminoethylthio)-6-deoxy-2,3-di-*O*-hexanoyl]cyclomaltoheptaose heptahydrochloride (21). Treatment of heptacarbamate **17** (664 mg, 0.18 mmol) with TFA following the standard procedure described in the general methods, followed by freeze-drying from a 0.1 N aq. HCl solution, gave pure compound **21** in virtually quantitative yield (583 mg).

$[\alpha]_D$ = +72.6 (*c* = 1.0 in MeOH).

^{1}H NMR (500 MHz, MeOD, Figure S8): δ = 5.37 (t, 7 H, $J_{2,3}$ = $J_{3,4}$ = 9.5 Hz, H-3), 5.16 (d, 7 H, $J_{1,2}$ = 3.5 Hz, H-1), 4.79 (dd, 7 H, H-2), 4.07 (bt, 7 H,$J_{5,6a}$ = $J_{5,6b}$ = 6.5 Hz, H-5), 3.90 (t, 7 H,$J_{4,5}$ = 9.0 Hz, H-4), 3.22 (d, 7 H,$J_{6a,6b}$ = 13.0 Hz, H-6a), 3.21 (bt, 14 H, $^3J_{H,H}$ = 7.0 Hz, C*H*$_2$NH$_2$), 3.04 (dd, 7H, H-6b), 3.02, 2.94 (2 dt, 14 H, $^2J_{H,H}$ = 14.5 Hz, $^3J_{H,H}$ = 7.5 Hz, CH_2S_{cyst}), 2.47–2.21 (m, 28 H, CH_2CO), 1.62 (m, 28H, C*H*$_2$CH$_2$CO), 1.33 (m, 56H, CH_3CH_2, $CH_3CH_2CH_2$), 0.92, 0.91 (2 t, 42 H,$^3J_{H,H}$ = 7.0 Hz, CH_3).

^{13}C NMR (125.7 MHz, MeOD, Figure S8): δ = 174.4, 174.3 (CO), 98.2 (C-1), 80.0 (C-4), 74.0 (C-5), 71.8 (C-2), 71.3 (C-3), 40.2 (CH_2NH_2), 35.2, 35.0 (*C*H$_2$CO), 34.4 (C-6), 32.6, 32.5 ($CH_3CH_2CH_2$), 31.7 (CH_2S_{cyst}), 25.6, 25.5 (*C*H$_2$CH$_2$CO), 23.6, 23.5 (CH_3CH_2), 14.4, 14.3 (CH_3).

ESI-MS (Figure S88): *m/z* 975.5 $[M + 3 H]^{3+}$, 1462.6 $[M + 2 H]^{2+}$.

Elemental analysis calculated (%) for $C_{140}H_{252}Cl_7N_7O_{42}S_7$: C 52.91, H 7.99, N 3.09; found: C 52.66, H 7.84, N 2.98.

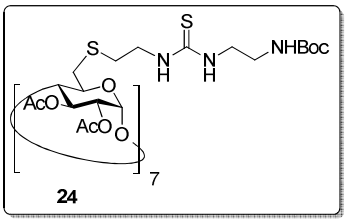

24

Heptakis[2,3-di-*O*-acetyl-6-(2-(*N*'-(2-*tert*-butoxycarbonylaminoethyl)thioureido)ethyl-thio)-6-deoxy]cyclomaltoheptaose (24). To a solution of compound **18** (125 mg, 42 µmol) and Et_3N (102 µL, 0.73mmol, 2.5 eq) in DCM (3 mL) a solution of 2-(*tert*-butoxycarbonylamino)ethyl-isothiocyanate **22**[186] (71 mg, 0.35 mmol, 1.2 eq) in DCM (2 mL) was added drop wise. The reaction mixture was stirred overnight at rt. The solvent was evaporated under reduced pressure and the residue was purified by flash column chromatography (40:1DCM-MeOH) to yield compound **24** as a white powder (140 mg, 94%).

R_f = 0.69 (9:1 DCM-MeOH). $[\alpha]_D$ = +69.0 (*c* = 0.4 in $CHCl_3$).

^{1}HNMR (500 MHz, $CDCl_3$, 313 K, Figure S9): δ = 7.20, 7.01 (2 bs, 14 H, NHCS), 5.44 (bs, 7 H, N*H*Boc), 5.24 (t, 7 H, $J_{2,3} = J_{3,4}$ = 8.8 Hz, H-3), 5.10 (d, 7 H, $J_{1,2}$ = 3.6 Hz, H-1), 4.78 (dd, 7 H, H-2), 4.17 (m, 7 H, H-5), 3.75 (t, 7 H, $J_{4,5}$ = 8.5 Hz, H-4), 3.74, 3.58 (2 bs, 28 H, C*H*$_2$NHCS), 3.29 (m, 14 H, $^3J_{H,H}$ = 5.6 Hz, C*H*$_2$NHBoc), 3.21 (bd, 7 H, $J_{6a,6b}$ = 13.0 Hz, H-6a), 3.03 (dd, 7 H, $J_{5,6b}$ = 7.6 Hz, H-6b), 2.94, 2.82 (2m, 14 H, CH_2S_{cyst}), 2.05, 2.00 (2 s, each 21 H, $COCH_3$), 1.42 (s, 63 H, $C(CH_3)_3$).

^{13}C NMR (125.7 MHz, $CDCl_3$, 313 K, Figure S9): δ = 182.6 (CS), 171.0, 169.6 (2 CO ester), 157.2 (CO carbamate), 97.2 (C-1), 80.2 (C-4), 79.7 (*C*CH_3), 72.0 (C-3), 71.3 (C-2), 70.9 (C-5), 45.4, 45.0 (*C*H_2NHCS), 40.5 (*C*H_2NHBoc), 34.1 (CH_2S_{cyst}), 33.3 (C-6), 28.9 ($C(CH_3)_3$), 21.0 ($COCH_3$).

ESI-MS (Figure S89): m/z 1221.0 $[M + 3 K]^{3+}$, 1820.5 $[M + 2 K]^{2+}$.

Elemental analysis calculated (%) for $C_{140}H_{231}N_{21}O_{56}S_{14}$: C 47.32, H 6.55, N 8.28, S 12.63; found: C 47.41, H 6.62, N 8.15, S 12.48.

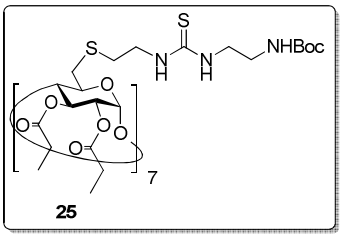

25

Heptakis[6-(2-(*N'*-(2-*tert*-butoxycarbonylaminoethyl)thioureido)ethylthio)-6-deoxy-2,3-di-*O*-propanoyl]cyclomaltoheptaose (25). To a solution of compound **19** (100 mg, 39 µmol) and Et_3N (94 µL, 0.68 mmol, 2.5 eq) in DCM (2 mL) a solution of 2-(*tert*-butoxycarbonylamino)ethylisothiocyanate **22**[186] (66 mg, 0.32 mmol, 1.2 eq) in DCM (1 mL) was added drop wise. The reaction mixture was stirred overnight at rt. Once evaporated the solvent under reduced pressure, the residue was purified by flash column chromatography (40:1 → 15:1 DCM-MeOH) to yield compound **25** as an off-white powder (108 mg, 75%).

R_f = 0.19 (20:1 DCM-MeOH). $[\alpha]_D$ = +73.9 (*c* = 1.0 in DCM).

^{1}H NMR (500 MHz, $CDCl_3$, Figure S10): δ = 7.25 (2 bs, 14H, NHCS), 5.63 (bs, 7H, N*H*Boc), 5.27 (t, 7H, $J_{2,3} = J_{3,4}$ = 8.5 Hz, H-3), 5.11 (d, 7H, $J_{1,2}$ = 2.7 Hz, H-1), 4.82 (dd, 7H, H-2), 4.20 (m, 7H, H-5), 3.78 (t, 7H, $J_{4,5}$ = 8.2 Hz, H-4), 3.73, 3.61 (2 m, 28H, CH_2NHCS), 3.30 (bs, 14H, CH_2NHBoc), 3.22 (bd, 7H, $J_{6a,6b}$ = 13.1 Hz, H-6a), 3.04 (m, 7H, H-6b), 2.95, 2.83 (2 m, 14H, CH_2S_{cyst}), 2.42-2.17 (m, 28H, CH_2CO), 1.45 (s, 63H, $C(CH_3)_3$), 1.12, 1.10 (2 t, 42H, $^3J_{H,H}$ = 7.5 Hz, CH_3).

^{13}C NMR (125.7 MHz, $CDCl_3$, 313 K, Figure S10): δ = 182.3 (CS), 174.1, 173.1 (2 CO ester), 157.3 (CO carbamate), 96.7 (C-1), 79.0 ($C(CH_3)_3$), 78.3 (C-4), 71.8 (C-5), 70.8 (C-3), 70.4 (C-2),43.8 (CH_2NHCS), 39.6 (CH_2NHBoc), 33.7 (C-6), 32.7 (CH_2S_{cyst}), 27.6 ($C(CH_3)_3$), 27.1, 27.0 (CH_2CO), 8.0 (CH_3).

ESI-MS (Figure S90): *m/z* 1286.3 $[M + 2 Na + K]^{3+}$, 1897.8 $[M + 2 Na]^{2+}$, 1917.5 $[M + Na + K]^{2+}$.

Elemental analysis calculated (%) for $C_{154}H_{259}N_{21}O_{56}S_{14}$: C 49.33, H 6.96, N 7.84, S 11.97; found: C 49.25, H 7.17, N 7.55, S 11.93.

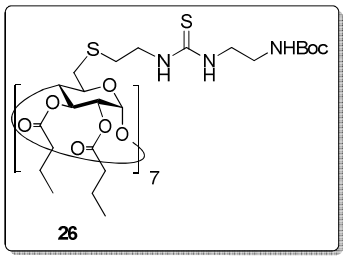

26

Heptakis[2,3-di-*O*-butanoyl-6-(2-(*N'*-(2-*tert*-butoxycarbonylaminoethyl)thioureido)-ethylthio)-6-deoxy]cyclomaltoheptaose (26). To a solution of compound **20** (81 mg, 29 µmol) and Et_3N (71 µL, 0.51 mmol, 2.5 eq) in DCM (2 mL) a solution of 2-(*tert*-butoxycarbonylamino)ethylisothiocyanate **22**[186] (49 mg, 0.24 mmol, 1.2 eq) in DCM (1 mL) was added drop wise. The reaction mixture was stirred overnight at rt. Then, the solvent was evaporated under reduced pressure and the resulting residue was purified by flash column chromatography (40:1 → 15:1 DCM-MeOH) to yield compound **26** as an off-white powder (97 mg, 84%).

R_f = 0.20 (20:1 DCM-MeOH). $[\alpha]_D$ = +38.5 (*c* = 1.0 in DCM).

^{1}H NMR (500 MHz, MeOD, 313 K, Figure S11): δ = 5.36 (t, 7H, $J_{2,3} = J_{3,4}$ = 8.2 Hz, H-3), 5.19 (d, 7H, $J_{1,2}$ = 2.7 Hz, H-1), 4.83 (dd, 7H, H-2), 4.23 (m, 7H, H-5), 3.96 (t, 7H, $J_{4,5}$ = 8.0 Hz, H-4), 3.77, 3.60 (2 m, 28H, CH_2NHCS), 3.28 (m, 21H, CH_2NHBoc, H-6a), 3.20 (dd, 7H, $J_{5,6a}$ = 4.1 Hz, $J_{6a,6b}$ = 9.8 Hz, H-6b), 2.97, 2.93 (2 m, 14H, CH_2S_{cyst}), 2.46-2.23 (m, 28H, CH_2CO), 1.67 (m, 28H, CH_2CH_3), 1.47(s, 63H, C$(CH_3)_3$), 1.00, 0.97 (2 t, 42H, $^3J_{H,H}$ = 7.2 Hz, CH_3).

^{13}C NMR (125.7 MHz, 313 K, MeOD, Figure S11): δ = 182.2 (CS), 173.1, 172.0 (2 CO ester), 157.3 (CO carbamate), 96.5 (C-1), 79.0 (*C*$(CH_3)_3$), 78.2 (C-4), 71.9 (C-5),70.5 (C-3), 70.3 (C-2), 43.9 (*C*H_2NHCS), 39.6 (*C*H_2NHBoc), 35.7, 35.6 (*C*H_2CO), 33.7 (C-6), 32.7 (CH_2S_{cyst}), 27.6 (C(*C*$H_3)_3$), 17.9, 17.8 (*C*H_2CH_3), 12.7 (CH_3).

ESI-MS (Figure S91): *m/z* 1995.6 $[M + 2\ Na]^{2+}$, 3966.6 $[M + Na]^+$.

Elemental analysis calculated (%) for $C_{168}H_{287}N_{21}O_{56}S_{14}$: C 51.13, H 7.33, N 7.45, S 11.38; found: C 51.34, H 7.36, N 7.48, S 11.29.

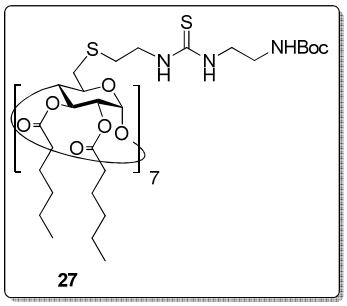

27

Heptakis[6-(2-(*N'*-(2-*tert*-butoxycarbonylaminoethyl)thioureido)ethylthio)-6-deoxy-2,3-di-*O*-hexanoyl]cyclomaltoheptaose (27). To a solution of compound **21** (150 mg, 47 µmol) and Et_3N (115 µL, 0.83 mmol, 2.5 eq) in DCM (3 mL) a solution of 2-(*tert*-butoxycarbonylamino)ethylisothiocyanate **22**[186] (80 mg, 0.40 mmol, 1.2 eq) in DCM (2 mL) was added drop wise. The reaction mixture was stirred overnight at rt. Once evaporated the solvent under reduced pressure, the resulting residue was purified by flash column chromatography (40:1 → 20:1DCM-MeOH) to yield compound **27** as an off-white powder (166 mg, 81%).

R_f = 0.53 (9:1 DCM-MeOH). $[\alpha]_D$ = +78.4 (*c* = 1.05 in DCM).

^{1}H NMR (500 MHz, $CDCl_3$, 313 K, Figure S12): δ = 7.19, 7.00 (2 bs, 14 H, NHCS), 5.46 (bs, 7 H, N*H*Boc), 5.25 (t, 7 H, $J_{2,3} = J_{3,4}$ = 8.8 Hz, H-3), 5.08 (d, 7 H, $J_{1,2}$ = 3.7 Hz, H-1), 4.76 (dd, 7 H, H-2), 4.15 (m, 7 H, H-5), 3.75 (t, 7 H, $J_{4,5}$ = 8.8 Hz, H-4), 3.72 (m, 14 H,C$H_2$$CH_2S_{cyst}$), 3.58 (m, 14 H, C$H_2$NHCS), 3.29 (m, 14 H, CH_2NHBoc), 3.20 (bd, 7 H, $J_{6a,6b}$ = 13.4 Hz, H-6a), 3.04 (dd, 7 H, $J_{5,6b}$ = 4.8 Hz, H-6b), 2.93, 2.81 (2 dt, 14 H, $^2J_{H,H}$ = 13.3 Hz, $^3J_{H,H}$ = 6.6 Hz, CH_2S_{cyst}), 2.38-2.11 (m, 28 H, CH_2CO), 1.56 (m, 28 H, C$H_2$$CH_2CO$), 1.42 (s, 9 H, $C(CH_3)_3$), 1.24 (m, 56 H, CH_3CH_2, $CH_3CH_2CH_2$), 0.90, 0.87 (2 t, each 21 H, $^3J_{H,H}$ = 7.1 Hz, CH_3).

^{13}C NMR (125.7 MHz, $CDCl_3$, 313 K, Figure S12): δ = 182.0 (CS), 173.4, 171.6 (2 CO ester), 156.9 (CO carbamate), 96.7 (C-1), 79.8 ($C(CH_3)_3$), 79.0 (C-4), 71.5 (C-5), 70.5 (C-3), 70.4 (C-2), 44.6 (CH_2NH), 43.8 ($CH_2CH_2S_{cyst}$), 40.0 (CH_2NHBoc), 34.0 (CH_2CO), 33.8 (C-6), 32.9 (CH_2S_{cyst}), 31.4, 31.2 (2 $CH_3CH_2CH_2$), 28.5 ($C(CH_3)_3$), 24.4, 24.3 (2 CH_2CH_2CO), 22.3 (CH_3CH_2), 13.8 (CH_3).

ESI-MS (Figure S92): *m/z* 1468.5 $[M + 3 Na]^{3+}$, 2191.2 $[M + 2 Na]^{2+}$.

Elemental analysis calculated (%) for$C_{196}H_{343}N_{21}O_{56}S_{14}$: C 54.26, H 7.97, N 6.78; found: C 54.10, H 7.84, N 6.67.

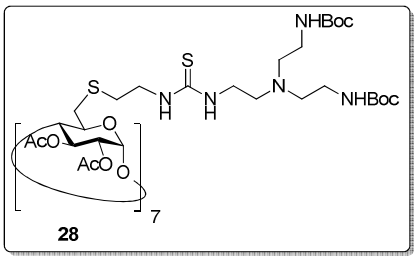

28

Heptakis[2,3-di-*O*-acetyl-6-(2-(*N*'-(2-(*N*,*N*-di-(2-(*N*-*tert*-butoxycarbonylamino)ethyl)-amino)ethyl)thioureido)ethylthio)-6-deoxy]cyclomaltoheptaose (28). To a solution of compound **18** (92 mg, 31 µmol) and Et_3N (74, µL, 0.54 mmol, 2.5 eq) in DCM (3 mL) a solution of 2-[bis(2-(*tert*-butoxycarbonylamino)ethyl)amino]ethylisothiocyanate **23**[177] (100 mg, 0.26 mmol, 1.2 eq) in DCM (2 mL) was added drop wise. The reaction mixture was stirred overnight at rt. After evaporation of the solvent under reduced pressure, the residue was purified by flash column chromatography (40:1 DCM-MeOH) to yield compound **28** as a white powder (141 mg, 95%).

R_f = 0.58 (9:1 DCM-MeOH). $[\alpha]_D$ = +51.0 (*c* = 0.98 in DCM).

^{1}H NMR (500 MHz, MeOD, 333 K, Figure S13): δ = 5.37 (t, 7 H, $J_{2,3}$ = $J_{3,4}$ = 9.0 Hz, H-3), 5.21 (d, 7 H, $J_{1,2}$ = 3.6 Hz, H-1), 4.83 (dd, 7 H,H-2), 4.20 (m, 7 H, H-5), 3.98 (t, 7 H, $J_{4,5}$ = 8.8 Hz, H-4), 3.80 (bt, 14 H, $^3J_{H,H}$ = 6.4 Hz, CH_2CH$_2$S$_{cyst}$), 3.58 (bt, 14 H,$^3J_{H,H}$ = 6.4 Hz, NCH$_2$CH_2NHCS), 3.29 (m, 7 H, H-6a), 3.17 (t, 35 H, H-6b, CH_2NHBoc), 2.96 (m, 14 H, CH$_2$S$_{cyst}$), 2.76 (bt, 14 H, $^3J_{H,H}$ = 6.1 Hz, NCH_2CH$_2$NHCS), 2.27 (bt, 28 H, $^3J_{H,H}$ = 6.1 Hz, CH_2CH$_2$NHBoc), 2.11, 2.10 (2 s, 42 H, COCH$_3$), 1.47 (s, 126 H, C(CH$_3$)$_3$).

^{13}C NMR (75.5 MHz, $CDCl_3$, 313 K, Figure S13): δ = 184.8 (CS), 172.9, 171.6 (2 CO ester), 158.8 (CO carbamate), 99.0 (C-1), 81.6 (*C*CH$_3$), 81.5 (C-4), 73.0 (C-5, C-3, C-2), 56.7 (*C*H$_2$CH$_2$NHBoc), 56.3 (NC*H*$_2$CH$_2$NHCS), 44.6 (*C*H$_2$CH$_2$S$_{cyst}$), 41.0 (NCH$_2$*C*H$_2$NHCS, *C*H$_2$NHBoc), 36.0 (C-6), 35.3 (CH$_2$S$_{cyst}$), 30.6 (C(*C*H$_3$)$_3$), 23.0, 22.9 (CO*C*H$_3$).

ESI-MS (Figure S93): *m/z* 1656.6 $[M + Na + 2 K]^{3+}$, 2456.8 $[M + 2 Na]^{2+}$, 2472.2 $[M + 2 K]^{2+}$, 2463.4 $[M + 2 Cl]^{2-}$.

Elemental analysis calculated (%) for $C_{203}H_{357}N_{35}O_{70}S_{14}$: C 50.20, H 7.41, N 10.09, S 9.24; found: C 50.01, H 7.22, N 9.81, S 8.94.

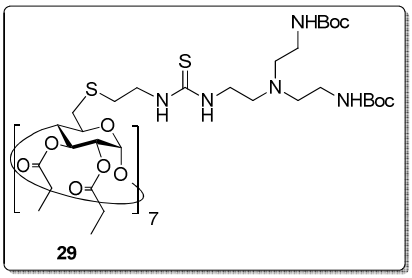

29

Heptakis[6-(2-(*N'*-(2-(*N*,*N*-di-(2-(*N*-*tert*-butoxycarbonylamino)ethyl)amino)ethyl)thio-ureido)ethylthio)-6-deoxy-2,3-di-*O*-propanoyl]cyclomaltoheptaose (29). To a solution of compound **19** (95 mg, 37 µmol) and Et_3N (90 µL, 0.64 mmol, 2.5 eq) in DCM (2 mL) a solution of 2-[bis(2-(*tert*-butoxycarbonylamino)ethyl)amino]ethylisothiocyanate **23**[177] (120 mg, 0.31 mmol, 1.2 eq) in DCM (1 mL) was added drop wise. The reaction mixture was stirred overnight at rt. After evaporation of the solvent under reduced pressure, the residue was purified by flash column chromatography (40:1 → 15:1 DCM-MeOH) to yield compound **29** as an off-white powder (114 mg, 62%).

R_f = 0.64 (9:1 DCM-MeOH). $[\alpha]_D$ = +37.8 (*c* = 1.0 in MeOH).

^{1}H NMR (500 MHz, MeOD, 323 K, Figure S14): δ = 5.36 (t, 7H, $J_{2,3} = J_{3,4}$ = 8.7 Hz, H-3), 5.18 (d, 7H, $J_{1,2}$ = 3.3 Hz, H-1), 4.83 (dd, 7H, H-2), 4.25 (m, 7H, H-5), 3.97 (t, 7H, $J_{4,5}$ = 8.3 Hz, H-4), 3.81 (bt, 14H, C*H*$_2$CH$_2$C$_{cyst}$), 3.56 (bt, 14H, NCH$_2$C*H*$_2$NHCS), 3.23 (m, 42H, H-6a, H-6b, C*H*$_2$NHBoc), 2.96 (m, 14H, C*H*$_2$S$_{cyst}$), 2.74 (t, 14H, $^3J_{H,H}$ = 6.0 Hz, NC*H*$_2$CH$_2$NHCS), 2.64 (t, 28H, $^3J_{H,H}$ = 6.0 Hz, C*H*$_2$CH$_2$NHBoc), 2.50-2.27 (m, 28H, C*H*$_2$CO), 1.48 (s, 126H, C(CH$_3$)$_3$), 1.15, 1.13 (2 t, 42H, $^3J_{H,H}$ = 7.7 Hz, CH$_3$).

^{13}C NMR (125.7 MHz, MeOD, 313 K, Figure S14): δ = 182.3 (CS), 174.0, 173.1 (2 CO ester), 157.1 (CO carbamate), 96.7 (C-1), 78.9 (*C*(CH$_3$)$_3$), 78.4 (C-4), 71.8 (C-5), 70.8 (C-3), 70.4 (C-2), 54.3 (*C*H$_2$CH$_2$NHBoc), 53.3 (NCH$_2$CH$_2$NHCS), 44.0 (*C*H$_2$CH$_2$S$_{cyst}$), 42.0

(NCH_2CH_2NHCS), 38.6 (CH_2NHBoc), 33.8 (C-6), 33.0 (CH_2S_{cyst}), 27.7 ($C(CH_3)_3$), 27.1, 27.0 (CH_2CO), 8.1, 8.0 (CH_3).

ESI-MS (Figure S94): *m/z* 1723.8 $[M + 3 K]^{3+}$, 2550.2 $[M + 2 Na]^{2+}$, 2558.3 $[M + Na + K]^{2+}$, 2543.4 $[M + Cl - H]^{2-}$.

Elemental analysis calculated (%) for $C_{217}H_{385}N_{35}O_{70}S_{14}$: C 51.57, H 7.68, N 9.70, S 8.88; found: C 51.18, H 7.67, N 9.23, S 8.99.

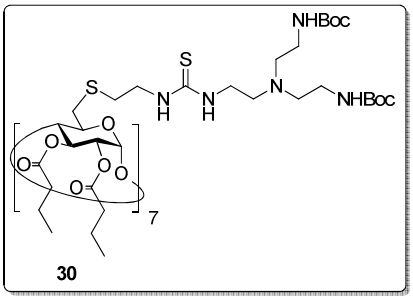

30

Heptakis[2,3-di-*O*-butanoyl-6-(2-(*N'*-(2-(*N*,*N*-di-(2-(*N*-*tert*-butoxycarbonylamino)-ethyl)amino)ethyl)thioureido)ethylthio)-6-deoxy]cyclomaltoheptaose (30). To a solution of compound **20** (100 mg, 36 µmol) and Et_3N (87 µL, 0.63 mmol, 2.5 eq) in DCM (2 mL) a solution of 2-[bis(2-(*tert*-butoxycarbonylamino)ethyl)amino]ethylisothiocyanate **23**[177] (117 mg, 0.30 mmol, 1.2 eq) in DCM (1 mL) was added drop wise. The reaction mixture was stirred overnight at rt. Then, the solvent was evaporated under reduced pressure and the resulting residue was purified by flash column chromatography (40:1 → 15:1DCM-MeOH) to give compound **30** (139 mg, 74%).

R_f = 0.63 (20:1 DCM-MeOH). $[\alpha]_D$ = +38.1 (*c* = 0.99 in MeOH).

^{1}H NMR (500 MHz, MeOD, 323 K, Figure S15): δ = 5.36 (t, 7H, $J_{2,3} = J_{3,4}$ = 8.7 Hz, H-3), 5.17 (d, 7H, $J_{1,2}$ = 3.7Hz, H-1), 4.83 (dd, 7H, H-2), 4.23 (m, 7H, H-5), 3.97 (t, 7H, $J_{4,5}$ = 8.3 Hz, H-4), 3.81 (t, 14H, $^3J_{H,H}$ = 6.5 Hz, $CH_2CH_2C_{cyst}$), 3.56 (m, 14H, NCH_2CH_2NHCS), 3.29 (m, 7H, H-6a), 3.21 (dd, 7 H, $J_{5,6b}$= 5.0 Hz, $J_{6a,6b}$ = 14.3 Hz, H-6b), 3.16 (t, 28 H, $^3J_{H,H}$ = 6.5 Hz,CH_2NHBoc), 2.96 (m, 14H, CH_2S_{cyst}), 2.74 (t, 14H, $^3J_{H,H}$ = 6.5 Hz, NCH_2CH_2NHCS), 2.53 (t, 28H, $^3J_{H,H}$ = 6.5 Hz, CH_2CH_2NHBoc), 2.47-2.23 (m, 28H,

C*H*$_2$CO), 1.67 (m, 28H, C*H*$_2$CH$_3$), 1.48 (s, 126H, C(CH$_3$)$_3$), 1.01, 0.98 (2 t, 42H, $^3J_{H,H}$ = 7.5 Hz, CH$_3$).

^{13}C NMR (125.7 MHz, MeOD, 313 K, Figure S15): δ = 173.1, 172.1 (2 CO ester), 157.1 (CO carbamate), 96.6 (C-1), 79.1 (*C*(CH$_3$)$_3$), 78.3 (C-4), 72.0 (C-5), 70.7 (C-3), 70.3 (C-2), 54.3 (*C*H$_2$CH$_2$NHBoc), 53.5 (NCH$_2$CH$_2$NHCS), 44.1 (*C*H$_2$CH$_2$S$_{cyst}$), 41.9 (NCH$_2$*C*H$_2$NHCS), 38.4 (*C*H$_2$NHBoc), 35.8, 35.6 (*C*H$_2$CO), 34.0 (C-6), 33.0 (CH$_2$S$_{cyst}$), 27.7 (C(*C*H$_3$)$_3$), 17.9, 17.8 (*C*H$_2$CH$_3$), 12.7 (CH$_3$).

ESI-MS (Figure S95): *m/z* 1772.9 [M + 3 Na]$^{3+}$, 2647.9 [M + 2 Na]$^{2+}$.

Elemental analysis calculated (%) for C$_{231}$H$_{413}$N$_{35}$O$_{70}$S$_{14}$: C 52.85, H 7.93, N 9.34, S 8.55; found: C 52.77, H 7.95, N 9.36, S 8.38.

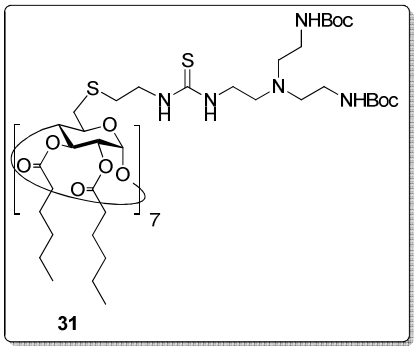

31

Heptakis[6-(2-(*N'*-(2-(*N*,*N*-di-(2-(*N*-*tert*-butoxycarbonylamino)ethyl)amino)ethyl)thio-ureido)ethylthio)-6-deoxy-2,3-di-*O*-hexanoyl]cyclomaltoheptaose (31). To a solution of compound **21** (68 mg, 21 µmol) and Et$_3$N (52 µL, 0.37 mmol, 2.5 eq) in DCM (1.5 mL) a solution of 2-[bis(2-(*tert*-butoxycarbonylamino)ethyl)amino]ethylisothiocyanate **23**[177] (70 mg, 0.18 mmol, 1.2 eq) in DCM (1 mL) was added drop wise. The reaction mixture was stirred overnight at rt. After evaporation of the solvent under reduced pressure, the resulting residue was purified by flash column chromatography (40:1 → 15:1 DCM-MeOH) yielding compound **31** (84 mg, 71%).

R_f = 0.65 (9:1 DCM-MeOH). $[\alpha]_D$ = +57.4 (*c* = 1.0 in DCM).

^{1}H NMR (300 MHz, CDCl$_3$, 313 K, Figure S16): δ = 7.22, 7.16 (2 bs, 14 H, NHCS), 5.29 (t, 7 H, $J_{2,3}$ = $J_{3,4}$ = 9.2 Hz, H-3), 5.24 (bs, 14 H, N*H*Boc), 5.08 (d, 7 H, $J_{1,2}$ = 3.5 Hz, H-1),

4.77 (dd, 7 H, H-2), 4.17 (m, 7 H, H-5), 3.83 (t, 7 H, $J_{4,5}$ = 9.2 Hz, H-4), 3.77 (m, 14 H, C*H*$_2$CH$_2$S$_{cyst}$), 3.54 (m, 14 H, NCH$_2$C*H*$_2$NHCS), 3.15 (m, 42 H, H-6a, H-6b, C*H*$_2$NHBoc), 2.87 (m, 14 H, CH$_2$S$_{cyst}$), 2.67 (bt, 14 H, $^3J_{H,H}$ = 5.5 Hz, NC*H*$_2$CH$_2$NHCS), 2.58 (bt, 28 H, $^3J_{H,H}$ = 5.2 Hz, C*H*$_2$CH$_2$NHBoc), 2.43-2.11 (m, 28 H, CH$_2$CO), 1.60 (m, 28 H, C*H*$_2$CH$_2$CO), 1.44 (s, 126 H, C(CH$_3$)$_3$), 1.30 (m, 56 H, C*H*$_2$CH$_3$, C*H*$_2$CH$_2$CH$_3$), 0.91, 0.89 (2 t, 42 H, $^3J_{H,H}$ = 7.8 Hz, CH$_3$).

^{13}C NMR (75.5 MHz, CDCl$_3$, 313 K, Figure S16): δ = 182.8 (CS), 173.8, 172.0 (2 CO ester), 156.9 (CO carbamate), 97.0 (C-1), 79.8 (*C*(CH$_3$)$_3$), 79.0 (C-4), 71.8 (C-5), 70.9 (C-3, C-2), 55.1 (*C*H$_2$CH$_2$NHBoc), 54.0 (NCH$_2$CH$_2$NHCS), 44.5 (*C*H$_2$CH$_2$S$_{cyst}$), 42.9 (NCH$_2$*C*H$_2$NHCS), 39.5 (*C*H$_2$NHBoc), 34.4, 34.2 (*C*H$_2$CO, C-6), 33.6 (CH$_2$S$_{cyst}$), 31.8, 31.7 (2 *C*H$_2$CH$_2$CH$_3$), 28.9 (C(*C*H$_3$)$_3$), 24.8, 24.7 (2 *C*H$_2$CH$_2$CO), 22.7 (*C*H$_2$CH$_3$), 14.2 (CH$_3$).

ESI-MS (Figure S96): *m/z* 1880.7 [M + 3 H]$^{3+}$, 2820.3 [M + 2 H]$^{2+}$.

Elemental analysis calculated (%) forC$_{259}$H$_{469}$N$_{35}$O$_{70}$S$_{14}$: C 55.13, H 8.38, N 8.69; found: C 54.76, H 8.21, N 8.50.

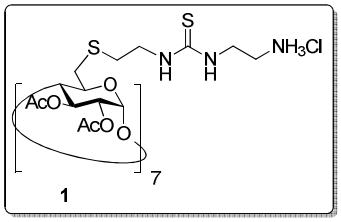

1

Heptakis[2,3-di-*O*-acetyl-6-(2-(*N*'-(2-aminoethyl)thioureido)ethylthio)-6-deoxy]cyclomaltoheptaose heptahydrochloride (1). Treatment of compound **24** (50 mg, 14 µmol) with anhydrous TFA (100 µL) at rt for 5 min, followed by freeze-drying immediately from a 0.1 N aq. HCl solution afforded pure compound **1** in virtually quantitative yield (43 mg).

$[\alpha]_D$ = +35.2 (*c* = 0.5 in MeOH).

^{1}H NMR (500 MHz, DMSO-d$_6$, 333 K, Figure S17): δ = 8.12 (bs, 14 H, NH$_2$), 7.97, 7.75 (2 bs, 14 H, NHCS), 5.22 (t, 7H, $J_{2,3}$ = $J_{3,4}$ = 9.0 Hz, H-3), 5.11 (d, 7H, $J_{1,2}$ = 3.7 Hz, H-1), 4.73 (dd, 7H, H-2), 4.14 (m, 7H, H-5), 3.90 (t, 7H, $J_{4,5}$ = 8.8 Hz, H-4), 3.72, 3.63 (2 bq,

28H, CH_2NHCS), 3.12 (m, 14H, H-6a, H-6b), 3.02 (bt, 14H, CH_2NH_2), 2.82 (m, 14H, CH_2S_{cyst}), 2.02, 2.00 (2s, 42H, $COCH_3$).

^{13}C NMR (100.6 MHz, DMSO-d_6, 323 K, Figure S17): δ = 183.2 (CS), 170.5, 169.7 (2 CO ester), 97.0 (C-1), 78.8 (C-4), 71.6 (C-5), 70.8 (C-2, C-3), 44.0, 41.7 (*C*H_2NHCS), 38.8 (CH_2NH_2), 33.7 (C-6), 32.8 (CH_2S_{cyst}), 21.0 ($COCH_3$).

ESI-MS (Figure S97): *m/z* 713.8 $[M + 4 H]^{4+}$, 951.7 $[M + 3 H]^{3+}$, 1426.7 $[M + 2 H]^{2+}$.

Elemental analysis calculated (%) for $C_{105}H_{182}Cl_7N_{21}O_{42}S_{14}$: C 40.58, H 5.90, N 9.46, S 14.44; found: C 40.54, H 6.15, N 9.33, S 14.79.

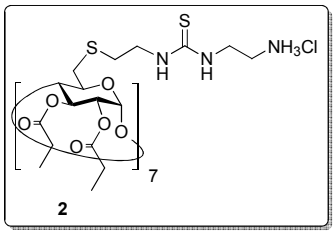

2

Heptakis[6-(2-(*N'*-(2-aminoethyl)thioureido)ethylthio)-6-deoxy-2,3-di-*O*-propanoyl]-cyclomaltoheptaose heptahydrochloride (2). Treatment of heptacarbamate **25** (35 mg, 9.3 µmol) with anhydrous TFA (90 µL) at rt for 5 min, followed by freeze-drying immediately from a 0.1 N aq. HCl solution yielded pure compound **2** (28 mg, 90%).

$[\alpha]_D$ = +36.9 (*c* = 0.5 in MeOH).

^{1}H NMR (500 MHz, DMSO-d_6, 333 K, Figure S18): δ = 8.11 (bs, 14 H, NH_2),7.96, 7.75 (2 bs, 14 H, NHCS), 5.24 (t, 7H, $J_{2,3} = J_{3,4}$ = 8.9 Hz, H-3), 5.10 (d, 7H, $J_{1,2}$ = 3.4 Hz, H-1), 4.74 (dd, 7H, H-2), 4.16 (m, 7H, H-5), 3.91 (t, 7H, $J_{4,5}$ = 8.6 Hz, H-4), 3.71, 3.64 (2 bq, 28H, CH_2NHCS), 3.12 (m, 14H, H-6a, H-6b), 3.02 (bt, 14H, CH_2NH_2), 2.83 (m, 14H, CH_2S_{cyst}), 2.37-2.20 (m, 28H, CH_2CO), 1.04, 1.03 (2 t, 42H, $^3J_{H,H}$ = 7.5 Hz, CH_3).

^{13}C NMR (125.7 MHz, DMSO-d_6, 323 K, Figure S18): δ = 183.2 (CS), 173.7, 172.9 (2 CO ester), 96.9 (C-1), 78.7 (C-4), 71.7 (C-5), 70.9 (C-3), 70.6 (C-2),43.1, 41.7, (*C*H_2NHCS), 38.9 (*C*H_2NH_2),33.8 (C-6), 32.8 (CH_2S_{cyst}),27.2 (*C*H_2CO), 9.1 (CH_3).

ESI-MS (Figure S98): *m/z* 762.7 $[M + 4 H]^{4+}$, 1017.6 $[M + 3 H]^{3+}$, 1525.5 $[M + 2 H]^{2+}$, 3048.8 $[M + H]^+$.

Elemental analysis calculated (%) for $C_{119}H_{210}Cl_7N_{21}O_{42}S_{14}$: C 43.26, H 6.41, N 8.90, S 13.59; found: C 43.34, H 6.33, N 8.84, S 13.34.

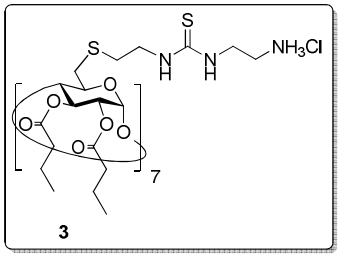

3

Heptakis[6-(2-(*N'*-(2-aminoethyl)thioureido)ethylthio)-2,3-di-*O*-butanoyl-6-deoxy]-cyclomaltoheptaose heptahydrochloride (3). Treatment of heptacarbamate **26** (88 mg, 22 µmol) with anhydrous TFA (0.5 mL) at rt for 5 min, followed by freeze-drying immediately from a 0.1 N aq. HCl solution yielded pure compound **3** in quantitative yield (78 mg).

$[\alpha]_D$ = +34.3 (*c* = 0.5 in MeOH).

^{1}H NMR (500 MHz, DMSO-d_6, 333 K, Figure S19): δ = 8.15 (bs, 14 H, NH_2), 7.97, 7.75 (2 bs, 14H, NHCS), 5.26 (t, 7H, $J_{2,3} = J_{3,4}$ = 8.8 Hz, H-3), 5.11 (d, 7H, $J_{1,2}$ = 3.0 Hz, H-1), 4.73 (dd, 7H, H-2), 4.17 (m, 7H, H-5), 3.91 (t, 7H, $J_{4,5}$ = 8.9 Hz, H-4), 3.73, 3.65 (2 bq, 28H, CH_2NHCS), 3.11 (m, 14H, H-6a, H-6b), 3.03 (bt, 14H, C$H_2$$NH_2$), 2.84 (m, 14H, C$H_2$$S_{cyst}$), 2.34, 2.22 (2 m, 28H, CH_2CO), 1.57 (m, 28H, C$H_2$$CH_3$), 0.92, 0.89 (2 t, 42H, $^3J_{H,H}$ = 7.4 Hz, CH_3).

^{13}C NMR (125.7 MHz, DMSO-d_6, 333 K, Figure S19): δ = 183.4 (CS), 172.8, 171.8 (2 CO ester), 96.7 (C-1), 78.6 (C-4), 71.6 (C-5), 70.7, 70.5 (C-3, C-2), 44.2, 43.1 (*C*H_2NHCS), 39.0 (*C*$H_2$$NH_2$), 35.8, 35.7 (*C*$H_2$CO), 34.1 (C-6), 32.9 ($CH_2S_{cyst}$), 18.1, 18.0 (*C*$H_2$$CH_3$), 13.7 ($CH_3$).

ESI-MS (Figure S99): *m/z* 812.5 $[M + 4 H]^{4+}$, 1082.4 $[M + 3 H]^{3+}$, 1623.1 $[M + 2 H]^{2+}$, 3245.1 $[M + H]^+$.

Elemental analysis calculated (%) for $C_{133}H_{238}Cl_7N_{21}O_{42}S_{14}$: C 45.63, H 6.85, N 8.40, S 12.82; found: C 45.51, H 7.01, N 8.35, S 12.57.

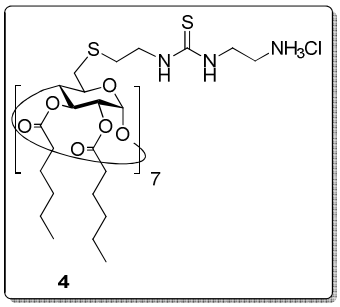

Heptakis[6-(2-(*N'*-(2-aminoethyl)thioureido)ethylthio)-6-deoxy-2,3-di-*O*-hexanoyl]-cyclomaltoheptaose heptahydrochloride (4). Treatment of compound **27** (56 mg, 13 µmol) with anhydrous TFA (100 µL) at rt for 5 min, followed by freeze-drying immediately from a 0.1 N aq. HCl solution yielded pure compound **4** in quantitative yield (50 mg).

$[\alpha]_D$ = + 80.7 (*c* = 1.0 in DMSO).

^{1}H NMR (500 MHz, DMSO-d_6, 333 K, Figure S20): δ = 8.08 (bs, 14 H, NH_2), 7.92, 7.72 (2 bs, 14 H, NHCS), 5.21 (t, 7 H, $J_{2,3}$ = $J_{3,4}$ = 8.8 Hz, H-3), 5.05 (d, 7 H, $J_{1,2}$ = 2.9 Hz,H-1), 4.67 (dd, 7H, H-2), 4.12 (m, 7 H, H-5), 3.85 (t, 7 H, $J_{4,5}$ = 8.8 Hz, H-4), 3.68 (m, 14 H, CH_2NHCS), 3.59 (m, 14 H, $CH_2CH_2S_{cyst}$), 3.10 (d, 14 H, H-6a, H-6b), 2.98 (t, 14 H, $^3J_{H,H}$ = 6.3 Hz, CH_2NH_2), 2.79, 2.77 (2 dt, 14 H, $^2J_{H,H}$ = 13.5 Hz, $^3J_{H,H}$ = 7.0 Hz, CH_2S_{cyst}), 2.35-2.11 (m, 28 H, CH_2CO), 1.50 (m, 28 H, CH_2CH_2CO), 1.24 (m, 56 H, CH_3CH_2, $CH_3CH_2CH_2$), 0.84, 0.83 (2 t, 42 H, $^3J_{H,H}$ = 7.1 Hz, CH_3).

^{13}C NMR (125.7 MHz, DMSO-d_6, 333 K, Figure S20): δ = 183.4 (CS), 172.9, 171.9 (2 CO), 96.7 (C-1), 78.5 (C-4), 71.5 (C-5), 70.7 (C-3, C-2), 44.2 ($CH_2CH_2S_{cyst}$), 41.7 (CH_2NHCS), 39.0 (CH_2NH_2), 34.0 (CH_2CO), 33.7 (C-6), 32.9 (CH_2S_{cyst}), 31.3, 31.1 (2 $CH_3CH_2CH_2$), 24.3, 24.2 (2 CH_2CH_2CO), 22.2 (CH_3CH_2), 14.0 (CH_3).

ESI-MS (Figure S100): *m/z* 910.2 $[M + 4 H]^{4+}$, 1213.4 $[M + 3 H]^{3+}$, 1819.2 $[M + 2 H]^{2+}$.

Elemental analysis calculated (%) for$C_{161}H_{294}Cl_7N_{21}O_{42}S_{14}$: C 49.67, H, 7.61, N 7.56; found: C 49.27, H 7.30, N 7.32.

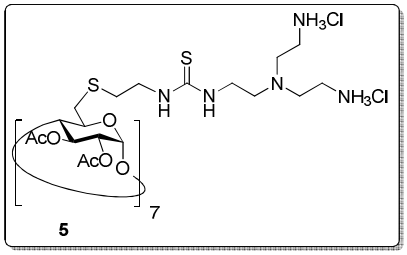

5

Heptakis[2,3-di-*O*-acetyl-6-(2-(*N*'-(2-(*N*,*N*-di-(2-aminoethyl)amino)ethyl)thioureido)-ethylthio)-6-deoxy]cyclomaltoheptaose tetradecahydrochloride (5). Treatment of compound **28** (50 mg, 10 µmol) with anhydrous TFA (100 µL) at rt for 5 min, followed by freeze-drying immediately from a 0.1 N aq HCl solution afforded pure compound **5** in quantitative yield (41 mg).

$[\alpha]_D$ = +25.1 (*c* = 0.5 in MeOH).

^{1}H NMR (500 MHz, 10:1 MeOD-D_2O, 333 K, Figure S21): δ = 5.33 (t, 7H, $J_{2,3} = J_{3,4}$ = 8.8 Hz, H-3), 5.21 (d, 7H, $J_{1,2}$ = 3.6 Hz, H-1), 4.83 (dd, 7H, H-2), 4.20 (m, 7H, H-5), 3.96 (t, 7H, $J_{4,5}$ = 8.6 Hz, H-4), 3.88 (bt, 14H, CH_2CH$_2$S$_{cyst}$), 3.78 (bt, 14H, NCH$_2$CH_2NHCS), 3.39 (m, 28H, CH_2NH$_2$), 3.33-3.18 (m, 56H, H-6a, H-6b, CH_2CH$_2$NH$_2$, NCH_2CH$_2$NHCS), 2.95 (m, 14H, CH_2S$_{cyst}$), 2.10, 2.08 (2s, 42H, COCH$_3$).

^{13}C NMR (100.6 MHz,15:1 MeOD-D_2O, 323 K, Figure S21): δ = 182.9 (CS), 171.3, 170.6 (2 CO ester), 96.7 (C-1), 78.7 (C-4), 72.1 (C-5), 70.9 (C-3, C-2), 52.7 (NCH_2CH$_2$NHCS), 51.1(CH_2CH$_2$NH$_2$), 44.1 (CH_2CH$_2$S$_{cyst}$), 40.4 (NCH$_2$CH_2NHCS), 36.4 (CH_2NH$_2$), 33.7 (C-6), 32.7 (CH$_2$S$_{cyst}$), 19.9, 19.8 (COCH$_3$).

ESI-MS (Figure S101): *m/z* 691.7 $[M + 5 H]^{5+}$, 864.6 $[M + 4 H]^{4+}$, 1152.7 $[M + 3 H]^{3+}$, 1728.7 $[M + 2 H]^{2+}$.

Elemental analysis calculated (%) for $C_{133}H_{259}Cl_{14}N_{35}O_{42}S_{14}$: C 40.28, H 6.58, N 12.36, S 11.32; found: C 40.10, H 6.66, N 12.56, S 11.32.

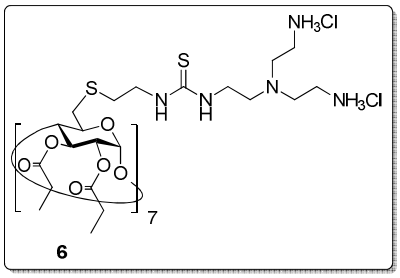

Heptakis[6-(2-(*N'*-(2-(*N*,*N*-di-(2-aminoethyl)amino)ethyl)thioureido)ethylthio)-6-deoxy-2,3-di-*O*-propanoyl]cyclomaltoheptaose tetradecahydrochloride (6). Treatment of compound **29** (100 mg, 19.8 µmol) with anhydrous TFA (0.5 mL) at rt for 5 min, followed by freeze-drying immediately from a 0.1 N aq HCl solution afforded pure compound **6** in quantitative yield (82 mg).

$[\alpha]_D$ = +33.2 (*c* = 0.25 in MeOH).

^{1}H NMR (500 MHz, 10:1 MeOD-D_2O, 323 K, Figure S22): δ = 5.32 (t, 7H, $J_{2,3} = J_{3,4}$ = 8.6 Hz, H-3), 5.18 (d, 7H, $J_{1,2}$ = 3.5 Hz, H-1), 4.84 (dd, 7H, H-2), 4.21 (m, 7H, H-5), 3.96 (t, 7H, $J_{4,5}$ = 8.3 Hz, H-4), 3.77 (bt, 14H, CH_2CH_2C$_{cyst}$), 3.72 (bt, 14H, NCH_2CH_2NHCS), 3.23 (m, 42H, H-6a, H-6b, CH_2NH_2), 3.00 (t, 28H, $^3J_{H,H}$ = 5.9 Hz, CH_2CH$_2$NH_2), 2.94 (m, 14H, CH_2S$_{cyst}$), 2.89 (t, 14H, $^3J_{H,H}$ = 5.9 Hz, NCH_2CH$_2$NHCS), 2.49-2.27 (m, 28H, CH_2CO), 1.13, 1.11 (2 t, 42H, $^3J_{H,H}$ = 7.5 Hz, CH_3).

^{13}C NMR (125.7 MHz, 5:1 MeOD-D_2O, 323 K, Figure S22): δ = 182.2 (CS), 174.9, 173.7 (2 CO ester), 96.6 (C-1), 78.3 (C-4), 72.0 (C-5), 70.9 (C-3), 70.4 (C-2), 52.2 (NCH_2CH$_2$NHCS), 51.0 (CH_2CH$_2$NH_2), 44.1 (CH_2CH$_2$S$_{cyst}$), 40.8 (NCH$_2$CH_2NHCS), 36.8 (CH_2NH_2), 33.9 (C-6), 32.7 (CH$_2$S$_{cyst}$), 27.2 (CH_2CO), 8.2, 8.1 (CH_3).

ESI-MS (Figure S102): *m/z* 931.1 [M + H + 3 Na]$^{4+}$, 1239.9 [M + 3 Na]$^{3+}$, 1827.3 [M + 2 H]$^{2+}$.

Elemental analysis calculated (%) for $C_{147}H_{287}Cl_{14}N_{35}O_{42}S_{14}\cdot 7H_2O$: C 41.17, H 7.07, N 11.43, S 10.47; found: C 40.93, H 6.89, N 11.35, S 10.22.

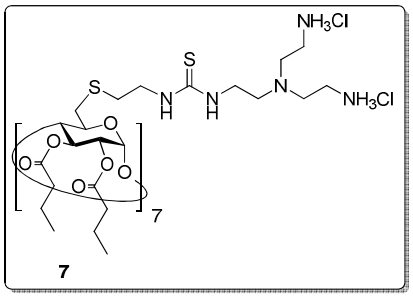

7

Heptakis[6-(2-(*N'*-(2-(*N*,*N*-di-(2-aminoethyl)amino)ethyl)thioureido)ethylthio)-2,3-di-*O*-butanoyl-6-deoxy-]cyclomaltoheptaose tetradecahydrochloride (7). Treatment of compound **30** (63 mg, 12 µmol) with anhydrous TFA (200 µL) at rt for 5 min, followed by freeze-drying immediately from a 0.1 N aq HCl solution afforded pure compound **7** in virtually quantitative yield (51 mg).

$[\alpha]_D$ = +30.0 (*c* = 0.5 in MeOH).

^{1}H NMR (500 MHz, 10:1MeOD-D_2O, 333 K, Figure S23): δ = 5.33 (t, 7H, $J_{2,3} = J_{3,4}$ = 8.6 Hz, H-3), 5.20 (d, 7H, $J_{1,2}$ = 3.6 Hz, H-1), 4.86 (dd, 7H, H-2),4.20 (m, 7H, H-5), 3.97 (t, 7H, $J_{4,5}$ = 8.4 Hz, H-4), 3.84 (bt, 14H, CH_2CH_2C$_{cyst}$), 3.80 (bq, 14H, NCH_2CH_2NHCS), 3.35 (t, 28H, $^3J_{H,H}$ = 6.2 Hz, CH_2NH_2), 3.29 (m, 14H, H-6a, H-6b), 3.24 (t, 28H, $^3J_{H,H}$ = 7.4 Hz, CH_2CH_2NH_2), 3.11 (t, 14H, $^3J_{H,H}$ = 6.4 Hz, NCH_2CH_2NHCS), 2.96 (m, 14H, CH_2S$_{cyst}$), 2.46-2.24 (m, 28H, CH_2CO), 1.66 (m, 28H, CH_2CH_3), 1.00, 0.96 (2 t, 42H, $^3J_{H,H}$ = 7.5 Hz, CH_3).

^{13}C NMR (100.6 MHz, 10:1MeOD-D_2O, 323 K, Figure S23): δ = 173.6, 172.3 (2 CO ester), 96.5 (C-1), 78.2 (C-4), 72.0 (C-5), 70.6 (C-3), 70.3 (C-2), 52.4 (NCH_2CH_2NHCS), 51.2 (CH_2CH_2NH_2), 44.1 (CH_2CH_2S$_{cyst}$), 40.9 (NCH_2CH_2NHCS), 36.9 (CH_2NH_2), 35.7, 35.6 (CH_2CO), 33.9 (C-6), 32.7 (CH_2S$_{cyst}$), 18.0, 17.9 (CH_2CH_3), 12.7 (CH_3).

ESI-MS (Figure S103): *m/z* 978.3 [M+ H+ 3 Na]$^{4+}$, 1283.2 [M + 3 H]$^{3+}$.

Elemental analysis calculated (%) for $C_{161}H_{315}Cl_{14}N_{35}O_{42}S_{14}$: C 44.36, H 7.28, N 11.25, S 10.30; found: C 44.54, H 7.44, N 11.36, S 10.55.

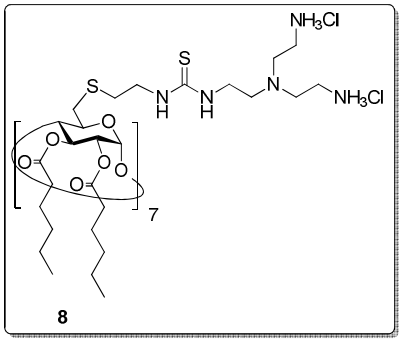

Heptakis[6-(2-(*N'*-(2-(*N*,*N*-di-(2-aminoethyl)amino)ethyl)thioureido)ethylthio)-6-deoxy-2,3-di-*O*-hexanoyl]cyclomaltoheptaose tetradecahydrochloride (8). Treatment of compound **31** (84 mg, 15 µmol) with anhydrous TFA (100 µL) at rt for 5 min, followed by freeze-drying immediately from a 0.1 N aq HCl solution afforded pure compound **8** in quantitative yield (70 mg).

$[\alpha]_D$ = +48.2 (*c* = 0.67 in MeOH).

^{1}H NMR (500 MHz, 5:1 MeOD-D_2O, 313 K, Figure S24): δ = 5.27 (t, 7 H, $J_{2,3}$ = $J_{3,4}$ = 8.6 Hz, H-3), 5.13 (d, 7 H, $J_{1,2}$ = 3.7 Hz, H-1), 4.82 (dd, 7 H, H-2), 4.14 (m, 7 H, H-5), 3.89 (t, 7 H, $J_{4,5}$ = 8.6 Hz, H-4), 3.73 (m, 28 H, CH_2CH$_2$S$_{cyst}$, NCH$_2$CH_2NHCS), 3.25 (t, 28 H, $^3J_{H,H}$ = 6.2 Hz, CH_2NH$_2$), 3.14 (m, 14 H, H-6a, H-6b), 3.14 (t, 28 H, CH_2CH$_2$NH$_2$), 2.97 (t, 14 H, $^3J_{H,H}$ = 6.5 Hz, NCH_2CH$_2$NHCS), 2.90 (m, 14 H, CH$_2$S$_{cyst}$), 2.50-2.15 (m, 28 H, CH$_2$CO), 1.60 (m, 28 H, CH_2CH$_2$CO), 1.30 (m, 56 H, CH_2CH$_3$, CH_2CH$_2$CH$_3$), 0.91, 0.89 (2 t, 42 H, $^3J_{H,H}$ = 7.8 Hz, CH$_3$).

^{13}C NMR (125.7 MHz, 5:1 MeOD-D_2O, 313 K, Figure S24): δ = 183.5 (CS), 175.0, 173.4 (2 CO ester), 98.1 (C-1), 80.1 (C-4), 73.1 (C-5), 71.9 (C-3) , 71.5 (C-2), 53.5 (NCH_2CH$_2$NHCS), 52.3 (CH_2CH$_2$NH$_2$), 45.4 (CH_2CH$_2$S$_{cyst}$), 42.1 (NCH$_2$CH_2NHCS), 38.1 (CH_2NH$_2$), 35.2 (C-6), 35.0 (CH_2CO), 33.9 (CH$_2$S$_{cyst}$), 32.3, 32.2 (2 CH_2CH$_2$CH$_3$), 25.4, 25.3 (2 CH_2CH$_2$CO), 23.2, 23.1 (2 CH_2CH$_3$), 14.2 (CH$_3$).

ESI-MS (Figure S104): *m/z* 849.2 [M + 5 H]$^{5+}$, 1061.2 [M + 4 H]$^{4+}$, 1414.4 [M + 3 H]$^{3+}$, 2120.7 [M + 2 H]$^{2+}$.

Elemental analysis calculated (%) for $C_{189}H_{371}N_{35}O_{42}S_{14}Cl_{14}$: C 47.78, H 7.87, N 10.32; found: C 47.45, H 7.34, N 10.35.

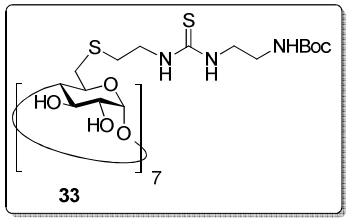

33

Heptakis[6-(2-(*N'*-(2-*tert*-butoxycarbonylaminoethyl)thioureido)ethylthio)-6-deoxy]-cyclomaltoheptaose (33). Saponification of compound **24** (214 mg, 60 µmol) was accomplished according to the procedure described in the general methods yielding compound **33** as an off-white powder (175 mg, 98%).

R_f = 0.50 (10:1:1 MeCN-H_2O-NH_4OH). $[\alpha]_D$ = +34.9 (*c* = 0.24 in MeOH).

^{1}HNMR (500 MHz, MeOD, 323 K, Figure S25): δ = 4.99 (d, 7 H, $J_{1,2}$ = 3.4 Hz, H-1), 4.05 (m, 7 H, H-5), 3.81 (t, 7 H, $J_{2,3}$ = $J_{3,4}$ = 9.3 Hz, H-3), 3.73, 3.58 (2 bs, 28 H, CH_2NHCS), 3.50 (m, 14 H, H-2, H-4), 3.26 (m, 21 H, H-6a, CH_2NHBoc), 2.98 (m, 7 H, H-6b), 2.92 (m, 14 H, CH_2S_{cyst}), 1.46 (bs, 63 H, $C(CH_3)_3$).

^{13}C NMR (125.7 MHz, MeOD, 323 K, Figure S25): δ = 183.7 (CS), 158.6 (CO), 104.1 (C-1), 86.4 (C-4), 80.6 ($C(CH_3)_3$), 74.5 (C-3), 74.4 (C-2), 73.5 (C-5), 45.3, 45.2 (CH_2NHCS), 41.2 (CH_2NHBoc), 35.0 (CH_2S_{cyst}), 33.8 (C-6), 29.1 ($C(CH_3)_3$).

ESI-MS (Figure S105): *m/z* 1504.9 $[M + 2 Na]^{2+}$.

Elemental analysis calculated (%) for $C_{112}H_{203}N_{21}O_{42}S_{14}$: C 45.37, H 6.90, N 9.92; found: C 45.11, H 6.69, N 9.80.

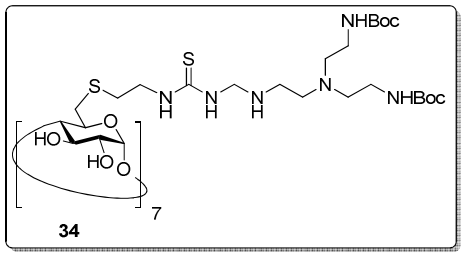

34

Heptakis[6-(2-(*N'*-(2-(*N*,*N*-di-(2-(*N*-*tert*-butoxycarbonylamino)ethyl)amino)ethyl)thio-ureido)ethylthio)-6-deoxy]cyclomaltoheptaose (34). Saponification of compound **28** (242 mg, 50 µmol) was accomplished according to the procedure described in the general methods yielding compound **34** as an off-white powder (211 mg, 99%).

R_f = 0.36 (10:1:1 MeCN-H_2O-NH_4OH). $[\alpha]_D$ = +33.3 (*c* = 0.8 in MeOH).

^{1}HNMR (500 MHz, MeOD, 313 K, Figure S26): δ = 4.96 (d, 7 H, $J_{1,2}$ = 3.5 Hz, H-1), 4.03 (m, 7 H, H-5), 3.79 (t, 7 H, $J_{2,3}$ = $J_{3,4}$ = 8.8 Hz, H-3), 3.74 (bt, 14 H, C*H*$_2$CH$_2$S$_{cyst}$), 3.51 (m, 28 H, H-2, H-4, NCH$_2$C*H*$_2$NHCS), 3.24 (m, 7 H, $J_{6a,6b}$ = 14.3 Hz, $J_{5,6a}$ = 1.8 Hz, H-6a), 3.12 (bt, 14 H, $^3J_{H,H}$ = 6.0 Hz, C*H*$_2$NHBoc), 2.97 (m, 7 H, $J_{5,6b}$ = 5.9 Hz, H-6b), 2.87 (m, 14 H, CH$_2$S$_{cyst}$), 2.69 (bt, 14 H, $^3J_{H,H}$ = 5.6 Hz, NC*H*$_2$CH$_2$NHCS), 2.59 (bt, 28 H, C*H*$_2$CH$_2$NHBoc), 1.44 (bs, 126 H, C(CH$_3$)$_3$).

^{13}C NMR (125.7 MHz, MeOD, 313 K, Figure S26): δ = 183.6 (CS), 158.5 (CO), 104.1 (C-1), 86.2 (C-4), 80.3 (*C*(CH$_3$)$_3$), 74.5 (C-3), 74.4 (C-2), 73.6 (C-5), 55.7 (*C*H$_2$CH$_2$NHBoc), 54.8 (NCH$_2$CH$_2$NHCS), 45.3 (*C*H$_2$CH$_2$S$_{cyst}$), 43.6 (NCH$_2$*C*H$_2$NHCS), 40.1 (*C*H$_2$NHBoc), 34.9 (C-6), 34.2 (CH$_2$S$_{cyst}$), 29.1 (C(*C*H$_3$)$_3$).

ESI-MS (Figure S106): *m/z* 1438.6 [M + H + 2 Na]$^{3+}$, 2146.8 [M + H + Na]$^{2+}$.

Elemental analysis calculated (%) for $C_{175}H_{329}N_{35}O_{56}S_{14}$: C 49.24, H 7.77, N 11.48; found: C 49.25, H 7.71, N 11.37.

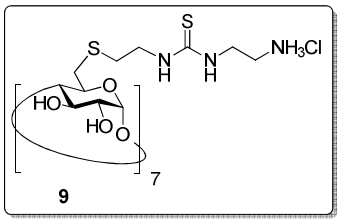

9

Heptakis[6-(2-(*N'*-(2-aminoethyl)thioureido)ethylthio)-6-deoxy]cyclomaltoheptaose heptahydrochloride (9). Treatment of compound **33** (40 mg, 13 µmol) with anhydrous TFA (100 µL) at rt for 5 min, followed by freeze-drying immediately from a 0.1 N aq. HCl solution afforded pure compound **9** in quantitative yield (34 mg).

$[\alpha]_D$ = +46.5 (*c* = 0.5 in H_2O).

^{1}HNMR (500 MHz, D_2O, 333 K, Figure S27): δ = 5.42 (d, 7 H, $J_{1,2}$ = 3.1 Hz, H-1), 4.25 (bt, 7 H, $J_{4,5}$ = 9.1 Hz, H-5), 4.20 (t, 7 H, $J_{2,3}$ = $J_{3,4}$ = 9.1 Hz, H-3), 4.14 (t, 14 H, $^3J_{H,H}$ = 6.0 Hz, CH_2CH_2NH_2), 3.99 (bs, 14 H, CH_2NHCS), 3.96 (dd, 7 H, H-2), 3.87 (t, 7 H, H-4), 3.55 (t, 14 H, $^3J_{H,H}$ = 6.0 Hz, CH_2NH_2), 3.52 (bd, 7 H, $J_{6a,6b}$ = 13.8 Hz, H-6a), 3.28 (dd, 7 H, $J_{5,6b}$ = 7.8 Hz, H-6b), 3.21 (t, 14 H, $^3J_{H,H}$ = 6.9 Hz, CH_2S_{cyst}).

^{13}C NMR (125.7 MHz, D_2O, 333 K, Figure S27): δ = 182.8 (CS), 101.6 (C-1), 84.1 (C-4), 73.6 (C-3), 72.5 (C-2), 72.0 (C-5), 44.3, 41.6 (*C*H_2NHCS), 39.8 (CH_2NH_2), 34.1 (C-6), 32.4 (CH_2S_{cyst}).

ESI-MS (Figure S107): *m/z* 755.8 $[M + 3 H]^{3+}$, 1132.9 $[M + 2 H]^{2+}$, 2264.5 $[M + H]^+$.

Elemental analysis calculated (%) for $C_{77}H_{154}Cl_7N_{21}O_{28}S_{14}$: C 36.71, H 6.16, N 11.68, S 17.82; found: C 36.48, H 5.95, N 11.44, S 17.49.

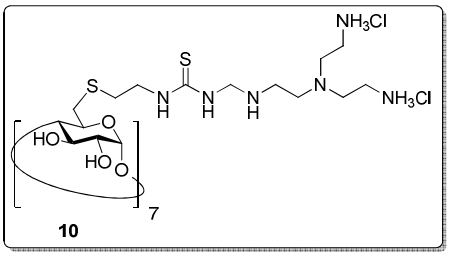

10

Heptakis[6-(2-(*N'*-(2-(*N*,*N*-di-(2-aminoethyl)amino)ethyl)thioureido)ethylthio)-6-deoxy]cyclomaltoheptaose tetradecahydrochloride (10). Treatment of compound **34** (105 mg, 25 µmol) with anhydrous TFA (200 µL) at rt for 5 min, followed by freeze-drying

immediately from a 0.1 N aq. HCl solution afforded pure compound **10** in virtually quantitative yield (82 mg).

$[\alpha]_D$ = +20.3 (*c* = 1.0 in H_2O).

^{1}HNMR (500 MHz, D_2O, 333 K, Figure S28): δ = 5.46 (d, 7 H, $J_{1,2}$ = 3.3 Hz, H-1), 4.30 (m, 7 H, H-5), 4.26 (t, 7 H, $J_{2,3}$ = $J_{3,4}$ = 9.5 Hz, H-3), 4.09 (m, 28 H, NCH_2CH_2NHCS, $CH_2CH_2S_{cyst}$), 4.02 (dd, 7 H, H-2), 3.98 (t, 7 H, H-4), 3.65 (m, 28 H, CH_2NH_2), 3.52 (m, 35 H, $CH_2CH_2NH_2$, H-6a), 3.40 (m, 21 H, H-6b, CH_2S_{cyst}), 3.29 (m, 14 H, NCH_2CH_2NHCS).

^{13}C NMR (75.5 MHz, D_2O, 333 K, Figure S28): δ = 181.9 (CS), 102.2 (C-1), 84.8 (C-4), 73.3 (C-3), 72.4 (C-2, C-5), 53.4 (NCH_2CH_2NHCS), 50.9 (NCH_2CH_2NHCS), 44.2 ($CH_2CH_2S_{cyst}$), 39.8 (CH_2NH_2), 35.2 ($CH_2CH_2NH_2$), 33.8 (C-6), 32.4 (CH_2S_{cyst}).

ESI-MS (Figure S108): *m/z* 717.5 $[M + 4 H]^{4+}$, 956.7 $[M + 3 H]^{3+}$, 1434.5 $[M + 2 H]^{2+}$.

Elemental analysis calculated (%) for$C_{105}H_{231}Cl_{14}N_{35}O_{28}S_{14}$: C 37.34, H 6.89, N 14.52; found: C 37.01, H 6.67, N 14.22.

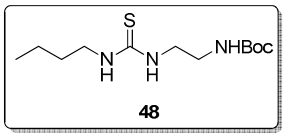

48

1-(2-(*tert*-Butoxycarbonylamino)ethyl)-3-butyl-2-thiourea (48). To a solution of 1-butylamine (25 µL, 0.25 mmol) and Et_3N (86 µL, 0.62 mmol, 2.5 eq) in DCM (1.5 mL) a solution of 2-(*tert*-butoxycarbonylamino)ethylisothiocyanate **22**[186] (50 mg, 0.25 mmol, 1 eq) in DCM (0.5 mL) was added drop wise. The reaction mixture was stirred for 4 h at rt. Then, the solvent was evaporated under reduced pressure and the resulting residue was purified by flash column chromatography (1:1 EtOAc-petroleum ether) to yield compound **48** (66 mg, 97%).

R_f = 0.50 (1:1 EtOAc-petroleum ether).

^{1}H NMR (300 MHz, MeOD, Figure S29): δ = 3.55 (m, 2 H, $CSNHCH_2CH_2NHBoc$), 3.42 (m, 2 H, $CSNHCH_2CH_2CH_2$), 3.23 (t, 2 H, $^3J_{H,H}$ = 6.0 Hz, CH_2NHBoc), 1.58 (m, 2 H, $CSNHCH_2CH_2CH_2$), 1.45 (s, 9 H, $C(CH_3)_3$), 1.38 (m, 2 H, $CSNHCH_2CH_2CH_2$), 0.96 (t, 3 H, $^3J_{H,H}$ = 6.8 Hz, CH_3).

^{13}C NMR (75.5 MHz, $CDCl_3$, Figure S29): δ = 181.5 (CS), 157.8 (CO carbamate), 80.2 ($C(CH_3)_3$), 43.7, 43.6 (CH_2NHCS), 39.8 (CH_2NHBoc), 30.8 ($CSNHCH_2CH_2CH_2$), 28.3 ($C(CH_3)_3$), 20.0 ($CSNHCH_2CH_2CH_2$), 13.7 (CH_3).

ESI-MS (Figure S109): *m/z* 276.2 $[M + H]^+$, 298.2 $[M + Na]^+$, 314.3 $[M + K]^+$.

Elemental analysis calculated (%) for $C_{12}H_{25}N_3O_2S$: C 52.33, H 9.15, N 15.26, S 11.64; found: C 52.72, N 15.67, H 9.16, S 11.50.

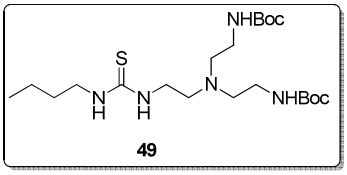

49

1-[2-(Bis(2-(*tert*-butoxycarbonylamino)ethyl)amino)ethyl]-3-butyl-2-thiourea (49). To a solution of 1-butylamine (7.7 µL, 77 µmol) and Et_3N (27 µL, 0.19 mmol, 2.5 eq) in DCM (1.5 mL) a solution of 2-[bis(2-(*tert*-butoxycarbonylamino)ethyl)amino]ethylisothiocyanate **23**[177] (30 mg, 77 µmol, 1 eq) in DCM (0.5 mL) was added drop wise. The reaction mixture was stirred overnight at rt. Then, the solvent was evaporated under reduced pressure and the resulting residue was purified by flash column chromatography (1:1 EtOAc-petroleum ether) to yield compound **49** (33 mg, 91%).

R_f = 0.18 (1:1 EtOAc-petroleum ether).

^{1}H NMR (300 MHz, MeOD, Figure S30): δ = 3.50 (m, 4 H, CH_2NHCS), 3.12 (t, 4 H, $^3J_{H,H}$ = 6.0 Hz, CH_2NHBoc), 2.68 (t, 2 H, $^3J_{H,H}$ = 6.1 Hz, $CSNHCH_2CH_2N$), 2.58 (t, 4 H, $^3J_{H,H}$ = 6.0 Hz, NCH_2CH_2NHBoc), 1.58 (m, 2 H, $CSNHCH_2CH_2CH_2$), 1.46 (s, 18 H, $C(CH_3)_3$), 1.39 (m, 2 H, $CSNHCH_2CH_2CH_2$), 0.96 (t, 3 H, $^3J_{H,H}$ = 7.3 Hz, CH_3).

^{13}C NMR (75.5 MHz, $CDCl_3$, Figure S30): δ = 183.0 (CS), 157.2 (CO carbamate), 80.1 ($C(CH_3)_3$), 56.0 (CH_2CH_2NHBoc, NCH_2CH_2NHCS), 44.4 (CH_2NHCS), 39.0 (CH_2NHBoc), 31.9 ($CSNHCH_2CH_2CH_2$), 28.9 ($C(CH_3)_3$), 20.4 ($CSNHCH_2CH_2CH_2$), 14.3 (CH_3).

ESI-MS (Figure S110): *m/z* 462.5 $[M + H]^+$, 468.5 $[M + Li]^+$, 484.5 $[M + Na]^+$, 500.4 $[M + K]^+$, 496.3 $[M + Cl]^-$.

Elemental analysis calculated (%) for $C_{21}H_{43}N_5O_4S$: C 54.63, H 9.39, N 15.17, S 6.95; found: C 54.23, H 9.48, N 15.11, S 6.87.

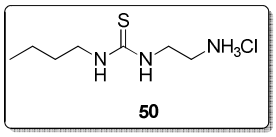

50

1-(2-Aminoethyl)-3-butyl-2-thiourea hydrochloride (50). Treatment of compound **48** (31 mg, 0.11 mmol) with TFA following the procedure described in the general methods, followed by freeze-drying from a 0.1 N aq. HCl solution, gave pure compound **50** in almost quantitative yield (23 mg, 96%).

^{1}H NMR (300 MHz, MeOD, Figure S31): δ = 3.87 (t, 2 H, $^3J_{H,H}$ = 6.0 Hz, CSNHC*H*$_2$CH$_2$NH$_2$), 3.44 (m, 2 H, CSNHC*H*$_2$CH$_2$CH$_2$), 3.18 (t, 2 H, $^3J_{H,H}$ = 6.0 Hz, C*H*$_2$NH$_2$), 1.58 (m, 2 H, CSNHCH$_2$C*H*$_2$CH$_2$), 1.40 (m, 2 H, CSNHCH$_2$CH$_2$C*H*$_2$), 0.96 (t, 3 H, $^3J_{H,H}$ = 7.3 Hz, CH$_3$).

^{13}C NMR (75.5 MHz, D$_2$O, Figure S31): δ = 180.0 (CS), 43.5 (CSNH*C*H$_2$CH$_2$NH$_2$), 41.1 (CSNHC*H*$_2$CH$_2$CH$_2$), 39.3 (*C*H$_2$NH$_2$), 30.0 (CSNHCH$_2$*C*H$_2$CH$_2$), 19.4 (CSNHCH$_2$CH$_2$*C*H$_2$), 13.0 (CH$_3$).

ESI-MS (Figure S111): *m/z* 176.1 $[M + H]^+$.

Elemental analysis calculated (%) for $C_7H_{18}ClN_3S$: C 39.70, H 8.57, N 19.84, S 15.14; found: C 39.93, H 8.84, N 19.46, S 14.76.

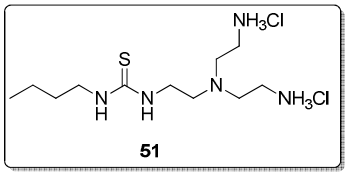

51

1-[2-(Bis(2-aminoethyl)amino)ethyl]-3-butyl-2-thiourea dihydrochloride (51). Treatment of compound **49** (33 mg, 71 µmol) with TFA following the procedure described in the general methods, followed by freeze-drying from a 0.1 N aq. HCl solution, gave pure compound **51** in quantitative yield (24 mg).

^{1}H NMR (300 MHz, MeOD, Figure S32): δ = 3.67 (t, 2 H, $^{3}J_{H,H}$ = 6.3 Hz, CSNHC*H*$_2$CH$_2$N), 3.43 (m, 2 H, CSNHC*H*$_2$CH$_2$CH$_2$), 3.13 (t, 4 H, $^{3}J_{H,H}$ = 6.0 Hz, C*H*$_2$NH$_2$), 2.89 (t, 4 H, $^{3}J_{H,H}$ = 6.1 Hz, NC*H*$_2$CH$_2$NH$_2$), 2.80 (t, 2 H, $^{3}J_{H,H}$ = 6.2 Hz, CSNHCH$_2$C*H*$_2$N), 1.56 (m, 2 H, CSNHCH$_2$C*H*$_2$CH$_2$), 1.38 (m, 2 H, CSNHCH$_2$CH$_2$C*H*$_2$), 0.95 (t, 3 H, $^{3}J_{H,H}$ = 7.3 Hz, CH$_3$).
^{13}C NMR (75.5 MHz, D$_2$O, Figure S32): δ = 181.0 (CS), 53.9 (N*C*H$_2$CH$_2$NHCS), 50.3 (*C*H$_2$CH$_2$NH$_2$), 38.9 (*C*H$_2$NHCS), 33.7 (*C*H$_2$NH$_2$), 30.1 (CSNHCH$_2$*C*H$_2$CH$_2$), 19.4 (CSNHCH$_2$CH$_2$*C*H$_2$), 13.0 (CH$_3$).
ESI-MS (Figure S112): *m/z* 262.3 [M + H]$^{+}$.
Elemental analysis calculated (%) for $C_{11}H_{29}Cl_2N_5S$: C 39.51, H 8.74, N 20.95, S 9.59; found: C 39.88, H 8.79, N 20.57, S 9.50.

3.2. New Compounds synthesized in Chapter 3

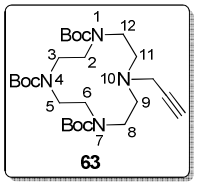

63

1,4,7-Tris(*tert*-butoxycarbonyl)-10-propargyl-1,4,7,10-tetraazacyclododecane (63).[350]
A solution of 1,4,7-tris(*tert*-butoxycarbonyl)-1,4,7,10-tetraazacyclododecane **61**[276b] (1.0 g, 2.12 mmol), propargyl bromide solution 80% in toluene (0.68 mL, 6.35 mmol, 3 eq) and Et$_3$N (0.88 mL, 6.35 mmol, 3 eq) in MeCN (11 mL) was stirred at rt for 48 h. Then, additional portions of propargyl bromide solution 80% in toluene (0.68 mL, 6.35 mmol, 3 eq) and Et$_3$N (0.88 mL, 1.35 mmol, 3 eq) were added and the suspension was stirred at rt for another 24 h. The resulting suspension was filtered and the solid residue extracted with DCM (2 x 5 mL). The combined filtrates were concentrated to dryness. The resulting residue was purified by flash column chromatography (1:1 EtOAc-petroleum ether) to give **63** (0.77 g, 71%).
R_f = 0.64 (1:1 EtOAc-petroleum ether).

^{1}H NMR (500 MHz, $CDCl_3$, 333 K, Figure S33): δ = 3.58 (bs, 2H, CH_2C≡CH), 3.54 (t, 4H, $^{3}J_{H,H}$ = 5.0 Hz, H-3, H-5), 3.40 (m, 8H, H-2, H-6, H-8, H-12), 2.90 (m, 4H, H-9, H-11), 2.26 (bs, 1H, C≡CH), 1.48, 1.47 (2 s, 27H, C(CH_3)$_3$).

^{13}C NMR (125.7 MHz, $CDCl_3$, 333 K, Figure S33): δ = 156.1 (CO), 80.1 (*C*(CH_3)$_3$), 79.7 (*C*≡CH), 76.2 (C≡*C*H), 53.5 (C-9, C-11), 50.0 (C-8, C-12), 47.8 (C-3, C-5), 47.6 (C-2, C-6), 40.8 (*C*H_2C≡CH), 28.9, 28.7 (C(*C*H_3)$_3$).

ESI-MS (Figure S113): *m/z* 511.4 $[M + H]^+$, 533.4 $[M + Na]^+$, 549.3 $[M + K]^+$.

Elemental analysis calculated (%) for$C_{26}H_{46}N_4O_6$: C 61.15, H9.08, N 10.97; found: C 61.22, H 9.22, N 10.67.

Alternatively, this reaction was also carried out under microwave irradiation: A solution of 1,4,7-tris(*tert*-butoxycarbonyl)-1,4,7,10-tetraazacyclododecane **61**[276b] (240 mg, 0.51 mmol), propargyl bromide solution 80% in toluene (0.16 mL, 1.53 mmol, 3 eq) and Et_3N (0.21 mL, 1.53 mmol, 3 eq) in MeCN (3 mL) was heated under microwave irradiation at 120 ºC for 0.5 h (40W). Then, additional portions of propargyl bromide solution 80% in toluene (0.16 mL, 1.53 mmol, 3 eq) and Et_3N (0.21 mL, 1.53 mmol, 3 eq) were added and the suspension was heated under microwave irradiation at 120 ºC for another 0.5 h. The resulting suspension was filtered and the solid residue extracted with DCM (2 x 1 mL). The combined filtrates were concentrated to dryness. The resulting residue was purified by column chromatography (1:1 EtOAc-petroleum ether) to give **63** (132 mg, 51%).

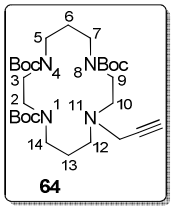

64

1,4,8-Tris(*tert*-butoxycarbonyl)-11-propargyl-1,4,8,11-tetraazacyclotetradecane (64). A solution of 1,4,8-tris(*tert*-butoxycarbonyl)-1,4,8,11-tetraazacyclotetradecane **62**[346] (250 mg, 0.50 mmol), propargyl bromide solution 80% in toluene (0.16 mL, 1.50 mmol, 3 eq) and Et_3N (0.20 mL, 1.50 mmol, 3 eq) in MeCN (3 mL) was stirred at rt for 48 h. Then, additional portions of propargyl bromide solution 80% in toluene (0.16 mL, 1.5 mmol, 3

eq) and Et_3N (0.20 mL, 1.5 mmol, 3 eq) were added and the suspension was stirred at rt for another 24 h. The resulting suspension was filtered and the solid residue extracted with DCM (2 x 1 mL). The combined filtrates were concentrated to dryness. The resulting residue was purified by flash column chromatography (95:5DCM-MeOH) to yield **64** (181 mg, 67%).

R_f = 0.69 (9:1 DCM-MeOH).

^{1}H NMR (500 MHz, $CDCl_3$, 333 K, Figure S34): δ = 3.41-3.24 (m, 4 H, H-2, H-3), 3.38 (d, 2 H, $^4J_{H,H}$ = 2.0 Hz, CH_2C≡CH), 3.33 (m, 2 H, H-9), 3.32 (t, 2 H, $^3J_{H,H}$ = 6.0 Hz, H-14), 3.28 (m, 4 H, $^3J_{H,H}$ = 7.0 Hz, H-5, H-7), 2.68 (bt, 2 H, $^3J_{H,H}$ = 5.5 Hz, H-10), 2.51 (bt, 2 H, $^3J_{H,H}$ = 6.0 Hz, H-12), 2.14 (m, 1 H, C≡CH), 1.90 (m, 2 H, $^3J_{H,H}$ = 7.0 Hz, H-6), 1.69 (m, 2 H, $^3J_{H,H}$ = 6.0 Hz, H-13), 1.45, 1.44 (2 s, 27 H, C$(CH_3)_3$).

^{13}C NMR (125.7 MHz, $CDCl_3$, 333 K, Figure S34): δ = 155.8, 155.5 (CO), 79.5, 79.4 (*C*$(CH_3)_3$), 78.1 (*C*≡CH), 73.1 (C≡*C*H), 52.7 (C-10), 51.2 (C-12), 47.7, 47.4, 47.3, 47.1, 46.7, 45.1 (C-2, C-3, C-5, C-7, C-9, C-14), 42.3 (*C*H_2C≡CH), 28.9 (C-6), 28.4 (C(*C*$H_3)_3$), 26.7 (C-13).

ESI-MS (Figure S114): *m/z* 539.4 $[M + H]^+$, 561.4 $[M + Na]^+$, 577.3 $[M + K]^+$.

Elemental analysis calculated (%) for $C_{28}H_{50}N_4O_6$: C 62.43, H 9.35, N 10.40; found: C , H , N.

Alternatively, this reaction was also carried out under microwave irradiation: A solution of 1,4,8-tris(*tert*-butoxycarbonyl)-1,4,8,11-tetraazacyclotetradecane **62**[346] (243 mg, 0.49 mmol), propargyl bromide solution 80% in toluene (0.16 mL, 1.48 mmol, 3 eq) and Et_3N (0.20 mL, 1.48 mmol, 3 eq) in MeCN (2.5 mL) was heated under microwave irradiation at 120 ºC for 0.5 h. Then, additional portions of propargyl bromide solution 80% in toluene (0.16 mL, 1.48 mmol, 3 eq) and Et_3N (0.20 mL, 1.48 mmol, 3 eq) were added and the suspension was heated under microwave irradiation at 120 ºC (40 W) for another 0.5 h. The resulting suspension was filtered and the solid residue extracted with DCM (2 x 1 mL). The combined filtrates were concentrated to dryness. The resulting residue was purified by flash column chromatography (95:5 DCM-MeOH) to give **64** (92 mg, 35%).

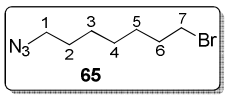

65

1-Azido-7-bromoheptane (65). To a solution of 1,7-dibromoheptane (1.19 g, 4.61 mmol) in DMSO (2 mL) was added NaN_3 (0.12 g, 1.85 mmol, 0.4 eq) and the reaction mixture was stirred at rt for 5 h. Then, water was added (15 mL) and the reaction mixture was extracted with Et_2O (3 x 10 mL). The organic layer was washed with brine (2 x 10 mL), dried over Na_2SO_4, filtered and evaporated to dryness. Solvents were evaporated and the resulting residue was purified by flash column chromatography (petroleum ether → 1:9 Et_2O-petroleum ether) to yield **65** (353 mg, 35%), together with 620 mg (52%) of recovered starting material.

R_f = 0.23 (petroleum ether).

^{1}H NMR (500 MHz, $CDCl_3$, Figure S35): δ = 3.41 (t, 2 H, $^3J_{H,H}$ = 7.0 Hz, H-7), 3.26 (t, 2 H, $^3J_{H,H}$ = 7.0 Hz, H-1), 1.86 (m, 2 H, $^3J_{H,H}$ = 7.0 Hz, H-6), 1.60 (m, 2 H, $^3J_{H,H}$ = 7.0 Hz, H-2), 1.45 (m, 2 H, $^3J_{H,H}$ = 7.0 Hz, H-5), 1.41-1.35 (m, 2 H, H-3), 1.37-1.31 (m, 2 H, H-4).

^{13}C NMR (125.7 MHz, $CDCl_3$, Figure S35): δ = 51.5 (C-1), 33.9 (C-7), 32.7 (C-6), 28.8 (C-2), 28.4 (C-5), 28.1 (C-3), 26.7 (C-4).

IR (NaCl): 2096 (N_3) cm^{-1}.

Elemental analysis calculated (%) for $C_7H_{14}N_3Br$: C 38.20, H 6.41, N 19.09; found: C 38.49, H 6.12, N 18.74.

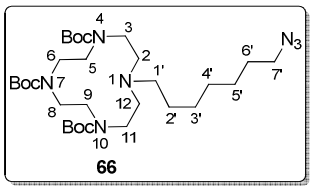

66

1-(7-Azido-*n*-hept-1-yl)-4,7,10-tris(*tert*-butoxycarbonyl)-1,4,7,10-tetraazacyclododecane (66). A suspension of 1,4,7-tris(*tert*-butoxycarbonyl)-1,4,7,10-tetraazacyclododecane **61**[276b] (300 mg, 0.63 mmol), compound **65** (182 mg, 0.83 mmol, 1.3 eq) and K_2CO_3 (114 mg, 0.83 mmol, 1.3 eq) in MeCN (5 mL) was heated under

microwave irradiation at 140 ºC for 2 h. Then, additional portions of **65** (182 mg, 0.83 mmol, 1.3 eq) and K_2CO_3 (114 mg, 0.83 mmol, 1.3 eq) were added and the suspension was heated under microwave irradiation at 140 ºC (60 W) for another 2 h. The resulting suspension was filtered and the solid residue extracted with DCM (2 x 1 mL). The combined filtrates were concentrated to dryness. The resulting residue was purified by flash column chromatography (1:1 EtOAc-petroleum ether) to give **66** (357 mg, 93%).

R_f = 0.40 (2:1 EtOAc-petroleum ether).

^{1}H NMR (500 MHz, $CDCl_3$, 323 K, Figure S36): δ = 3.50, 3.43 (2m, 8 H, H-5, H-6, H-8, H-9), 3.28-3.20 (m, 4 H, H-3, H-11), 3.21 (t, 2 H, $^3J_{H,H}$ = 7.0 Hz, H-7'), 2.60 (m, 4 H, H-2, H-12), 2.47 (t, 2 H, $^3J_{H,H}$ = 8.0 Hz, H-1'), 1.56 (m, 2 H, $^3J_{H,H}$ = 7.0 Hz, H-6'), 1.48 (m, 2H, H-2'), 1.45, 1.43 (2 s, 27 H, $C(CH_3)_3$), 1.33 (m, 4H, H-3', H-5'), 1.24 (m, 2H, H-4').

^{13}C NMR (125.7 MHz, $CDCl_3$, 323 K, Figure S36): δ = 155.9, 155.7 (CO), 79.5, 79,3 ($C(CH_3)_3$), 57.7 (C-2, C-12), 54.2 (C-1'), 53.1 (C-7'), 49.9, 48.2 (C-5, C-6, C-8, C-9), 48.0 (C-3, C-11), 29.2 (C-3'), 29.0 (C-6'), 28.8, 28.6 ($C(CH_3)_3$), 27.8 (C-4'), 26.8 (C-5'), 24.3 (C-2').

IR (NaCl): 2096 (N_3) cm^{-1}.

ESI-MS (Figure S115): *m/z* 612.4 $[M + H]^+$, 634.4 $[M + Na]^+$, 650.3 $[M + K]^+$.

Elemental analysis calculated (%) for $C_{30}H_{57}N_7O_6$: C 58.89, H 9.39, N 16.03; found: C 58.98, H 9.43, N 15.71.

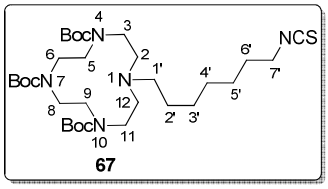

67

1-(7-Isothiocyanato-*n*-hept-1-yl)-4,7,10-tris(*tert*-butoxycarbonyl)-1,4,7,10-tetraaza-cyclododecane (67). To a solution of **66** (177 mg, 0.29 mmol), in dioxane (4 mL) under N_2, was added TPP (91 mg, 0.35 mmol, 1.2 eq) and the reaction mixture was stirred at rt for 15 min. Then, CS_2 (0.17 mL, 2.89 mmol, 10 eq) was added and the reaction mixture was stirred at rt for 16 h. The reaction was concentrated to dryness. The resulting residue

was purified by flash column chromatography (1:4 → 1:2 EtOAc-petroleum ether) to give **67** (130 mg, 71%).

R_f = 0.67 (1:1 EtOAc-petroleum ether).

^{1}H NMR (500 MHz, $CDCl_3$, 333 K, Figure S37): δ = 3.51, 3.35 (2m, 8 H, H-5, H-6, H-8, H-9), 3.46 (t, 2 H, $^3J_{H,H}$ = 6.5 Hz, H-7'), 3.24 (m, 4 H, H-3, H-11), 2.61 (m, 4 H, H-2, H-12), 2.54 (m, 2 H, H-1'), 1.67 (m, 2 H, $^3J_{H,H}$ = 7.0 Hz, H-6'), 1.44, 1.42 (2 s, 27 H, $C(CH_3)_3$), 1.43-1.36 (m, 2H, H-2'), 1.33 (m, 4H, H-3',H-5'), 1.26 (m, 2H, H-4').

^{13}C NMR (125.7 MHz, $CDCl_3$, 333 K, Figure S37): δ = 155.8, 155.4 (CO), 131.1 (NCS), 79.4, 79,2 ($C(CH_3)_3$), 54.6 (C-2, C-12), 53.0 (C-1'), 49.8, 47.7 (C-5, C-6, C-8, C-9), 48.1 (C-3, C-11), 45.0 (C-7'), 29.9 (C-6'), 28.7 (C-3'), 28.6, 28.5 ($C(CH_3)_3$), 27.6 (C-4'), 26.5 (C-5'), 24.2 (C-2').

IR (NaCl): 2171, 2096 (NCS) cm^{-1}.

ESI-MS (Figure S116): *m/z* 628.3 $[M + H]^+$, 650.3 $[M + Na]^+$, 666.3 $[M + K]^+$.

Elemental analysis calculated (%) for $C_{31}H_{57}N_5O_6S$: C 59.30, H 9.15, N 11.15, S 5.11; found: C 59.19, H 9.03, N 10.94, S 4.79.

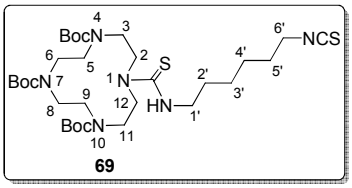

69

***N*-[4,7,10-Tris(*tert*-butoxycarbonyl)-1,4,7,10-tetraazacyclododec-1-yl]-*N'*-(6-isothiocyanato-*n*-hex-1-yl)thiourea (69).** To a solution of 1,6-hexamethylenediisothiocyanate **68**[278] (0.56 g, 2.79 mmol, 3 eq) and Et_3N (0.39 mL, 2.79 mmol, 3 eq) in DCM (12 mL), a solution of 1,4,7-tris(*tert*-butoxycarbonyl)-1,4,7,10-tetraazacyclododecane **61**[276b] (0.44 g, 0.93 mmol) in DCM (6 mL) was added drop wise. The reaction mixture was then stirred at rt for 16 h. Solvents were evaporated and the resulting residue was purified by flash column chromatography (1:2 EtOAc-petroleum ether) to yield **69** (531 mg, 85%).

R_f = 0.59 (1:1 EtOAc-petroleum ether).

^{1}H NMR (500 MHz, $CDCl_3$, 313 K, Figure S38): δ = 5.80 (bs, 1 H, NH), 3.82 (m, 4 H, H-2, H-12), 3.61 (m, 2 H, H-1'), 3.49 (m, 4 H, H-3, H-11), 3.48 (t, 2 H, $^3J_{H,H}$ = 6.5 Hz, H-6'), 3.38 (m, 8 H, H-5, H-6, H-8, H-9), 1.69 (m, 2 H, H-5'), 1.62 (m, 2 H, $^3J_{H,H}$ = 7.0 Hz, H-2'), 1.45, 1.44 (2 s, 27 H, $C(CH_3)_3$), 1.43 (m, 2 H, H-4'), 1.40 (m, 2 H, H-3').

^{13}C NMR (125.7 MHz, $CDCl_3$, 313 K, Figure S38): δ = 182.9 (CS), 156.9, 156.7 (CO), 130.5 (NCS), 80.5, 80.4 ($C(CH_3)_3$), 53.6 (C-2, C-12), 50.4 (C-5, C-6, C-8, C-9), 50.0 (C-3, C-11), 45.8 (C-1'), 45.1 (C-6'), 30.0 (C-5'), 29.2 (C-2'), 28.6 ($C(CH_3)_3$), 26.4 (C-3'), 26.2 (C-4').

IR (NaCl): 2181, 2105 (NCS) cm^{-1}.

ESI-MS (Figure S117): *m/z* 673.3 $[M + H]^+$, 695.3 $[M + Na]^+$, 711.3 $[M + K]^+$.

Elemental analysis calculated (%) for $C_{31}H_{56}N_6O_6S_2$: C 55.33, H 8.39, N 12.49, S, 9.53; found: C 55.48, H 8.75, N 12.43, S 9.18.

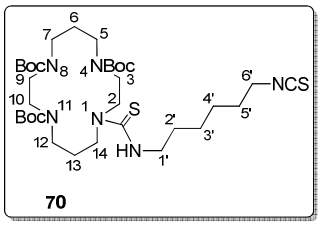

70

***N*-[4,8,11-Tris(*tert*-butoxycarbonyl)-1,4,8,11-tetraazacyclotetradec-1-yl]-*N'*-(6-isothiocyanato-*n*-hex-1-yl)thiourea (70).** To a solution of 1,6-hexamethylenediisothiocyanate **68**[278] (120 mg, 0.65 mmol, 3 eq) and Et_3N (90 µL, 0.65 mmol, 3 eq) in DCM (3 mL), a solution of 1,4,8-tris(*tert*-butoxycarbonyl)-1,4,8,11-tetraazacyclotetradecane **62**[346] (108 mg, 0.22 mmol) in DCM (1 mL) was added drop wise and then the reaction mixture was stirred at rt for 16 h. Solvents were evaporated and the resulting residue was purified by flash column chromatography (1:2 → 1:1 EtOAc-petroleum ether) to yield **70** (139 mg, 90%).

R_f = 0.43 (1:1 EtOAc-petroleum ether).

^{1}H NMR (500 MHz, $CDCl_3$, 313 K, Figure S39): δ = 6.82 (m, 1 H, NH), 3.93 (m, 2 H, H-14), 3.62 (m, 2 H, H-1'), 3.57 (m, 2 H, H-2), 3.47 (t, 2 H, $^3J_{H,H}$ = 7.0 Hz, H-6'), 3.41-3.34

(m, 4 H, H-9, H-10), 3.31 (m, 4 H, H-3, H-12), 3.34-3.23 (m, 4 H, H-5, H-7), 1.86 (m, 2 H, $^3J_{H,H}$ = 6.5 Hz, H-13), 1.74 (m, 2 H, $^3J_{H,H}$ = 7.0 Hz, H-6), 1.67 (m, 2 H, $^3J_{H,H}$ = 7.0 Hz, H-5'), 1.65 (m, 2 H, $^3J_{H,H}$ = 7.0 Hz, H-2'), 1.43, 1.42, 1.41 (3 s, 27 H, C(CH_3)$_3$), 1.40 (m, 2 H, H-4'), 1.38 (m, 2 H, H-3').

^{13}C NMR (125.7 MHz, $CDCl_3$, 313 K, Figure S39): δ = 182.1 (CS), 156.1, 156.0, 155.0 (CO), 130.5 (NCS), 80.9, 80.1, 80.0 (*C*(CH_3)$_3$), 53.6 (C-2), 50.5 (C-14), 48.5 (C-9, C-10), 47.1 (C-3), 46.7 (C-5, C-7), 46.2 (C-12), 46.4 (C-1'), 45.1 (C-6'), 29.9 (C-5'), 28.8 (C-6), 28.7 (C-2'), 28.5, 28.4 (C(*C*H_3)$_3$), 28.0 (C-13), 26.4 (C-3'), 26.3 (C-4').

IR (NaCl): 2180, 2103 (NCS) cm^{-1}.

ESI-MS (Figure S118): *m/z* 701.6 $[M + H]^+$, 723.7 $[M + Na]^+$, 739.6 $[M + K]^+$.

Elemental analysis calculated (%) for $C_{33}H_{60}N_6O_6S_2$: C 56.54, H 8.63, N 11.99, S 9.15; found: C 56.20, H 8.52, N 11.86, S 9.22.

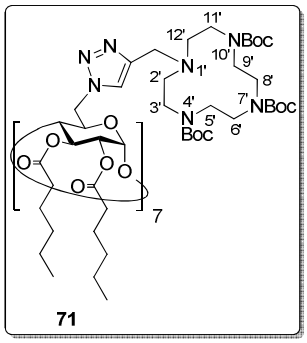

71

Heptakis[6-(4-(4,7,10-tris(*tert*-butoxycarbonyl)-1,4,7,10-tetraazacyclododecyl-1-methyl)-1*H*-1,2,3-triazol-1-yl)-6-deoxy-2,3-di-*O*-hexanoyl]cyclomaltoheptaose (71). To a solution of heptakis(6-azido-6-deoxy-2,3-di-*O*-hexanoyl)cyclomaltoheptaose **54**[180b] (80 mg, 30 µmol) and **63** (117 mg, 0.23 mmol, 1.1 eq) in ^{t}BuOH-H_2O (3:1, 4 mL) the silica-supported Cu(I) catalyst Si-BPA·Cu$^+$[180a] (7 mg, 30 mg per mmol of alkyne) was added and the reaction mixture was refluxed for 16 h. Then, the solvent was removed under reduced pressure, the residue was taken in DCM (4 mL), and the catalyst was filtered. After evaporation of the solvent, the residue was purified by flash column chromatography (30:1 → 9:1 DCM-MeOH) to yield compound **71** (182 mg, 97%).

R_f = 0.55 (9:1 DCM-MeOH). $[\alpha]_D$ = +13.8 (*c* = 1.0 in MeOH).

^{1}H NMR (500 MHz, MeOD, 333 K, Figure S40): δ = 8.05 (bs, 7H, $CH_{triazole}$), 5.55-5.35 (m, 14H, H-1, H-3), 5.06-4.78 (m, 14H, H-6), 4.74 (m, 7H, H-2), 4.58 (m, 7H, H-5), 4.02 (m, 14H, $CH_{2triazole}$), 3.70-3.52 (m, 35H, H-4, H-6', H-8'), 3.52-3.33 (m, 56H, H-3', H-5', H-9', H-11'), 2.82-2.56 (m, 28H, H-2', H-12'), 2.53-2.19 (m, 28H, CH_2CO), 1.65 (m, 28H,CH_2CH_2CO), 1.50, 1.46 (2s, 189H, $C(CH_3)_3$), 1.43-1.29 (m, 56H, C$H_2CH_2CH_3$), 0.95 (m, 42H, CH_3).

^{13}C NMR (125.7 MHz, MeOD, 333 K, Figure S40): δ = 172.9, 171.9 (CO ester), 156.0 (CO carbamate), 141.1 ($C_{triazole}$), 126.9 ($CH_{triazole}$), 96.7 (C-1), 79.6 ($C(CH_3)_3$), 77.2 (C-4), 70.1 (C-3), 69.9 (C-2, C-5), 53.8 (C-2', C-12'), 50.3 (C-6), 49.4-47.5 (C-3', C-5', C-9', C-11'), 46.3(C-6', C-8'), 42.6 ($CH_{2triazole}$), 33.5, 33.7 (CH_2CO), 31.2, 31.0 ($CH_2CH_2CH_3$), 27.8, 27.7 ($C(CH_3)_3$), 24.1 (CH_2CH_2CO), 22.0 (CH_2CH_3), 12.9 (CH_3).

ESI-MS (Figure S119): *m/z* 3150.9 $[M + 2 Na]^{2+}$.

Elemental analysis calculated (%) for $C_{308}H_{525}N_{49}O_{84}$: C 59.11, H 8.45, N 10.97; found: C 59.33, H 8.50, N 10.73.

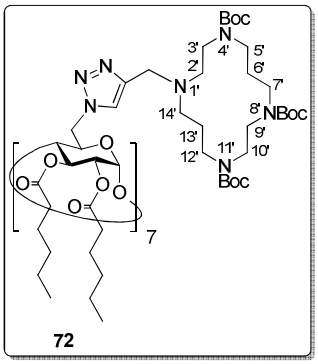

72

Heptakis[6-(4-(4,8,11-tris(*tert*-butoxycarbonyl)-1,4,8,11-tetraazacyclotetradecyl-1-methyl)-1*H*-1,2,3-triazol-1-yl)-6-deoxy-2,3-di-*O*-hexanoyl]cyclomaltoheptaose (72). To a solution of heptakis(6-azido-6-deoxy-2,3-di-*O*-hexanoyl)cyclomaltoheptaose **54**[180b] (68 mg, 25 µmol) and **64** (105 mg, 0.19 mmol, 1.1 eq) in ^{t}BuOH-H_2O (3:1, 4 mL) the silica-supported Cu(I) catalyst Si-BPA·Cu^{+}[180a] (6 mg, 30 mg per mmol of alkyne) was

added and the reaction mixture was refluxed for 16 h. Then, the solvent was removed under reduced pressure, the residue was taken in DCM (4 mL), and the catalyst was filtered. After evaporation of the solvent, the residue was purified by flash column chromatography (95:5 DCM-MeOH) to yield compound **72** (136 mg, 84%).

R_f = 0.58 (9:1 DCM-MeOH). $[\alpha]_D$ = +10.2 (*c* = 1.0 in MeOH).

^{1}H NMR (500 MHz, MeOD, 333 K, Figure S41): δ = 8.00 (bs, 7 H, $CH_{triazole}$), 5.55 (m, 7 H, H-1), 5.50 (t, 7 H, $J_{2,3}$ = $J_{3,4}$ = 9.5 Hz, H-3), 4.93 (m, 14 H, H-6), 4.74 (dd, 7 H, $J_{1,2}$ = 3.0 Hz, H-2), 4.57 (m, 7 H, H-5), 3.89 (bd, 7 H, $^2J_{H,H}$ = 12.5 Hz, $CH_{2\text{-a-triazole}}$), 3.83 (bd, 7 H, $CH_{2\text{-b-triazole}}$), 3.57 (bt, 7 H, $J_{4,5}$ = 9.5 Hz, H-4), 3.48-3.31 (m, 84 H, H-3', H-5', H-7', H-9', H-10', H-12'), 2.69 (m, 14 H, H-2'), 2.49 (m, 14 H, H-14'), 2.46-2.18 (m, 28 H, CH_2CO), 1.95 (m, 14 H, H-6'), 1.75 (m, 14 H, H-13'), 1.62 (m, 28 H, CH_2CH_2CO), 1.49, 1.48, 1.46 (3s, 189 H, $C(CH_3)_3$), 1.42-1.30 (m, 56 H, $CH_2CH_2CH_3$), 0.94 (m, 42 H, CH_3).

^{13}C NMR (125.7 MHz, MeOD, 333 K, Figure S41): δ = 172.8, 171.9 (CO ester), 156.1, 155.9, 155.8 (CO carbamate), 142.8 ($C_{triazole}$), 126.4 ($CH_{triazole}$), 96.7 (C-1), 79.7, 79.6 ($C(CH_3)_3$), 77.1 (C-4), 70.2 (C-5), 69.9 (C-2, C-3), 52.6 (C-2'), 51.3 (C-14'), 50.3 (C-6), 47.6 ($CH_{2triazole}$), 47.1, 46.8, 46.6, 45.5, 45.1, 41.9 (C-3′, C-5′, C-7′, C-9′, C-10′, C-12′), 33.8, 33.5 (CH_2CO), 31.2, 31.0 ($CH_2CH_2CH_3$), 28.6 (C-6'), 27.7, 27.6, 27.5 ($C(CH_3)_3$), 26.5 (C-13'), 24.1 (CH_2CH_2CO), 22.0 (CH_2CH_3), 12.9 (CH_3).

ESI-MS (Figure S120): *m/z* 2174.7 $[M + 3\ Na]^{3+}$, 3250.5 $[M + 2\ Na]^{2+}$.

Elemental analysis calculated (%) for $C_{322}H_{553}N_{49}O_{84}$: C 59.91, H 8.63, N 10.63; found: C 60.08, H 8.61, N 10.51.

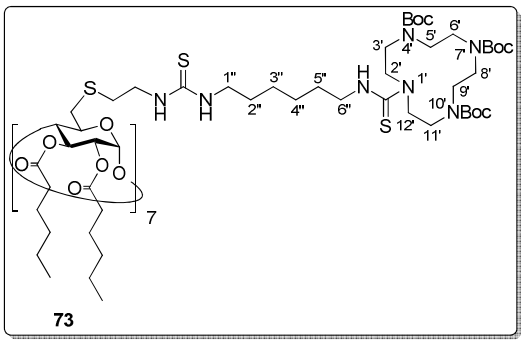

73

Heptakis{6-[2-(*N'*-(*N*'-(4,7,10-tris(*tert*-butoxycarbonyl)-1,4,7,10-tetraazacyclododec-1-yl)-thioureido-*n*-hex-1-yl)thioureido)ethylthio]-6-deoxy-2,3-di-*O*-hexanoyl}cyclomaltoheptaose (73). To a solution of compound **21** (61 mg, 19 µmol) and Et_3N (0.02 mL, 0.15 mmol, 1.1 eq) in DCM (4 mL) **69** (100 mg, 0.15 mmol, 1.1 eq) was added and the reaction mixture was stirred in a sealed reaction vial at 40 ºC for 72 h assuring that pH value was maintained at 9. Then, solvents were evaporated under reduced pressure and the resulting residue was purified by size exclusion chromatography in MeOH to yield **73** (109 mg, 75%).

R_f = 0.50 (95:5 DCM-MeOH). $[\alpha]_D$ = +43.3 (*c* = 1.0 in DCM).

^{1}H NMR (500 MHz, MeOD, 333 K, Figure S42): δ = 5.34 (t, 7 H, $J_{2,3}$ = $J_{3,4}$ = 8.5 Hz, H-3), 5.19 (d, 7 H, $J_{1,2}$ = 3.0 Hz, H-1), 4.85 (dd, 7 H, H-2), 4.22 (m, 7 H, H-5), 3.95 (t, 7 H, $J_{4,5}$ = 8.5 Hz, H-4), 3.89 (m, 28 H, H-2', H-12'), 3.80 (m, 14 H, CH_2N_{cyst}), 3.65 (t, 14 H, $^3J_{H,H}$ = 7.0 Hz, H-1''), 3.57 (m, 28 H, H-3', H-11'), 3.50 (m, 56 H, H-5′, H-6′, H-8′, H-9′), 3.49 (m, 14 H, H-6''), 3.30 (m, 7 H, H-6a), 3.20 (dd, 7 H, $J_{6a,6b}$ = 14.0 Hz, $J_{5,6b}$ = 6.5 Hz, H-6b), 2.96 (m, 14 H, CH_2S_{cyst}), 2.50-2.24 (m, 28 H, CH_2CO), 1.64 (m, 56 H, H-2'', H-5'', C$H_2$$CH_2CO$), 1.52, 1.51 (2 s, 189 H,$C(CH_3)_3$), 1.44 (m, 28 H, H-3'', H-4''), 1.43-1.30 (m, 56 H, CH_2CH_2CH_3), 0.95 (m, 42 H, CH_3).

^{13}C NMR (125.7 MHz, MeOD, 333 K, Figure S42): δ = 182.6, 182.0 (CS), 173.3, 172.0 (CO ester), 157.2, 156.8 (CO carbamate), 96.9 (C-1), 80.6, 80.5 ($C(CH_3)_3$), 78.7 (C-4), 71.9 (C-5),70.7 (C-3), 70.3 (C-2), 52.7 (C-2', C-12'), 50.2, 49.9 (C-5′, C-6′, C-8′, C-9′), 49.5 (C-3′, C-11′), 45.8 (C-1″), 44.0, 43.9 (C-6″, CH_2N_{Cyst}), 34.0 (C-6), 33.8, 33.7 (CH_2CO), 32.9 (CH_2S_{cyst}), 31.2, 31.1 ($CH_2CH_2CH_3$), 29.0, 28.9 (C-2″, C-5″),27.7, 27.6 ($C(CH_3)_3$), 26.5 (C-3″, C-4″), 24.2 (CH_2CH_2CO), 22.1, 22.0 (CH_2CH_3), 13.1, 12.9 (CH_3).

ESI-MS (Figure S121): *m/z* 2567.8 $[M + 3 Na]^{3+}$, 3839.4 $[M + 2 Na]^{2+}$.

Elemental analysis calculated (%) for $C_{357}H_{637}N_{49}O_{84}S_{21}$: C 56.17, H 8.41, N 8.99, S 8.82; found: C 56.29, H 8.16, N 8.99, S 8.46.

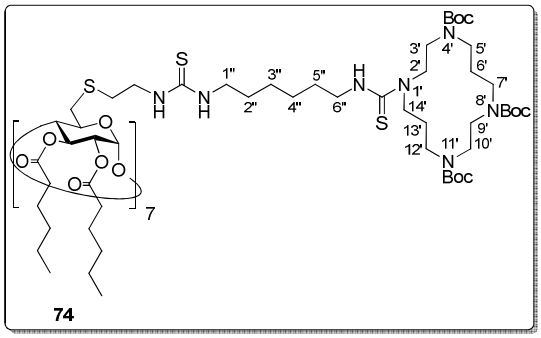

Heptakis{6-[2-(*N'*-(*N'*-(4,8,11-tris(*tert*-butoxycarbonyl)-1,4,8,11-tetraazacyclotetradec-1-yl)-thioureido-*n*-hex-1-yl)thioureido)ethylthio]-6-deoxy-2,3-di-*O*-hexanoyl}cyclomaltoheptaose (74). To a solution of compound **21** (59 mg, 19 µmol) and Et_3N (0.02 mL, 0.14 mmol, 1.1 eq) in DCM (4 mL), **70** (100 mg, 0.14 mmol, 1.1 eq) was added and the reaction mixture was stirred in a sealed reaction vial at 40 ºC for 72 h assuring that pH value was maintained at 9. Then, solvents were evaporated under reduced pressure and the resulting residue was purified by size exclusion chromatography in MeOH to yield **74** (111 mg, 77%).

R_f = 0.49 (95:5 DCM-MeOH). $[\alpha]_D$ = +34.1 (*c* = 1.0 in MeOH).

^{1}H NMR (500 MHz, MeOD, 333 K, Figure S43): δ = 5.34 (t, 7 H, $J_{2,3} = J_{3,4}$ = 8.5 Hz, H-3), 5.19 (d, 7 H, $J_{1,2}$ = 3.3 Hz, H-1), 4.85 (dd, 7 H, H-2), 4.21 (m, 7 H, H-5), 3.95 (t, 7 H, $J_{4,5}$ = 8.5 Hz, H-4), 3.85 (m, 14 H, H-2'), 3.81 (m, 14H, H-14′), 3.80 (m, 14 H, CH_2N_{cyst}),3.65 (t, 14H, $^3J_{H,H}$ = 7.0 Hz, H-1″), 3.56 (m, 14H, H-3′), 3.51, 3.45 (2m, 28H, H-9′, H-10′), 3.50 (m, 14H, H-6″), 3.44 (m, 14H, H-12′), 3.43-3.37 (m, 28H, H-5′, H-7′), 3.30 (m, 7 H, H-6a), 3.20 (m, 7 H, H-6b), 2.96 (m, 14 H, CH_2S_{cyst}), 2.51-2.23 (m, 28 H, CH_2CO), 1.93 (m, 14H, H-13′), 1.84 (m, 14H, H-6′), 1.66 (m, 56H, H-2″, H-5″, C*H*$_2$CH$_2$CO), 1.50 (s, 189 H, $C(CH_3)_3$),1.45 (m, 28H, H-3″, H-4″), 1.43-1.31 (m, 56H, C*H*$_2$C*H*$_2$CH$_3$), 0.95 (m, 42 H, CH_3).

^{13}C NMR (125.7 MHz, MeOD, 333 K, Figure S43): δ = 182.0, 181.5 (CS), 173.3, 172.0 (CO ester), 156.4, 155.9 (CO carbamate), 96.9 (C-1), 80.3, 80.0 (*C*$(CH_3)_3$), 78.8 (C-4), 71.9 (C-5), 70.7 (C-3), 70.3 (C-2), 50.4 (C-2'), 49.5 (C-14′), 49.0, 48.3 (C-9′, C-10′, C-12′),47.2 (C-3′), 46.6 (C-5′, C-7′), 45.9 (C-1″), 44.1, 43.9 (C-6″, CH_2N_{Cyst}), 34.0 (C-6),

33.8, 33.7 (CH_2CO), 32.9 (CH_2S_{cyst}), 31.2, 31.1 ($CH_2CH_2CH_3$), 29.0, 28.9 (C-2″, C-5″), 28.0 (C-6′), 27.7, 27.6 ($C(CH_3)_3$), 27.0 (C-13′), 26.5 (C-3″, C-4″), 24.2 (CH_2CH_2CO), 22.1, 22.0 (CH_2CH_3), 13.1, 12.9 (CH_3).

ESI-MS (Figure S122): *m/z* 1991.1 $[M + 2 Na + 2 K]^{4+}$, 2646.5 $[M + Na + 2 K]^{3+}$, 3957.8 $[M + 2 K]^{2+}$.

Elemental analysis calculated (%) for $C_{371}H_{665}N_{49}O_{84}S_{21}$: C 56.91, H 8.56, N 8.77; found: C 56.88, H 8.94, N 8.54.

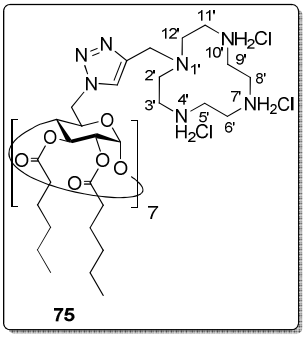

75

Heptakis[6-(4-(1,4,7,10-tetraazacyclododecyl-1-methyl)-1*H*-1,2,3-triazol-1-yl)-6-deoxy-2,3-di-*O*-hexanoyl]cyclomaltoheptaose henicosahydrochloride (75). Treatment of compound **71** (80 mg, 13 µmol) with TFA following the procedure described in the general methods, followed by freeze-drying from a 0.1 N aq. HCl solution, gave pure compound **75** in virtually quantitative yield (63 mg, 99%).

$[\alpha]_D$ = +20.0 (*c* = 1.0 in 1:1 MeOH-H_2O).

^{1}H NMR (500 MHz, 5:1 MeOD-D_2O, 333 K, Figure S44): δ = 8.27 (bs, 7H, $CH_{triazole}$), 5.53 (m, 14H, H-1, H-3), 4.95 (m, 14H, H-6), 4.70 (dd, 7H, $J_{2,3}$ = 10.0 Hz, $J_{1,2}$ = 3.3 Hz, H-2), 4.60 (m, 7H, H-5), 4.06 (m, 14H, $CH_{2triazole}$), 3.69 (t, 7H, $J_{3,4} = J_{4,5}$ = 9.5 Hz, H-4), 3.35 (m, 56H, H-3′, H-5′, H-9′, H-11′), 3.24 (m, 28H, H-6′, H-8′), 3.02 (m, 28H, H-2′, H-12′), 2.54-2.16 (m,28H, CH_2CO), 1.63 (m, 28H, CH_2CH_2CO), 1.36 (m, 56H, $CH_2CH_2CH_3$), 0.93 (m, 42H, CH_3).

^{13}C NMR (125.7 MHz, 5:1 MeOD-D_2O, 333 K, Figure S44): δ = 173.4, 172.1 (CO ester), 141.3 ($C_{triazole}$), 127.7 ($CH_{triazole}$), 96.8 (C-1), 77.3 (C-4), 70.2 (C-2), 70.1 (C-5), 69.8 (C-3),

50.4 (C-6), 48.0 (C-2', C-12'), 46.9 ($CH_{2triazole}$), 44.3 (C-5′, C-9′), 43.0 (C-3′, C-11′), 41.2 (C-6′, C-8′), 33.8 (CH_2CO), 31.2, 31.1 ($CH_2CH_2CH_3$), 24.2 (CH_2CH_2CO), 22.1, 22.0 (CH_2CH_3), 12.9 (CH_3).

ESI-MS (Figure S123): *m/z* 1065.8 $[M + 3 Na + K]^{4+}$, 1420.5 $[M + 3 K]^{3+}$, 2115.5 $[M + 2 K]^{2+}$.

Elemental analysis calculated (%) for $C_{203}H_{378}N_{49}O_{42}Cl_{21}$: C 49.54, H 7.74, N 13.94; found: C 49.54, H 7.39, N 13.62.

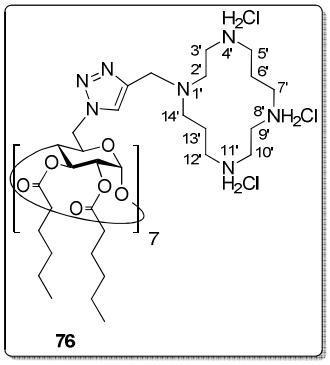

Heptakis[6-(4-(1,4,8,11-tetraazacyclotetradecyl-1-methyl)-1*H*-1,2,3-triazol-1-yl)-6-deoxy-2,3-di-*O*-hexanoyl]cyclomaltoheptaose henicosahydrochloride (76). Treatment of compound **72** (60 mg, 9 µmol) with TFA following the procedure described in the general methods, followed by freeze-drying from a 0.1 N aq. HCl solution, gave pure compound **76** in virtually quantitative yield (47 mg, 99%).

$[\alpha]_D$ = +15.0 (*c* = 1.0 in 1:1 MeOH-H_2O).

^{1}H NMR (500 MHz, 5:1 MeOD-D_2O, 333 K, Figure S45): δ = 8.24 (bs, 7H, $CH_{triazole}$), 5.56 (m, 7H, H-1), 5.55 (t, 7H, $J_{2,3} = J_{3,4}$ = 9.5 Hz, H-3), 4.96 (m, 14H, H-6), 4.68 (dd, 7H, $J_{1,2}$ = 3.0 Hz, H-2), 4.63 (m, 7H, H-5), 4.15 (d, 7H, $^2J_{H,H}$ = 15.0 Hz, $CH_{2\text{-a-triazole}}$), 4.08 (d, 7H, $CH_{2\text{-b-triazole}}$), 3.71 (t, 7H, $J_{4,5}$ = 9.5 Hz, H-4), 3.56-3.35 (m, 28H, H-9', H-10'), 3.40 (m, 14H, H-7′), 3.36 (m, 14H, $^3J_{H,H}$ = 6.0 Hz, H-12′), 3.31 (m, 14H, H-3′), 3.24 (m, 14H, H-5′), 3.06 (m, 14H, H-2′), 2.99 (m, 14H, H-14′), 2.49-2.13 (m, 28H, CH_2CO), 2.22 (m, 14H, H-6′),

2.02 (m, 14H, H-13′), 1.65 (m, 28H, C*H*$_2$CH$_2$CO), 1.35 (m, 56H, C*H*$_2$C*H*$_2$CH$_3$), 0.93 (bt, 42H, $^3J_{H,H}$ = 7.0 Hz, CH$_3$).

^{13}C NMR (125.7 MHz, 5:1 MeOD-D$_2$O, 333 K, Figure S45): δ = 173.6, 172.3 (CO ester), 139.6 (C$_{triazole}$), 128.5 (CH$_{triazole}$), 96.8 (C-1), 77.2 (C-4), 70.4 (C-2), 70.0 (C-5), 69.7 (C-3), 50.4 (C-6), 50.2 (C-14'), 48.7 (C-2′), 45.4 (C-5′), 44.9 (CH$_{2triazole}$), 44.7, 44.4 (C-9′, C-10′), 43.6 (C-3′), 43.0 (C-12'), 41.6 (C-7'), 33.7 (*C*H$_2$CO), 31.2, 31.1 (*C*H$_2$CH$_2$CH$_3$), 24.2, 24.1 (*C*H$_2$CH$_2$CO), 22.1 (C-6'), 22.0 (*C*H$_2$CH$_3$), 21.7(C-13), 13.1 (CH$_3$).

ESI-MS (Figure S124): *m/z* 2212.1 [M + 2 Cl]$^{2-}$, 4387.3 [M + Cl]$^-$.

Elemental analysis calculated (%) for C$_{217}$H$_{385}$N$_{49}$O$_{42}$: C 59.88, H 8.92, N 15.77; found: C 59.98, H 9.01, N 15.56.

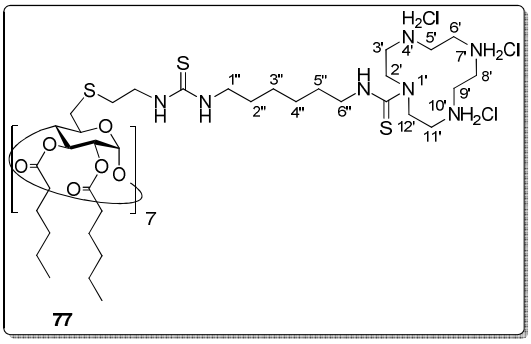

77

Heptakis{6-[2-(*N'*-(*N*'-(1,4,7,10-tetraazacyclododec-1-yl)thioureido-*n*-hex-1-yl)thioureido)ethylthio]-6-deoxy-2,3-di-*O*-hexanoyl}cyclomaltoheptaose henicosahydrochloride (77). Treatment of compound **73** (47 mg, 6 µmol) with TFA following the procedure described in the general methods, followed by freeze-drying from a 0.1 N aq. HCl solution, gave pure compound **77** in virtually quantitative yield (40 mg, 99%).

[α]$_D$ = +26.7 (*c* = 1.0 in MeOH).

^{1}H NMR (500 MHz, 5:1 MeOD-D$_2$O, 333 K, Figure S46): δ = 5.32 (t, 7H, $J_{2,3}$ = $J_{3,4}$ = 9.5 Hz, H-3), 5.18 (d, 7H, $J_{1,2}$ = 3.5 Hz, H-1), 4.85 (dd, 7H, H-2), 4.19 (m, 7H, H-5), 4.07 (m, 28H, H-2', H-12'), 3.93 (t, 7H, $J_{4,5}$ = 8.5 Hz, H-4), 3.78 (m, 14H, CH$_2$N$_{cyst}$), 3.67 (t, 14H, $^3J_{H,H}$ = 7.0 Hz, H-1″), 3.47 (m, 14H, H-6″), 3.44 (m, 28H, H-6′, H-8′), 3.33 (m, 56H, H-3′,

H-5′, H-9′, H-11′), 3.32 (m, 7H, H-6a), 3.18 (m, 7H, H-6b), 2.95 (m, 14H, CH_2S_{cyst}), 2.49-2.24 (m, 28H, CH_2CO), 1.81-1.58 (m, 56H, H-2″, H-5″, CH_2CH_2CO), 1.43 (m, 28H, H-3″, H-4″), 1.41-1.30 (m, 56H, $CH_2CH_2CH_3$), 0.94 (m, 42H, CH_3).

^{13}C NMR (125.7 MHz, 5:1 MeOD-D_2O, 333 K, Figure S46): δ = 183.4, 181.5 (CS), 173.7, 172.3 (CO ester), 96.9 (C-1), 78.9 (C-4), 71.9 (C-5), 70.7 (C-3), 70.3 (C-2), 50.6 (C-2′, C-12′), 46.9 (C-5′, C-9′), 46.4 (C-1″), 44.7 (C-3′, C-11′), 44.6 (C-6″), 44.4 (C-6′, C-8′), 44.0 (CH_2N_{cyst}), 34.0 (C-6), 33.8 (CH_2CO), 32.8 (CH_2S_{cyst}), 31.2, 31.0 ($CH_2CH_2CH_3$), 28.8, 28.5 (C-2″, C-5″), 26.4 (C-3″, C-4″), 24.2 (CH_2CH_2CO), 22.0 (CH_2CH_3), 13.2, 13.0 (CH_3).

ESI-MS (Figure S125): *m/z* 1383.9 $[M + 4\ H]^{4+}$, 1875.9 $[M + Na + 2\ K]^{3+}$, 2797.9 $[M + Na + K]^{2+}$.

Elemental analysis calculated (%) for$C_{252}H_{469}N_{49}O_{42}S_{21}$: C 54.72, H 8.55, N 12.41, S 12.17; found: C 54.64, H 8.84, N 12.66, S 12.06.

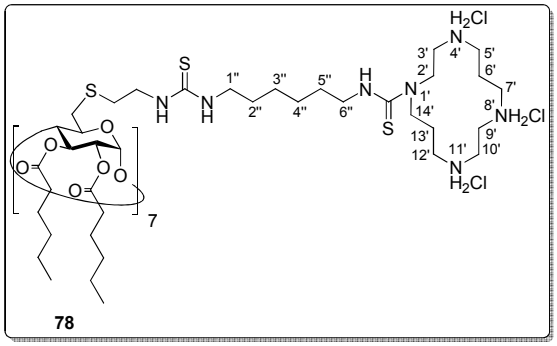

78

Heptakis{6-[2-(*N'*-(*N'*-(1,4,8,11-tetraazacyclotetradec-1-yl)thioureido-*n*-hex-1-yl)thioureido)ethylthio]-6-deoxy-2,3-di-*O*-hexanoyl}cyclomaltoheptaose henicosahydrochloride (78). Treatment of compound **74** (111 mg, 14 µmol) with TFA following the procedure described in the general methods, followed by freeze-drying from a 0.1 N aq. HCl solution, gave pure compound **78** (90 mg, 97%).

$[\alpha]_D$ = +37.6 (*c* = 1.0 in 1:1 MeOH-H_2O).

^{1}H NMR (500 MHz, 5:1 MeOD-D_2O, 333 K, Figure S47): δ = 5.32 (t, 7H, $J_{2,3} = J_{3,4}$ = 8.5 Hz, H-3), 5.18 (m, 7H, H-1), 4.85 (bd, 7H, H-2), 4.29 (m, 14H, H-2'), 4.20 (m, 7H, H-5), 3.93 (m, 7H, H-4), 3.92 (m, 14H, H-14′), 3.78 (m, 14 H, CH_2N_{cyst}), 3.65 (t, 14H, $^3J_{H,H}$ = 7.0

Hz, H-1″), 3.59-3.49 (m, 28H, H-9′, H-10′), 3.53 (m, 14H, H-3′), 3.50, 3.32 (2m, 28H, H-5′, H-7′), 3.47 (m, 14H, H-6″), 3.34 (m, 14H, H-12′), 3.29 (m, 7 H, H-6a), 3.20 (m, 7 H, H-6b), 2.95 (m, 14 H, CH_2S_{cyst}), 2.50-2.23 (m, 28 H, CH_2CO), 2.28 (m, 14H, H-6′), 2.24 (m, 14H, H-13′), 1.73-1.58 (m, 56H, H-2″, H-5″, CH_2CH_2CO), 1.41 (m, 28 H, H-3″, H-4″), 1.40-1.29 (m, 56H, C$H_2CH_2CH_3$), 0.94 (m, 42H, CH_3).

^{13}C NMR (125.7 MHz, 5:1 MeOD-D_2O, 333 K, Figure S47): δ = 182.8, 181.6 (CS), 173.7, 172.3 (CO ester), 96.9 (C-1), 78.8 (C-4), 71.9 (C-5), 70.7 (C-3), 70.3 (C-2), 48.2 (C-2'), 47.8 (C-14′), 46.3 (C-1″), 45.0 (C-5′, C-7′), 44.5 (C-3′), 44.1 (C-6″), 44.0 (C-12′, CH_2N_{Cyst}), 42.4, 42.2 (C-9′, C-10′), 34.0 (C-6), 33.8 (CH_2CO), 32.9 (CH_2S_{cyst}), 31.2, 31.0 ($CH_2CH_2CH_3$), 28.8, 28.6 (C-2″, C-5″), 26.4 (C-3″, C-4″), 24.2 (CH_2CH_2CO), 23.8 (C-13′), 22.0 (CH_2CH_3), 21.6 (C-6′), 13.2, 13.0 (CH_3).

ESI-MS (Figure S126): *m/z* 1443.5 $[M + 2 H + 2 Na]^{4+}$, 1933.5 $[M + 3 Na]^{3+}$.

Elemental analysis calculated (%) for $C_{266}H_{518}N_{49}O_{42}S_{21}Cl_{21}$: C 49.20, H 8.04, N 10.57, S 10.37; found: C 49.21, H 8.29, N 10.50, S,10.17.

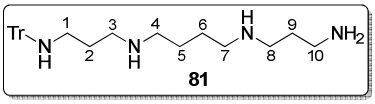

81

***N*-Tritylspermine (81).** To a solution of spermine (2 g, 9.88 mmol) in dry DCM (20 mL) under nitrogen atmosphere triphenylmethyl chloride (276 mg, 0.99 mmol, 0.1 eq) was added in small portions at 0 ºC. The reaction mixture was allowed to warm to rt and stirred overnight. Then, the reaction mixture was washed with H_2O (2 x 15 mL). The organic layer was dried over Na_2SO_4, filtered and the solvent was removed under reduced pressure to yield compound **81** (416 mg, 95 % on the basis of tripehnylpmethyl chloride). The unreacted spermine was reused for another reaction cycle after concentrating the aqueous layer to dryness .

^{1}H NMR (500 MHz, $CDCl_3$, Figure S48): δ = 7.48 (d, 6 H, $^3J_{H,H}$ = 7.5 Hz, H_{ar}-2), 7.26 (t, 6 H, $^3J_{H,H}$ = 7.5 Hz, H_{ar}-3), 7.17 (t, 3 H, $^3J_{H,H}$ = 7.5 Hz, H_{ar}-4), 2.73 (t, 2 H, $^3J_{H,H}$ = 7.3 Hz, H-1), 2.67 (m, 4 H, H-3, H-8), 2.61 (m, 4 H, H-4, H-7), 2.21 (t, 2 H, $^3J_{H,H}$ = 7.2 Hz, H-10), 1.67 (m, 2 H, H-9), 1.61 (m, 2 H, H-2), 1.51 (m, 9 H, H-5, H-6, NH, NH_2).

^{13}C NMR (125.7 MHz, MeOD, Figure S48): δ = 146.2, 128.7, 127.8, 126.2 (Ph), 70.9 (*C*Ph$_3$), 50.0 (C-4, C-7), 48.6, 47.9 (C-3, C-8), 42.2 (C-10), 40.6 (C-1), 33.8 (C-2), 31.0 (C-9), 28.0, 27.9 (C-5, C-6).

ESI-MS (Figure S127): *m/z* 445.5 [M + H]$^+$.

Elemental analysis calculated (%) for $C_{29}H_{40}N_4 \cdot 2H_2O$: C 72.46, H 9.23, N 11.66; found: C 72.69, H 9.07, N 11.73.

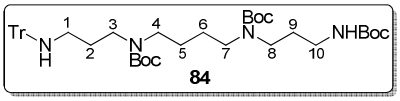

84

***N*^{1}-(3-*tert*-Butoxycarbonylaminopropyl)-*N*^{4}-(3-(tritylamino)propyl)bis(*N*^{1},*N*^{4}-*tert*-butoxycarbonyl)butane-1,4-diamine (84).** To a solution of compound **81** (157 mg, 0.35 mmol) in DCM (5 mL) was added drop wise a solution of di-*tert*-butyl dicarbonate (255 mg, 1.17 mmol, 3.3 eq) in DCM (5 mL). The reaction mixture was stirred at rt overnight. Then, solvents were evaporated under reduced pressure and the resulting residue was purified by flash column chromatography (1:2 EtOAc-petroleum ether) yielding compound **84** as a white solid (301 mg, 86%).

R_f = 0.42 (1:2 EtOAc-petroleum ether).

^{1}H NMR (500 MHz, $CDCl_3$, Figure S49): δ = 7.48 (d, 6 H, $^3J_{H,H}$ = 7.4 Hz, H_{ar}-2), 7.27 (t, 6 H, $^3J_{H,H}$ = 7.4 Hz, H_{ar}-3), 7.18 (t, 3 H, $^3J_{H,H}$ = 7.4 Hz, H_{ar}-4), 5.32, 4.80 (2 bs, 1 H each, N*H*Tr, N*H*Boc), 3.27-3.12 (m, 10 H, H-3, H-4, H-7, H-8, H-10), 2.14 (m, 2 H, H-1), 1.69 (m, 4 H, H-2, H-9), 1.54 (m, 4 H, H-5, H-6), 1.46 (bs, 18 H, C(CH$_3$)$_3$), 1.42 (bs, 9 H, C(CH$_3$)$_3$).

^{13}C NMR (125.7 MHz, $CDCl_3$, Figure S49): δ = 156.1, 155.5 (CO), 146.2, 128.6, 127.8, 126.2 (Ph),79.5, 79.2, 78.8 (*C*(CH$_3$)$_3$), 70.9 (*C*Ph$_3$), 46.8, 46.4 (C-4, C-7), 45.1, 43.9 (C-3, C-8), 41.1 (C-1), 37.4 (C-10), 30.3 (C-2), 29.4 (C-9), 28.5 (C(*C*H$_3$)$_3$), 26.0, 25.6 (C-5, C-6).

ESI-MS (Figure S128): *m/z* 745.6 [M + H]$^+$, 767.5 [M + Na]$^+$, 743.5 [M – H]$^-$, 779.6 [M + Cl]$^-$.

Elemental analysis calculated (%) for $C_{44}H_{64}N_4O_6$: C 70.94, H 8.66, N 7.52; found: C 70.91, H 8.90, N 7.52.

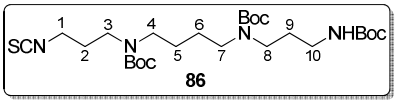

86

4,9,13-Tris(*tert*-butoxycarbonyl)-4,9,13-triazatridecyl-1-isothiocyanate (86). Compound **84** (229 mg, 0.23 mmol) was treated with a solution of 2% TFA in DCM (5 mL) at rt for 1.5 h. Then, the solvent was removed to yield crude 1,4,9-tris(*tert*-butoxycarbonyl)spermine which subsequently was suspended in a 1:1 mixture of H_2O-DCM (5 mL). $CaCO_3$ (232 mg, 2.32 mmol, 10 eq) was added and the mixture was vigorously stirred for a few minutes. The suspension was then cooled to 0 ºC, $CSCl_2$ (27 µL, 0.35 mmol, 1.5 eq) was added and the reaction mixture was further stirred for 1 h. The organic phase was decanted, the solvent was evaporated and the resulting residue was purified by flash column chromatography (1:2 EtOAc-petroleum ether) to yield compound **86** (92 mg, 73%).

R_f = 0.34 (1:2 EtOAc-petroleum ether).

^{1}H NMR (500 MHz, $CDCl_3$, Figure S50): δ = 5.29 (N*H*Boc), 3.56 (t, 2 H, $^3J_{H,H}$ = 6.5 Hz, H-1), 3.30 (t, 2 H, $^3J_{H,H}$ = 6.6 Hz, H-10), 3.20, 3.11 (2 m, 8 H, H-3, H-4, H-7, H-8), 1.92 (m, 2 H, H-9), 1.66 (m, 2 H, H-2), 1.50 (m, 4 H, H-5, H-6), 1.47 (bs, 18 H, $C(CH_3)_3$), 1.44 (s, 9 H, $C(CH_3)_3$).

^{13}C NMR (125.7 MHz, $CDCl_3$, Figure S50): δ = 155.8, 155.2 (CO), 130.4 (NCS), 79.6, 79.3, 78.6($C(CH_3)_3$), 47.3 (C-1), 46.6, 46.0 (C-4, C-7), 43.9, 42.6 (C-3, C-8), 37.4 (C-10), 28.8 (C-2), 28.2 ($C(CH_3)_3$), 25.7 (C-9), 25.3 (C-5, C-6).

ESI-MS (Figure S129): *m/z* 567.5 $[M + Na]^+$, 583.4 $[M + K]^+$, 543.4 $[M - H]^-$, 579.5 $[M + Cl]^-$.

Elemental analysis calculated (%) for $C_{26}H_{48}N_4O_6S$: C 57.33, H 8.88, N 10.28, S 5.89; found: C 57.53, H 8.99, N 9.95, S 6.01.

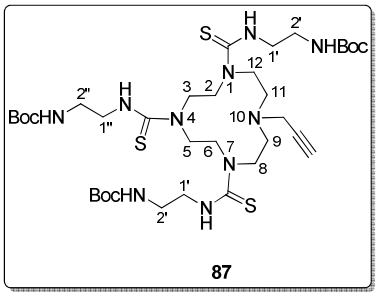

87

1,4,7-Tris(*N'*-(2-*tert*-butoxycarbonylaminoethyl)thioureido)-10-propargyl-1,4,7,10-tetraazacyclododecane (87). To a solution of compound **60**[274] (135 mg, 0.42 mmol) and Et_3N (212 µL, 1.53 mmol, 1.2 eq) in DCM (8 mL) a solution of 2-(*tert*-butoxycarbonylamino)ethylisothiocyanate **22**[186] (284 mg, 1.40 mmol, 1.1 eq) in DCM (2 mL) was added drop wise. The reaction mixture was stirred overnight at rt maintaining pH 9. After evaporation of the solvent under reduced pressure, the resulting residue was purified by flash column chromatography (1:1 EtOAc-petroleum ether) yielding compound **87** as a white solid (333 mg, 96%).

R_f = 0.66 (1:1 EtOAc-petroleum ether).

^{1}H NMR (400 MHz, MeOD, 333 K, Figure S51): δ = 4.04 (m, 4 H, H-3, H-5), 3.89 (m, 8 H, H-2, H-6, H-8, H-12), 3.77 (t, 2 H, $^3J_{H,H}$ = 6.0 Hz, H-1''), 3.71 (bs, 2 H, CH_2C≡CH), 3.68 (t, 4 H, $^3J_{H,H}$ = 6.0 Hz, H-1'), 3.36 (t, 2 H, $^3J_{H,H}$ = 6.1 Hz, H-2''), 3.28 (t, 4 H, $^3J_{H,H}$ = 6.1 Hz, H-2'), 2.98 (m, 4 H, H-9, H-11), 2.62 (m, 1 H, C≡CH), 1.46 (s, 27 H, C(CH_3)$_3$).

^{13}C NMR(100.6 MHz, MeOD, 333 K, Figure S51): δ = 183.0, 182.4 (CS), 157.4 (CO), 79.1 (*C*(CH_3)$_3$), 77.3 (*C*≡CH), 74.0 (C≡*C*H), 53.5 (C-9, C-11), 50.5 (C-2, C-3, C-5, C-6, C-8, C-12), 46.0 (C-1', C-1''), 40.4 (*C*H_2C≡CH), 39.8 (C-2', C-2''), 27.5 (C(*C*H_3)$_3$).

ESI-MS (Figure S130): *m/z* 839.4 $[M + Na]^+$, 855.4 $[M + K]^+$, 815.3 $[M - H]^-$, 851.2 $[M + Cl]^-$.

Elemental analysis calculated (%) for $C_{35}H_{64}N_{10}O_6S_3$: C 51.44, H 7.89, N 17.14, S 11.77; found: C 51.64, H 7.82, N 16.84, S 11.39.

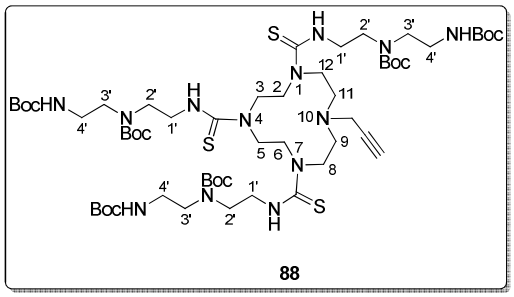

88

1,4,7-Tris[*N'*-(2-(*N*-(*tert*-butoxycarbonyl)-*N*-(2-(*tert*-butoxycarbonylamino)ethyl)-amino)ethyl)]thioureido-10-propargyl-1,4,7,10-tetraazacyclododecane (88). To a solution of compound **60**[274] (226 mg, 0.71 mmol) and Et_3N (355 µL, 2.56 mmol, 1.2 eq) in DCM (9 mL) a solution of 2-[*N*-(*tert*-butoxycarbonyl)-*N*-[2-(*tert*-butoxycarbonylamino)ethyl]amino]ethyl isothiocyanate **85**[177] (810 mg, 2.34 mmol, 1.1 eq) in DCM (5 mL) was added drop wise. The reaction mixture was stirred overnight at rt maintaining pH 9. After evaporation of the solvent under reduced pressure, the resulting residue was purified by flash column chromatography (2:1 EtOAc-petroleum ether) yielding compound **88** as a white solid (782 mg, 88%).

R_f = 0.56 (2:1 EtOAc-petroleum ether).

^{1}H NMR (500 MHz, MeOD, 333 K, Figure S52): δ = 4.03 (m, 4 H, H-3, H-5), 3.85 (m, 8 H, H-2, H-6, H-8, H-12), 3.73 (t, 6 H, $^3J_{H,H}$ = 6.1 Hz, H-1'), 3.68 (bs, 2 H, CH_2C≡CH), 3.53 (t, 2 H, $^3J_{H,H}$ = 6.1 Hz, H-2'), 3.47 (t, 4 H, $^3J_{H,H}$ = 6.1 Hz, H-2'), 3.41-3.35 (m, 6 H, H-3'), 3.25, 3.24 (2 t, 6 H, $^3J_{H,H}$ = 6.2 Hz, H-4'), 2.97 (m, 4 H, H-9, H-11), 2.62 (t, 1 H, $^4J_{H,H}$ = 2.2 Hz, C≡CH), 1.50, 1.46 (2 s, 27 H each, C(CH_3)$_3$).

^{13}C NMR (100.6 MHz, MeOD, 333 K, Figure S52): δ = 182.9, 182.4 (CS), 156.8, 156.5 (CO), 80.1, 78.8 (*C*(CH_3)$_3$), 77.4 (*C*≡CH), 74.0 (C≡*C*H), 53.7 (C-9, C-11), 50.5 (C-2, C-3, C-5, C-6, C-8, C-12), 46.6 (C-2', C-3'), 44.2 (C-1'), 40.7 (*C*H_2C≡CH), 39.0 (C-4'), 27.6, 27.5 (C(*C*H_3)$_3$).

ESI-MS (Figure S131): *m/z* 1268.7 $[M + Na]^+$, 1284.6 $[M + K]^+$.

Elemental analysis calculated (%) for $C_{56}H_{103}N_{13}O_{12}S_3$: C 53.95, H 8.33, N 14.61, S 7.72; found: C 53.60, H 7.99, N 14.67, S 7.84.

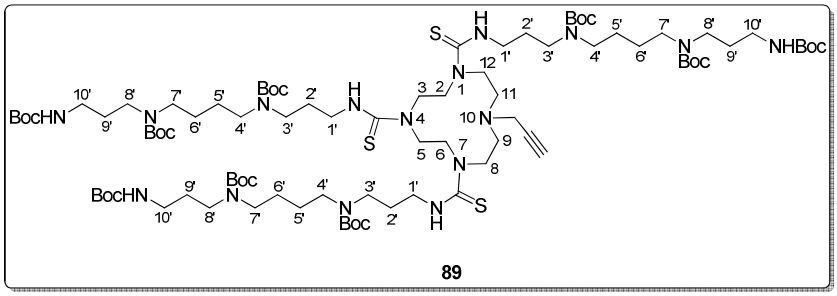

89

1,4,7-Tris[*N'*-(3-((4-((3-(*tert*-butoxycarbonyl)amino)propyl)(*tert*-butoxycarbonyl)-amino)butyl)(*tert*-butoxycarbonyl)amino)propyl)]thioureido-10-propargyl-1,4,7,10-tetraazacyclododecane (89). To a solution of compound **60**[274] (27 mg, 83 µmol) and Et_3N (42 µL, 0.30 mmol, 1.2 eq) in DCM (5 mL) a solution of compound **86** (150 mg, 0.28 mmol, 1.1 eq) in DCM (2 mL) was added drop wise. The reaction mixture was stirred overnight at rt maintaining pH 9. After evaporation of the solvent under reduced pressure, the resulting residue was purified by flash column chromatography (1:1 EtOAc-petroleum ether) yielding compound **89** as a white solid (105 mg, 68%).

R_f = 0.38 (2:1 EtOAc-petroleum ether).

^{1}H NMR (400 MHz, MeOD, 333 K, Figure S53): δ = 4.05 (m, 4 H, H-3, H-5), 3.89 (m, 8 H, H-2, H-6, H-8, H-12), 3.71 (bs, 2 H, CH_2C≡CH), 3.68 (t, 2 H, $^3J_{H,H}$ = 6.7 Hz, H-1'), 3.60 (t, 4 H, $^3J_{H,H}$ = 6.7 Hz, H-1'), 3.35 (t, 2 H, $^3J_{H,H}$ = 6.7 Hz, H-3'), 3.26 (m, 22 H, H-3', H-4', H-7', H-8'), 3.07 (m, 6 H, H-10'), 2.99 (m, 4 H, H-9, H-11), 2.63 (t, 1 H, $^4J_{H,H}$ = 2.3 Hz, C≡CH), 1.92 (m, 2 H, H-2'), 1.85 (m, 4 H, H-2'), 1.73 (m, 6 H, H-9'), 1.56 (m, 12 H, H-5', H-6'), 1.50 (s, 9 H, $C(CH_3)_3$), 1.49 (s, 18 H, $C(CH_3)_3$), 1.48 (s, 27 H, $C(CH_3)_3$), 1.46 (s, 27 H, $C(CH_3)_3$).

^{13}C NMR (100.6 MHz, MeOD, 333 K, Figure S53): δ = 182.6, 182.0 (CS), 156.9, 156.2, 156.1 (CO), 79.7, 79.6, 78.7 ($C(CH_3)_3$), 77.4 (*C*≡CH), 74.0 (C≡*C*H), 53.6 (C-9, C-11), 50.8 (C-2, C-3, C-5, C-6, C-8, C-12), 44.6 (C-3', C-4', C-7', C-8'), 43.2 (C-1'), 40.6 (*C*H_2C≡CH), 37.8 (C-10'), 29.2 (C-9'), 27.5 (C-2'), 27.5 ($C(CH_3)_3$), 25.6 (C-5', C-6').

ESI-MS (Figure S132): *m/z* 942.4 $[M + 2 Na]^{2+}$, 1867.0 $[M + Na]^+$, 1843.1 $[M - H]^-$, 1878.0 $[M + Cl]^-$.

Elemental analysis calculated (%) for $C_{89}H_{166}N_{16}O_{18}S_3$: C 57.95, H 9.07, N 12.15; found: C 58.17, H 9.23, N 12.48.

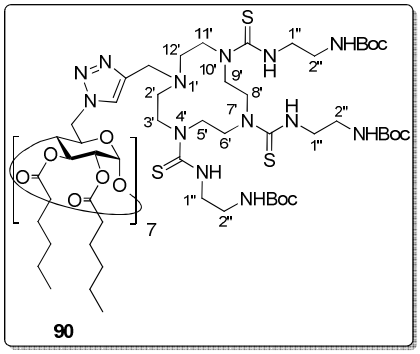

90

Heptakis[6-(4-(4,7,10-tris(*N'*-(2-*tert*-butoxycarbonylaminoethyl)thioureido)-1,4,7,10-tetraazacyclododecyl-1-methyl)-1*H*-1,2,3-triazol-1-yl)-6-deoxy-2,3-di-*O*-hexanoyl]-cyclomaltoheptaose (90). To a solution of heptakis(6-azido-6-deoxy-2,3-di-*O*-hexanoyl)cyclomaltoheptaose **54**[180b] (8.5 mg, 3.2 μmol) and compound **87** (20 mg, 25 μmol, 1.1 eq) in acetonitrile (0.5 mL) bis(triphenylphosphine)copper(I)iodide **93**[289] (1.8 mg, 2.5 μmol, 0.1 eq relative to the alkyne) was added and the reaction mixture was heated under microwave irradiation to 85 ºC for 1 h (60 W). Then, the solvent was evaporated and the resulting residue was purified by size exclusion chromatography in MeOH to yield compound **90** (20 mg, 75%). As determined by integration of characteristic ^{1}H NMR signals, the average degree of substitution of heterogeneous compound **90** was estimated 85%.

R_f = 0.61 (9:1 DCM-MeOH). $[\alpha]_D$ = +19.5 (*c* = 1.0 in MeOH).

^{1}H NMR (500 MHz, MeOD, 323 K, Figure S54): δ = 7.82 (bs, 6 H, $CH_{triazole}$), 5.72-4.65 (m, 35 H, H-1, H-2, H-3, H-6), 4.33-3.52 (m, 126 H, H-4, H-5, $CH_{2triazole}$, H-1'',H-3', H-5', H-6', H-8', H-9', H-11'), 3.52-3.10 (m, 35 H, H-2''), 3.05-2.63 (m, 24 H, H-2', H-12'), 2.60-2.09 (m, 28 H, CH_2CO), 1.64 (m, 28 H, CH_2CH_2CO), 1.46 (bs, 149 H, $C(CH_3)_3$), 1.37 (m, 56 H, CH_3CH_2, $CH_3CH_2CH_2$), 0.95 (m, 42 H, CH_3).

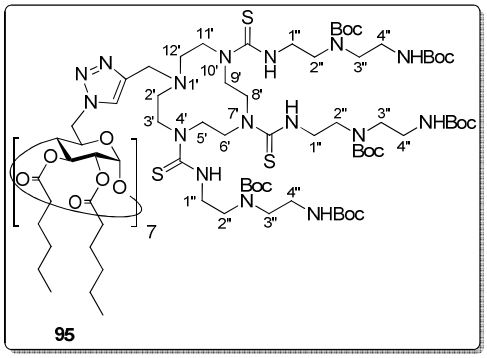

95

Heptakis[6-(4-(4,7,10-tris(*N*'-(2-*N*-((*N*-*tert*-butoxycarbonylaminoethyl)*tert*-butoxy-carbonyl)amino)ethyl)thioureido)-1,4,7,10-tetraazacyclododecyl-1-methyl)-1*H*-1,2,3-triazol-1-yl)-6-deoxy-2,3-di-*O*-hexanoyl]cyclomaltoheptaose (95). To a solution of heptakis(6-azido-6-deoxy-2,3-di-*O*-hexanoyl)cyclomaltoheptaose **54**[180b] (5.6 mg, 2.1 µmol) and compound **88** (20 mg, 16 µmol, 1.1 eq) in acetonitrile (0.5 mL) bis(triphenylphosphine)copper(I)iodide **93**[289] (1.2 mg, 1.6 µmol, 0.1 eq relative to the alkyne) was added and the reaction mixture was heated under microwave irradiation to 85 ºC for 1 h (60 W). Then, the solvent was evaporated and the resulting residue was purified by size exclusion chromatography in MeOH to yield compound **95** (12 mg, 50%). As determined by integration of characteristic ^{1}H NMR signals, the average degree of substitution of heterogeneous compound **95** was estimated 80%.

R_f = 0.26 (9:1 DCM-MeOH). $[\alpha]_D$ = +15.6 (*c* = 0.6 in MeOH).

^{1}H NMR (500 MHz, MeOD, 323 K, Figure S55): δ = 8.10 (bs, 5 H, $CH_{triazole}$), 6.40-4.64(m, 35 H, H-1, H-2, H-3, H-6), 4.39-3.63 (m, 92 H, H-4, H-5, $CH_{2triazole}$, H-3', H-5', H-6', H-8', H-9', H-11'), 3.59-3.35 (m, 101 H, H-1'', H-2'', H-3''), 3.25 (m, 34 H, H-4''), 3.06-2.66 (m, 22 H, H-2', H-12'), 2.56-2.17 (m, 28 H, CH_2CO), 1.63 (m, 28 H, CH_2CH_2CO), 1.50, 1.46 (2 bs, each 151 H, $C(CH_3)_3$), 1.37 (m, 56 H, CH_3CH_2, $CH_3CH_2CH_2$), 0.95 (m, 42 H, CH_3).

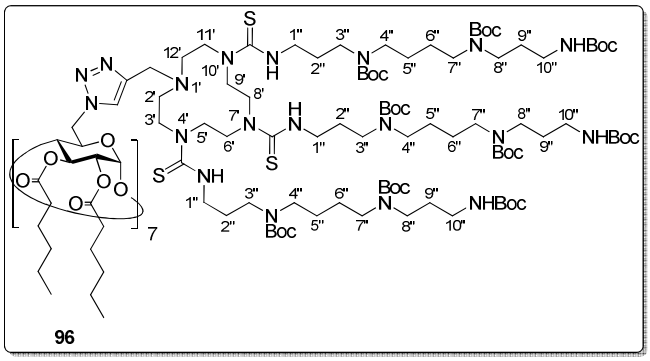

96

Heptakis[6-(4-(4,7,10-tris(*N'*-(-(3-((4-((3-(*tert*-butoxycarbonyl)amino)propyl)(*tert*-butoxycarbonyl)amino)butyl)(*tert*-butoxycarbonyl)amino)propyl))thioureido)-1,4,7,10-tetraazacyclododecyl-1-methyl)-1*H*-1,2,3-triazol-1-yl)-6-deoxy-2,3-di-*O*-hexanoyl]cyclomaltoheptaose (96). To a solution of heptakis(6-azido-6-deoxy-2,3-di-*O*-hexanoyl)cyclomaltoheptaose **54**[180b] (4.7 mg, 1.8 µmol) and compound **89** (25 mg, 13.6 µmol, 1.1 eq) in acetonitrile (0.5 mL) bis(triphenylphosphine)copper(I)iodide **93**[289] (1.0 mg, 1.4 µmol, 0.1 eq relative to the alkyne) was added and the reaction mixture was heated under microwave irradiation to 85 ºC for 1 h (60 W). Then, the solvent was evaporated and the resulting residue was purified by size exclusion chromatography in MeOH to yield compound **96** (8.4 mg, 31%). As determined by integration of characteristic ^{1}H NMR signals, the average degree of substitution of heterogeneous compound **96** was estimated 73%.

R_f = 0.25 (9:1 DCM-MeOH). $[\alpha]_D$ = +6.37 (*c* = 0.4 in MeOH).

^{1}H NMR (500 MHz, MeOD, 323 K, Figure S56): δ = 7.85 (bs, 5 H, $CH_{triazole}$), 5.70-4.81 (m, 35 H, H-1, H-2, H-3, H-6), 3.78-3.50 (m, 32 H, H-4, H-5, $CH_{2triazole}$, H-1'', H-3', H-5', H-6', H-8', H-9', H-11'), 3.32-3.20 (m, 122 H, H-3'', H-4'', H-7'', H-8''), 3.07 (t, 31 H, $^{3}J_{H,H}$ = 6.4 Hz, H-10''), 3.00-2.81 (m, 20 H, H-2', H-12'), 2.57-2.17 (m, 28 H, CH_2CO), 1.98-1.79 (m, 31 H, H-2''), 1.72 (m, 31 H, H-9''), 1.61 (m, 28 H, CH_2CH_2CO), 1.56 (m, 61 H, H-5'', H-6''), 1.49, 1.46 (2 bs, 414 H, $C(CH_3)_3$), 1.37 (m, 56 H, CH_3CH_2, $CH_3CH_2CH_2$), 0.95 (m, 42 H, CH_3).

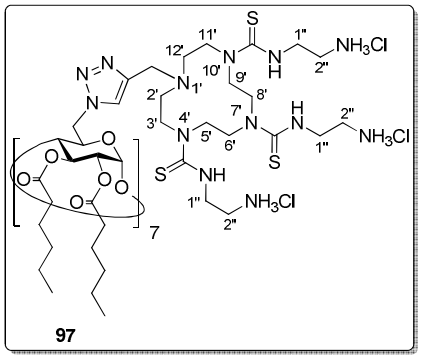

97

Heptakis[6-(4-(4,7,10-tris(*N'*-(2-aminoethyl)thioureido)-1,4,7,10-tetraazacyclo-dodecyl-1-methyl)-1*H*-1,2,3-triazol-1-yl)-6-deoxy-2,3-di-*O*-hexanoyl]cyclomalto-heptaose henicosahydrochloride (97). Treatment of compound **90** (20 mg, 2.4 µmol) with TFA following the procedure described in the general methods, followed by freeze-drying from a 0.1 N aq. HCl solution, gave compound **97** in quantitative yield (15 mg).

$[\alpha]_D$ = +18.3 (*c* = 0.4 in MeOH).

^{1}H NMR (500 MHz, MeOD, 323 K, Figure S57): δ = 7.86 (bs, 6 H, $CH_{triazole}$), 5.72-4.61 (m, 35 H, H-1, H-2, H-3, H-6), 4.42-3.59 (m, 126 H, H-4, H-5, $CH_{2triazole}$, H-1'', H-3', H-5', H-6', H-8', H-9', H-11'), 3.49-3.18 (m, 35 H, H-2''), 3.07-2.63 (m, 24 H, H-2', H-12'), 2.62-2.15 (m, 28 H, CH_2CO), 1.65 (m, 28 H, CH_2CH_2CO), 1.38 (m, 56 H, CH_3CH_2, $CH_3CH_2CH_2$),0.95 (m, 42 H, CH_3).

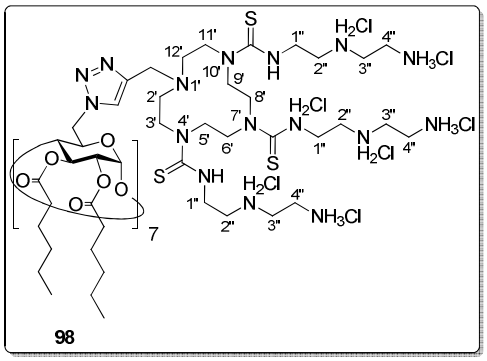

Heptakis[6-(4-(4,7,10-tris*(N'*-(2-(*N*-2-aminoethyl)aminoethyl)thioureido)-1,4,7,10-tetraazacyclododecyl-1-methyl)-1*H*-1,2,3-triazol-1-yl)-6-deoxy-2,3-di-*O*-hexanoyl]cyclomaltoheptaose dotetracontahydrochloride (98). Treatment of compound **95** (11 mg, 1.0 µmol) with TFA following the procedure described in the general methods, followed by freeze-drying from a 0.1 N aq. HCl solution, gave compound **98** in quantitative yield (8.4 mg).

$[\alpha]_D$ = +15.0 (*c* = 0.6 in MeOH).

^{1}H NMR (500 MHz, MeOD, 323 K, Figure S58): δ = 7.85 (bs, 5 H, $CH_{triazole}$), 5.66-4.68 (m, 35 H, H-1, H-2, H-3, H-6), 4.40-3.85 (m, 92 H, H-4, H-5, $CH_{2triazole}$, H-3', H-5', H-6', H-8', H-9', H-11'), 3.78-3.40 (m, 134 H, H-1'', H-2'', H-3'', H-4''), 2.66-2.07 (m, 50 H, CH_2CO, H-2', H-12'), 1.65 (m, 28 H, CH_2CH_2CO), 1.38 (m, 56 H, CH_3CH_2, $CH_3CH_2CH_2$), 0.96 (m, 42 H, CH_3).

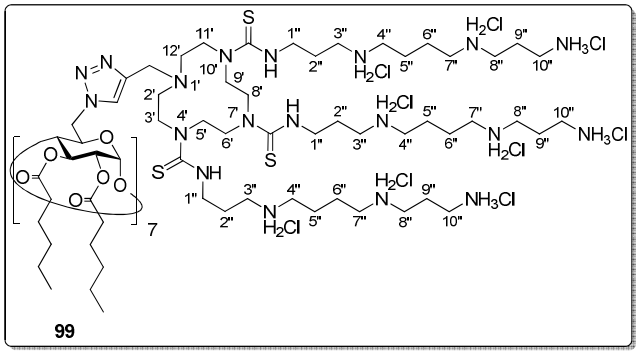

Heptakis[6-(4-(4,7,10-tris(*N'*-(3-((4-(3-aminopropyl)aminobutyl)aminopropyl))thio-ureido)-1,4,7,10-tetraazacyclododecyl-1-methyl)-1*H*-1,2,3-triazol-1-yl)-6-deoxy-2,3-di-*O*-hexanoyl]cyclomaltoheptaose trishexacontahydrochloride (99). Treatment of compound **96** (8 mg, 0.5 µmol) with TFA following the procedure described in the general methods, followed by freeze-drying from a 0.1 N aq. HCl solution, gave compound **99** in quantitative yield (6 mg).

$[\alpha]_D$ = +7.86 (*c* = 0.4 in MeOH).

^{1}H NMR (500 MHz, MeOD, 323 K, Figure S59): δ = 7.86 (bs, 5 H, $CH_{triazole}$), 5.66-4.64 (m, 35 H, H-1, H-2, H-3, H-6), 4.44-3.44 (m, 32 H, H-4, H-5, $CH_{2triazole}$, H-1'', H-3', H-5', H-6', H-8', H-9', H-11'), 3.28-3.10 (m, 173 H, H-3'', H-4'', H-7'', H-8'', H-10'', H-2', H-12'), 2.52-1.87 (m, 151 H, CH_2CO, H-2'', H-5'', H-6'', H-9''), 1.65 (m, 28 H, CH_2CH_2CO), 1.38 (m, 56 H, CH_3CH_2, $CH_3CH_2CH_2$), 0.95 (m, 42 H, CH_3).

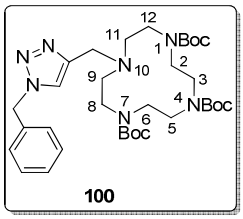

1,4,7-Tris(*tert*-butoxycarbonyl)-10-((1-benzyl-1*H*-1,2,3-triazol-4-yl)methyl)-1,4,7,10-tetraazacyclododecane (100). To a solution of compound **63** (50 mg, 97.9 µmol) and

benzyl azide (19.2 mg, 0.15 mmol, 1.5 eq) in THF (2 mL) 2,6-lutidine (3.5 µL, 29.4 µmol, 0.3 eq) and CuI·P(OEt)$_3$ (0.5 mg, 1.5 µmol, 1.5 mol-%) were added and the reaction mixture was heated under microwave irradiation to 110 ºC for 20 min (60 W). Then, the solvent was evaporated and the resulting residue was purified by flash column chromatography (95:5 DCM-MeOH) to obtain compound **100** (56 mg, 89%).

R_f = 0.50 (9:1 DCM-MeOH).

^{1}H NMR (400 MHz, $CDCl_3$, 323 K, Figure S60): δ = 7.37 (m, 4 H, $CH_{triazole}$, Ar), 7.25 (m, 2 H, Ar), 5.51 (s, 2 H, C*H*$_2$Ph), 3.88 (s, 2 H, $CH_{2triazole}$), 3.53, 3.33 (2 m, 12 H, H-2, H-3, H-5, H-6, H-8, H-12), 2.67 (m, 4 H, H-9, H-11), 1.49, 1.43 (2 s, 27 H, $C(CH_3)_3$).

^{13}C NMR (100.6 MHz, $CDCl_3$, 323 K, Figure S60): δ = 155.8, 155.4 (CO carbamate), 143.4 ($C_{triazole}$), 134.8 ($Ar_{quaternary}$), 129.1, 128.7, 127.9 (Ar), 122.7 ($CH_{triazole}$), 79.5, 79.2 (*C*$(CH_3)_3$), 54.9 (C-9, C-11), 54.1 (*C*H_2Ph), 49.8, 47.8 (C-2, C-3, C-5, C-6, C-8, C-12), 46.1 ($CH_{2triazole}$), 29.6, 28.7, 28.5 ($C(CH_3)_3$).

ESI-MS (Figure S133): *m/z* 666.3 $[M + Na]^+$, 682.3 $[M + K]^+$.

Elemental analysis calculated (%) for $C_{33}H_{53}N_7O_6$: C 61.56, H 8.30, N 15.23; found: C 61.76, H 8.34, N 15.55.

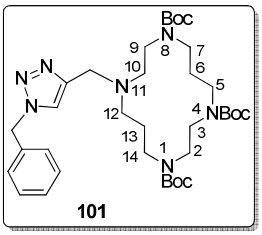

101

1,4,8-Tris(*tert*-butoxycarbonyl)-11-((1-benzyl-1*H*-1,2,3-triazol-4-yl)methyl)-1,4,8,11-tetraazacyclotetradecane (101). To a solution of compound **64** (30.5 mg, 56.6 µmol) and benzyl azide (11.3 mg, 84.9 µmol, 1.5 eq) in THF (2 mL) 2,6-lutidine (2.1 µL, 17.0 µmol, 0.3 eq) and CuI·P(OEt)$_3$ (0.3 mg, 0.8 µmol, 1.5 mol-%) were added and the reaction mixture was heated under microwave irradiation to 110 ºC for 20 min (60 W). Then, the solvent was evaporated and the resulting residue was purified by flash column chromatography (95:5 DCM-MeOH) to obtain compound **101** (23.6 mg, 62%).

R_f = 0.45 (9:1 DCM-MeOH).

^{1}H NMR (500 MHz, $CDCl_3$, 323 K, Figure S61): δ = 7.37 (m, 4 H, $CH_{triazole}$, Ar), 7.29 (m, 2 H, Ar), 5.52 (s, 2 H, C*H*$_2$Ph), 3.77 (s, 2 H, $CH_{2triazole}$), 3.38-3.26 (m, 12 H, H-3, H-5, H-7, H-9, H-10, H-12), 2.64 (t, 2 H, $^3J_{H,H}$ = 5.4 Hz, H-2), 2.45 (t, 2 H, $^3J_{H,H}$ = 5.4 Hz, H-14), 1.89 (m, 2 H, $^3J_{H,H}$ = 6.4 Hz, H-6), 1.71 (m, 2 H, $^3J_{H,H}$ = 6.4 Hz, H-13), 1.47, 1.44 (2 s, 27 H, $C(CH_3)_3$).

^{13}C NMR (125.7 MHz, $CDCl_3$, 323 K, Figure S61): δ = 155.7, 155.5 (CO carbamate), 144.6 ($C_{triazole}$), 134.9 ($Ar_{quaternary}$), 129.1, 128.6, 127.9 (Ar), 122.3 ($CH_{triazole}$), 79.5, 79.4 (*C*$(CH_3)_3$), 54.1 (*C*H_2Ph), 53.2 (C-2), 51.6 (C-14), 49.2 ($CH_{2triazole}$), 47.6, 47.2, 46.9, 45.6 (C-3, C-5, C-7, C-9, C-10, C-12), 28.8 (C-6), 28.5, 28.4 (C(*C*$H_3)_3$), 26.8 (C-13).

ESI-MS (Figure S134): *m/z* 694.3 $[M + Na]^+$, 710.3 $[M + K]^+$.

Elemental analysis calculated (%) for $C_{35}H_{57}N_7O_6$: C 62.57, H 8.55, N 14.59; found: C 62.17, H 8.51, N 14.98.

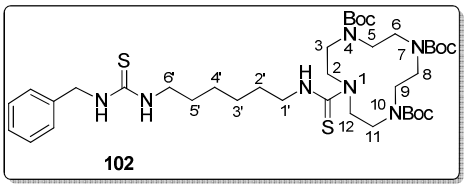

102

***N*-[4,7,10-Tris(*tert*-butoxycarbonyl)-1,4,7,10-tetraazacyclododec-1-yl]-*N'*-[6-(*N'*-benzyl)thioureido-*n*-hex-1-yl]thiourea (102).** To a solution of benzyl amine (9 µL, 81.7 µmol, 1.1 eq) and Et_3N (10 µL, 81.7 µmol, 1.1 eq) in DCM (3.5 mL) **69** (50 mg, 74.3 µmol) was added and the reaction mixture was stirred in a sealed reaction vial at 45 ºC for 24 h assuring that pH value was maintained at 9. Then, solvents were evaporated under reduced pressure and the resulting residue was purified by flash column chromatography (3:2 EtOAc-petroleum ether → 45:5:3 EtOAc-EtOH-H_2O) to afford **102** (64 g, 88%).

R_f = 0.65 (2:1 EtOAc-petroleum ether).

^{1}H NMR (500 MHz, $CDCl_3$, 323 K, Figure S62): δ = 7.32 (m, 5 H, Ar), 6.33 (bs, 1 H, N*H*Bn), 6.09, 5.83 (2 bs, 2 H, NH), 4.69 (d, 2 H, $^3J_{H,H}$ = 5.4 Hz, C*H*$_2$Ph), 3.82 (m, 4 H, H-2, H-12), 3.62 (q, 2 H, $^3J_{H,H}$ = 5.8 Hz, H-1'), 3.50 (m, 4 H, H-3, H-11), 3.46 (m, 2 H, H-6'),

3.40 (m, 8 H, H-5, H-6, H-8, H-9), 1.59 (m, 4 H, H-2', H-5'), 1.47, 1.46 (2 s, 27 H, $C(CH_3)_3$), 1.35 (m, 4 H, H-3', H-4').

^{13}C NMR (125.7 MHz, $CDCl_3$, 323 K, Figure S62): δ = 183.0, 182.7 (CS), 156.7, 156.6 (CO carbamate), 137.5 ($Ar_{quaternary}$), 128.7, 127.7, 127.6 (Ar), 80.5, 80.4, 80.3 ($C(CH_3)_3$), 53.5 (C-2, C-12), 50.3 (C-5, C-6, C-8, C-9), 49.9 (C-3, C-11), 48.5 (CH_2Ph), 45.6 (C-1'), 44.3 (C-6'), 29.0, 28.8 (C-2', C-5'), 28.5, 28.4 ($C(CH_3)_3$), 26.3, 26.2 (C-3', C-4').

ESI-MS (Figure S135): *m/z* 802.4 $[M + Na]^+$.

Elemental analysis calculated (%) for $C_{38}H_{65}N_7O_6S_2$: C 58.51, H 8.40, N 12.57, S 8.22; found: C, H, N, S.

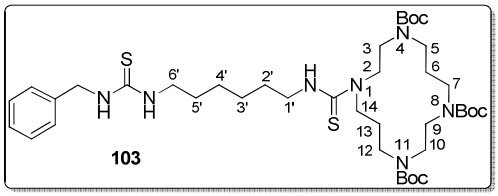

***N*-[4,8,11-Tris(*tert*-butoxycarbonyl)-1,4,8,11-tetraazacyclotetradec-1-yl]-*N'*-[6-(*N'*-benzyl)thioureido-*n*-hex-1-yl]thiourea (103).** To a solution of benzyl amine (8.6 µL, 78.5 µmol, 1.1 eq) and Et_3N (10 µL, 78.5 µmol, 1.1 eq) in DCM (3.5 mL) **70** (50 mg, 71.3 µmol) was added and the reaction mixture was stirred in a sealed reaction vial at 45 ºC for 48 h assuring that pH value was maintained at 9. Then, solvents were evaporated under reduced pressure and the resulting residue was purified by flash column chromatography (3:2 EtOAc-petroleum ether → EtOAc) to afford **103** (48 mg, 83%).

Rf = 0.16 (1:1 EtOAc-petroleum ether).

^1H NMR (500 MHz, $CDCl_3$, 323 K, Figure S63): δ = 7.32 (m, 5 H, Ar), 6.49 (bs, 1 H, N*H*Bn), 6.34, 6.11 (2 bs, 2 H, NH), 4.69 (d, 2 H, $^3J_{H,H}$ = 5.3 Hz, CH_2Ph), 3.92 (m, 2 H, H-14), 3.63 (m, 4 H, H-2, H-1'), 3.46 (m, 2 H, H-10), 3.40 (m, 4 H, H-9, H-6'), 3.34 (m, 8 H, H-3, H-5, H-7, H-12), 1.88 (m, 2 H, H-13), 1.77 (m, 2 H, H-6), 1.64 (m, 2 H, H-2'), 1.57 (m, 2 H, H-5'), 1.47 (s, 27 H, $C(CH_3)_3$), 1.37 (m, 4 H, H-3', H-4').

^{13}C NMR (125.7 MHz, $CDCl_3$, 323 K, Figure S63): δ = 182.7, 182.1 (CS), 156.0, 155.7, 155.6 (CO carbamate), 137.6 ($Ar_{quaternary}$), 128.7, 127.6 (Ar), 80.8, 80.1, 80.0 ($C(CH_3)_3$),

50.4 (C-14), 48.5 (*C*H_2Ph), 47.0 (C-2), 46.6, 46.2, 46.1 (C-3, C-5, C-7, C-9, C-10, C-12), 44.3 (C-1', C-6'), 28.8 (C-2', C-5'), 28.5 (C-6), 28.4, 28.3 (C(*C*H_3)$_3$), 27.9 (C-13), 26.3 (C-3', C-4').

ESI-MS (Figure S136): *m/z* 830.5 $[M + Na]^+$.

Elemental analysis calculated (%) for $C_{40}H_{69}N_7O_6S_2$: C 59.45, H 8.61, N 12.13; found: C 59.26, H 9.10, N 11.61.

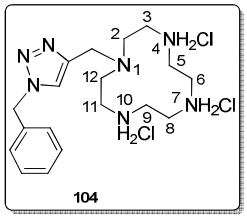

104

1-[(1-Benzyl-1*H*-1,2,3-triazol-4-yl)methyl]-1,4,7,10-tetraazacyclododecane trihydrochloride (104). Treatment of compound **100** (66 mg, 0.10 mmol) with TFA following the procedure described in the general methods, followed by freeze-drying from a 0.1 N aq. HCl solution, gave compound **104** in virtually quantitative yield (46 mg).

^{1}H NMR (400 MHz, 5:1 MeOD-D_2O, 333 K, Figure S64): δ = 8.01 (s, 1 H, $CH_{triazole}$), 7.39 (m, 5 H, Ar), 5.63 (s, 2 H, C*H*$_2$Ph), 3.97 (s, 2 H, $CH_{2triazole}$), 3.24, 3.06 (2 m, 12 H, H-3, H-5, H-6, H-8, H-9, H-11), 2.98 (t, 4 H, $^3J_{H,H}$ = 5.6 Hz, H-2, H-12).

^{13}C NMR (100.6 MHz, 5:1 MeOD-D_2O, 333 K, Figure S64): δ = 143.2 ($C_{triazole}$), 135.0 ($Ar_{quaternary}$), 128.8, 128.4, 127.9 (Ar), 124.1 ($CH_{triazole}$), 53.9 (*C*H_2Ph), 48.5 (C-2, C-12), 47.1 ($CH_{2triazole}$), 44.8, 42.7, 42.1 (C-3, C-5, C-6, C-8, C-9, C-11).

ESI-MS (Figure S137): *m/z* 344.2 $[M + H]^+$.

Elemental analysis calculated (%) for $C_{18}H_{32}Cl_3N_7$: C 62.94, H 8.51, N 28.55; found: C, H, N.

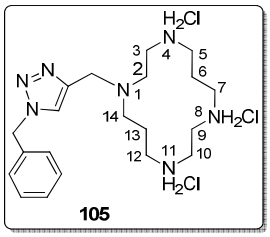

1-[(1-Benzyl-1*H*-1,2,3-triazol-4-yl)methyl]-1,4,8,11-tetraazacyclotetradecane trihydrochloride (105). Treatment of compound **101** (23 mg, 34 µmol) with TFA following the procedure described in the general methods, followed by freeze-drying from a 0.1 N aq. HCl solution, afforded compound **105** in quantitative yield (16 mg).

^{1}H NMR (400 MHz, 5:1 MeOD-D_2O, 333 K, Figure S65): δ = 8.00 (s, 1 H, $CH_{triazole}$), 7.41 (m, 5 H, Ar), 5.63 (s, 2 H, CH_2Ph), 3.84 (s, 2 H, $CH_{2triazole}$), 3.29 (m, 4 H, H-9, H-10), 3.13-3.03 (m, 8 H, H-3, H-5, H-7, H-12), 2.89 (m, 4 H, H-2, H-14), 2.09 (m, 2 H, $^{3}J_{H,H}$ = 6.4 Hz, H-6), 1.92 (m, 2 H, $^{3}J_{H,H}$ = 5.4 Hz, H-13).

^{13}C NMR (100.6 MHz, 5:1 MeOD-D_2O, 333 K, Figure S65): δ = 144.6 ($C_{triazole}$), 135.1 ($Ar_{quaternary}$), 128.9, 128.5, 128.1 (Ar), 123.8 ($CH_{triazole}$), 54.2 (*C*H_2Ph), 54.0, 52.6 (C-2, C-14), 47.1, 46.4 (C-9, C-10), 46.8 ($CH_{2triazole}$), 46.6, 45.2, 44.0 (C-3, C-5, C-7, C-12), 24.4 (C-13), 22.7 (C-6).

ESI-MS (Figure S138): *m/z* 372.3 $[M + H]^+$, 406.1 $[M + Cl]^-$.

Elemental analysis calculated (%) for $C_{20}H_{36}Cl_3N_7$: C 64.66, H 8.95, N 26.39; found: C, H, N.

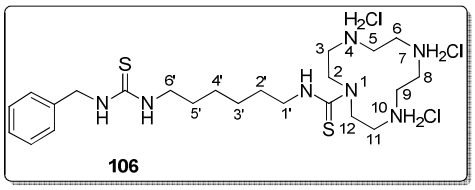

***N*-(1,4,7,10-Tetraazacyclododec-1-yl)-*N'*-[6-(*N'*-benzyl)thioureido-*n*-hex-1-yl]thiourea trihydrochloride (106).** Treatment of compound **102** (64 mg, 82 µmol) with TFA following

the procedure described in the general methods, followed by freeze-drying from a 0.1 N aq. HCl solution, afforded compound **106** in quantitative yield (48 mg).

^{1}H NMR (500 MHz, 5:1 MeOD-D_2O, 333 K, Figure S66): δ = 7.34 (m, 5 H, Ar), 4.71 (s, 2 H, C*H*$_2$Ph), 4.05 (t, 4 H, $^{3}J_{H,H}$ = 5.0 Hz, H-2, H-12), 3.65 (t, 2 H, $^{3}J_{H,H}$ = 7.4 Hz, H-1'), 3.49 (t, 2 H, $^{3}J_{H,H}$ = 7.3 Hz, H-6'), 3.42, 3.31 (2 m, 12 H, H-3, H-5, H-6, H-8, H-9, H-11), 1.68 (m, 2 H, H-2'), 1.61 (m, 2 H, H-5'), 1.38 (m, 4 H, H-3', H-4').

^{13}C NMR (125.7 MHz, 5:1 MeOD-D_2O, 333 K, Figure S66): δ = 186.3 (CS), 130.9, 129.8, 129.7 (Ar), 53.1 (C-2, C-12), 49.4 (C-1'), 48.9, 46.9 (C-3, C-5, C-6, C-8, C-9, C-11), 47.3 (*C*H$_2$Ph), 46.6 (C-6'), 31.2, 31.0 (C-2', C-5'), 28.8, 28.6 (C-3', C-4').

ESI-MS (Figure S139): *m/z* 480.3 $[M + H]^+$, 514.1 $[M + Cl]^-$.

Elemental analysis calculated (%) for $C_{23}H_{44}Cl_3N_7S_2$: C 46.89, H 7.53, N 16.64, S 10.89; found: C, H, N, S.

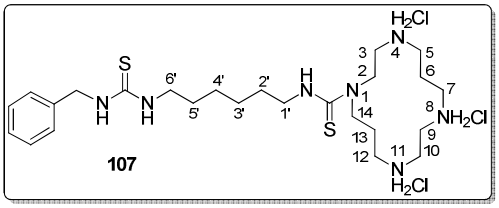

***N*-(1,4,8,11-Tetraazacyclotetradec-1-yl)-*N'*-[6-(*N'*-benzyl)thioureido-*n*-hex-1-yl]thiourea trihydrochloride (107).** Treatment of compound **103** (55 mg, 68 µmol) with TFA following the procedure described in the general methods, followed by freeze-drying from a 0.1 N aq. HCl solution, afforded compound **107** in quantitative yield (42 mg).

^{1}H NMR (500 MHz, 5:1 MeOD-D_2O, 333 K, Figure S67): δ = 7.34 (m, 5 H, Ar), 4.70 (s, 2 H, C*H*$_2$Ph), 4.25 (t, 2 H, $^{3}J_{H,H}$ = 6.7 Hz, H-2), 3.87 (t, 2 H, $^{3}J_{H,H}$ = 7.4 Hz, H-14), 3.63 (t, 2 H, $^{3}J_{H,H}$ = 7.4 Hz, H-1'), 3.49, 3.30 (2 m, 14 H, H-3, H-5, H-7, H-9, H-10, H-12, H-6'), 2.23 (m, 4 H, H-6, H-13), 1.67 (m, 2 H, H-2'), 1.60 (m, 2 H, H-5'), 1.38 (m, 4 H, H-3', H-4').

^{13}C NMR (125.7 MHz, 5:1 MeOD-D_2O, 333 K, Figure S67): δ = 185.6 (CS), 131.0, 129.8, 129.7 (Ar), 48.8 (C-2), 47.3 (*C*H$_2$Ph), 46.9 (C-14), 46.8 (C-1'), 46.5, 45.1, 44.8 (C-3, C-5, C-7, C-9, C-10, C-12, C-6'), 28.7, 28.6 (C-2', C-5'), 26.4 (C-3', C-4'), 24.3 (C-6, C-13).

ESI-MS (Figure S140): *m/z* 508.3 $[M + H]^+$, 542.2 $[M + Cl]^-$.

Elemental analysis calculated (%) for $C_{25}H_{48}Cl_3N_7S_2$: C 48.65, H 7.84, N 15.89, S 10.39; found: C, H, N, S.

3.3. New Compounds synthesized in Chapter 4

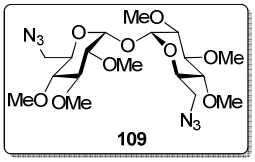

109

6,6'-Diazido-6,6'-dideoxy-2,2',3,3',4,4'-hexa-*O*-methyl-α,α'-trehalose (**109**)**.** To a solution of 6,6'-diazido-6,6'-dideoxy-α,α'-trehalose **108**[269] (0.56 g, 1.31 mmol) in dry DMF (15 mL) under N_2 atmosphere at 0 ºC NaH (0.63 g, 15.8 mmol, 2 eq, 60% dispersion in mineral oil) and methyl iodide (0.98 mL, 15.8 mmol, 2 eq) were sequentially added. The reaction mixture was allowed to warm to rt and stirred overnight. Then, the reaction was quenched by addition of water (15 mL). The reaction mixture was then concentrated under reduced pressure and the residue was taken in DCM (15 mL) and washed with water (2 x 15 mL). The organic layer was dried over Na_2SO_4, filtered and evaporated to dryness. The crude product was purified by flash column chromatography (1:2 EtOAc-petroleum ether) to furnish **109** in 72% yield (0.45 g).

R_f = 0.41 (1:2 EtOAc-petroleum ether). $[\alpha]_D$ = +161.8 (*c* = 1.0 in MeOH).

^{1}H NMR (500 MHz, $CDCl_3$, Figure S68): δ = 5.19 (d, 2 H, $J_{1,2}$ = 3.7 Hz, H-1), 4.07 (ddd, 2 H, $J_{4,5}$ = 9.9 Hz, $J_{5,6b}$ = 5.5 Hz, $J_{5,6a}$ = 2.7 Hz, H-5), 3.64, 3.57, 3.48 (3 s, 6 H each, OCH_3), 3.51 (t, 2 H, $J_{2,3}$ = $J_{3,4}$ = 9.2 Hz, H-3), 3.45 (m, 4 H, H-6a, H-6b), 3.20 (dd, 2 H, H-2), 3.08 (dd, 2 H, H-4).

^{13}C NMR (125.7 MHz, $CDCl_3$, Figure S68): δ = 93.2 (C-1), 82.8 (C-3), 81.6 (C-2), 80.4 (C-4), 70.5 (C-5), 60.8, 60.7, 58.6 (OCH_3), 51.5 (C-6).

ESI-MS (Figure S141): *m/z* 499.5 $[M + Na]^+$, 515.5 $[M + K]^+$.

Elemental analysis calculated (%) for $C_{18}H_{32}N_6O_9$: C 45.37, H 6.77, N 17.64; found: C 45.32, H 6.66, N 17.41.

RP-HPLC: t_R = 10.5 min (according to the RP-HPLC analytical procedure described in the *General Methods* section).

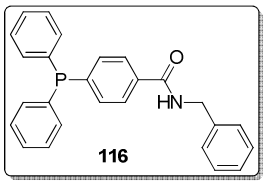

116

***N*-Benzyl-4-(diphenylphosphino)benzamide (116).** To a solution of 4-(diphenylphosphino)benzoic acid **112**[334] (0.68 g, 2.2 mmol) in DMF (20 mL) DIPEA (0.42 mL, 2.5 mmol, 1.1 eq) and TBTU (0.72 g, 2.2 mmol, 1 eq) were sequentially added. The reaction mixture was stirred for 5 min and then benzylamine (0.24 mL, 2.2 mmol, 1 eq) was added. The reaction mixture was stirred at rt overnight. The solvent was evaporated and the residue was taken in DCM, and successively washed with 1 M aq. HCl, saturated aq. $NaHCO_3$, brine and H_2O. The organic layer was dried over Na_2SO_4, filtered and evaporated to dryness. The crude product was purified by flash column chromatography (1:6 → 1:3 EtOAc-petroleum ether) to afford **116** as a white solid (729 mg, 83%).

R_f = 0.55 (1:3 EtOAc-petroleum ether).

^{1}H NMR (500 MHz, $CDCl_3$, Figure S69): δ =7.75 (d, 2 H, $^3J_{H,H}$ = 7.6 Hz, C*H*CCONH), 7.38-7.29 (m, 17 H, Ar), 6.46 (bs, 1 H, NH), 4.66 (d, 2 H, $^3J_{H,H}$ = 5.6 Hz, CH_2).

^{13}C NMR (125.7 MHz, $CDCl_3$, Figure S69): δ = 167.0 (CO), 138.1 (P*C*CHCHCCONH), 136.4, 136.3 (*C*P), 134.4 (*C*CH_2NH), 134.0, 133.8 (PC*C*H), 133.7, 133.5 (PC*C*HCHCCONH), 129.1 (*C*CONH, *C*HCHCCH_2NH), 128.8 (PCCHCH*C*H), 128.7, 128.6 (PCCH*C*H), 127.9 (*C*HCCH_2NH), 127.7 (*C*HCHCHCCH_2NH), 126.9, 126.8 (*C*HCCONH), 44.2 (*C*H_2).

^{31}P NMR (202.5 MHz, $CDCl_3$, Figure S69): δ = -6.21 (s).

ESI-MS (Figure S142): *m/z* 396.4 $[M + H]^+$, 418.4 $[M + Na]^+$, 434.3 $[M + K]^+$, 394.2 $[M – H]^-$.

Elemental analysis calculated (%) for $C_{26}H_{22}NOP$: C 78.97, H 5.61, N 3.54; found: C 78.48, H 5.82, N 3.42.

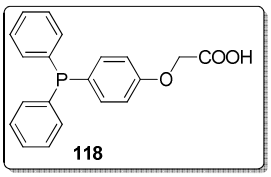

118

[4-(Diphenylphosphino)phenoxy]acetic acid (118). To a solution of (4-iodophenoxy)acetic acid **117** (1.39 g, 5 mmol) and Et_3N (1.39 mL, 10 mmol, 2 eq) in degassed MeCN (30 mL) under N_2 $Pd(AcO)_2$ (1.1 mg, 5 µmol, 0.1% eq) and diphenylphosphine (0.87 mL, 5 mmol, 1 eq) were sequentially added. The intensely orange-red colored reaction mixture was refluxed at 85 °C for 12 h. The volatiles were then evaporated and the residue was suspended in water (15 mL), taken to basic pH by adding KOH (0.56 g, 10 mmol, 2 eq) and washed with Et_2O (3 x 20 mL). The aqueous layer was then acidified to pH 2 by addition of 1.8 M HCl and extracted with Et_2O (3 x 20 mL). The collected organic phase was washed with water (15 mL), dried over Na_2SO_4, filtered and evaporated to dryness. The crude product was purified by flash column chromatography (1:2 → 2:1 EtOAc-petroleum ether) to afford **118** as a white solid (1.57 g, 93%).

R_f = 0.35 (1% AcOH in 2:1 EtOAc-petroleum ether).

^{1}H NMR (400 MHz, $CDCl_3$, Figure S70): δ = 9.04 (bs, 1 H, COOH), 7.38-7.28 (m, 12 H, Ar), 6.93 (dd, 2 H, $^3J_{H,H}$ = 8.8 Hz, $^4J_{H,P}$ = 0.9 Hz, C*H*COCH$_2$COOH), 4.71 (s, 2 H, C*H$_2$*).

^{13}C NMR (100.6 MHz, $CDCl_3$, Figure S70): δ = 173.6 (CO), 158.1 (*C*OCH$_2$COOH), 138.5 (P*C*CHCHCOCH$_2$COOH), 137.5, 137.4 (*C*P), 135.8, 135.6 (PC*C*HCHCOCH$_2$COOH), 133.6, 133.4 (PC*C*H), 128.7, 128.6, 128.5 (PCCH*C*H, PCCHCH*C*H), 114.9, 114.8 (*C*HCOCH$_2$COOH), 64.7 (*C*H$_2$).

^{31}P NMR (162 MHz, $CDCl_3$, Figure S70): δ = -7.02 (s).

ESI-MS (Figure S143): *m/z* 335.0 $[M - H]^-$.

Elemental analysis calculated (%) for $C_{20}H_{17}O_3P$: C 71.42, H 5.09; found: C 71.54, H 5.38.

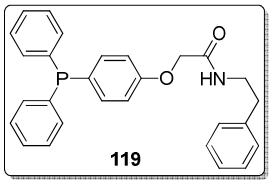

119

***N*-Benzyl-[4-(diphenylphosphino)phenoxy]acetamide (119).** To a solution of compound **118** (100 mg, 0.30 mmol) in DMF (10 mL) DIPEA (54 µL, 0.33 mmol, 1.1 eq) and TBTU (96 mg, 0.3 mmol, 1 eq) were sequentially added. The reaction mixture was stirred for 5 min and then benzylamine (33 µL, 0.3 mmol, 1 eq) was added. The reaction mixture was stirred at rt overnight. The solvent was then evaporated and the residue was taken in DCM, washed with 1 M aq. HCl, saturated aq. $NaHCO_3$, brine and H_2O. The organic layer was dried over Na_2SO_4, filtered and evaporated to dryness. The crude product was purified by flash column chromatography (1:3 EtOAc-petroleum ether) to yield **119** as a white solid (75 mg, 59%).

R_f = 0.23 (1:3 EtOAc-petroleum ether).

^{1}H NMR (400 MHz, $CDCl_3$, Figure S71): δ = 7.37-7.29 (m, 17 H, Ar), 6.92 (d, 2 H, $^3J_{H,H}$ = 8.4 Hz, C*H*COCH$_2$CONH), 4.59 (m, 3 H, OC*H$_2$*CO, CONHC*H$_a$*), 4.57 (m, 1 H, CONHC*H$_b$*).

^{13}C NMR (75.5 MHz, $CDCl_3$, Figure S71): δ = 167.9 (CO), 157.8 (*C*OCH$_2$CONH), 137.6 (P*C*CHCHCOCH$_2$CONH), 135.9, 135.5 (*C*P), 133.6, 133.4 (PC*C*HCHCOCH$_2$CONH), 132.1 (*C*CH$_2$NH), 128.8, 128.6, 128.5, 127.7 (PC*C*H, PCCH*C*H, PCCHCH*C*H, *C*HCHCCH$_2$NH, *C*HCCH$_2$NH, *C*HCHCHCCH$_2$NH), 115.1, 114.8 (*C*HCOCH$_2$CONH), 67.3 (O*C*H$_2$CONH), 43.1 (CONH*C*H$_2$).

^{31}P NMR (162 MHz, $CDCl_3$, Figure S71): δ = -7.03 (s).

ESI-MS (Figure S144): *m/z* 448.2 $[M + Na]^+$, 464.2 $[M + K]^+$.

Elemental analysis calculated (%) for $C_{27}H_{24}NO_2P$: C 76.22, H 5.69, N 3.29; found: C 76.00, H 5.90, N 3.46.

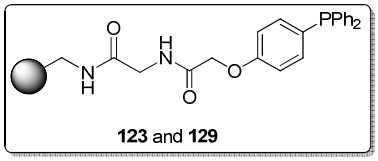

123 and **129**

Phosphine-functionalized PS resins 123 and 129. Commercially available AM-PS resin (2.0 g, 0.39 mmol·g^{-1}) was placed in a plastic syringe and allowed to swell in DMF for 20 min. Fmoc-Gly-OH (0.70 g, 2.34 mmol, 3 eq) was dissolved in a minimum amount of DMF. DIPEA (0.54 mL, 3.12 mmol, 4 eq) and TBTU (0.75 g, 2.34 mmol, 3 eq) were then sequentially added to the glycine solution. The mixture was stirred for approximately 5 min until complete dissolution of TBTU. Then, the solution was added to the swollen resin and the mixture was incubated rt overnight. Disappearance of amino groups was monitored by Kaiser test.[337] The resin was then washed with DMF (6 x 2 min) and DCM (4 x 2 min). The resin was finally dried under vacuum to constant weight. Resin substitution was estimated to be close to the nominal value (0.39 mmol·g^{-1}) by UV determination of the dibenzofulvene released from a portion of resin upon 2% DBU in DMF treatment according to standard procedures.

Fmoc was removed by treating the resin with 20% v/v piperidine in DMF at rt for 20 min, followed by rinsing the resin with degassed DMF (6 x 2 min) and degassed DCM (4 x 2 min) under N_2 to prevent oxidation during phosphine coupling.

To a solution of phosphine **118** (0.54 g, 1.63 mmol, 2.1 eq) in dry and degassed DCM under N_2 atmosphere DMAP (0.20 g, 1.63 mmol, 2.1 eq) and DIC (0.20 g, 1.63 mmol, 2.1 eq) were sequentially added. The mixture was stirred for approximately 5 min under N_2 and the solution was subsequently transferred to the resin. After incubation for 16 h, the resin was then washed under N_2 stream with dry DCM (6 x 2 min) and dried under vacuum to constant weight. The resin was stored under an inert atmosphere to prevent phosphine oxidation. Successful phosphine incorporation was confirmed by appearance of the corresponding resonance at ca. -6 ppm in the ^{31}P NMR spectra.

^{31}P NMR (121 MHz, DMF, Figure S72): δ = -7.78 (s). Minute amounts (< 5%) of oxide phosphine (signal at ca. 32 ppm) were observed. Final resin loading (due to resin mass increase) was estimated in 0.34 mmol·g^{-1}.

For the synthesis of the diluted version of resin **129**, the coupling of the initial amino acid was effected using a mixture of Fmoc-Gly-OH and Boc-Gly-OH (1:9 in a molar basis). Thus, AM-PS resin (2.0 g, 0.39 mmol·g^{-1}) was treated with mixture of Fmoc-Gly-OH (68 mg, 0.23 mmol, 0.3 eq), Boc-Gly-OH (0.37 g, 2.1 mmol, 2.7 eq), DIPEA (0.54 mL, 3.12 mmol, 4 eq) and TBTU (0.75 g, 2.34 mmol, 3 eq) in DMF. After disappearance of amino groups, the resin was then washed with DMF (6 x 2 min) and DCM (4 x 2 min). Then Boc protecting groups were removed by treatment with a 1:1 mixture of TFA-DCM for 1 h and the resin was washed with DCM (4 x 2 min), 5% DIPEA in DCM and neat DCM again (4 x 2 min). Free amino groups were capped by treating the DMF-swollen resin with a 1:1 Ac_2O-Py mixture (10 eq each) for 1 h. The resin was finally rinsed with DMF (6 x 2 min) and DCM (4 x 2 min). Phosphine installation on the diluted resin was effected as described for **123**.

^{31}P NMR (121 MHz, DMF, Figure S73): δ = -7.78 (s). Minute amounts (< 5%) of oxide phosphine (signal at ca. 32 ppm) were observed. Final resin loading (due to resin mass increase) was estimated in 40 µmol·g^{-1}.

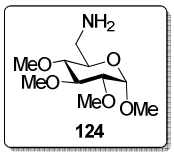

124

Methyl 6-amino-6-deoxy-2,3,4-tri-*O*-methyl-α-D-glucopyranoside (124). Amine **124** was obtained from methyl 6-azido-6-deoxy-2,3,4-tri-O-methyl-α-D-glucopyranoside **91**[280] (35 mg, 136 µmol, 2 eq) and resin **123** (0.2 g, 0.34 mmol·g^{-1}) using the catch-and-release protocol as described in *procedure A* (*General Methods for Solid-Phase Synthesis*) in 89% yield (14 mg).

ESI-MS (Figure S145): *m/z* 236.1 $[M + H]^+$, 258.1 $[M + Na]^+$.

Alternatively, compound **124** was prepared in solution as follows: To a mixture of methyl 6-azido-6-deoxy-2,3,4-tri-*O*-methyl-α-D-glucopyranoside **91**[280] (100 mg, 0.38 mmol) and Et_3N (106 µL, 0.77 mmol, 2 eq) in MeOH (3 mL) was added 1,3-propanedithiol (77 µL, 0.77 mmol, 2 eq). The reaction mixture was stirred at rt overnight and solvents were subsequently evaporated under reduced pressure. The resulting residue was purified by flash column chromatography (30:2:1 MeCN-H_2O-NH_4OH) to yield compound **124** (88 mg, 98%).

R_f = 0.19 (30:2:1 MeCN-H_2O-NH_4OH). $[\alpha]_D$ = +41.6 (*c* = 1.0 in MeOH).

^{1}H NMR (300 MHz, MeOD, Figure S74): δ = 4.86 (d, 1 H, $J_{1,2}$ = 3.6 Hz, H-1), 3.59, 3.54, 3.49, 3.42 (4 s, 3 H each, OCH_3), 3.45 (ddd, 1 H, $J_{4,5}$ = 10.4 Hz, $J_{5,6b}$ = 5.7 Hz, $J_{5,6a}$ = 2.7 Hz, H-5), 3.39 (m, 1 H, H-3), 3.20 (dd, 1 H, $J_{2,3}$ = 9.6 Hz, H-2), 2.98 (dd, 1 H, H-6a), 2.59 (dd, 1 H, $J_{3,4}$ = 9.0 Hz, H-4), 2.71 (dd, 1 H, $J_{6a,6b}$ = 13.2 Hz, H-6b).

^{13}C NMR (75.5 MHz, MeOD, Figure S74): δ = 97.0 (C-1), 83.2 (C-3), 81.6 (C-4), 81.3 (C-2), 71.0 (C-5), 59.6, 59.4, 57.4, 54.1 (OCH_3), 42.2 (C-6).

ESI-MS (Figure S146): *m/z* 236.1 $[M + H]^+$, 258.2 $[M + Na]^+$, 471.3 $[2 M + H]^+$.

Elemental analysis calculated (%) for $C_{10}H_{21}NO_5$: C 51.05, H 9.00, N 5.95; found: C 51.23, H 9.04, N 5.96.

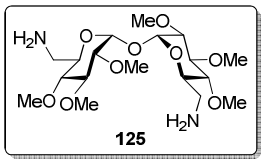

125

6,6'-Diamino-6,6'-dideoxy-2,2',3,3',4,4'-hexa-*O*-methyl-α,α'-trehalose (125). To a solution of compound **109** (49 mg, 96 µmol) in MeOH (1.5 mL) Pd/C (5 mg, 10% w/w) was added. The reaction mixture was stirred at rt for 24 h at 2 bar hydrogen pressure. Then, the reaction mixture was filtered over celite to remove the catalyst. The solvent was evaporated yielding compound **125** (43 mg, 97%). The crude product was used without further purification.

R_f = 0.15 (10:1:1 MeCN-H_2O-NH_4OH). $[\alpha]_D$ = +33.1 (*c* = 0.52 in MeOH).

^{1}H NMR (500 MHz, $CDCl_3$, Figure S75): δ = 5.14 (d, 2 H, $J_{1,2}$ = 3.5 Hz, H-1), 3.83 (ddd, 2 H, $J_{4,5}$ = 9.6 Hz, $J_{5,6b}$ = 6.1 Hz, $J_{5,6a}$ = 2.8 Hz, H-5), 3.64, 3.58, 3.47 (3 s, 6 H each, OCH_3), 3.55 (t, 2 H, $J_{2,3}$ = $J_{3,4}$ = 9.2 Hz, H-3), 3.16 (dd, 2 H, H-2), 3.03 (m, 4 H, H-4, H-6a), 2.81 (dd, 2 H, $J_{6a,6b}$ = 13.1 Hz, H-6b).

^{13}C NMR (125.7 MHz, $CDCl_3$, Figure S75): δ = 92.8 (C-1), 83.0 (C-3), 81.8 (C-2), 80.9 (C-4), 71.9 (C-5), 60.8, 60.5, 58.8 (OCH_3), 42.7 (C-6).

ESI-MS (Figure S147): *m/z* 425.5 $[M+H]^+$, 447.4 $[M + Na]^+$.

Elemental analysis calculated (%) for $C_{18}H_{36}N_2O_9$: C 50.93, H 8.55, N 6.60; found: C 50.70, H 8.24, N 6.45.

RP-HPLC: t_R = 5.4 min (according to the RP-HPLC analytical procedure described in the *General Methods* section).

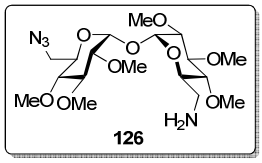

126

6-Amino-6'-azido-6,6'-dideoxy-2,2',3,3',4,4'-hexa-*O*-methyl-α,α'-trehalose (126). Compound **126** was obtained from compound **109** (32 mg, 68 µmol, 2 eq) and resin **123** (0.1 g, 0.34 $mmol \cdot g^{-1}$) using the catch-and-release protocol as described in *procedure A* (*General Methods for Solid-Phase Synthesis*) in 52 % yield (8 mg).

HPLC: t_R= 6.3 min (according to the RP-HPLC analytical procedure described in the *General Methods* section).

ESI-MS (Figure S148): *m/z* 451.4 $[M + H]^+$, 473.4 $[M + Na]^+$.

Alternatively, compound **126** was prepared in solution by statistical reduction of a single azido group as follows: To a mixture of compound **109** (100 mg, 0.21 mmol), Et_3N (58 µL, 0.42 mmol, 2 eq) and 1,3-propanedithiol (3 µL, 0.02 mmol, 0.1 eq) in 2-propanol-DMF (2:1, 3 mL) was added $NaBH_4$ (8.7 mg, 0.23 mmol, 1.1 eq). The reaction mixture was stirred at rt for 4.5 h, and then H_2O (1 mL) was added and solvents were evaporated under reduced pressure. The resulting residue was purified by flash column chromatography (30:2:1 MeCN-H_2O-NH_4OH) to yield compound **126** (38 mg, 40%).

R_f = 0.36 (30:2:1 MeCN-H_2O-NH_4OH). $[\alpha]_D$ = +101.2 (*c* = 1.0 in MeOH).

^{1}H NMR (500 MHz, $CDCl_3$, Figure S76): δ = 5.18, 5.17 (2 d, 1 H each, $J_{1,2}$ = 3.7 Hz, H-1, H-1'), 4.09 (ddd, 1 H, $J_{4,5}$ = 9.9 Hz, $J_{5,6b}$ = 5.2 Hz, $J_{5,6a}$ = 2.7 Hz, H-5'), 3.84 (ddd, 1 H, $J_{4,5}$ = 12.8 Hz, $J_{5,6b}$ = 5.8 Hz, $J_{5,6a}$ = 2.7 Hz, H-5), 3.65, 3.64, 3.59, 3.58, 3.49, 3.48 (6 s, 3 H each, OCH_3), 3.53 (2 t, 1 H each, $J_{2,3}$ = $J_{3,4}$ = 9.7 Hz, H-3, H-3'), 3.47-3.42 (m, 2 H, H-6a', H-6b'), 3.20, 3.18 (2 dd, 1 H each, H-2, H-2'), 3.10-3.01 (m, 3 H, H-4, H-4', H-6a), 2.83 (dd, 1 H, $J_{6a,6b}$ = 13.5 Hz, H-6b).

^{13}C NMR (125.7 MHz, $CDCl_3$, Figure S76): δ = 93.1, 93.0 (C-1, C-1'), 83.0, 82.8 (C-3, C-3'), 81.8, 81.6 (C-2, C-2'), 80.8, 80.4 (C-4, C-4'),71.9 (C-5'), 70.4 (C-5), 60.8, 60.6, 58.7 (OCH_3), 51.5 (C-6'), 42.6 (C-6).

ESI-MS (Figure S149): *m/z* 451.5 $[M + H]^+$, 473.4 $[M + Na]^+$.

Elemental analysis calculated (%) for $C_{18}H_{34}N_4O_9$: C 47.99, H 7.61, N 12.44; found: C 47.67, H 7.54, N 12.35.

RP-HPLC: t_R = 6.3 min (according to the RP-HPLC analytical procedure described in the *General Methods* section).

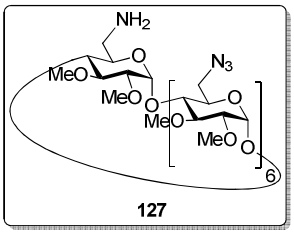

127

6^{I}-Amino-6^{II-VII}-hexaazido-6^{I-VII}-heptadeoxy-2^{I-VII},3^{I-VII}-tetradeca-*O*-methylcyclomalto-heptaose (127). Monoamine **127** was obtained from heptakis(6-azido-6-deoxy-2,3-di-*O*-methyl)cyclomaltoheptaose **110**[180a] (153 mg, 0.1 mmol, 2 eq) and resin **123** (0.15 g, 0.34 mmol·g^{-1}) using the catch-and-release protocol as described in *procedure A* (*General Methods for Solid-Phase Synthesis*) in 79% yield (60 mg).

HPLC: t_R = 9.2min (according to the RP-HPLC analytical procedure described in the *General Methods* section).

ESI-MS (Figure S150): m/z 1480.6 $[M + H]^+$, 1502.5 $[M + Na]^+$.

Alternatively, compound **127** was prepared in solution by statistical reduction of a single azido group as follows: To a solution of heptakis(6-azido-6-deoxy-2,3-di-*O*-methyl)cyclomaltoheptaose **110**[180a] (262 mg, 0.17 mmol) in 2-propanol (10 mL) under nitrogen atmosphere, Et_3N (48 µL, 0.35 mmol, 2 eq), 1,3-propanedithiol (1.75 µL, 17 µmol, 0.1 eq) and $NaBH_4$ (7.3 mg, 0.19 mmol, 1.1 eq) were added, and the reaction mixture was vigorously stirred overnight. The reaction was quenched by addition of water (2 mL). The solvent was evaporated under reduced pressure and the residue was diluted with DCM (20 mL) and washed with 1 M aq. NaOH (3 x 5 mL). The organic layer was dried, filtered and concentrated. The resulting residue was purified by flash column chromatography (20:1 → 9:1 DCM-MeOH) to obtain the starting material and compound **127** as an amorphous white solid. Yield: 56 mg (23 %) along with unreacted starting material (126 mg, 48%).

R_f = 0.50 (9:1 DCM-MeOH). $[\alpha]_D$ = +149.1 (*c* = 1.0 in DCM).

^{1}H NMR (500 MHz, MeOD, 333 K, Figure S77): δ =5.27 (d, 1H, $J_{1,2}$ = 3.7 Hz, H-1^{II}), 5.22-5.18 (m, 6 H, H-1$^{I,III-VII}$), 3.95-3.84 (m, 11 H, H-5^{II-VII}, H-6a^{II-VI}), 3.81-3.78 (dd, 1 H, H-6a^{VII}), 3.77-3.74 (ddd, 1 H, H-5^{I}), 3.70-3.50 (m, 20 H, H-4^{I-VII}, H-3^{I-VII}, H-6b^{II-VII}), 3.66 (m, 21 H, OCH_3 $^{I-VII}$), 3.55 (m, 21 H, OCH_3 $^{I-VII}$), 3.26-3.21 (m, 7 H, H-2^{I-VII}), 3.19-3.16 (dd, 1 H, H-6a^{I}), 3.07-3.02 (dd, 1 H, H-6b^{I}).

1D-TOCSY (500 MHz, MeOD, H-6a^{I} irradiation): δ =5.21 (d, 1 H, $J_{1,2}$ = 2.8 Hz, H-1^{I}), 3.75 (ddd, 1 H, $J_{4,5}$ = 8.4 Hz, $J_{5,6a}$ = 2.9 Hz, $J_{5,6b}$ = 5.6 Hz, H-5^{I}), 3.58-3.52 (m, 2 H, H-3^{I}, H-4^{I}), 3.22 (dd, 1 H, $J_{2,3}$ = 8.6 Hz, H-2^{I}), 3.16 (dd, 1 H, H-6a), 3.04 (dd, 1 H, H-6b, $J_{6a,6b}$ = 14.0 Hz).

1D-TOCSY (500 MHz, MeOD, H-2^{II} irradiation): δ =5.25 (d, 1 H, $J_{1,2}$ = 3.9 Hz, H-1^{II}), 3.92 (ddd, 1 H, H-5 ^{II}), 3.85 (d, 1 H, H-6a^{II}), 3.69 (dd, 1 H, $J_{6a,6b}$ = 14.0 Hz, $J_{5,6b}$ = 4.0 Hz, H-6b ^{II}), 3.6 (t, 1 H, H-4 ^{II}), 3.52 (t, 1 H, $J_{2,3}$ = $J_{3,4}$ = 9.1 Hz, H-3 ^{II}), 3.23 (dd, 1 H, $J_{2,3}$ = 9.9 Hz, H-2 ^{II}).

^{13}C NMR (125.7 MHz, MeOD, 333 K, Figure S77): δ = 100.6-100.4 (C-1^{I-VII}), 84.0-82.1 (C-2^{I-VII},C-3^{I-VII}, C-4^{I-VII}), 73.8-73.2 (C-5^{I-VII}), 62.8-62.4 (OCH_3), 60.2-59.9 (OCH_3), 54.1-53.9 (C-6^{II-VII}), 43.9 (C-6^{I}).

ESI-MS (Figure S151): *m/z* 1480.7 $[M + H]^+$, 1502.6 $[M + Na]^+$.

Elemental analysis calculated (%) for $C_{56}H_{93}N_{19}O_{28}$: C 45.43, H 6.33, N 17.98; found: C 45.08, H 6.27, N 17.61.

RP-HPLC: t_R = 9.2 min (according to the RP-HPLC analytical procedure described in the *General Methods* section).

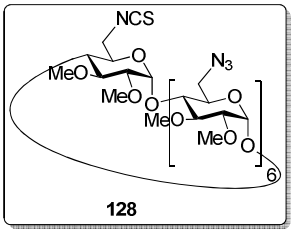

6^{II-VII}-Hexaazido-6^{I-VII}-heptadeoxy-6^{I}-isothiocyanato-2^{I-VII},3^{I-VII}-tetradeca-*O*-methyl-cyclomaltoheptaose (128). Monoisothiocyanate **128** was obtained from heptakis(6-azido-6-deoxy-2,3-di-*O*-methyl)cyclomaltoheptaose **110**[180a] (153 mg, 0.1 mmol, 2 eq) and resin **123** (0.15 g, 0.34 mmol·g^{-1}) using the catch-and-release protocol as described in *procedure B* (*General Methods for Solid-Phase Synthesis*) in 86% yield (67 mg).

HPLC: t_R= 13.7 min (according to the RP-HPLC analytical procedure described in the *General Methods* section).

ESI-MS (Figure S152): *m/z* 1544.6 $[M + Na]^+$.

Alternatively, compound **128** was prepared in solution as follows: To a solution of compound **127** (50 mg, 34 µmol) in DCM-H_2O (1:1, 6 mL), thiophosgene (5 µL, 68 µmol, 2 eq) and $CaCO_3$ (14 mg, 0.14 mmol, 4 eq) were added and the suspension was vigorously stirred at rt for 5 h. The organic layer was diluted with DCM(10 mL) and decanted, then dried over Na_2SO_4, filtered and concentrated. The residue was purified by flash column chromatography (3:1 EtOAc-petroleum ether) to give compound **128**. Yield: 29 mg (58 %).

R_f = 0.55 (4:1 EtOAc-petroleum ether). $[\alpha]_D$ = +163.2 (*c* = 0.9 in DCM).

^{1}H NMR (500 MHz, $CDCl_3$, Figure S78): δ =5.11-5.08 (m, 7 H, H-1^{I-VII}), 3.97 (dd, 1 H, $J_{6a,5}$ = 2.4 Hz, $J_{6a,6b}$ = 14.8 Hz, H-$6a^{I}$), 3.91 (dd, 1 H, $J_{6a,5}$ = 5.1 Hz, H-$6b^{I}$), 3.84-3.65 (m, 7 H,

H-5$^{I\text{-}VII}$), 3.84-3.45 (m, 12 H, H-6a,b$^{II\text{-}VI}$), 3.63 (m, 21 H, OCH_3 $^{I\text{-}VII}$), 3.55-3.45 (m, 14 H, H-3$^{I\text{-}VII}$, H-4$^{I\text{-}VII}$), 3.52 (m, 21 H, $OCH_3$$^{I\text{-}VII}$), 3.21-3.15 (m, 7 H, H-2$^{I\text{-}VII}$).

1D-TOCSY (500 MHz, $CDCl_3$, H-6a^{I} irradiation): δ = 5.10 (s, 1 H, H-1^{I}), 4.04-3.90 (m, 14 H, H-6a^{I}, H-6b^{I}), 3.60-3.40 (m, 2 H, H-3^{I,} H-4^{I}), 3.22 (m, 1 H, H-2^{I}).

^{13}C NMR (125.7 MHz, $CDCl_3$, Figure S78): δ = 99.0 (C-1$^{I\text{-}VII}$), 81.9-81.3 (C-2$^{I\text{-}VII}$,C-3$^{I\text{-}VII}$, C-4$^{I\text{-}VII}$), 71.3 (C-5$^{I\text{-}VII}$), 61.9 (OCH_3 $^{I\text{-}VII}$), 59.3 (OCH_3 $^{I\text{-}VII}$), 52.2 (C-6$^{I\text{-}VII}$).

ESI-MS (Figure S153): *m/z* 1544.7 $[M + Na]^+$.

Elemental analysis calculated (%) for$C_{57}H_{91}N_{19}O_{28}S$: C 44.97, H 6.02, N 17.48, S 1.45; found: C 44.71, H 5.90, N 17.31, S 1.86.

RP-HPLC: t_R = 13.7min (according to the RP-HPLC analytical procedure described in the *General Methods* section).

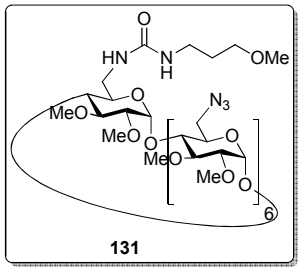

131

6^{I}-[*N*'-(3-methoxypropyl)ureido]-6$^{II\text{-}VII}$-hexaazido-6$^{I\text{-}VII}$-heptadeoxy-2$^{I\text{-}VII}$,3$^{I\text{-}VII}$-tetradeca-*O*-methylcyclomaltoheptaose (131). Monourea **131** was obtained from heptakis(6-azido-6-deoxy-2,3-di-*O*-methyl)cyclomaltoheptaose **110**[180a] (52 mg, 35 µmol, 2 eq) and resin **129** (0.5 g, 35 µmol·g^{-1}) using the catch-and-release protocol as described in *procedure C* (*General Methods for Solid-Phase Synthesis*) in 76% yield (21 mg).

^{1}H NMR (500 MHz, MeOD, 323 K, Figure S79): δ = 5.29-5.15 (m, 7 H, H-1$^{I\text{-}VII}$), 4.03 (m, 2 H, CH_2O), 3.93-3.80 (m, 14 H, H-5$^{I\text{-}VII}$, H-6a$^{I\text{-}VII}$), 3.67-3.63, 3.56-3.51 (2 m, 45 H, OCH_3), 3.62-3.56 (m, 7 H, H-6b$^{I\text{-}VII}$), 3.61-3.47 (m, 14 H, H-3$^{I\text{-}VII}$, H-4$^{I\text{-}VII}$), 3.24-3.21 (m, 7 H, H-2$^{I\text{-}VII}$).

^{13}C NMR (125.7 MHz, MeOD, Figure S79): δ = 158.0 (CO), 98.2-97.9 (C-1^{I-VII}), 81.8-79.7 (C-2^{I-VII}, C-3^{I-VII}, C-4^{I-VII}, CH_2O), 71.0 (C-5^{I-VII}), 60.6 (OCH_3 $^{I-VII}$), 57.8 (OCH_3 $^{I-VII}$), 51.7 (C-6^{II-VII}), 42.0 (C-6^{I}, CH_2N), 29.7 ($CH_2CH_2CH_2$).

ESI-MS (Figure S154): *m/z* 1617.6 $[M + Na]^+$.

HPLC: t_R = 12.9 min (according to the RP-HPLC analytical procedure described in the *General Methods* section).

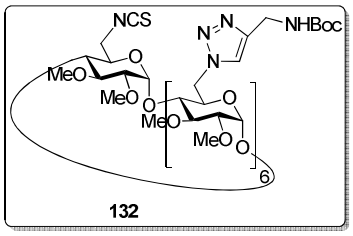

132

6-$^{II-VII}$-Hexakis[(*N-tert*-butoxycarbonylaminomethyl-1*H*-1,2,3-triazol-1-yl]-6^{I-VII}-heptadeoxy-6^{I}-isothiocyanato-2^{I-VII},3^{I-VII}-tetradeca-*O*-methylcyclomaltoheptaose (132). Monoisothiocyanate **132** was obtained from heptakis(6-azido-6-deoxy-2,3-di-*O*-methyl)cyclomaltoheptaose **110**[180a] (52 mg, 35 µmol, 2 eq) and resin **129** (0.5 g, 35 µmol·g^{-1}) using the catch-and-release protocol as described in *General Methods for Solid-Phase Synthesis* in 59% yield (25 mg).

R_f = 0.39 (20:1 DCM-MeOH). $[\alpha]_D$ = +121.0 (*c* = 0.5 in MeOH).

^{1}H NMR (500 MHz, MeOD, 323 K, Figure S80): δ = 7.89-7.73 (m, 6 H, triazole), 5.48-5.39 (m, 6 H, H-1^{II-VII}), 5.17 (m, 1 H, H-1^{I}), 4.33 (m, 2 H, H-6a^{I}, H-6b^{I}), 4.24 (m, 7 H, H-5^{I-VII}), 3.67-3.49 (m, 80 H, H-3^{I-VII}, H-4^{I-VII}, H-6a^{II-VII}, H6b^{II-VII}, C*H*$_2$NHBoc, OCH_3 $^{I-VII}$), 3.11 (m, 6 H, H-2^{I-VII}), 1.45, 1.43 (2 s, 9 H each, $C(CH_3)_3$), 1.42 (bs, 18 H, $C(CH_3)_3$), 1.40, 1.38 (2 s, 9 H each, $C(CH_3)_3$).

ESI-MS (Figure S155): *m/z* 1249.5 $[M + 2 Na]^{2+}$, 2475.7 $[M + Na]^+$, 2487.8 $[M + Cl]^-$.

RP-HPLC: t_R = 12.8 (according to the RP-HPLC analytical procedure described in the *General Methods* section).

REFERENCES

[1] C. Ortiz Mellet, J. M. García Fernández, J. M. Benito, *Chem. Soc. Rev.* **2011**, *40*, 1586-1608.

[2] M. E. Davis, *Mol. Pharm.* **2009**, *6*, 659-668.

[3] (a) S. A. Rosenberg, P. Aebersold, K. Cornetta, A. Kasid, R. A. Morgan, R. Moen, E. M. Karson, M. T. Lotze, J. C. Yang, S. L. Topalian, M. J. Merino, K. Culver, A. D. Miller, R. M. Blaese, W. F. Anderson, *N. Engl. J. Med.* **1990**, *323*, 570-578. (b) R. M. Blaese, K. W. Culver, A. D. Miller, C. S. Carter, T. Fleisher, M. Clerici, G. Shearer, L. Chang, Y. Chiang, P. Tolstoshev, J. J. Greenblatt, S. A. Rosenberg, H. Klein, M. Berger, C. A. Mullen, W. J. Ramsey, L. Muul, R. A. Morgan, W. F. Anderson, *Science* **1995**, *270*, 475-480.

[4] C. Sheridan, *Nat. Biotechnol.* **2011**, *29*, 121-128.

[5] M. Cavazzana-Calvo, S. Hacein-Bey, B. G. de Saint, F. Gross, E. Yvon, P. Nusbaum, F. Selz, C. Hue, S. Certain, J. L. Casanova, P. Bousso, F. L. Deist, A. Fischer, *Science* **2000**, *288*, 669-672.

[6] M. Cavazzana-Calvo, E. Payen, O. Negre, G. Wang, K. Hehir, F. Fusil, J. Down, M. Denaro, T. Brady, K. Westerman, R. Cavallesco, B. Gillet-Legrand, L. Caccavelli, R. Sgarra, L. Maouche-Chretien, F. Bernaudin, R. Girot, R. Dorazio, G.-J. Mulder, A. Polack, A. Bank, J. Soulier, J. Larghero, N. Kabbara, B. Dalle, B. Gourmel, G. Socie, S. Chretien, N. Cartier, P. Aubourg, A. Fischer, K. Cornetta, F. Galacteros, Y. Beuzard, E. Gluckman, F. Bushman, S. Hacein-Bey-Abina, P. Leboulch, *Nature* **2010**, *467*, 318-322.

[7] The Journal of Gene Medicine, © 2013 John Wiley and Sons Ltd, http://www.wiley.co.uk/genmed/clinical (Last visited on July 26th 2013).

[8] M. A. Branca, *Nat. Biotechnol.* **2005**, *23*, 519-521.

[9] S. Hacein-Bey-Abina, A. Garrigue, G. P. Wang, J. Soulier, A. Lim, E. Morillon, E. Clappier, L. Caccavelli, E. Delabesse, K. Beldjord, V. Asnafi, E. MacIntyre, L. Dal Cortivo, I. Radford, N Brousse, F. Sigaux, D. Moshous, J. Hauer, A. Borkhardt, B. H. Belohradsky, U. Wintergerst, M. C. Velez, L. Leiva, R. Sorensen, N. Wulffraat, S. Blanche, F. D. Bushman, Alain Fischer, M. Cavazzana-Calvo, *J. Clin. Invest.* **2008**, *118*, 3132-3142.

[10] C. Uherek, W. Wels, *Adv. Drug Deliv. Rev*. **2000**, *44*, 153-166.

[11] S. T. Crooke, *Biochim. Biophys. Acta*. **1999**, *1489*, 31-43.

[12] R. A. Stull, F. C. Szoka, Jr. *Pharm Res*. **1995**, *12*, 465-483.

[13] S. Akhtar, M. D. Hughes, A. Khan, M. Bibby, M. Hussain, Q. Nawaz, J. Double, P. Sayyed, *Adv. Drug Deliv. Rev.* **2000**, *44*, 3-21.

[14] Y. Dorsett, T. Tuschl, *Nat. Rev. Drug Discov.* **2004**, *3*, 318-329.

[15] S. D. Jayasena, *Clin. Chem*. **1999**, *45*, 1628-1650.

[16] (a) J. B. Opalinska, A. M. Gewirtz, *Nat. Rev. Drug Discov.* **2002**, *1*, 503-514. (b) http://www.clinicaltrials.gov, ClinicalTrials.gov Identifiers: NCT01274455, NCT01182857, NCT00599781, NCT00300521, NCT01347346 (Last visited on July 15th 2013).

[17] S. D. Patil, D. J. Burgess, *AAPS Newsmagazine* **2003**, 6, 27-27.

[18] (a) K. K. L. Phua, K. W. Leong, S. K. Nair, *J. Control. Release* **2013**, *166*, 227-233. (b) K. Shimizu, S. Kawakami, K. Hayashi, H. Kinoshita, K. Kuwahara, K. Nakao, M. Hashida, S. Konishi, *PLOS ONE* **2012**, *7*, e41319. (c) L. J. Wolff, J. A. Wolff, M. G. Sebestyen, *Hum. Gene Ther.* **2009**, *20*, 374-388.

[19] R. Niven, R. Pearlman, T. Wedeking, J. Mackeigan, P. Noker, L. Simpson-Herren, J. G. Smith, *J. Pharm. Sci.* **1998**, *87*, 1292-1299.

[20] M. S. Al-Dosari, X. Gao, *AAPS J.* **2009**, *11*, 671-681.

[21] L. Xu, T. Anchordoquy, *J. Pharm. Sci.* **2011**, *100*, 38-52.

[22] P. Opanasopit, M. Nishikawa, M. Hashida, *Crit. Rev. Ther. Drug* **2002**, *19*, 191-233.

[23] R. J. Boado, W. M. Pardridge, *Bioconjugate Chem.* **1992**, *3*, 519-523.

[24] G. Sahay, D. Y. Alakhova, A. V. Kabanov, *J. Control. Release* **2010**, *145*, 182-195.

[25] D. V. McAllister, M. G. Allen, M. R. Prausnitz, *Annu. Rev. Biomed. Eng*. **2000**, *2*, 289-313.

[26] L. Huang, E. Viroonchatapan, in *Nonviral Vectors for Gene Therapy* (Eds.: L. Huang, M.-C. Hung, E. Wagner), Academic Press, San Diego, **1999**, pp 3-22.

[27] S. Agrawal, R. Zhang, in *Oligonucleotides as Therapeutic Agents*, (Ciba Foundation Symposium, Vol. 209) Wiley, Weinheim, **1997**, 209 60-78.

[28] (a) T. Suda, X. Gao, D. B. Stolz, D. Liu, *Gene Ther.* **2007**, *14*, 129-137. (b) T. Suda, D. Liu, *Mol. Ther.* **2007**, *15*, 2063-2069.

[29] S. Mehier-Humbert, R. H. Guy, *Adv. Drug Deliv. Rev.* **2005**, *57*, 733-753.

[30] J. J. Drabick, J. Glasspool-Malone, S. Somiari, A. King, R. W. Malone, *Mol. Ther.* **2001**, *3*, 249-255.

[31] (a) H. Kamiya, H. Tsuchiya, J. Yamazaki, H. Harashima, *Adv. Drug Deliv. Rev*. **2001**, *52*, 153-164. (b) C. Mah, B. J. Byrne, T. R. Flotte, *Clin. Pharmacokinet*. **2002**, *41*, 901-911.

[32] M. A. Kay, J. C. Glorioso, L. Naldini, *Nat. Med.* **2001**, *7*, 33-40.

[33] (a) S. McTaggart, M. Al-Rubeai, *Biotechnol. Adv*. **2002**, *20*, 1-31. (b) C. K. Tai, N. Kasahara, *Front. Biosci.* **2008**, *13*, 3083-3095. (c) C. J. Buchholz, L. J. Duerner, S. Funke, I. C. Schneider, *Comb. Chem. HTP Screen.* **2008**, *11*, 99-110.

[34] (a) F. Kreppel, S. Kochanek, *Mol. Ther.* **2008**, *16*, 16-29. (b) D. Descamps, K. Benihoud, *Curr. Gene Ther.* **2009**, *9*, 115-127.

[35] (a) Z. J. Wu, A. Asokan, R. J. Samulski, *Mol. Ther.* **2006**, *14*, 316-327. (b) H. Buening, L. Perabo, O. Coutelle, S. Quadt-Humme, M. Hallek, *J. Gene Med.* **2008**, *10*, 717-733. (c) K. Vig, R. Herzog, D. Martin, E. G. Moore, V. A. Dennis, S. Pillai, S. R. Singh, *Gene Ther. Mol. Biol.* **2008**, 12B, 277-292. (d) K. Stieger, E. Lheriteau, P. Moullier, F. Rolling, *ILAR J.* **2009**, *50*, 206-240.

[36] (a) Z. S. Guo, S. H. Thorne, D. L. Bartlett, *Biochim. Biophys. Acta* **2008**, *1785*, 217-231. (b) C. E. Gómez, J. L. Nájera, M. Krupa, M. Esteban, *Gene Deliv. Ther.* **2008**, *8*, 97-120.

[37] (a) D. K. Kirn, S. H. Thorne, *Nat. Rev. Cancer* **2009**, *9*, 64-71. (b) A. Frentzen, Y. A. Yu, N. Chen, Q. Zhang, S. Weibel, V. Raab, A. A. Szalay, *Proc. Natl. Acad. Sci. USA* **2009**, *106*, 12915-12920. (c) Z. S. Guo, D. L. Bartlett, *Expert Opin. Biol. Ther.* **2004**, *4*, 901-917.

[38] A. L. Epstein, *Gene Ther.* **2009**, *16*, 709-715.

[39] Y.-H H. Lien, L.-W. Lai, *Drugs Aging*. **2002**, *19*, 553-560.

[40] J. K. Wolf, A. D. Jenkins, *Int. J. Oncol*. **2002**, *21*, 461-468.

[41] K. R. Martin, R. L. Klein, H. A. Quigley, *Methods* **2002**, *28*, 267-275.

[42] J. S. Chamberlain, *Hum. Mol. Genet*. **2002**, *11*, 2355-2362.

[43] S. Nayak, R. W. Herzog, *Gene Ther.* **2010**, *17*, 295-304.

[44] (a) L. E. Rosenberg, A. N. Schechter, *Science* **2000**, *287*, 1751-1751. (b) B. Gansbacher, *J. Gene Med*. **2003**, *5*, 261-262. (c) M. E. Gore, *Gene Ther*. **2003**, *10*, 4-4.

[45] (a) http://www.uniqure.com/products/glybera/ (Last visited on July 15th 2013.) (b) http://www.ema.europa.eu/ema/index.jsp?curl=pages/news_and_events/news/2012/07/news_detail_001574.jsp&mid=WC0b01ac058004d5c1 (Last visited on July 15th 2013.)

[46] Z. Peng, *Hum. Gene Ther.* **2005**, *16*, 1016-1027.

[47] S. E. Frew, Sarah, S. M. Sammut, A. F. Shore, J. K. Ramjist, S. Al-Bader, R. Rezaie, A. S. Daar, P. A. Singer, *Nat. Biotechnol.* **2008**, *26*, 37-53.

[48] (a) J. Guo, H. Xin, *Science* **2006***, 314*, 1232-1235. (b) G. Walsh, *Nat. Biotechnol.* **2006**, *24*, 769-776.

[49] A. Aiuti, L. Biasco, S. Scaramuzza, F. Ferrua, M. P. Cicalese, C. Baricordi, F. Dionisio, A. Calabria, S. Giannelli, M. C. Castiello, M. Bosticardo, C. Evangelio, A. Assanelli, M. Casiraghi, S. Di Nunzio, L. Callegaro, C. Benati, P. Rizzardi, D. Pellin, C. Di Serio, M. Schmidt, C. Von Kalle, J. Gardner, N. Mehta, V. Neduva, D. J. Dow, A. Galy, R. Miniero, A. Finocchi, A. Metin, P. Banerjee, J. Orange, S. Galimberti, M. G. Valsecchi, A. Biffi, E. Montini, A. Villa, F. Ciceri, M. G. Roncarolo, L. Naldini, *Science* **2013**, *341*, DOI: 10.1126/science.1233151.

[50] A. Biffi, E. Montini, L. Lorioli, M. Cesani, F. Fumagalli, T. Plati, C. Baldoli, S. Martino, A. Calabria, S. Canale, F. Benedicenti, G. Vallanti, L. Biasco, S. Leo, N. Kabbara, G. Zanetti, W. B. Rizzo, N. A. L. Mehta, M. P. Cicalese, M. Casiraghi, J. J. Boelens, U. Del Carro, D. J. Dow, M. Schmidt, A. Assanelli, V. Neduva, C. Di Serio, E. Stupka, J. Gardner, C. von Kalle, C. Bordignon, Fabio Ciceri, A. Rovelli, M. G. Roncarolo, A. Aiuti, M. Sessa, L. Naldini, *Science* **2013**, *341*, DOI: 10.1126/science.1233158.

[51] http://www.cbsnews.com/8301-204_162-57593387/gene-therapy-using-part-of-hiv-virus-treats-two-rare-childhood-diseases/ (Last visited on July 16th 2013.)

[52] http://www.sciencenews.org/view/generic/id/351534/description/Gene_therapy_treats_children_with_rare_diseases (Last visited on July 16th 2013.)

[53] A. M. L. Lever, *Expert Opin. Ther. Pat.* **1998**, *8*, 983-990.

[54] W. Zhao, M. Kobayashi, M. Hosokawa, P. Seth, *Curr. Genomics* **2002**, *3*, 163-180.

[55] M. A. Mintzer, E. E. Simanek, *Chem. Rev.* **2009**, *109*, 259-302.

[56] R. J. Christie, N. Nishiyama, K. Kataoka, *Endocrinology* **2010**, *151*, 466-473.

[57] (a) R. Srinivas, S. Samanta, A. Chaudhuri, *Chem. Soc. Rev*. **2009**, *38*, 3326-3338. (b) I. S. Zuhorn, J. B. F. N. Engberts, D. Hoekstra, *Eur. Biophys. J.* **2007**, *36*, 349-362. (c) W. L. Li, F. C. Szoka, *Pharm. Res*. **2007**, *24*, 428-449.

[58] (a) T. G. Park, J. H. Jeong, S. W. Kim, *Adv. Drug Deliv. Rev*. **2006**, *58*, 467-486. (b) D. Putnam, *Nat. Mater.* **2006**, *5*, 439-451. (c) M. Thomas, A. M. Klibanov, *Appl. Microbiol. Biotechnol*. **2003**, *62*, 27-34. (d) C. Tros de Ilarduya, Y. Sun, N. Düzgüneç, *Eur. J. Pharm. Sci*. **2010**, *40*, 159-170.

[59] D. J. Glover, H. J. Lipps, D. A. Jans, *Nat. Rev. Genet.* **2005**, *6*, 299-310.

[60] E. Mastrobattista, M. A. E. M. van der Aa, W. E. Hennink, D. J. A. Crommelin, *Nat. Rev. Drug Discov.* **2006**, *5*, 115-121.

[61] A. Elouahabi, J.-M. Ruysschaert, *Mol. Ther*. **2005**, *11*, 336-347.

[62] (a) C. K. Chan, D. A. Jans, *Gene Ther.* **2001**, *8*, 166-171. (b) K. Itaka, K. Kataoka, *Eur. J. Pharm. Biopharm.* **2009**, *71*, 475-483.

[63] (a) M. Kursa, G. F. Walker, V. Roessler, M. Ogris, W. Roedl, R. Kircheis, E. Wagner, *Bioconjugate Chem*. **2003**, *14*, 222-231. (b) R. M. Schiffelers, A. Ansari, J. Xu, Q. Zhou, Q. Tang, G. Storm, G. Molema, P. Y. Lu, P. V. Scaria, M. C. Woodle, *Nucleic Acids Res.* **2004**, *32*, e149. (c) H. Mok, T.-G. Park, *Macromol. Biosci.* **2009**, *9*, 731-743.

[64] T. Kakudo, S. Chaki, S. Futaki, I. Nakase, K. Akaji, T. Kawakami, K. Maruyama, H. Kamiya, H. Harashima, *Biochemistry* **2004**, *43*, 5618-5628.

[65] J.-P. Behr, *Chimia* **1997**, *51*, 34-36.

[66] (a) R. N. Cohen, M. J. Rashkin, X. Wen, F. C. Szoka Jr., *Drug Discov. Today: Technol.* **2005**, *2*, 111-118. (b) A. Mesika, V. Kiss, V. Brumfeld, G. Ghosh, Z. Reich, *Hum. Gene Ther.* **2005**, *16*, 200-208.

[67] (a) J. J. Ludtke, G. Zhang, M. G. Sebestyen, J. A. Wolff *J. Cell Sci.* **1999**, *112*, 2033-2041. (b) K. H. Bremner, L. W. Seymour, A. Logan, M. L. Read, *Bioconjugate Chem.* **2004**, *15*, 152-161. (c) V. Escriou, M. Carriere, D. Scherman, P. Wils, *Adv. Drug Deliv. Rev.* **2003**, *55*, 295-306.

[68] G. F. Walker, C. Fella, J. Pelisek, J. Fahrmeir, S. Boeckle, M. Ogris, E. Wagner, *Mol. Ther.* **2005**, *11*, 418-425.

[69] (a) F. J. Verbaan, C. Oussoren, C. J. Snel, D. J. A. Crommelin, W. E. Hennink, G. Storm, *J. Gene Med.* **2004**, *6*, 64-75. (b) J. H. Jeong, S. W. Kim, T. G. Park, *Prog. Polym. Sci.* **2007**, *32*, 1239-1274.

[70] K. Knop, R. Hoogenboom, D. Fischer, U. S. Schubert, *Angew. Chem. Int. Ed.* **2010**, *49*, 6288-6308.

[71] P. L. Felgner, T. R. Gadek, M. Holm, R. Roman, H. W. Chan, M. Wenz, J. P. Northrop, G. M. Ringold, M. Danielsen, *Proc. Natl. Acad. Sci. USA* **1987**, *84*, 7413-7417.

[72] (a) D. Zhi, S. Zhang, S. Cui, Y. Zhao, Y. Wang, D. Zhao, *Bioconjugate Chem.* **2013**, *24*, 487-519. (b) D. Zhi, S. Zhang, B. Wang, Y. Zhao, B. Yang, S. Yu, *Bioconjugate Chem.* **2010**, *21*, 563-577.

[73] G. Basha, T. I. Novobrantseva, N. Rosin, Y. Y. C. Tam, I. M. Hafez, M. K. Wong, T. Sugo, V. M. Ruda, J. Qin, B. Klebanov, M. Ciufolini, A. Akinc, Y. K. Tam, M. J. Hope, P. R. Cullis, *Mol. Ther.* **2011**, *19*, 2186-2200.

[74] W. Liang, J. K. W. Lam, *Endosomal Escape Pathways for Non-Viral Nucleic Acid Delivery Systems* in *Molecular Regulation of Endocytosis* (Ed.: Brian Ceresa), InTechOpen, **2012**.

[75] P. P. Karmali, A. Chaudhuri, *Med. Res. Rev*. **2007**, *27*, 696-722.

[76] Z. Ma, J. L. Zhang, S. Alber, J. Dileo, Y. Negishi, D. Stolz, S. Watkins, L. Huang, B. Pitt, S. Li, *Am. J. Respir. Cell Mol. Biol.* **2002**, *27*, 151-159.

[77] X. Gao, L. Huang, *Biochem. Biophys. Res. Commun*. **1991**, *179*, 280-285.

[78] J.-P. Behr, B. Demeneix, J. P. Loeffler, J. Perez-Mutul, *Proc. Natl. Acad. Sci. USA* **1989**, *86*, 6982-6986.

[79] J.-S. Remy, C. Sirlin, P. Vierling, J.-P. Behr, *Bioconjugate Chem*. **1994**, *5*, 647-654.

[80] (a) J. Leblond, N. Mignet, C. Largeau, J. Seguin, D. Scherman, J. Herscovici, *Bioconjugate Chem.* **2008**, *19*, 306-314. (b) J. Leblond, N. Mignet, C. Largeau, M.-V. Spanedda, J. Seguin, D. Scherman, J. Herscovici, *Bioconjugate Chem.* **2007**, *18*, 484-493. (c) J. Leblond, N. Mignet, L. Leseurre, C. Largeau, M. Bessodes, D. Scherman, J. Herscovici, *Bioconjugate Chem.* **2006**, *17*, 1200-1208.

[81] (a) M. Sainlos, M. Hauchecorne, N. Oudrhiri, S. Zertal-Zidani, A. Aissaoui, J.-P. Vigneron, J.-M. Lehn, P. Lehn, *ChemBioChem* **2005**, *6*, 1023-1033. (b) L. Desigaux, M.

Sainlos, O. Lambert, R. Chevre, E. Letrou-Bonneval, J.-P. Vigneron, P. Lehn, J.-M. Lehn, B. Pitard, *Proc. Natl. Acad. Sci. USA* **2007**, *104*, 16534-16539.

[82] A. Gissot, M. Camplo, M. W. Grinstaff, P. Barthelemy, *Org. Biomol. Chem.* **2008**, *6*, 1324-1333.

[83] K. Wang, X. Yan, Y. Cui, Q. He, J. Li, *Bioconjugate Chem*. **2007**, *18*, 1735-1738.

[84] (a) G. Zuber, L. Zammut-Italiano, E. Dauty, J.-P. Behr, *Angew. Chem. Int. Ed.* **2003**, *42*, 2666-2669. (b) G. Zuber, M. Dontenwill, J.-P. Behr, *Mol. Pharm.* **2009**, 6, 1544-1552.

[85] W. D. Henner, I. Kleber, R. Benzinger, *J. Virol.* **1973**, *12*, 741-747.

[86] O. Boussif, F. Lezoualc'h, M. A. Zanta, M. D. Mergny, D. Scherman, B. Demeneix, J.-P. Behr, *Proc. Natl. Acad. Sci. USA* **1995**, *92*, 7297-7301.

[87] A. C. Hunter, *Adv. Drug Deliv. Rev.* **2006**, *58*, 1523-1531.

[88] U. K. Laemmli, *Proc. Natl. Acad. Sci. USA*, **1975**, *72*, 4288-4292.

[89] A. Akinc, R. Langer, *Biotechnol. Bioeng*. **2002**, *78*, 503-508.

[90] P. Van de Wetering, J.-Y. Cherng, H. Talsma, W. E. Hennink, *J. Control. Rel.* **1997**, *49*, 59-69. (b) P. Van de Wetering, E. E. Moret, N. M. E. Schuurmans-Nieuwenbroek, M. J. Van Steenbergen, W. E. Hennink, *Bioconjugate Chem.* **1999**, *10*, 589-597.

[91] P. Van de Wetering, N. M. E. Schuurmans-Nieuwenbroek, W. E. Hennink, G. Storm, *J. Gene Med.* **1999**, *1*, 156-165.

[92] M. Wang, S. Sun, K. A. Alberti, Q. Xu, *ACS Synth. Biol.* **2012**, *1*, 403-407.

[93] J. J. Green, R. Langer, D. G. Anderson, *Acc. Chem. Res.* **2008**, *41*, 749-759.

[94] M. Neu, D. Fischer, T. Kissel, *J. Gene Med.* **2005**, *7*, 992-1009.

[95] (a) D. Wang, A. S. Narang, M. Kotb, A. O. Gaber, D. D. Miller, S. W. Kim, R. I. Mahato, *Biomacromolecules* **2002**, *3*, 1197-1207. (b) S.-O. Han, R. I. Mahato, S. W. Kim, *Bioconjugate Chem.* **2001**, *12*, 337-345.

[96] M. Thomas, A. M. Klibanov, *Proc. Natl. Acad. Sci. USA* **2002**, *99*, 14640-14645.

[97] S. Patnaik, K. C. Gupta, *Expert Opin. Drug Deliv.* **2013**, *10*, 215-228.

[98] B. Demeneix, Z. Hassani, J.-P. Behr, *Curr. Gene Ther.* **2004**, *4*, 445-455.

[99] C. Biesa, C.-M. Lehra, J. F. Woodley. *Adv. Drug Deliv. Rev.* **2004**, *56*, 425-435.

[100] H. Zhang, Y. Ma, X.-L. Sun, *Med. Res. Rev.* **2010**, *30*, 270-289.

[101] S. Mao, W. Sun, T. Kissel, *Adv. Drug Deliv. Rev.* **2010**, *62*, 12-27.

[102] For a recent survey on the use of naturally-occurring carbohydrate polymers in gene delivery, see: A. Sizovs, P. M. McLendon, S. Srinivasachari, T. M. Reineke, *Top. Curr. Chem.* **2010**, *296*, 131-190.

[103] K. Raemdonck, T. F. Martens, K. Braeckmans, J. Demeester, S. C. De Smedt, *Adv. Drug Deliv. Rev.* **2013**, *65*, doi 10.1016/j.addr.2013.05.002.

[104] (a) L. Wightman, R. Kircheis, V. Rossler, S. Carotta, R. Ruzicka, M. Kursa, E. Wagner, *J. Gene Med.* **2001**, *3*, 362-372. (b) Y. H. Choi, F. Liu, J.-S. Kim, Y. K. Choi, J.-S. Park, S. W. Kim, *J. Control. Release* **1998**, *54*, 39-48. (c) K. M. Kitchens, M. E. H. El-Sayed, H. Ghandehari, *Adv. Drug Deliv. Rev.* **2005**, *57*, 2163-2176.

[105] S. Aoshima, S. Kanaoka, *Chem. Rev.* **2009**, *109*, 5245-5287.

[106] S. M. Moghimi, P. Symonds, J. C. Murray, A. C. Hunter, G. Debska A. Szewczyk, *Mol. Ther.* **2005**, *11*, 990-995.

[107] C. Ortiz Mellet, J. M García Fernández, J. M. Benito, *Carbohydr. Chem.* **2012**, *38*, 338-375.

[108] S. Höbel, A. Loos, D. Appelhans, S. Schwarz, J. Seidel, B. Voit, A. Aigner, *J. Control. Release* **2011**, *149*, 146-158.

[109] (a) S. P. Strand, M. M. Issa, B. E. Christensen, K. M. Vårum, P. Artursson, *Biomacromolecules* **2008**, *9*, 3268-3276. (b) S. P. Strand, S. Lelu, N. K. Reitan, C. de Lange Davies, P. Artursson, K. M. Vårum, *Biomaterials* **2010**, *31*, 975-987.

[110] M. Ahmed, X. Jiang, Z. Deng, R. Narain, *Bioconjugate Chem.* **2009**, *20*, 2017-2022.

[111] M. Ahmed, Z. Deng, R. Narain, *ACS Appl. Mater. Interfaces* **2009**, *9*, 1980-1987.

[112] J.-M. Li, M.-X. Zhao, H. Su, Y.-Y. Wang, C.-P. Tan, L.-N. Ji, Z.-W. Mao, *Biomaterials* **2011**, *32*, 7978-7987.

[113] (a) J. Li, X. J. Loh, *Adv. Drug. Deliv. Rev.* **2008**, *60*, 1000-1017. (b) J. J. Li, F. Zhao, J. Li, *Appl. Microbiol. Biotechnol.* **2011**, *90*, 427-443.

[114] (a) G. Y. Wu, C. H. Wu, *J. Biol. Chem.* **1987**, *262*, 4429-4432. (b) G. Y. Wu, C. H. Wu, *J. Biol. Chem.* **1988**, *263*, 14621-14624.

[115] S.-J. Kim, H. Ise, M. Goto, K. Komura, C.-S. Cho, T. Akaike, *Biomaterials* **2011**, *32*, 3471-3480.

[116] D. B. Rozema, D. L. Lewis, D. H. Wakefield, S. C. Wong, J. J. Klein, P. L. Roesch, S. L. Bertin, T. W. Reppen, Q. Chu, A. V. Blokhin, J. E. Hagstrom, J. A. Wolff, *Proc. Natl. Acad. Sci USA* **2007**, *104*, 12982-12987.

[117] (a) M.-A. Zanta, O. Boussif, A. Adib, J.-P. Behr, *Bioconjugate Chem.* **1997**, *8*, 839-844. (b) S. S. Diebold, M. Kursa, E. Wagner, M. Cotten, M. Zenke, *J. Biol. Chem.* **1999**, *274*, 19087-19094. (c) T. Bettinger, J.-S. Remy, P. Erbacher, *Bioconjugate Chem.* **1999**, *10*, 558-561.

[118] (a) P. Erbacher, A. C. Roche, M. Monsigny, P. Midoux, *Bioconjugate Chem.* **1995**, *6*, 401-410. (b) J. C. Perales, T. Ferkol, H. Beegen, O. D. Ratnoff, R. W. Hanson, *Proc. Natl. Acad. Sci. USA* **1994**, *91*, 4086-4090. (c) T. Ferkol, J. C. Perales, F. Mularo, R. W. Hanson, *Proc. Natl. Acad. Sci. USA* **1996**, *93*, 101-105.

[119] H. Arima, S. Yamashita, Y. Mori, Y. Hayashi, K. Motoyama, K. Hattori, T. Takeuchi, H. Jono, Y. Ando, F. Hirayama, K. Uekama, *J. Control. Release* **2010**, *146*, 106-117.

[120] (a) K. Motoyama, Y. Nakashima, Y. Aramaki, F. Hirayama, K. Uekama, H. Arima, *J. Drug Deliv.* **2011**, Article ID 476137, doi:10.1155/2011/476137. (b) T. Montier, P. Delépine, T. Benvegnu, V. Ferrières, M.-L. Miramon, S. Dagorn, C. Guillaume, D. Plusquellec, C. Férec, *Blood Cells Mol. Dis.* **2004**, *32*, 271-282. (c) M. Hashida, S. Kawakami, F. Yamashita, *Chem. Pharm. Bull.* **2005**, *53*, 871-880.

[121] (a) H. Arima, Y. Chihara, M. Arizono, S. Yamashita, K. Wada, F. Hirayama, K. Uekama, *J. Control. Release* **2006**, *116*, 64-74. (b) Y. Chihara, H. Arima, M. Arizono, K. Wada, F. Hirayama, K. Uekama, *J. Incl. Phenom. Macrocycl. Chem.* **2006**, *56*, 89-93.

[122] C. Rondanino, M. T. Bousser, M. Monsigny, A. C. Roche, *Glycobiology* **2003**, *13*, 509-519.

[123] (a) A. C. Roche, I. Fajac , S. Grosse, N. Frison, C. Rondanino, R. Mayer, M. Monsigny, *Cell. Mol. Life Sci.* **2003**, *60*, 288-297. (b) M. Monsigny, C. Rondanino, E. Duverger, I. Fajac, A.-C. Roche, *Biochim. Biophys. Acta* **2004**, *1673*, 94-103.

[124] (a) S. Grosse, A. Tremeau-Bravard, Y. Aron, P. Briand, I. Fajac, *Gene Ther.* **2002**, *9*, 1000-1007. (b) M. Hashimoto, M. Morimoto, H. Saimoto, Y. Shigemasa, T. Sato, *Bioconjugate Chem.* **2006**, *17*, 309-316.

[125] S. Grosse, G. Thévenot, M. Monsigny, I. Fajac, *J. Gene Med.* **2006**, *8*, 845-851.

[126] (a) H. Akita, T. Masuda, T. Nishio, K. Niikura, K. Ijiro, H. Harashima, *Mol. Pharm.* **2011**, *8*, 1436-1442. (b) T. Masuda, H. Akita, T. Nishio, K. Niikura, K. Kogure, K. Ijiro, H. Harashima, *Biomaterials* **2008**, *29*, 709-723.

[127] M. Breton, J.-F. Berret, C. Bourgaux, T. Kral, M. Hof, C. Pichon, M. Bessodes, D. Scherman, N. Mignet, *Langmuir* **2011**, *27*, 12336-12345.

[128] P. Vicennati, A. Giuliano, G. Ortaggi, A. Masotti, *Curr. Med. Chem.* **2008**, *15*, 2826-2839.

[129] M. Huang, C.-W. Fong, E. Khor, L.-Y. Lim, *J. Control. Release* **1999**, *106*, 391-406.

[130] C. Troiber, E. Wagner, *Bioconjugate Chem.* **2011**, *22*, 1737-1752.

[131] C. Lin, J. F. J. Engbersen, *J. Control. Release* **2008**, *132*, 267-272.

[132] Y. Liu, L. Wenning, M. Lynch, T. M. Reineke, *J. Am. Chem. Soc.* **2004**, *126*, 7422-4723.

[133] M. Metzke, N. O'Connor, S. Maiti, E. Nelson, Z. Guan, *Angew. Chem. Int. Ed.* **2005**, *44*, 6529-6533.

[134] N. P. Ingle, B. Malone, T. M. Reineke, *Trends Biotechnol.* **2011**, *29*, 443-453.

[135] (a) Y. Liu, T. M. Reineke, *J. Am. Chem. Soc.* **2005**, *127*, 3004-3015. (b) Y. Liu, T. M. Reineke, *Bioconjugate Chem.* **2006**, *17*, 101-108.

[136] Y. Liu, T. M. Reineke, *Biomacromolecule*s **2010**, *11*, 316-325.

[137] C.-C. Lee, Y. Liu, T. M. Reineke, *Bioconjugate Chem.* **2008**, *19*, 428-440.

[138] Y. Liu, T. M. Reineke, *Bioconjugate Chem.* **2007**, *18*, 19-30.

[139] K. M. Fichter, N. P. Ingle, P. M. McLendon, T. M. Reineke, *ACS Nano* **2013**, *7*, 347-364.

[140] http://www.techulon.com/products (Last visited on July 15th 2013.)

[141] T. M. Reineke, M. E. Davis, *Bioconjugate Chem.* **2003**, *14*, 247-254.

[142] (a) S. Srinivasachari, Y. Liu, G. Zhang, L. Prevette, T. M. Reineke, *J. Am. Chem. Soc.* **2006**, *125*, 8176-8184. (b) S. Srinivasachari, Y. Liu, L. Prevette, T. M. Reineke, *Biomaterials* **2007**, *28*, 2885-2898.

[143] R. D. Lins, C. S. Pereira, P. H. Hünenberger, *Proteins* **2004**, *55*, 177-186.

[144] M. Meldal, C. W. Tornøe, *Chem. Rev.* **2008**, *108*, 2952-3015.

[145] M. Ahmed, R. Narain, *Prog. Polym. Sci.* **2013**, *38*, 767-790.

[146] (a) M. Ahmed, R. Narain, *Biomaterials* **2011**, *32*, 5279-5290. (b) M. Ahmed, R. Narain, *Biomaterials* **2012**, *33*, 3990-4001.

[147] (a) A. Villiers, *Compt. Rend*. **1891**, *112*, 412-437. (b) A. Villiers, *Compt. Rend*. **1891**, *112*, 536-538.

[148] (a) F. Schardinger, *Z. Unters. Nahr. Genussm*. **1903**, *6*, 865-880. (b) F. Schardinger, *Wiener Klin. Wochenschr*. **1904**, *17*, 207-209. (c) F. Schardinger, *Zentralbl. Bakteriol. Parasitenkd. Abt. II* **1905**, *14*, 772-781. (d) F. Schardinger, *Zentralbl. Bakteriol. Parasitenkd. Abt. II* **1911**, *29*, 188-197.

[149] (a) K. Freudenberg, M. Meyer-Delius, *Ber. Chem.* **1938**, *71*, 1596. (b) K. Freudenberg, E. Schaaf, G. Dumpert, T. Ploetz, *Naturwiss* **1939**, *27*, 850.

[150] K. Freudenberg, F. Cramer, H. Plieninger, German Pat. 895,769 (**1953**).

[151] (a) *Cyclodextrins and their complexes* (Ed.: H. Doziuk), Wiley-VCH, Weinheim, **2006**. (b) T. Loftsson, D. Duchêne, *Int. J. Pharm.* **2007**, *329*, 1. (c) *Cyclodextrins in pharmacy* (Eds.: K. H. Frömming, J. Szejtli), Kluwer Academic Publishers, Dordrecht, **1994**.

[152] The effects derived from CD-drug interactions and their relevance in the pharmaceutical industry have been covered in excellent comprehensive accounts. See for instance: (a) T. Loftsson, M. E. Brewster, *J. Pharm. Pharmacol.* **2010**, *62*, 1607-1621. (b) *Cyclodextrins in pharmaceutics, cosmetics and biomedicine* (Ed.: E. Bilensoy), Wiley-VCH, Weinheim, **2011**.

[153] (a) F. J. Otero-Espinar, A. Luzardo-Álvarez, J. Blanco-Méndez, *Mini Rev. Med. Chem.* **2010**, *10*, 715-725. (b) C. Alvarez-Lorenzo, B. Blanco-Fernandez, A. M. Puga, A. Concheiro, *Adv. Drug Deliv. Rev.* **2013**, *65*, doi: 10.1016/j.addr.2013.04.016.

[154] M. E. Davis, M. E. Brewster, *Nat. Rev. Drug Discov.* **2004**, *3*, 1023-1035.

[155] (a) H. M. C. Marques, J. Hadgraft, I. W. Kellaway, G. Taylor, *Int. J. Pharm.* **1991**, *77*, 303-307. (b) H.-Y. Li, P. C. Seville, I. J. Williamson, J. C. Birchall, *J. Gene Med.* **2005**, *7*, 1035-1039. (c) N. Jessel, M. Oulad-Abdelghani, F. Meyer, P. Lavalle, Y. Haîkel, P. Schaaf, J.-C. Voegel, *Proc. Natl. Acad. Sci. USA* **2006**, *103*, 8618-8621. (d) X. Zhang, K. K. Sharma, M. Boeglin, J. Ogier, D. Mainard, J.-C. Voegel, Y. Mély, N. Benkirane-Jessel, *Nano Lett.* **2008**, *8*, 2432-2436.

[156] H. Gonzalez, S. J. Hwang, M. E. Davis, *Bioconjugate Chem.***1999**, *10*, 1068-1074.

[157] (a) S. J. Hwang, N. C. Bellocq, M. E. Davis, *Bioconjugate Chem.* **2001**, *12*, 280-290. (b) T. M. Reineke, M. E. Davis, *Bioconjugate Chem.* **2003**, *14*, 255-261. (c) S. R. Popielarski, S. Mishra, M. E. Davis, *Bioconjugate Chem.* **2003**, *14*, 672-678. (d) M. E. Davis, S. H. Pun, N. C. Bellocq, T. M. Reineke, S. R. Popielarski, S. Mishra, J. D. Heidel, *Curr. Med. Chem.* **2004**, *11*, 179-197.

[158] S. Mishra, P. Webster, M. E. Davis, *Eur. J. Cell Biol.* **2004**, *83*, 97-111.

[159] (a) N. C. Bellocq, S. H. Pun, G. S. Jensen, M. E. Davis, *Bioconjugate Chem.* **2003**, *14*, 1122-1132. (b) D. W. Bartlett, M. E. Davis, *Bioconjugate Chem.* **2007**, *18*, 456-468.

[160] (a) S. H. Pun, F. Tack, C. C. Bellocq, J. Cheng, B. H. Grubbs, G. S. Jensen, M. E. Davis, M. Brewster, M. Janicot, B. Janssens, W. Floren, A. Bakker, *Cancer Biol. Ther.* **2004**, *3*, 641-650. (b) S. Hu-Lieskovan, J. D. Heidel, D. W. Bartlett, M. E. Davis, T. J. Triche, *Cancer Res.* **2005**, *65*, 8984-8992. (c) D. W. Bartlett, M. E. Davis, *Biotechnol. Bioeng.* **2008**, *99*, 975-985.

[161] (a) J. D. Heidel, Z. Yu, J. Y. Liu, S. M. Rele, Y. Liang, R. K. Zeidan, D. J. Kornbrust, M. E. Davis, *Proc. Natl. Acad. Sci. USA* **2007**, *104*, 5715-5721. (b) M. E. Davis, J. E. Zuckerman, C. H. J. Choi, D. Seligson, A. Tolcher, C. A. Alabi, Y. Yen, J. D. Heidel, A. Ribas, *Nature* **2010**, *464*, 1067-1070.

[162] For the most recent updates, see: http://www.arrowheadresearch.com/programs/calaa-01 (Last visited on July 16th 2013) or http://clinicaltrials.gov/ct2/show/NCT00689065 (Last visited on July 16th 2013).

[163] S. Srinivasachari, T. M. Reineke, *Biomaterials* **2009**, *30*, 928-938.

[164] (a) K. Wada, H. Arima, T. Tsutsuma, Y. Chihara, K. Hattori, F. Hirayama, K. Uekama, *J. Control. Release* **2005**, *104*, 397-413. (b) Y. Hayashi, Y. Mori, S. Yamashita, K. Motoyama, T. Higashi, H. Jono, Y. Ando, H. Arima, *Mol. Pharm.* **2012**, *9*, 1645-1653.

[165] (a) F. Zhao, H. Yin, Z. Zhang, J. Li, *Biomacromolecules* **2013**, *14*, 476-484. (b) Q.-Y. Jiang, L.-H. Lai, J. Shen, Q.-Q. Wang, F.-J. Xu, G.-P. Tang, *Biomaterials* **2011**, *32*, 7253-7262. (c) M. Liu, Z. H. Li, F. J. Xu, L. H. Lai, Q.-Q. Wang, G.-P. Tang, W. T. Yang, *Biomaterials* **2012**, *33*, 2240-2250.

[166] (a) T. Ooya, H. S. Choi, A. Yamashita, N. Yui, Y. Sugaya, A. Kano, A. Maruyama, H. Akita, R. Ito, K. Kogure, H. Harashima, *J. Am. Chem. Soc.* **2006**, *128*, 3852-3853. (b) J.

Li, C. Yang, H. Li, X. Wang, S. H. Goh, J. L. Ding, D. Y. Wang, K. W. Leong, *Adv. Mater.* **2006**, *18*, 2969-2974. (c) J. Li, X. J. Xian, *Adv. Drug Deliv. Rev.* **2008**, *60*, 1000-1017. (d) Y. Zhou, H. Wang, C. Wang, Y. Li, W. Lu, S. Chen, J. Luo, Y. Jiang, J. Chen, *Mol. Pharm.* **2012**, *9*, 1067-1076.

[167] S.-A. Cryan, A. Holohan, R. Donohue, R. Darcy, C. M. O'Driscoll, *Eur. J. Pharm. Sci.* **2004**, *21*, 625-633.

[168] (a) N. Mourtzis, K. Eliadou, C. Aggelidou, V. Sophianopoulou, I. M. Mavridis, K. Yannakopoulou, *Org. Biomol. Chem.* **2007**, *5*, 125-131. (b) N. Mourtzis, M. Paravatou, I. M. Mavridis, M. L. Roberts, K. Yannakopoulou, *Chem. Eur. J.* **2008**, *14*, 4188-4200.

[169] S. Srinivasachari, K. M. Fichter, T. M. Reineke, *J. Am. Chem. Soc.* **2008**, *130*, 4618-4627.

[170] V. Bennevault-Celton, A. Urbach, O. Martin, C. Pichon, P. Guégan, P. Midoux, *Bioconjugate Chem.* **2011**, *22*, 2404-2414.

[171] For a recent review dealing with the concept of ''pre-organized'' systems in gene delivery, see: C. Ortiz Mellet, J. M. Benito, J. M. García Fernández, *Chem. Eur. J.* **2010**, *16*, 6728-6742.

[172] (a) S.-A. Cryan, R. Donohue, B. J. Ravoo, R. Darcy, C. M. O'Driscoll, *J. Drug. Deliv. Sci. Technol.* **2004**, *14*, 57-62. (b) A. McMahon, E. Gomez, R. Donohue, D. Forde, R. Darcy, C. M. O'Driscoll, *J. Drug. Deliv. Sci. Technol.* **2008**, *18*, 303-307.

[173] J. M. García Fernández, J. M. Benito, C. Ortiz Mellet, *Pure Appl. Chem.* **2013**, *85*, doi: 10.1351/PAC-CON-12-10-13.

[174] A. Díaz-Moscoso, P. Balbuena, M. Gómez-García, C. Ortiz Mellet, J. M. Benito, L. Le Gourriérec, C. Di Giorgio, P. Vierling, A. Mazzaglia, N. Micali, J. Defaye, J. M. García Fernández, *Chem. Commun.* **2008**, 2001-2003.

[175] A. Gadelle, J. Defaye, *Angew. Chem. Int. Ed.* **1991**, *30*, 78-80.

[176] J. L. Jiménez Blanco, P. Bootello, J. M. Benito, C. Ortiz Mellet, J. M. García Fernández, *J. Org. Chem.* **2006**, *71*, 5136-5143.

[177] A. Díaz-Moscoso, L. Le Gourriérec, M. Gómez-García, J. M. Benito, P. Balbuena, F. Ortega-Caballero, N. Guilloteau, C. Di Giorgio, P. Vierling, J. Defaye, C. Ortiz Mellet, J. M. García Fernández, *Chem. Eur. J.* **2009**, *15*, 12871-12888.

[178] F. Ortega-Caballero, C. Ortiz Mellet, L. Le Gourriérec, N. Guilloteau, C. Di Giorgio, P. Vierling, J. Defaye, J. M. García Fernández, *Org. Lett.* **2008**, *10*, 5143-5146.

[179] C. Bienvenu, A. Martinez, J. L. Jimenez Blanco, C. Di Giorgio, P. Vierling, C. Ortiz Mellet, J. Defaye, J. M. García Fernández, *Org. Biomol. Chem.* **2012**, *10*, 5570-5581.

[180] (a) A. Méndez-Ardoy, N. Guilloteau, C. Di Giorgio, P. Vierling, F. Santoyo-Gonzalez, C. Ortiz Mellet, J. M. García Fernández, *J. Org. Chem.* **2011**, *76*, 5882-5894. (b) A. Méndez-Ardoy, M. Gómez-García, C. Ortiz Mellet, N. Sevillano, M. D. Girón, R. Salto, F. Santoyo-González, J. M. García Fernández, *Org. Biomol. Chem.* **2009**, *7*, 2681-2684.

[181] A. Méndez-Ardoy, K. Urbiola, C. Aranda, C. Ortiz-Mellet, J. Manuel García-Fernández, C. Tros de Ilarduya, *Nanomedicine* **2011**, *6*, 1697-1707.

[182] A. Díaz-Moscoso, D. Vercauteren, J. Rejman, J. M. Benito, C. Ortiz Mellet, S. C. de Smedt, J. M. García Fernández, *J. Control. Release* **2010**, *143*, 318-325.

[183] (a) A. Díaz-Moscoso, N. Guilloteau, C. Bienvenu, A. Méndez-Ardoy, J. L. Jiménez Blanco, J. M. Benito, L. Le Gourriérec, C. Di Giorgio, P. Vierling, J. Defaye, C. Ortiz Mellet, J. M. García Fernández, *Biomaterials* **2011**, *32*, 7263-7273. (b) N. Symens, A. Méndez-Ardoy, A. Díaz-Moscoso, E. Sánchez-Fernández, K. Remaut, J. Demeester, J. M. García Fernández, S. C. De Smedt, J. Rejman, *Bioconjugate Chem.* **2012**, *23*, 1276-1289.

[184] K. Chmurski, J. Defaye, *Supramol. Chem*. **2000**, *12*, 221-224.

[185] (a) M. Gómez-García, J. M. Benito, D. Rodríguez-Lucena, J.-X. Yu, K. Chmurski, C. Ortiz Mellet, R. Gutiérrez Gallego, A. Maestre, J. Defaye, J. M. García Fernández, *J. Am. Chem. Soc.* **2005**, *127*, 7970-7971. (b) M. Gómez-García, J. M. Benito, R. Gutiérrez-Gallego, A. Maestre, C. Ortiz Mellet, J. M. García Fernández, J. L. Jiménez Blanco, *Org. Biomol. Chem.* **2010**, *8*, 1849-1860. (c) M. Gómez-García, J. M. Benito, A. P. Butera, C. Ortiz Mellet, J. M. García Fernández, J. L. Jiménez Blanco, *J. Org. Chem.* **2012**, *77*, 1273-1288.

[186] D. M. Kneeland, K. Ariga, V. M. Lynch, C. Y. Huang, E. V. Anslyn, *J. Am. Chem. Soc*. **1993**, *115*, 10042-10055.

[187] J. L. Jiménez Blanco, C. Sainz Barría, J. M. Benito, C. Ortiz Mellet, J. Fuentes, F. Santoyo-González, J. M. García Fernández, *Synthesis* **1999**, 1907-1914.

[188] A. Díaz-Moscoso, A. Méndez-Ardoy, F. Ortega-Caballero, J. M. Benito, C. Ortiz Mellet, J. Defaye, T. M. Robinson, A. Yohannes, V. A. Karginov, J. M. García Fernández, *ChemMedChem* **2011**, 6, 181-192.

[189] O. S. Tee, C. Mama, X.-X. Du, *J. Org. Chem.* **1990**, *55*, 3603-3609.

[190] C. Ortiz Mellet, J. M. García Fernández, H. Law, K. Chmurski, J. M. Benito, J. Defaye, M. L. O'Sullivan, H. N. Caro, *Chem. Eur. J.* **1998**, *4*, 2523-2531.

[191] D. Duchêne, G. Ponchel, D. Wouessidjewe, *Adv. Drug Deliv. Rev.* **1999**, *36*, 29-40.

[192] Y. Kawabata, M. Matsumoto, M. Tanaka, H. Takahashi, Y. Irinatsu, S. Tamara, W. Tagaki, H. Nakahara, K. Fukuda, *Chem. Lett.* **1986**, *11*, 1933-1934.

[193] (a) B. J. Ravoo, R. Darcy, *Angew. Chem. Int. Ed.* **2000**, *39*, 4324-4326. (b) A. Mazzaglia, R. Donohue, B. J. Ravoo, R. Darcy, *Eur. J. Org. Chem.* **2001**, 1715-1721. (c) P. Falvey, C. W. Lim, R. Darcy, T. Revermann, U. Karst, M. Giesbers, A. T. M. Marcelis, A. Lazar, A. W. Coleman, D. N. Reinhoudt, B. J. Ravoo, *Chem. Eur. J.* **2005**, *11*, 1171-1180.

[194] (a) D. Nolan, R. Darcy, B. J. Ravoo, *Langmuir* **2003**, *19*, 4469-4472. (b) B. J. Ravoo, J. C. Jacquier, G. Wenz, *Angew. Chem. Int. Ed.* **2003**, *42*, 2066-2070. (c) A. Mazzaglia, D. Forde, D. Garozzo, P. Malvagna, B. J. Ravoo, R. Darcy, *Org. Biomol. Chem.* **2004**, *2*, 957-960.

[195] F. Sallas, R. Darcy, *Eur. J. Org. Chem.* **2008**, 957-969.

[196] (a) J. N. Israelachvilli, *Intermolecular and Surface Forces: With Application to Colloidal and Biological Systems*, AcademicPress, New York, **1985**. (b) J.-H.Fuhrhop, J. Koning, *Membranes and Molecular Assemblies: The Synkinetic Approach*, Royal Society of Chemistry, Cambridge, **1994**.

[197] S. McNicholas, A. Rencurosi, L. Lay, A. Mazzaglia, L. Sturiale, M. Perez, R. Darcy, *Biomacromolecules* **2007**, *8*, 1851-1857.

[198] (a) R. Darcy, B. J. Ravoo, A. Mazzaglia, E. Kan, C. M. O'Driscoll, *Proceedings Twelfth International Symposium on Cyclodextrins*, Kluwer Academic, Dordrecht, **2004**, 665. (b) R. Darcy, L. J. Penkler, B. J. Ravoo, *PCT/IE01/00057*, **2002**.

[199] T. Sukegawa, T. Furuike, K. Niikura, A. Yamagishi, K. Monde, S.-I. Nishimura, *Chem. Commun.* **2002**, 430-431.

[200] C. Byrne, F. Sallas, D. K. Rai, J. Ogier, R. Darcy, *Org. Biomol. Chem.* **2009**, *7*, 3763-3771.

[201] V. Villari, A. Mazzaglia, R. Darcy, C. M. O'Driscoll, N. Micali, *Biomacromolecules* **2013**, *14*, 811-817.

[202] R. Donohue, A. Mazzaglia, B. J. Ravoo, R. Darcy, *Chem. Commun.* **2002**, 2864-2865.

[203] A. Méndez-Ardoy, M. Gómez-García, A. Gèze, J.-L. Putaux, D. Wouessidjewe, C. Ortiz Mellet, J. Defaye, J. M. García Fernández, J. M. Benito, *Med. Chem.* **2012**, *8*, 524-532.

[204] P. L. Du Noüy *J. Gene Physiol.* **1925**, *7*, 625-633.

[205] (a) M. Wilhelm, C. L. Zhao, Y. Wang, R. Xu, M. A. Winnik, G. R. Jean Luc Mura, M. D. Croucher, *Macromolecules* **1991**, *24*, 1033-1040. (b) F. K. Wolf, A. M. Hofmann, H. Frey, *Macromolecules* **2010**, *43*, 3314-3324. (c) A. M. Hofmann, F. Wurm, H. Frey, *Macromolecules* **2011**, *44*, 4648-4657. (d) C.-L. Zhao, M. A. Winnik, *Langmuir* **1990**, *6*, 514-516.

[206] (a) Y.-C. Lin, P.-I. Wang, S.-W. Kuo, *Soft Matter* **2012**, *8*, 9676-9684. (b) K. A. Udachin, J. A. Ripmeester, *J. Am. Chem. Soc.* **1998**, *120*, 1080-1081. (c) A. Muñoz de la Peña, T. T. Ndou, J. B. Zung, K. L. Greene, D. H. Live, I. M. Warner, *J. Am. Chem. Soc.* **1991**, *113*, 1572-1577. (d) G. Nelson, I. M. Warner, *J. Phys. Chem.* **1990**, *94*, 576-581.

[207] Y. W. Cho, J.-D. Kim, K. Park, *J. Pharm. Pharmacol*. **2003**, *55*, 721-734.

[208] S. Guo, L. Huang, *J. Nanomater.* **2011**, *2011*, ID 742895.

[209] P. Midoux, G. Breuzard, J. P. Gomez, C. Pichon, *Curr. Gene Ther.* **2008**, *8*, 335-352.

[210] (a) C. Gonçalves, E. Mennesson, R. Fuchs, J. P. Gorvel, P. Midoux, C. Pichon, *Mol. Ther*. **2004**, *10*, 373-385. (b) J. Rejman, A. Bragonzi, M. Conese, *Mol. Ther.* **2005**, *12*, 468-474. (c) K. von Gersdorff, N. N. Sanders, R. Vandenbroucke, S. C. De Smedt, E. Wagner, M. Ogris, *Mol. Ther.* **2006**, *14*, 745-753.

[211] N. Ferrer-Miralles, E. Vázquez, A. Villaverde, *Trends Biotechnol.* **2008**, *5*, 267-275.

[212] C. M. Carr, C. Chaudhry, P. S. Kim, *Proc. Natl. Acad. Sci. USA* **1997**, *94*, 14306-14313.

[213] Y. Xu, F. C. Szoka, *Biochemistry* **1996**, *35*, 5616-5623.

[214] (a) Y. Obata, S. Tajima, S. Takeoka, *J. Control. Release* **2010**, *142*, 267-276. (b) S. C. Semple, A. Akinc, J. Chen, A. P. Sandhu, B. L. Mui, C. K. Cho, D. W. Sah, D. Stebbing, E. J. Crosley, E. Yaworski, I. M. Hafez, J. R. Dorkin, J. Qin, K. Lam, K. G. Rajeev, K. F. Wong, L. B. Jeffs, L. Nechev, M. L. Eisenhardt, M. Jayaraman, M. Kazem, M. A. Maier, M. Srinivasulu, M. J. Weinstein, Q. Chen, R. Alavarez, S. A. Barros, S. De, S. K. Klimuk, T. Borland, V. Kosovrasti, W. L. Cantley, Y. K. Tam, M. Manoharan, M. A: Ciufolini, M. A. Tracy, A. de Fougerolles, I. MacLachlan, P. R. Cullis, T. D. Madden, M. J. Hope, *Nat. Biotechnol.* **2010**, *28*, 172-176.

[215] J. Nguyen, F. C. Szoka, *Acc. Chem. Res.* **2012**, *45*, 1153-1162.

[216] I. S. Blagbrough, A. A. Metwally, A. J. Geall in A. E. Pegg, R. A. Casero, Jr. (Eds.), *Polyamines: Methods and Protocols,* Methods in Molecular Biology, vol. 720, Springer Science+Business Media, LLC **2011**, ch. 32, 493-503.

[217] S. Babić, A. J. M. Horvat, D. Mutavdžić Pavlovićm, M. Kaštelan-Macan, *Trends Anal. Chem.* **2007**, 26, 1043-1061.

[218] M. Andrasi, P. Buglyo, L. Zekany, A. Gaspar, *J. Pharm. Biomed. Anal*. **2007**, *44*, 1040-1047.

[219] C. Frassineti, S. Ghelli, P. Gans, A. Sabatini, M. S. Moruzzi, A. Vacca, *Anal. Biochem*. **1995**, 231, 374-382.

[220] A. G. Blackman, *Polyhedron* **2005**, *24*, 1-39.

[221] G. Wenz, C. Strassning, C. Thiele, A. Engelke, B. Morgenstern, K. Hegetschweiler, *Chem. Eur. J.* **2008**, *14*, 7202-7211.

[222] J. Heidel, S. Mishra, M. E. Davis, in T. Scheper (series eds.), D. V. Schaffer, Weichang Zhou (volume eds.), *Advances in Biochemical Engineering/Biotechnology - Gene Therapy and Gene Delivery Systems, Molecular Conjugates*, Springer-Verlag Berlin Heidelberg **2005**, ch. 2, 7-40.

[223] A. F. Adler, K. W. Leong, *Nano Today* **2010**, *5*, 553-556.

[224] G. T. Hess, W. H. Humphries Iv, N. C. Fay, C. K. Payne, *Biochim. Biophys. Acta: Mol. Cell Res.* **2007**, *1773*, 1583-1588.

[225] C. M. Wiethoff, J. G. Koe, G. S. Koe, C. R. Middaugh, *J. Pharm. Sci.* **2004**, *93*, 108-123.

[226] D. X. Liu, *Adv. Drug Deliv. Rev.* **1997**, *24*, 201-213.

[227] (a) C. Tros de Ilarduya, Y. Sunb, N. Düzgünes¸ *Eur. J. Pharm. Sci.* **2010**, *40*, 159-170. (b) L. Wasungu, D. Hoekstra, *J. Control. Release* **2006**, *116*, 255-264.

[228] http://www.malvern.com/labeng/technology/dynamic_light_scattering/classical_90_degree_ scattering.htm (Last visited on may 30th 2013.)

[229] http://www.malvern.com/labeng/technology/zeta_potential/zeta_potential_lde.htm (Last visited on may 30th 2013.)

[230] S. Nimesh, A. Goyal, V. Pawar, S. Jayaraman, P. Kumar, R. Chandra, Y. Singh, K. C. Gupta, *J. Control. Release* **2006**, *110*, 457-468.

[231] M.-H. Louis, S. Dutoit, Y. Denoux, P. Erbacher, E. Deslandes, J.-P. Behr, P. Gauduchon, L. Poulain, *Cancer Gene Ther.* **2006**, *13*, 367-374.

[232] L. Le Gourriérec, C. Di Giorgio, J. Greiner, P. Vierling, *New J. Chem.* **2008**, *32*, 2027-2042.

[233] C. Chittimalla, L. Zammut-Italiano, G. Zuber, J.-P. Behr, *J. Am. Chem. Soc.* **2005**, *127*, 11436-11441.

[234] (a) H.-P. Hsieh, J. G. Muller, C. J. Burrows, *J. Am. Chem. Soc.* **1994**, *116*, 12077-12078. (b) A. J. Geall, I. S. Blagbrough, *Tetrahedron Lett*. **1998**, *39*, 443-446. (c) M. Liu, H. Zhao, S. Chen, H. Yu, Y. Zhang, X. Quan, *Chem. Commun.* **2011**, *47*, 7749-7751.

[235] D. V. Schaffer, N. A. Fidelman, N. Dan, D. A. Lauffenburger, *Biotechnol. Bioeng.* **2000**, *67*, 598-606.

[236] M. Ruponen, S. Ronkko, P. Honkakoski, J. Pelkonen, M. Tammi, A. Urtti, *J. Biol. Chem.* **2001**, *276*, 33875-33880.

[237] I. Moret, J. E. Peris, V. M. Guillem, M. Benet, F. Revert, F. Dasi, A. Crespo, S. Alino, *J. Control. Release* **2001**, *76*, 169-181.

[238] (a) S. Asgatay, S. Franceschi-Messant, E. Perez, P. Vicendo, I. Rico-Lattes, E. Phez, M. P. Rols, *Int. J. Pharm.* **2004**, *285*, 121-133. (b) S. Höbel, C. M. C. Appeldoorn, P. J. Gaillard, A. Aigner, *Pharmaceut.* **2011**, *4*, 1591-1606.

[239] (a) Q.-D. Huang, J. Ren, W.-J. Ou, Y. Fu, M.-Q.Cai, J. Zhang, W. Zhu, X.-Q. Yu, *Chem. Biol. Drug Des.* **2012**, *79*, 879-887. (b) Q.-D. Huang, H. Chen, L.-H. Zhou, J. Huang, J. Wu, X.-Q. Yu, *Chem. Biol. Drug Des.* **2008**, *71*, 224-229.

[240] M. Suchý, R. H. E. Hudson, *Eur. J. Org. Chem.* **2008**, 4847-4865.

[241] (a) H. Stetter, W. Frank, *Angew. Chem. Int. Ed.* **1976**, *15*, 686-687. (b) J. F. Desreux, *Inorg. Chem.* **1980**, *19*, 1319-1324.

[242] (a) S. Amin, J. R. Morrow, C. Lake, M. R. Churchill, *Angew. Chem. Int. Ed.* **1994**, *33*, 773-775. (b) L. Carlton, R. D. Hancock, H. Maumela, K. P. Wainwright, *J. Chem. Soc., Chem. Commun.* **1994**, 1007-1008. (c) H. Maumela, R. D. Hancock, L. Carlton, J. H. Reibenspies, K. P. Wainwright, *J. Am. Chem. Soc.* **1995**, *117*, 6698-6707.

[243] D. D. Dischino, E. J. Delaney, J. E. Emswiler, G. T. Gaughan, J. S. Prasad, S. K. Srivastava, M. F. Tweedle, *Inorg. Chem.* **1991**, *30*, 1265-1269.

[244] (a) M. Moreau, O. Raguin, J.-M. Vrigneaud, B. Collin, C. Bernhard, X. Tizon, F. Boschetti, O. Duchamp, F. Brunotte, F. Denat, *Bioconjugate Chem.* **2012**, *23*, 1181-1188. (b) J. K. Uppal, P. P. Hazari, Raunak, K. Chuttani, M. Allard, N. K. Kaushik, A. K. Mishra, *Org. Biomol. Chem.* **2011**, *9*, 1591-1599.

[245] X. Sun, J. Kim, A. E. Martell, M. J. Welch, C. J. Anderson, *Nucl. Med. Biol.* **2004**, *3*, 1051-1059.

[246] J. Wen, Z. Geng, Y. Yin, Z. Zhang, Z. Wang, *Dalton Trans.* **2011**, *40*, 1984-1989.

[247] A. Thibon, V. C. Pierre, *Anal. Bioanal. Chem*. **2009**, *394*, 107-120.

[248] Y. Shiraishi, S. Sumiya, Y. Kohno, T. Hirai, *J. Org. Chem.* **2008**, *73*, 8571-8574.

[249] (a) M.-Q. Wang, J-L. Liu, J.-Y. Wang, D.-W. Zhang, J. Zhang, F. Streckenbach, Z. Tang, H.-H. Lin, Y. Liu, Y.-F. Zhao, X.-Q. Yu, *Chem. Commun.* **2011**, *47*, 11059-11061. (b) Y.-G. Fang, J. Zhang, S.-Y. Chen, N. Jiang, H.-H. Lin, Y. Zhang, X.-Q. Yu, *Bioorg. Med. Chem.* **2007**, *15*, 696-701.

[250] (a) S.-H. Wan, F. Liang, X. Q. Xiong, L. Yang, X.-J. Wu, P. Wang, X. Zhou, C.-T. Wu, *Bioorg. Med. Chem. Lett*. **2006**, *16*, 2804-2806. (b) C. S. Jeung, J. B. Song, Y. H. Kim,

J. Suh, *Bioorg. Med. Chem. Lett.* **2001**, *11*, 3061-3164. (c) T. Koike, E. Kimura, *J. Am. Chem. Soc.* **1991**, *113*, 8935-8941. (d) E. Kimura, M. Shionoya, A. Hoshino, T. Ikeda, Y. Yamado, *J. Am. Chem. Soc.* **1992**, *114*, 10134-10137. (e) Q.-X. Xiang, J. Zhang, P.-Y. Liu, C.-Q. Xia, Z.-Y. Zhou, R.-G. Xie, X.-Q. Yu, *J. Inorg. Biochem.* **2005**, *99*, 1661-1669. (f) W. Peng, P.-Y. Liu, N. Jiang, H.-H. Lin, G.-L. Zhang, X.-Q. Yu, *Bioorg. Chem.* **2005**, *33*, 374-385. (g) Q.-L. Li, J. Huang, G.-L. Zhang, N. Jiang, C.-Q. Xia, H.-H. Lin, J. Wu, X.-Q. Yu, *Bioorg. Med. Chem.* **2006**,*14*, 4151-4157. (h) C.-Q. Xia, L. Jiang, J. Zhang, S.-Y. Chen, H.-H. Lin, X,-Y. Tan, Y. Yue, X.-Q. Yu, *Bioorg. Med. Chem.* **2006**,*14*, 5756-5764. (i) X.-Y. Wang, J. Zhang, K. Li, N. Jiang, S.-Y. Chen, H.-H. Lin, Y. Huang, L.-J. Ma, X.-Q. Yu, *Bioorg. Med. Chem.* **2006**, *14*, 6745-6751. (j) C.-Q. Xia, N. Jiang, J. Zhang, S.-Y. Chen, H.-H. Lin, X.-Y. Tan, Y. Yue, X.-Q. Yu, *Bioorg. Med. Chem.* **2006**, *14*, 5756-5764.

[251] J. Suh, W. S. Chei, *Curr. Opin. Chem. Biol.* **2008**, *12*, 207-213.

[252] E. De Clercq, *Nat. Rev. Drug Discov.* **2003**, *2*, 581-587.

[253] (a) C. Trabaud, J. Dessolin, P. Vileghe, M. Bouygues, J. C. Chermann, M. Camplo, J. K. Kraus, *Bioorg. Med. Chem. Lett.* **1997**, *7*, 1353-1358. (b) G. J. Bridger, R. T. Skerlj, D. Thornton, S. Padmanabhan, S. A. Martellucci, G. W. Henson, M. J. Abrams, N. Yamamoto, K. De Vreese, R. Pauwels, E. De Clercq, *J. Med. Chem.* **1995**, *38*, 366-378. (c) E. De Clercq, N. Yamamoto, R. Pauwels, M. Baba, D. Schols, H. Nakashima, J. Balzarini, Z. Debyser, B. A. Murrer, D. Schwartz, D. Thornton, G. Bridger, S. Fricker, G. Henson, M. Abrams, D. Picker, *Proc. Natl. Acad. Sci. USA* **1992**, *89*, 5286-5290. (d) Y. Inouye, T. Kanamori, T. Yoshida, T. Koike, M. Shionoya, H. Fujioka, E. Kimura, *Biol. Pharm. Bull.* **1996**, *19*, 456-458.

[254] (a) S. Nimmagadda, M. Pullambhatla, K. Stone, G. Green, Z. M. Bhujwalla, M. G. Pomper, *Cancer Res.* **2010**, *70*, 3935-3944. (b) O. Jacobson, I. D. Weiss, L. Szajek, J. M. Farber, D. O. Kiesewetter, *Bioorg. Med. Chem.* **2009**, *17*, 1486-1493.

[255] B. Le Bon, N. Van Craynest, J.-M. Daoudi, C. Di Giorgio, A. J. Domb, and P. Vierling, *Bioconjugate Chem.* **2004**, *15,* 413-423.

[256] R. M. Izatt, K. Pawlak, J. S. Bradshaw, R. L. Bruening, *Chem. Rev.* **1991**, *91*, 1721-2085.

[257] G. J. Bridger, R. T. Skerlj, S. Padmanabhan, S. A. Martellucci, G. W. Henson, M. J. Abrams, H. C. Joao, M. Witvrouw, K. De Vreese, R. Pauwels, E. De Clercq, *J. Med. Chem.* **1996**, *39*, 109-119.

[258] H. Cheng, R. Zhou, L. Liu, B. Du, R. Zhuo, *Genetica* **2000**, *108*, 53-56.

[259] (a) Q.-D. Huang, W.-J.Ou, H. Chen, Z.-H.Feng, J.-Y.Wang, J. Zhang, W. Zhu, X.-Q.Yu, *Eur. J. Pharm. Biopharm.* **2011**, *78*, 326-335. (b) Q.-D. Huang, G.-X. Zhong, Y. Zhang, J. Ren, Y. Fu, J. Zhang, W. Zhu, X.-Q. Yu, *PLoS ONE* **2011**, *6*, e23134.

[260] (a) J.-L. Liu, Q.-P. Ma, Q.-D. Huang, W.-H. Yang, J. Zhang, J.-Y. Wang, W. Zhu, X.-Q. Yu, *Eur. J. Med. Chem.* **2011**, *46*, 4133-4141. (b) Q.-D. Huang, J. Ren, H. Chen, W.-J. Ou, J. Zhang, Y. Fu, W. Zhu, X.-Q. Yu, *ChemPlusChem* **2012**, *77*, 584-591.

[261] R. U. Islam, J. Hean, W. A. L. van Otterlo, C. B. de Konig, P. Arbuthnot, *Bioorg. Med. Chem. Lett.* **2009**, *19*, 100-103.

[262] K. Lia, N. Wanga, F. Yanga, Z.-W. Zhang, L.-H. Zhoua, S.-Y. Chena, H.-H. Lin, Y.-F. Tianc, X.-Q. Yu, *Chem. Biodivers.* **2009**, *6*, 754-763.

[263] L.-H. Zhou, M. Yang, H. Zhou, J. Zhang, K. Li, Y.-Z. Xiang, N. Wang, Y.-F. Tianand, X.-Q. Yu, *Chem. Biol. Drug Des.* **2009**, *73*, 216-224.

[264] Y.-Z. Xiang, Z.-H. Feng, J. Zhang, Y.-L. Liao, C.-J. Yu, W.-J. Yi, W. Zhu, X.-Q. Yu, *Org. Biomol. Chem.* **2010**, *8*, 640-647.

[265] W.-J. Yi, Z.-H. Feng, Q.-F. Zhang, J. Zhang, L.-D. Li, W. Zhu, X.-Q. Yu, *Org. Biomol. Chem* **2011**, *9*, 2413-2421.

[266] S. Li, Y. Wang, S. Wang, J. Zhang, S.-F. Wu, B.-L. Wang, W. Zhu, X.-Q. Yu, *Bioorg. Med. Chem.* **2012**, *20*, 1380-1387.

[267] C. Li, H. Tian, N. Rong, K. Liu, F. Liu, Y. Zhu, R. Qiao, Y. Jiang, *Biomacromolecules* **2011**, *12*, 298-305.

[268] J. Li, Y. Zhu, S. T. Hazeldine, S. M. Firestine, D. Oupický, *Biomacromolecules* **2012**, *13*, 3220-3227.

[269] J. M. García Fernández, C. Ortiz Mellet, J. L. Jiménez Blanco, J. Fuentes Mota, A. Gadelle, A. Coste-Sarguet, J. Defaye, *Carbohydr.* Res. **1995**, *268*, 57-71.

[270] J. E. Richman, T. J. Atkins, *J. Am. Chem. Soc.* **1974**, *96*, 2268-2270.

[271] T. J. Atkins, J. E. Richman, W. F. Oettle, *Org. Synth.* **1978**, *58*, 86.

[272] J. Huang, Z. Zhou, T. H. Chan, *Synthesis* **2009**, *14*, 2341-2344.

[273] V. Montembault, H. Mouaziz, V. Blondeau, R. Touchard, J. C. Sotif, J. C. Brosse, *Synth. Commun.* **1999**, *29*, 4279-4294.

[274] J. K. Molloy, O. Kotova, R. D. Peacock, T.Gunnlaugsson, *Org. Biomol. Chem.* **2012**, *10*, 314-322.

[275] L. M. De León-Rodríguez, Z. Kovacs, A. C. Esqueda-Oliva, A. D. Miranda-Olvera, *Tetrahedron Lett.* **2006**, *47*, 6937-6940.

[276] (a) S. Brandès, C. Gros, F. Denat, P. Pullumbi, R. Guilard, *Bull. Soc. Chim. Fr.* **1996**, *133*, 65-73. (b) E. Kimura, S. Aoki, T. Koike, M. Shiro, *J. Am. Chem. Soc.* **1997**, *119*, 3068-3076.

[277] M. I. García-Moreno, P. Díaz-Pérez, J. M. Benito, C. Ortiz Mellet, J. Defaye, J. M. García Fernández, *Carbohydr. Res.* **2002**, *337*, 2329-2334.

[278] G. Li, H. Tajima, T. Ohtani, *J. Org. Chem.* **1997**, *62*, 4539-4540.

[279] A. Megia-Fernandez, M. Ortega-Muñoz, J. Lopez-Jaramillo, F. Hernandez-Mateo, F. Santoyo-Gonzalez, *Adv. Synth. Catal.* **2010**, *352*, 3306-3320.

[280] M. Bueno Martínez, F. Zamora Mata, M. T. Ugalde Donoso, J. A. Galbis Pérez, *Carbohydr. Res.* **1992**, *230*, 191-195.

[281] (a) M. Alodan, W. Smyrl, *Electrochim. Acta* **1998**, *44*, 299-309. (b) C. Yarnitzky, R. Schrieber-Stanger, *J. Electroanal. Chem.* **1986**, *214*, 65-78. (c) M. Schuster, B. Kugler, K.H. König, *J. Anal. Chem.* **1990**, *338*, 717-723. (d) D. Jia, A.-M. Zhu, M. Ji, Y. Zhang, *J. Coord. Chem.* **2008**, *61*, 2307-2314.

[282] E. Rodríguez-Fernández, J. L. Manzano, J. J. Benito, R. Hermosa, E. Monte, J. J. Criado, *J. Inorg. Biochem.* **2005**, *99*, 1558-1572.

[283] (a) N. H. Shah, K. Kirshenbaum, *Macromol. Rapid Commun*. **2008**, *29*, 1134-1139. (b) K. Takasu, T. Azuma, Y. Takemoto, *Tetrahedron Lett.* **2010**, *51*, 2737-2740. (c) K. Takasu, T. Azuma, I. Enkhtaivan, Y. Takemoto, *Molecules* **2010**, *15*, 8327-8348.

[284] S. Lal, S. Díez-González, *J. Org. Chem.* **2011**, *76*, 2367-2373.

[285] (a) T. R. Chan, R. Hilgraf, K. B. Sharpless, V. V. Fokin, *Org. Lett.* **2004**, *6*, 2853-2855. (b) R. Ribeiro-Viana, J. J. García-Vallejo, D. Collado, E. Pérez-Inestrosa, K. Bloem, Y. van Kooyk, J. Rojo, *Biomacromolecules* **2012**, *13*, 3209-3219.

[286] (a) H. Staudinger, J. Meyer, *Helv. Chim. Acta* **1919**, *2*, 635-646. (b) M. Koehn, R. Breinbauer, *Angew. Chem. Int. Ed.* **2004**, *43*, 3106-3116.

[287] Z. Gonda, Z. Novák, *Dalton Trans.* **2010**, *39*, 726-729.

[288] (a) M. Malkoch, K. Schleicher, E. Drockenmuller, C. J. Hawker, T. P. Russell, P. Wu, V. V. Fokin, *Macromolecules* **2005**, *38*, 3663-3678. (b) P. Wu, A. K. Feldman, A. K. Nugent, C. J. Hawker, A. Scheel, B. Voit, J. Pyun, J. M. J. Frechet, K. B. Sharpless, V. V. Fokin, *Angew. Chem. Int. Ed.* **2004**, *43*, 3928-3932.

[289] G. A. Bowmaker , J. C. Dyason , P. C. Healy , L. M. Engelhardt , C. Pakawatchai, A. H. White, *J. Chem. Soc., Dalton Trans.* **1987**, 1089-1097.

[290] P. F. Barron , J. C. Dyason , P. C. Healy , L M. Engelhardt , C.Pakawatchai , V. A. Patrick, A. H. White, *J. Chem. Soc., Dalton Trans.* **1987**, 1099-1106.

[291] V. Bennevault-Celton, A. Urbach, O. Martin, C. Pichon, P. Guégan, P. Midoux, *Bioconjuagte Chem.* **2011**, *21*, 2404-2414.

[292] A. R. Khan, P. Forgo, K. J. Stine, V. T. D´Souza, *Chem. Rev.* **1998**, *98*, 1977-1996.

[293] (a) C. Fraschini, L. Greffe, H. Driguez, M. R. Vignon, *Carbohydr. Res.* **2005**, *340*, 1893-1899. (b) K. Hara, K. Fujita, N. Kuwahara, T. Tanimoto, H. Hashimoto, K. Koizumi, S. Kitahata, *Biosci. Biotech. Biochem.* **1994**, *58*, 652-659. (c) K. Koizumi, T. Tanimoto, Y. Okada, K. Hara, K. Fujita, H. Hashimoto, S. Kitahata, *Carbohydr. Res.* **1995**, *278*, 129-142. (d) C. Simiand, S. Cottaz, C. Bosso, H. Driguez, *Biochimie* **1992**, *74*, 75-80.

[294] C. Ortiz Mellet, J. M. García Fernández, J. M. Benito, in *Monographs in Supramolecular Chemistry No. 13, Supramolecular Systems in Biomedical Fields* (Ed.: H.-J. Schneider), RSC, **2013**, pp 94-139.

[295] (a) J. Bjerre, C. Rousseau, L. Marinescu, M. Bols, *Appl. Microbiol. Biotechnol.* **2008**, *81*, 1-11. (b) R. Breslow, *Acc. Chem. Res.* **1995**, *28*, 146-153. (c) J. Bjerre, E. H. Nielsen, M. Bols, *Eur. J. Org. Chem.* **2008**, 745-752. (d) J. Bjerre, T. H. Fenger, L. G. Marinescu, M. Bols, *Eur. J. Org. Chem.* **2007**, 704-710. (e) H. L. Chen, B. Zhao, Z. Wang, *J. Inclus. Phenom. Macrocycl. Chem.* **2006**, *56*, 17-21. (f) L. G. Marinescu, M. Bols, *Angew. Chem. Int. Ed.* **2006**, *45*, 4590-4593. (g) F. Ortega-Caballero, J. Bjerre, L. S. Laustsen, M. Bols, *J. Org. Chem.* **2005**, *70*, 7217-7226. (h) C. Rousseau, F. Ortega-Caballero, L. U. Nordstrom, B. Christensen, T. E. Petersen, M. Bols, *Chem. Eur. J.*

2005, *11*, 5094-5101. (i) F. Ortega-Caballero, C. Rousseau, B. Christensen, T. E. Petersen, M. Bols, *J. Am. Chem. Soc.* **2005**, *127*, 3238-3239. (j) R. Breslow, S. D. Dong, *Chem. Rev.* **1998**, *98*, 1997-2011.

[296] (a) J. M. Haider, Z. Pikramenou, *Chem. Soc. Rev.* **2005**, *34*, 120-132. (b) T. Ogoshi, A. Harada, *Sensors* **2008**, *8*, 4961-4982. (c) Y. Liu, N. Zhang, Y. Chen, L. H. Wang, *Org. Lett.* **2007**, *9*, 315-318. (d) A. Yamauchi, Y. Sakashista, K. Hirose, T. Hayashita, I. Suzuki, *Chem. Commun.* **2006**, 4312-4314. (e) Y. Liu, Y. Chen, *Acc. Chem. Res.* **2006**, *39*, 681-691. (f) N. Smiljanic, V. Moreau, D. Yockot, J. M. Benito, J. M. García Fernández, F. Djedaïni-Pilard, *Angew. Chem. Int. Ed.* **2006**, *45*, 5465-5468.

[297] (a) Z.-Y. Dong, S.-Z. Mao, K. Liang, J.-Q. Liu, G.-M. Luo, J.-C. Shen, *Chem. Eur. J.* **2006**, *12*, 3575-3579. (b) F. Hapiot, S. Tilloy, E. Monflier, *Chem. Rev.* **2006**, *106*, 767-781. (c) C. Jeunesse, D. Armspach, D. Matt, *Chem. Commun.* **2005**, 5603-5614. (d) H. Bricout, F. Hapiot, A. Ponchel, S. Tilloy, E. Monflier, *Curr. Org. Chem.* **2010**, 14, 1296-1307. (e) F. Hapiot, A. Ponchel, S. Tilloy, E. Monflier, *C. R. Chim.* **2011**, *14*, 149-166. (f) C. Yang, C. Ke, W. Liang, G. Fukuhara, T. Mori, Y. Liu, Y. Inoue, *J. Am. Chem. Soc.* **2011**, *133*, 13786-13789.

[298] A. Bom, M. Bradley, K. Cameron, J. K. Clark, J. van Egmond, H. Feilden, E. J. MacLean, A. W. Muir, R. Palin, D. C. Rees, M.-Q. Zhang, *Angew. Chem. Int. Ed.* **2002**, *41*, 265-270.

[299] J. M. Benito, M. Gómez-Gracía, C. Ortiz Mellet, I. Baussanne, J. Defaye, J. M. García Fernández, *J. Am. Chem. Soc.* **2004**, *126*, 10355-10363.

[300] (a) R. J. Coulston, H. Onagi, S. F. Lincoln, C. J. Easton, *J. Am. Chem. Soc.* **2006**, *128*, 14750-14751. (b) H. Tian, Q. C. Wang, *Chem. Soc. Rev.* **2006**, *35*, 361-374. (c) G. Wenz, B. H. Han, A. Muller, *Chem. Rev.* **2006**, *106*, 782-817.

[301] (a) D.-E. Lee, H. Koo, I.-C. Sun, J. H. Ryu, K. Kim, I. C. Kwon, *Chem. Soc. Rev.* **2012**, *41*, 2656-2672. (b) S. S. Kelkar, T. M. Reineke, *Bioconjugate Chem.* **2011**, *22*, 1879-1903.

[302] (a) A. Hybl, R. E. Rundle, D. E. William, *J. Am. Chem. Soc*. **1965**, *87*, 2779-2788. (b) W. Saenger, M. Noltemeyer, P. C. Manor, B. Himgerty, B. Klar, *Bioorg. Chem*. **1976**, *5*, 187-195.

[303] H. Law, J. M. Benito, J. M. García Fernández, L. Jicsinszky, S. Crouzy, J. Defaye, *J. Phys. Chem. B* **2011**, *115*, 7524-7532.

[304] J. Defaye, A. Gadelle, A. Guillier, R. Darcy, T. O'Sullivan, *Carbohydr. Res.* **1989**, *192*, 251-258.

[305] B. Brady, N. Lynam, T. O'Sullivan, C. Ahern, R. Darcy, *Org. Synth.* **2000**, *77*, 221-224.

[306] (a) T. T. Nielsen, V. Wintgens, C. Amiel, R. Wimmer, K. L. Larsen, *Biomacromolecules* **2010**, *11*, 1710-1715. (b) H.-S. Byun, N. Zhong, R. Bittman, *Org. Synth.* **2000**, *77*, 225-230.

[307] (a) E. Z. Messmer, *Phys. Chem.* **1927**, 126, 369-416. (b) Y. Matsui, T. Kurita, Y. Date, *Bull. Chem. Soc. Jpn.* **1972**, *45*, 3229-3229. (c) Y. Matsui, K. Kinugawa, *Bull. Chem. Soc. Jpn.* **1985**, *58*, 2981-2986. (d) M. Darj, E. R. Malinovski, *Appl. Spectrosc.* **2002**, *56*, 257-265. (e) E. Norkus, G. Grinciene, T. Vuorinen, E. Butkus, R. Vaitkus, *Supramol. Chem.* **2003**, *15*, 425-431. (f) P. K. Bose, P. L. Polavarapu, *Carbohydr. Res.* **2000**, *323*, 63-72. (g) E. Norkus, G. Grinciené, T. Vuorinen, R. J. Vaitkus, *J. Incl. Phenom. Macrocycl.Chem.* **2004**, *48*, 147-150. (h) R. Fuchs, N. Habermann, P. Klüfers, *Angew. Chem. Int. Ed.* **1993**, *32*, 852-854.

[308] M. Sollogoub, *Eur. J. Org. Chem.* **2009**, 1295-1303.

[309] J. Boger, D. G. Brenner, J. R. Knowles, *J. Am. Chem. Soc.* **1979**, *101*, 7630-7631.

[310] I. Tabushi, K. Shimokawa, N. Shimizu, H. Shirakata, K. Fujita, *J. Am. Chem. Soc.* **1976**, *98*, 7855-7856.

[311] (a) D. Armspach, L. Poorters, D. Matt, B. Benmerad, F. Balegroune, L. Toupet*c*, *Org. Biomol. Chem.* **2005**, *3*, 2588-2592. (b) R. Gramage-Doria, D. Rodríguez-Lucena, D. Armspach, C. Egloff, M. Jouffroy, D. Matt, L. Toupet, *Chem. Eur. J.* **2011**, *17*, 3911-3921.

[312] (a) P. Balbuena, D. Lesur, M. J. González Álvarez, F. Mendicuti, C. Ortiz Mellet, J. M. García Fernández, *Chem. Commun.* **2007**, 3270-3272. (b) P. Balbuena, R. Gonçalves-Pereira, J. L. Jiménez Blanco, M. I. García-Moreno, D. Lesur, C. Ortiz Mellet, J. M. García Fernández, *J. Org. Chem.* **2013**, 78, 1390-1403.

[313] E. Engeldinger, D. Armspach, D. Matt, *Chem. Rev.* **2003**, *103*, 4147-4173.

[314] F. Bellia, D. La Mendola, C. Pedone, E. Rizzarelli, M. Savianoc, G. Vecchio, *Chem. Soc. Rev.* **2009**, *38*, 2756-2781.

[315] D. Armspach, D. Matt, *Carbohydr. Res.* **1998**, *310*, 129-133.

[316] L. Poortes, D. Armspach, D. Matt, *Eur. J. Org. Chem.* **2003**, 1377-1381.

[317] M. Jouffroy, R. Gramage-Doria, D. Armspach, D. Matt, L. Toupet, *Chem. Commun.* **2012**, *48*, 6028-6030.

[318] M. Petrillo, L. Marinescu, C. Rosseau, M. Bols, *Org. Lett.* **2009**, *11*, 1983-1985.

[319] (a) A. J. Pearce, P. Sinaÿ, *Angew. Chem. Int. Ed.* **2000**, *39*, 3610-3612. (b) T. Lecourt, A. Herault, A. J. Pearce, M. Sollogoub, P. Sinaÿ, *Chem. Eur. J.* **2004**, *10*, 2960-2971.

[320] (a) B. du Roizel, J.-P. Baltaze, P. Sinaÿ, *Tetrahedron Lett.* **2002**, *43*, 2371-2373. (b) X. Luo, Y. Chen, J. G. Huber, Y. Zhang, P. Sinaÿ, *C. R. Chimie* **2004**, *7*, 25-28. (c) S. Xiao, M. Yang, P. Sinaÿ, Y. Blériot, M. Sollogoub, Y. Zhang, *Eur. J. Org. Chem.* **2010**, 1510-1516.

[321] R. Ghosh, P. Zhang, A. Wang, C.-C. Ling, *Angew. Chem. Int. Ed.* **2012**, *51*, 1548-1552.

[322] (a) E. Zaborova, M. Guitet, G. Prencipe, Y. Blériot, M. Ménand, M. Sollogoub, *Angew. Chem. Int. Ed.* **2013**, *52*, 639-644. (b) G. K. Rawal, S. Rani, S. Ward, C.-C. Ling, *Org. Biomol. Chem.* **2010**, *8*, 171-180. (c) G. K. Rawal, S. Rani, C.-C. Ling, *Tetrahedron Lett.* **2009**, *50*, 4633-4636. (d) S. Guieu, M. Sollogoub, *J. Org. Chem.* **2008**, *73*, 2819-2828.

[323] S. Guieu, M. Sollogoub, *Angew. Chem. Int. Ed.* **2008**, *47*, 7060-7063.

[324] (a) K.-M. Sung, D. W. Mosley, B. R. Peelle, S. Zhang, J. M. Jacobson, *J. Am. Chem. Soc.* **2004**, *126*, 5064-5065. (b) J. G. Worden, A. W. Shaffer, Q. Huo, *Chem. Commun.* **2004**, 518-519.

[325] G. Di Fabio, G. Malgieri, C. Isernia, J. D'Onofrio, M. Gaglione, A. Messere, A. Zarrellia, L. De Napolia, *Chem. Commun.* **2012**, *48*, 3875-3877.

[326] R. B. Merrifield, *J. Am. Chem. Soc.*, 1963, **85**, 2149-2154.

[327] (a) R. C. D. Brown, *J. Chem. Soc.*, *Perkin Trans. 1*, **1998**, 3293-3320. (b) R. Brown, *Contemp. Org. Synth.* **1997**, *4*, 216-237. (c) P. H. H. Hermkens, H. C. J. Ottenheijm, D. C. Rees, *Tetrahedron* **1997**, *53*, 5643-5678.

[328] (a) A. Kirschning, H. Monenschein, R. Wittenberg, *Angew. Chem. Int. Ed.* **2001**, *40*, 650-679. (b) S. V. Ley, I. R. Baxendale, R. N. Bream, P. S. Jackson, A. G. Leach, D. A. Longbottom, M. Nesi, J. S. Scott, R. I. Storer, S. J. Taylor, *J. Chem. Soc., Perkin Trans. 1* **2000**, 3815-4195. (c) D. H. Drewry, D. M. Coe, S. Poon, *Med. Res. Rev.* **1999**, *19*, 97-148. (d) S. V. Ley, I. R. Baxendale, *Nat. Rev. Drug Discov.* **2002**, *1*, 573-586.

[329] (a) Immobilized Catalysts (Ed.: A. Kirschning) *Top. Curr. Chem.* **2004**, Vol. 242. (b) W. Solodenko, Y. Frenzel, A. Kirschning, in *Polymeric Materials in Organic Synthesis and Catalysis* (Ed.: M. R. Buchmeiser), Wiley-VCH, Weinheim, **2003**, pp. 201-240. (c) C. A. McNamara, M. J. Dixon, M. Bradley *Chem. Rev.* **2002**, *102*, 3275-3300.

[330] (a) T. A. Keating, R. W. Armstrong, *J. Am. Chem. Soc*. **1996**, *118*, 2574-2583. (b) J. M. J. Fréchet, L. J. Nuyens, *Can. J. Chem.* **1976**, *54*, 926-934. (c) J. Y. Wong, C. C. Leznoff, *Can. J. Chem*. **1973**, *51*, 2452-2456. (d) I. T. Harrison, S. Harrison, *J. Am. Chem. Soc*. **1967**, *89*, 5723-5724.

[331] A. Kirschning, H. Monenschein, R. Wittenberg, *Chem. Eur. J.* **2000**, *6*, 4445-4450.

[332] (a) S. S. van Berkel, M. B. van Eldijk, J. C. M. van Hest, *Angew. Chem. Int. Ed.* **2011**, *50*, 8806-8827. (b) E. Saxon, C. R. Bertozzi, *Science* **2000**, *287*, 2007-2010. (c) B. L. Nilsson, L. L. Kiessling, R. T. Raines, *Org. Lett.* **2000**, *2*, 1939-1941.

[333] F. Palacios, C. Alonso, D. Aparicio, G. Rubiales, J. M. de los Santos, *Tetrahedron* **2007**, *63*, 523-575.

[334] O. Herd, A. Heßler, M. Hingst, M. Tepper, O. Stelzer, *J. Organomet. Chem.* **1996**, *522*, 69-76.

[335] (a) E. Atherton, R. C. Sheppard, in *Solid Phase Peptide Synthesis: A Practical Approach*. IRL Press: Oxford; **1989**. (b) J. Meienhofer, M. Waki, E. P. Heimer, T. J. Lambros, R. C. Makofske, C.-D. Chang, *Int. J. Pept. Prot. Res.* **1979**, *13*, 35-42.

[336] (a) M. Gude, J. Ryf, P. D. White, *Lett. Pept. Sci.* **2002**, *9*, 203-206. (b) C. E. Freeman, A. G. Howard, *Talanta* **2005**, *65*, 574-577.

[337] E. Kaiser, R. L. Colescott, C. D. Bossinger, P. I. Cook, *Anal. Biochem.* **1970**, *34*, 595-598.

[338] M. Meldal, *Tetrahedron Lett.* **1992**, *33*, 3077-3080.

[339] R. Zhang, Q. Li, J. Zhang, J. Li, G. Ma, Z. Su, *React. Funct. Polym.* **2012**, *72*, 773-780.

[340] J. M. García Fernández, C. Ortiz Mellet, V. M. Díaz Pérez, J. Fuentes, J. Kovács, I. Pintér, *Tetrahedron Lett.* **1997**, *38*, 4161-4164.

[341] C. V. N. S. Varaprasad, D. Barawkar, H. El Abdellaoui, S. Chakravarty, M. Allan, H. Chen, W. Zhang, J. Z. Wu, R. Tam, R. Hamatake, S. Lang, Z. Hong, *Bioorg. Med. Chem. Lett.* **2006**, *16*, 3975-3980.

[342] G. Zemplén, A. Kunz, *Berichte der Deutschen chemischen Gesellschaft* **1924**, *57*, 1357-1359.

[343] (a) V. Krchnák, J. Vágner, M. Lebl, *Int. J. Pept. Protein Res.* **1988**, *32*, 415-416. (b) M. Flegel, R. C. Sheppard, *J. Chem. Soc., Chem. Commun.* **1990**, 536-538.

[344] M. E. Attardi, G. Porcu, M. Taddei, *Tetrahedron Lett.* **2000**, *41*, 7391-7394.

[345] J. Gaucheron, C. Boulanger, C. Santaella, N. Sbirrazzouli, O. Boussif, P. Vierling, *Bioconjugate Chem*. **2001**, 12, 949-963.

[346] C. Schickaneder, F. W. Heinemann, R. Alsfasser, *Eur. J. Inorg. Chem.* **2006**, 2357-2363.

[347] M. Shao, Y. Zhao, *Tetrahedron Lett.* **2010**, *51*, 2892-2895.

[348] H. Lebel, V. Paquet, *J. Am. Chem. Soc.* **2004**, *126*, 320-328.

[349] S. M. Rummelt, M. Ranocchiari, J. A. van Bokhoven, *Org. Lett.* **2012**, *14*, 2188-2190.

[350] K. Jobe, C. H. Brennan, M. Motevalli, S. M. Goldup, M. Watkinson, *Chem. Commun.* **2011**, *47*, 6036-6038.